

Birla Central Library

PILANI (Jaipur State)

Class No :- 629.1323

Book No :- WA26E

Accession No :- 18939

**ELEMENTARY
APPLIED
AERODYNAMICS**

ELEMENTARY
APPLIED
AERODYNAMICS

BY
T. G. WHITLOCK

OXFORD UNIVERSITY PRESS
LONDON: HUMPHREY MILFORD

OXFORD UNIVERSITY PRESS
AMEN HOUSE, E.C. 4
LONDON EDINBURGH GLASGOW
LEIPZIG NEW YORK TORONTO
MELBOURNE CAPE TOWN BOMBAY
CALCUTTA MADRAS SHANGHAI
HUMPHREY MILFORD
PUBLISHER TO THE
UNIVERSITY

FIRST EDITION 1931

Reprinted photographically in Great Britain in
1935 (with corrections), 1938, and 1943, by
LOWE & BRYDONE, Printers, Ltd., London

PREFACE

THIS book, it is hoped, will fill to some extent the gap which still exists between the popular non-technical books on aeronautics and the advanced mathematical works on aerodynamics. It is the outcome of an attempt to provide an elementary text-book suitable for students of moderate mathematical ability and attainment, who require an introduction to the subject involving little else but elementary algebra and trigonometry and the fundamental principles of mechanics.

Within the mathematical limits imposed the book is fairly complete, and deals in turn with the performance and theory of aerofoils, aeroplane and airscrew performance, control and stability, scale effect, and airscrew theory. Several fully worked-out examples are given in the text to illustrate methods and principles, while there are also a few short sets of examples to be worked through by the student. A list of the principal formulae in aerodynamics is given for ease of reference.

It has been thought desirable to include some treatment of the modern aerofoil theory which is now so widely used in aeroplane and airscrew design. The complex mathematics involved in the full development of the theory has been necessarily omitted, but the principal features and results have been included. Those readers who have access to wind channels should find many interesting laboratory experiments provided by the experimental verification of the effects of induced velocity and centre line camber.

The author wishes to thank the Controller of His Majesty's Stationery Office for permission to use many diagrams and data taken from the various Reports and Memoranda of the Aeronautical Research Committee. He also wishes freely to

acknowledge his indebtedness to the many existing works on aerodynamics, especially to Bairstow's *Applied Aerodynamics*, Glauert's *Aerofoil and Airscrew Theory*, and Warner's *Airplane Design*. Finally, he desires to thank the Clarendon Press for all the help which they have given him.

T. G. W.

December 1930.

CONTENTS

PRINCIPAL FORMULAE IN AERODYNAMICS I

I.—INTRODUCTION.

Aeroplane parts, the wind channel, the pitot tube, air speed indicator, relative density, indicated air speed, the altimeter, the standard atmosphere 5

II.—THE AEROFOIL.

Forces on a flat plate, lift and drag, lift and drag coefficients of aerofoil, effect of incidence, the weight-lift equation, stalling speed, wing loading, the lift-drag ratio, the moment coefficient and centre of pressure 15

III.—ELEMENTS OF AIRFLOW.

Streamlines, viscosity and skin friction, form drag, streamline bodies, airflow over aerofoil, the slotted wing, the pressure distribution over an aerofoil, Bernoulli's equation, circulation and origin of lift 35

IV.—THE AEROPLANE WING.

Lift distribution across the span, three-dimensional flow, the trailing vortices, the induced velocity, induced and profile drag, aspect ratio corrections, non-rectangular aerofoils, biplane effect, stagger, curvature of streamlines, distribution of lift between biplane wings, channel wall constraint 48

V.—THE AEROFOIL IN TWO-DIMENSIONAL FLOW.

The perfect fluid, the boundary layer, the origin of lift, circulation, aerofoil characteristics for infinite aspect ratio, camber effects, effect of thickness 69

VI.—PARASITE DRAG.

Value of streamlining, struts, wires, the fuselage, the turbulence ring, airship envelopes, the undercarriage, the tail unit, interference, incidence effects, distribution of parasite drag, drag of complete aeroplane 81

VII.—AEROPLANE PERFORMANCE.

Slipstream effect, horse-power available and horse-power required, performance charts, calculation of speed and climb, angle of climb, gliding angle, effect of change of weight, performance at height, ceiling, supercharging, the rapid prediction of speed and ceiling, wing loading and power loading in performance, drag analysis, the $\text{span}^2/\text{weight}$ ratio, aeroplane characteristics 94

VIII.—THE AIRSCREW.

Engine power and torque, the power curve, airscrew torque, airscrew thrust, thrust and torque coefficients, efficiency, pitch, calculation of airscrew performance, supercharging, effect of body behind an airscrew, tip speed, the slipstream factor 125

IX.—THE EQUILIBRIUM OF THE AEROPLANE.

Determination of the centre of gravity, the mean chord, C.G. coordinates, moment of wing forces about the C.G., thrust and body moments, downwash, tail setting, tail plane characteristics, tail plane efficiency, tail moment, tail setting to trim, tail plane drag. 146

X.—CONTROL AND MANŒUVRE.

Axes of reference, the control surfaces, balancing, elevator characteristics, aileron rolling and yawing movements, rudder yawing moment, turning, load factor, speed and loading in a turn, looping, autorotation and spinning, the slot-cum-aileron device 164

XI.—STABILITY.

Definitions, longitudinal static stability, analysis of wing and tail moment curves, longitudinal dynamic stability, directional stability, rolling stability, the dihedral angle and stability in sideslip, spiral instability. 185

XII.—SCALE EFFECT.

Dimensional theory, Reynolds' number, the variable-density wind channel, aerofoil lift, drag and moment, parasite drag, full-scale lift and drag 197

XIII.—AIRSCREW THEORY.

The simple blade element theory, thrust and torque grading curves, efficiency, the simple momentum theory, the modified blade element theory, the vortex theory, the partial efficiencies of an airscrew 208

APPENDIX.—THEORY OF AEROFOILS.

Calculation of the angle of no-lift and the moment coefficient at zero lift 231

INDEX 237

ANSWERS TO EXAMPLES 241

PRINCIPAL FORMULAE IN AERODYNAMICS

Chapter

- I. Indicated Air Speed . $V_i = V\sqrt{\sigma}$.
- II. Aerofoil Lift . . . $L = k_L \rho S V^2$
 Aerofoil Drag . . . $D = k_D \rho S V^2$
 Weight-Lift Equation $W = k_L \rho S V^2$
 Moment about Leading Edge . . . $M = k_m c \rho S V^2$
 Centre of Pressure Coefficient . . . $k_{C.P.} = \frac{k_m}{k_L \cos \alpha + k_D \sin \alpha}$
 (or $k_{C.P.} = \frac{k_m}{k_L}$ approximately).
- III. Bernoulli's Equation . $p + \frac{1}{2} \rho V^2 = H$.
- IV. Aspect Ratio . . . $A = \frac{4s^2}{S}$
 Induced Drag Coefficient of Aerofoil $k_{D_1} = \frac{2}{\pi A} k_L^2$
 Effect of Induced Velocity $\alpha = \alpha_0 + \frac{2}{\pi A} k_L$
 $k_D = k_{D_0} + \frac{2}{\pi A} k_L^2$
 Aspect Ratio Correction $\alpha' - \alpha = \frac{2}{\pi} \left(\frac{1}{A'} - \frac{1}{A} \right) k_L$
 $k_{D'} - k_D = \frac{2}{\pi} \left(\frac{1}{A'} - \frac{1}{A} \right) k_L^2$
 Biplane Effect . . . $\alpha = \alpha_0 + \frac{2}{\pi A} (1 + \sigma) k_L$
 $k_D = k_{D_0} + \frac{2}{\pi A} (1 + \sigma) k_L^2$
 or $k_{D_1} = \frac{S}{2\pi s_1^2 - 2\sigma s_1 s_2 + s_2^2} k_L^2$
 (for unequal wings).

2 Principal Formulae in Aerodynamics

Chapter

V. Aerofoil of Infinite

$$\begin{aligned} \text{Aspect Ratio} \quad & k_L = 0.052(\alpha + \beta) \\ & k_m = -0.25k_L + k_{m_0} \\ & \left. \begin{aligned} \beta &= 2\gamma \\ k_{m_0} &= -\frac{\pi}{2}\gamma \end{aligned} \right\} \text{where } \gamma \text{ is cam-} \\ & \quad \quad \quad \text{ber of circular} \\ & \quad \quad \quad \text{centre line} \\ & k_L = 2\pi\gamma \text{ for minimum } k_{D_0}. \end{aligned}$$

$$\text{VII. Horse-power Required} \quad H.P_r = \frac{DV}{550}$$

$$\text{Horse-power Available} \quad H.P_a = \eta P$$

$$\begin{aligned} \text{Rate of Climb} \quad & \text{Climb (ft./min.)} = \frac{Z \times 33000}{W} \\ & \text{or } \frac{T-D}{W} \times V \times 60 \end{aligned}$$

$$\text{Airscrew Thrust} \quad TV = \eta P 550$$

$$\text{Best Gliding Angle} \quad \tan \theta = \frac{1}{L/D (\max)}.$$

$$\text{VIII. Airscrew Thrust} \quad T = k_T \rho n^2 D^4$$

$$\text{Airscrew Torque} \quad Q = k_Q \rho n^2 D^5$$

$$\text{Airscrew Efficiency} \quad \eta = \frac{1}{2\pi} \frac{k_T}{k_Q} \frac{V}{nD}$$

$$\text{Slipstream Factor} \quad \frac{R}{R_0} = a + b \frac{T}{\rho V^2 D^2}.$$

IX. Wing Moment about C.G.

$$M_w = k_m^- c \rho S V^2, \text{ where}$$

$$k_m^- = k_m + h k_L + k k_x$$

$$k_x = k_L \sin \alpha - k_D \cos \alpha$$

Incidence and Setting of Tail Plane

$$\alpha' = \alpha - \epsilon + \alpha_t$$

Principal Formulae in Aerodynamics 3

Chapter

$$\begin{aligned} \text{Downwash} \quad . \quad . \quad \text{Average figures } \epsilon &= \frac{70k_L}{A} \\ &\quad \text{(for monoplane)} \\ &= \frac{110k_L}{A} \\ &\quad \text{(for biplane)} \end{aligned}$$

$$\text{Tail Moment} \quad . \quad . \quad M_t = -k_L' l \rho S' V^2$$

$$\text{Moment Equation} \quad . \quad k_m c \rho S V^2 = k_L' l \rho S' V^2.$$

$$\begin{aligned} \text{X. Stalling Speed in a} \quad V_s' &= \frac{V_s}{\sqrt{\cos \phi}} \\ \text{Turn} \quad . \quad . \quad . \end{aligned}$$

The above formulae have been indicated where they occur in the text by printing the serial numbers in heavy type.

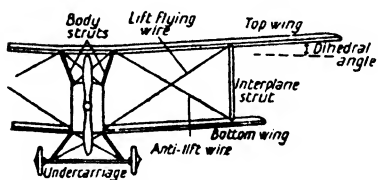
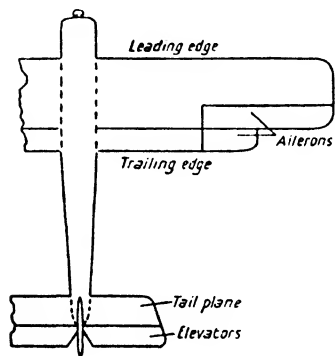
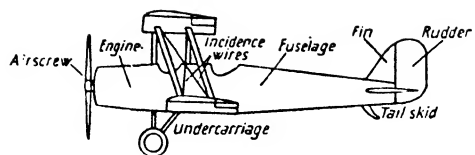


FIG. 1. AEROPLANE NOMENCLATURE.

I

INTRODUCTION

Air Forces. When a body is in motion through the air, or when it is held at rest in a moving air-stream, it experiences reactions which are known as air forces.

✓ **Aerodynamics.** Aerodynamics is the name given to the study of the air forces acting on a body due to the relative motion of the body and the air, and in its application to the aeroplane deals with

- (a) the determination of the air forces acting on the aeroplane, ✓
- and (b) the effect of these forces on the behaviour of the aeroplane. ✓

Air Speed. The speed of an aeroplane relative to the air is called its air speed, and agrees with the actual speed over the ground only if the aeroplane is flying in still air. It must be realized at once that it is the relative speed upon which the air forces depend.

Aeroplane Parts. The names of the various parts of an aeroplane are given in Fig. 1. The wings or main planes are fabric-covered structures which, on account of the air forces experienced by them due to the relative speed of the aeroplane, provide a vertical lifting force which balances the weight of the aeroplane. The necessary speed is provided by the airscrew which, on being rotated by the engine, experiences an air force in a forward direction and so urges the aeroplane through the air.

At the rear end of the body or fuselage are certain wing-like surfaces for stability and control. The tail plane is a stabilizing surface which experiences a small lifting force of the same nature as the main plane lift, the function of this force being to give the aeroplane fore-and-aft stability and equilibrium. The rear part of the tail plane consists of the elevators which are movable surfaces under the control of the pilot. By altering the position of the elevators relative to the tail plane proper, the

pilot can vary the amount of tail plane lift and so control the fore-and-aft attitude of the aeroplane.

In a similar manner directional stability and control are obtained from the air forces acting on the fixed stabilizing fin and movable rudder.

At the rear edges of the wings are further movable control surfaces called the ailerons, movement of which calls into play air forces tending to roll or bank the aeroplane.

The undercarriage is the structure upon which the aeroplane makes its preliminary run in acquiring sufficient 'flying speed' for the development of the main plane lift, and upon which it alights in landing. In order to prevent damage to the tail while the aeroplane is moving on the ground, a skid is fixed to the fuselage underneath the tail plane; this also acts as a brake during the landing run.

The Wind Channel. Many of the air forces acting on the various parts of an aeroplane cannot be directly calculated, but have to be obtained from experiments on models.

Now the air forces on a body are the same whether the body is moving through the air or the air is moving past the body, provided that the air speed is the same in each case. In experimental laboratory work on models it is clearly desirable and more practicable to keep the model at rest and make the air pass over it. The apparatus used in such work is called a Wind Channel, and a typical wind channel, as used at the National Physical Laboratory, is shown in Fig. 2.

It consists of a long wooden box through which the air is drawn and in which the model is mounted. The air current is produced by an airscrew *E* driven by an electric motor. The air is drawn through the trumpet mouth *A* and passes through a honeycomb *B*, the object of which is to disperse any eddies existing in the air and so ensure that the air-stream through the working portion *C*, where the model is mounted, is uniform and free from turbulence. Glass doors or windows are let in to the channel at *D* for the setting-up and viewing of the model. After passing through the working portion the air enters the rear part

called the distributor. The distributor has specially perforated walls through which the air is squeezed out. This breaks up the stream and allows the air to return to the laboratory at a low velocity.

The model is mounted on a spindle connected to a balance,

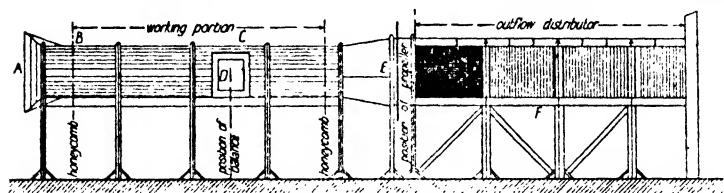


FIG. 2. The Wind Channel.

by means of which the forces on the model can be measured. In some experiments the model is inverted and a wire suspension method of setting-up is used, the forces then being measured by balances on the channel roof.

The channels in this country are mostly 4 or 7 ft. square. On the continent there are circular channels, while at the National Physical Laboratory there is a channel called the Duplex channel, measuring 14 ft. by 7 ft., in which models as large as $\frac{1}{4}$ scale can be tested. More often than not the different parts of the aeroplane are tested separately in wind channel work; this allows the use of larger scale models and shows how each component plays its part. This method, however, cannot be used indiscriminately for any component, as the behaviour of one part of an aeroplane is often considerably modified by the presence of another.

The air speed used in wind channel experiments varies from about 40 to 100 ft. per second. Aeroplane speeds are, of course, much higher than this, but it will be shown in the later chapters how air forces on aeroplanes at high speeds can be calculated from model data obtained at low speeds.

The Pitot Tube. The speed of an air-stream in a wind channel is measured by means of an instrument known as the Pitot Tube. This consists of two fine tubes (often concentric,

but shown separate in the figure) facing the air-stream, the front end of one tube *A* (called the dynamic tube) being open, while the other tube *B* (called the static tube) is closed but has its sides perforated by small holes. The rear ends of the tubes are connected to the different arms of a *U*-tube pressure gauge.

The principle of working lies in the fact that, when an air-stream passes over the two tubes, the pressure in the static tube is the normal pressure of the general stream, but the pressure in

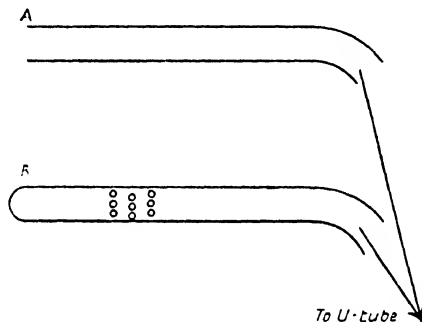


FIG. 3. The Pitot Tube.

the dynamic tube is greater than this by $\frac{1}{2}\rho V^2$, where V is the velocity in feet per second and ρ (the Greek letter *rho*) is the density in slugs per cubic foot.¹ Hence the difference in the level of the two arms of the pressure gauge is due to a pressure difference of $\frac{1}{2}\rho V^2$, so that if the density is known the velocity can be calculated.

The value $\frac{1}{2}\rho V^2$ for the pressure difference in the two tubes is deduced from Bernoulli's equation; for proof see p. 44.

Air Speed Indicators. A pitot is also fitted on all aeroplanes, often on one of the interplane struts. The tubes are usually separate and are connected to an instrument called the Air Speed Indicator (A.S.I.) fixed on the instrument board in the

¹ Since pressures are measured in lb. per square foot the density must be measured in gravitational mass units or slugs, so that, if w is the weight of one cubic foot of air, the density $\rho = \frac{w}{g}$ slugs per cubic foot.

pilot's cockpit. The A.S.I. is a small box divided into two compartments by an airtight but movable diaphragm. The dynamic tube is connected to one side of the diaphragm, and the static tube to the other. Difference in pressure is then registered by a movement of the diaphragm which, in its turn, moves a pointer on a dial reading in miles per hour. Since the pressure difference is $\frac{1}{2}\rho V^2$ the dial can only be made to give true air speeds for one particular value of ρ , and air speed indicators are all designed on a value for ρ of 0.00237 which corresponds to a pressure of 760 mm. at a temperature of 15° C. This is called the *standard density* and is denoted by ρ_0 . The correction to be applied to the recorded speed for any other value of the density is given later.

The Atmosphere. The density of the atmosphere is not constant, and the value of ρ_0 given above represents an average ground level value only. The density depends upon the pressure and temperature, both of which may vary from day to day. Again, the density decreases as the height above the earth's surface increases, although the density at any given height is not constant owing to the variations in pressure and temperature at that height.

From the well-known laws of Boyle and Charles the relation between the pressure, density and temperature may be written

$$\frac{p}{\rho} = kT. \quad \dots \quad (1)$$

where p is the pressure (generally expressed in millimetres),

T is the absolute temperature (i.e. the actual centigrade temperature plus 273),

and k is a constant.

Hence, if the density is known for one particular value of the pressure and one particular value of the temperature, its value may be calculated for any other conditions of pressure and temperature. The known standard conditions are as given above, viz.:

$$\rho = 0.00237 \text{ when } p = 760 \text{ and } T = 288.$$

Example. Find the density at a height where the temperature is -12° C. and the pressure is 456 mm.

From the standard ground level conditions we have

$$\frac{760}{0.00237} = k \times 288.$$

Let ρ be the required density. Then, since $T = 273 - 12 = 261$, we have

$$\frac{456}{\rho} = k \times 261.$$

Hence, by division, we get

$$\frac{760}{0.00237} \times \frac{\rho}{456} = \frac{288}{261}$$

$$\begin{aligned} \text{i.e.} \quad \rho &= \frac{0.00237 \times 456 \times 288}{760 \times 261} \\ &= 0.00157. \end{aligned}$$

Relative Density. The ratio of the density at any height to the standard density is called the relative density and is denoted by the Greek letter σ (*sigma*). Hence

$$\rho = \sigma \rho_0 \quad \dots \quad (2)$$

Combination of equations (1) and (2) leads to the equation

$$\sigma = \frac{p \times 288}{760 \times T} \quad \dots \quad (3)$$

Indicated Air Speed. The speed actually recorded by the A.S.I. is called the indicated air speed and is denoted by V_i ; it gives the true speed only if the density is the standard density ρ_0 .

Consider an aeroplane flying at a true speed V at a height where the relative density is σ . Then the pressure difference measured by the pitot is given by $p = \frac{1}{2} \rho V^2 = \frac{1}{2} \sigma \rho_0 V^2$. Also, if V_i is the indicated air speed, $p = \frac{1}{2} \rho_0 V_i^2$; whence

$$V_i^2 = \sigma V^2$$

or

$$V_i = V \sqrt{\sigma} \quad \dots \quad (4)$$

The above equation enables the indicated air speed to be corrected for density to give the true speed.

Example. Find the true air speed corresponding to an indicated air speed of 100 miles per hour at a height at which the density is 0.00132.

Since $\sigma = \frac{0.00132}{0.00237}$, the true speed is given by

$$\begin{aligned} V &= V_i / \sqrt{\sigma} = 100 \times \sqrt{\frac{0.00237}{0.00132}} \\ &= 134 \text{ m.p.h.} \end{aligned}$$

The Altimeter or Aneroid. The instrument which gives the pilot an approximate idea of his height above the ground is called the altimeter and relies for its design on the decrease of atmospheric pressure with height. It is, in effect, an aneroid barometer recording pressures.

It consists of a hollow metal box exhausted of air, and records the atmospheric pressure by movement of the lid. Suitable mechanism and gearing transfers this movement to a pointer on a dial graduated in hundreds and thousands of feet, the zero reading corresponding to the standard pressure of 760 mm., and the graduation being based on the approximate law $h = -62,700 \log p/p_0$, where p is the pressure at height h and p_0 is the standard pressure. This law has been deduced theoretically on the assumption that the temperature remains constant at all heights at 10° C. Actually, the difference in height of two points is proportional also to the mean temperature; therefore, since the temperature decreases as the height increases, it follows that the height indicated by the aneroid is greater than the true height, the error increasing as the height increases. Nevertheless the aneroid gives the pilot a very good idea of his height; even on a very cold day at 20,000 ft. the error is not likely to exceed about 1,500 to 2,000 ft.

The Standard Atmosphere. The reduction of pressure; density and temperature with height has a marked effect on the top speed and rate of climb of an aeroplane, for the horse-power of the engine and the air forces on the aeroplane are both affected by atmospheric changes. The later chapters will show that the

Introduction

performance of an aeroplane (i.e. its speed and climb) falls off as the height increases. Since, however, the atmospheric conditions at any given height may vary from day to day, the performance at that height may vary also, and so the word performance has no precise meaning. In order to obviate this difficulty, a 'standard' atmosphere has been fixed which gives roughly the average atmospheric conditions up to a height of 30,000 ft., and upon which all aeroplane performances are calculated and compared.

This standard atmosphere is defined by Table I given below, densities and pressures being expressed relative to 0.00237 slugs and 760 mm. respectively. The last column of the table gives the aneroid height corresponding to the standard height, and illustrates to some extent the magnitude of the difference between aneroid height and true height arising from the assumption of a constant temperature.

The relative density is shown plotted against standard height in Fig. 140. Although aneroid height is included in the table, it will be found that aneroids vary among themselves and require to be calibrated in accurate aeronautical work.

The use of the table is illustrated by the following example:

Example. At a certain height the following readings were taken:

Aneroid height 15,000 ft.

Temperature -18.5° C.

Indicated air speed 102 m.p.h.

On calibration the aneroid height was found to correspond to 432 mm. Find the standard height and true speed.

From equation (3)

$$\begin{aligned}\sigma &= \frac{p \times 288}{760 \times T} \\ &= \frac{432 \times 288}{760 \times 254.5} \\ &= 0.646.\end{aligned}$$

Hence from the curve of Fig. 140, the standard height is 14,250 ft. Also, from equation (4), the true speed is given by

Introduction

13

$$V = \frac{V_i}{\sqrt{\sigma}}$$

$$= \frac{102}{\sqrt{0.646}}$$

$$= 126.9 \text{ m.p.h.}$$

TABLE I. STANDARD HEIGHT

<i>Standard height (feet).</i>	<i>Relative density σ.</i>	<i>Relative pressure p.</i>	<i>Tempera- ture °C.</i>	<i>Aneroid height (feet).</i>
0	1.000	1.000	15.0	0
1,000	0.971	0.964	13.0	990
2,000	0.943	0.930	11.0	1,980
3,000	0.915	0.896	9.0	2,970
4,000	0.888	0.864	7.0	3,980
5,000	0.862	0.832	5.0	4,990
6,000	0.836	0.801	3.0	6,020
7,000	0.811	0.772	1.0	7,040
8,000	0.786	0.743	- 1.0	8,080
9,000	0.762	0.715	- 3.0	9,130
10,000	0.738	0.688	- 5.0	10,180
11,000	0.715	0.661	- 7.0	11,240
12,000	0.693	0.636	- 9.0	12,300
13,000	0.671	0.611	- 11.0	13,380
14,000	0.650	0.587	- 12.5	14,470
15,000	0.629	0.564	- 14.5	15,550
16,000	0.609	0.542	- 16.5	16,650
17,000	0.589	0.520	- 18.5	17,760
18,000	0.570	0.499	- 20.5	18,870
19,000	0.551	0.479	- 22.5	20,000
20,000	0.533	0.460	- 24.5	21,130
21,000	0.515	0.440	- 26.5	22,260
22,000	0.498	0.422	- 28.5	23,430
23,000	0.481	0.404	- 30.5	24,600
24,000	0.464	0.387	- 32.5	25,760
25,000	0.448	0.371	- 34.5	26,930
26,000	0.432	0.355	- 36.5	28,140
27,000	0.417	0.340	- 38.5	29,340
28,000	0.402	0.325	- 40.5	30,550
29,000	0.387	0.311	- 42.5	31,760
30,000	0.374	0.297	- 44.5	33,000

EXAMPLES

1. Given that the density of the air is 0.00237 slugs at 760 mm. at 15° C., calculate the density at a height at which the pressure is 426 mm. and the temperature is -15.5° C.

2. In the previous example, find the relative density and give the standard height corresponding to this density.

3. At a certain height the aneroid read $5,000$ ft. and the temperature was 2° C. On calibration this aneroid height was found to correspond to a pressure of 630 mm. Calculate the density at this height and give the corresponding standard height.

4. A certain aneroid reads $10,000$ ft. when the pressure is 521 mm. Show that the difference in the corresponding standard heights for temperatures of -2° C. and -12° C. is about 1150 ft.

5. An aeroplane climbs from ground level to $15,000$ ft. (standard) at a constant indicated air speed of 65 miles per hour. Calculate the true air speeds at heights of $3,000$, $6,000$, $9,000$ and $12,000$ ft.

6. Find the standard height at which the true air speed is always 25 per cent. greater than the indicated air speed.

II

THE AEROFOIL

THE wings may be considered the most important part of an aeroplane, for their function is to provide a lifting force which will overcome gravity and so maintain the aeroplane in the air. As an introduction to the behaviour of an aeroplane wing, and as an illustration of the origin and nature of air forces generally, it is convenient to study the air forces acting on a thin flat plate exposed to an air-stream. An aeroplane wing differs from a flat plate principally in its cross-section. Whereas the section of the plate is a thin rectangle, that of the wing is curved or 'cambered' and is known as an **aerofoil section**, the wing itself being termed an **aerofoil**. There are a large number of aerofoil sections in common use; some typical ones are given in Fig. 8. Such shapes are the outcome of careful research carried out to ascertain the most efficient types of aerofoils. The flat plate, however, formed the subject of early experiments, and from these experiments a fundamental law of aerodynamics was established.

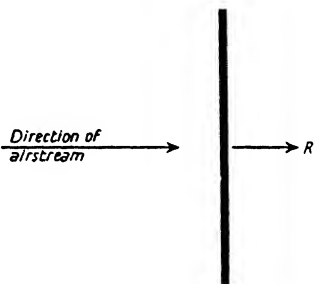


FIG. 4. Plate at right angles to Airstream.

The Flat Plate. Consider, first of all, a thin flat plate held at right angles to an air-stream as shown in Fig. 4. As the air moves past the plate, some of the particles of the air are deflected from their straight line paths, and so there is a change in the momentum of the air. Hence, by Newton's laws of motion, the plate must experience a reaction which is equal and opposite to the rate of change of momentum. This reaction is a resistance and is familiar to everyone as 'head resistance.'

The fundamental law which has been established experi-

mentally in the wind-channel states that, to a good order of accuracy, the reaction R may be taken to vary directly as the density of the air ρ , the area of the plate S and the square of the air speed V ; in other words

$$R = k\rho SV^2 \quad (1)$$

where k is a constant for any particular shape of plate. (See also Chapter III, p. 35).

This equation holds, of course, whatever system of units is used. In this country and in America, ρ is measured in slugs, S in square feet and V in feet per second, so that R is measured in lb. weight.

The value of k can be obtained from experiment, and the use of the above equation then enables the force on any *geometrically similar* plate to be calculated for any speed and density.

Example. Calculate the resistance of a flat plate held at right angles to an air-stream of 60 miles per hour, given that $k = 0.57$, $\rho = 0.00237$ and the area of the plate is 12 sq. ft. What would be the resistance at a height of 15,000 ft.?

The given density is the standard density ρ_0 , and the resistance is given by

$$\begin{aligned} R &= k\rho_0 SV^2 \\ &= 0.57 \times 0.00237 \times 12 \times 88^2, \text{ since } V = 88 \text{ (in f.p.s.)} \\ &= 125.5 \text{ lb.} \end{aligned}$$

At 15,000 ft.,

$$\begin{aligned} R' &= k\rho SV^2 = k\sigma\rho_0 SV^2 \\ &= \sigma \times k\rho_0 SV^2 \\ &= 0.629 \times 125.5 \\ &= 78.9 \text{ lb.} \end{aligned}$$

Now consider the plate to be held at an angle to the air-stream as in Fig. 5. Again the same law holds, but, in this case, the reaction is inclined to the air-stream (although still nearly at right angles to the plate), and the value of k depends, not only on the shape of the plate, but also on the angle between the plate

~~and the air stream.~~ This angle is called the angle of incidence and is denoted by the Greek letter α (*alpha*).

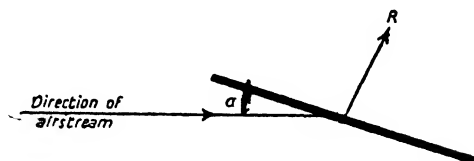


FIG. 5. Plate Inclined to Airstream.

The nature of this force shows at once how a flat plate may be used as a lifting surface. For, if the angle between the vertical and the line of action of R is denoted by the Greek letter γ (*gamma*),

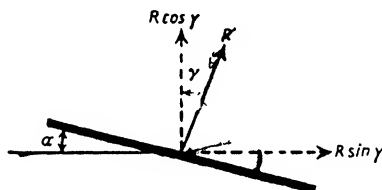


FIG. 6. Lift and Drag Components.

R may be resolved into its two components $R \cos \gamma$ and $R \sin \gamma$ as shown in Fig. 6.

The former is, of course, the lifting force, known as the Lift and denoted by L ; the latter is a resistance or Drag and is denoted by D . Thus

$$L = R \cos \gamma \quad . \quad . \quad . \quad . \quad . \quad (2)$$

$$D = R \sin \gamma \quad . \quad . \quad . \quad . \quad . \quad (3)$$

For all values of α between 0° and 90° the resultant reaction R can be resolved into its components L and D as above. In the case of an aeroplane, D is a resistance which has to be overcome by the thrust of the airscrew, and is the price which has to be paid for the development of the lift.

At 0° incidence the lift clearly vanishes, and the resultant

reaction is a pure resistance again as shown in Fig. 7. The resistance in this case is not so much head resistance as skin friction, and is discussed more fully in the next chapter.



FIG. 7. Plate Parallel to Airstream.

The Aerofoil. A thin flat plate is unsatisfactory as an aeroplane wing for two reasons; firstly, it is necessary from structural considerations to have a certain depth of wing, and, secondly, the plate is far from being the most efficient type of lifting surface. By curving the plate it is possible to increase the lift, while, by increasing its thickness and giving it more of a fish-shaped appearance, it is possible to reduce its drag. This is roughly the manner in which an aerofoil is designed, the amount of curving and thickness being determined by the particular requirements of the aeroplane for which it is intended.

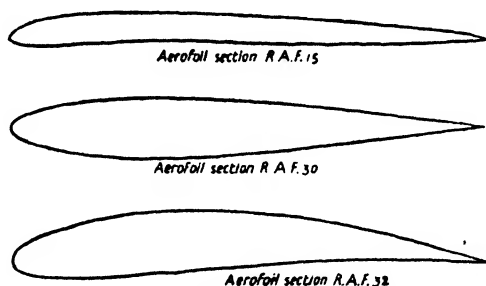


FIG. 8. Typical Aerofoil Sections.

Lift and Drag Coefficients. Equations (2) and (3) may be put into a more convenient form as follows:

$$\begin{aligned} L &= R \cos \gamma = k \rho S V^2 \cos \gamma = k \cos \gamma \cdot \rho S V^2, \\ D &= R \sin \gamma = k \rho S V^2 \sin \gamma = k \sin \gamma \cdot \rho S V^2. \end{aligned}$$

Now it is found from experiment that γ , like k , varies with incidence. Hence $k \cos \gamma$ and $k \sin \gamma$ are simply numbers de-

pending upon α , and, if they are denoted by k_L and k_D respectively, the equations for lift and drag become

$$L = k_L \rho S V^2 \quad (4)$$

and

$$D = k_D \rho S V^2 \quad (5)$$

k_L and k_D are called absolute or non-dimensional coefficients, k_L being termed the lift coefficient and k_D the drag coefficient. They are called coefficients as they are numerical values only and have no dimensions in mass, length or time like forces and velocities. (In many countries, including Germany and America, it is customary to use lift and drag coefficients C_L and C_D , defined by the equations

$$L = C_L \cdot \frac{1}{2} \rho S V^2 \quad (6)$$

and

$$D = C_D \cdot \frac{1}{2} \rho S V^2 \quad (7)$$

Thus $C_L = 2k_L$ and $C_D = 2k_D$, and it is a simple matter to change from one set of coefficients to another.)

In wind channel work the resultant force R on an aerofoil is not measured as a whole, but its components L and D are measured separately. The values of the lift and drag in lb. are then reduced to coefficient form by means of the equations

$$k_L = \frac{L}{\rho S V^2} \text{ and } k_D = \frac{D}{\rho S V^2}, \text{ and the values of } k_L \text{ and } k_D \text{ so}$$

obtained for different angles of incidence then express the characteristics of the aerofoil non-dimensionally, without any reference to the particular size of the aerofoil or to the particular air speed used in the experiments. If the lift and drag in lb. of any geometrically similar wing are required for any given size, speed and density, they can be obtained at once by multiplying the coefficients by $\rho S V^2$.

Effect of Incidence. With regard to the variation of k_L and k_D with incidence, all aerofoils exhibit the same general characteristics, and for the purposes of illustration it is sufficient to consider one aerofoil only. The characteristics of an aerofoil depend upon its aerofoil section and its plan form. It is usual to define the plan form by the ratio of the length of the aerofoil from wing tip to wing tip (known as the span of the aerofoil and

denoted by $2s$) to the distance between the front or leading edge of the aerofoil and the rear or trailing edge (known as the **chord** of the aerofoil section and denoted by c),¹ this ratio being termed the **aspect ratio**.

The aerofoil chosen for illustration is a rectangular aerofoil of aspect ratio (A.R.) 6, having for its aerofoil section No. 1 of Fig. 8, a section known as R.A.F. 15 and one which has been

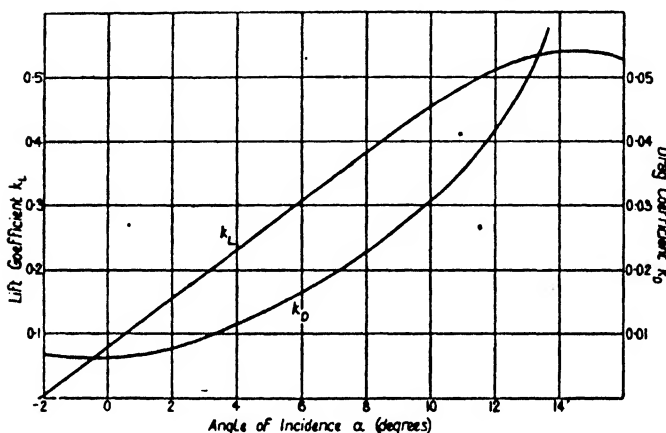


FIG. 9. Aerofoil Characteristics (R.A.F. 15, Aspect Ratio 6).

used extensively in this country. The characteristics are shown graphically in Fig. 9, where k_L and k_D are plotted against α . The actual experimental points are not given, but the curves represent the best mean curves drawn through the points.

The important features of the diagram are as follows:

(1) The aerofoil still gives a small lift at 0° incidence, the lift not vanishing until an angle of -2.1° is reached.

The angle at which the lift of an aerofoil vanishes is called the **angle of no-lift**, and varies from 0° for a symmetrical section like No. 2 of Fig. 8 to as high a figure as -7.3° for a thick, highly

¹ The length of the chord is measured along the straight line tangential to the under-surface at front and rear, except in the case of symmetrical sections, or other sections with convex upper- and under-surfaces, when it is measured along the line joining the leading and trailing edges.

cambered section like No. 3. It is obvious, of course, that a symmetrical section must have a no-lift angle of 0° .

(2) As α increases, k_L increases up to a certain point and then decreases. Up to an angle of about 8° the curve is practically straight, but beyond this incidence k_L begins to lose its steady rate of increase, and the curve bends over until, at an angle of 14° , k_L reaches its maximum value of 0.54.

The angle at which k_L reaches its maximum value is called the critical angle of the aerofoil, and the corresponding value of k_L is written $k_{L\max}$. The value of $k_{L\max}$ varies considerably with the aerofoil section; thus for aerofoil No. 3 its value is as high as 0.655.

(3) Over a considerable portion of the range of incidence between the no-lift and critical angles k_L and α are connected by a linear law, which for this particular aerofoil is

$$k_L = 0.038(\alpha + 2.1),$$

and which holds up to an angle of incidence of about 8° .

The slope of this line is almost independent of the aerofoil section, but varies with the aspect ratio.

(4) The drag coefficient has a minimum value at an angle of incidence of about -0.5° . On either side of this angle it rises fairly rapidly. The magnitude and position of the minimum drag both vary from one aerofoil to another, although the drag curve is always roughly parabolic in shape.

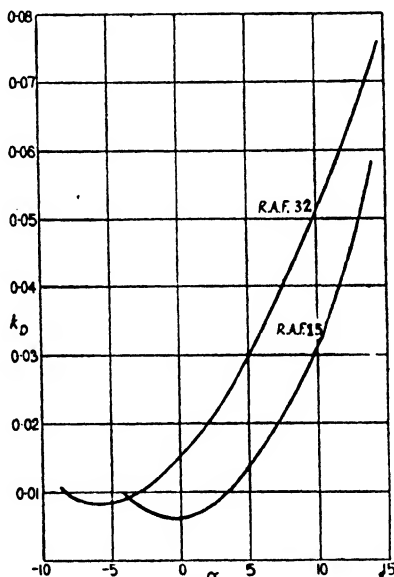


FIG. 10. Wing Drag Curves.

The Aerofoil

Discussion of the variation is left till later, but Fig. 10, which gives the drag curves for two aerofoils of the same aspect ratio, shows how the drag may vary with wings of different section.

✓ **The Weight-Lift Equation.** Since the weight of an aeroplane is balanced by the lift on the wings, the weight-lift equation gives

$$W = k_L \rho S V^2 \quad \dots \quad (9)$$

where W is the total weight of the aeroplane in lb.

Although this equation is sufficiently accurate for most practical purposes, it is not strictly correct.

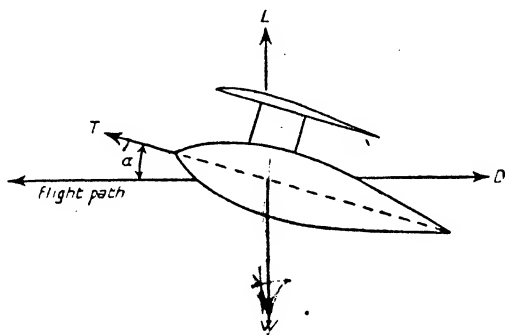


FIG. 11. Forces on Aeroplane in Level Flight.

For consider an aeroplane flying horizontally at a constant speed, and for simplicity suppose that the aeroplane has one wing only and that the chord of the wing is parallel to the centre line of the aeroplane. In order that the lift may be large enough to support the aeroplane, the wing and therefore the body will, in general, be inclined at a definite angle of incidence to the flight path as shown in Fig. 11. The aeroplane is therefore moving crabwise, that is to say, it is not moving in the direction of its centre line.

The forces acting on the aeroplane are as shown, T being the thrust of the airscrew and D being the total drag, i.e. the wing drag plus the drag of the rest of the aeroplane. There is also a

small lifting force on the tail plane, but this is small and may be neglected in comparison with the main wing lift L . Its neglect, however, is another small source of inaccuracy.

The forces may now be resolved in a direction at right angles to the flight path, giving

$$W = L + T \sin \alpha.$$

But in normal flight α is small and never exceeds its critical angle; $\sin \alpha$ is therefore small and, in consequence, $T \sin \alpha$ may generally be neglected in comparison with L , so that the equation reduces to the simple form (9).

In the case of an aeroplane climbing, or gliding at moderate angles to the horizontal, the problem is a little more complex, but for all normal flight conditions equation (9) is sufficiently accurate.

By means of this equation the angle of incidence and the wing drag of an aeroplane can be calculated for any steady speed of flight, given the weight W , the wing area S , the density ρ and a diagram of wing characteristics like Fig. 9. For the equation may be written

$$k_L = \frac{W}{\rho S V^2} \quad \dots \quad (10)$$

so that for any given speed k_L may be calculated at once. The corresponding angle of incidence and drag coefficient k_D can then be read from the diagram of wing characteristics, the actual wing drag in lb. next being obtained by multiplying k_D by $\rho S V^2$.

Example. Find the angles of incidence and the corresponding values of the wing drag at speeds of 70, 80, 90 and 100 miles per hour for an aeroplane weighing 3,400 lb. and having 400 sq. ft. of wing area, given that the density is the standard density and the wing characteristic curves are as in Fig. 9.

We tabulate as under:

Speed. m.p.h.	V . f.p.s.	k_L . ($= W / \rho S V^2$)	α . (from diagram)	k_D .	Wing Drag. lb.
70	102.7	0.340	6.85	0.0190	190
80	117.3	0.261	4.8	0.0131	171
90	132.0	0.206	3.3	0.0099	164
100	146.7	0.167	2.3	0.0082	167

The Aerofoil

✓ **Stalling Speed.** From the above example it will be seen that the incidence and the lift coefficient both increase as the speed decreases. Every aerofoil, however, has a maximum value of the lift coefficient; hence, when the wing reaches the critical angle at which k_L has its maximum value, the corresponding speed is the minimum speed of flight.

This is known as the stalling speed and can be calculated as follows:

From equation (9),

$$V^2 = \frac{W}{k_L \rho S}$$

Hence, if the stalling speed in feet per second is denoted by V_s ,

$$V_s = \sqrt{\frac{W}{k_{L \max} \rho S}} \quad \dots \dots (11)$$

For the aeroplane in the previous example the stalling speed is given by

$$\begin{aligned} V_s &= \sqrt{\frac{3400}{0.54 \times 0.00237 \times 400}} \\ &= 81.5 \text{ f.p.s.} \\ &\text{i.e. } 55.6 \text{ m.p.h.} \end{aligned}$$

Consider now what happens when the speed of an aeroplane is gradually reduced. As the speed decreases the incidence gradually increases until the critical angle is reached and the aeroplane is flying at its minimum speed. If this angle is exceeded, the lift coefficient begins to decrease, and the wings cannot provide a lifting force sufficient to support the aeroplane; in consequence of this the nose of the aeroplane falls, and the aeroplane commences to dive earthwards in an automatic endeavour to regain flying speed. This motion is referred to as the stall, and the critical angle is sometimes called the stalling angle. When once an aeroplane stalls, it is out of the control of the pilot until it has recovered flying speed by diving and by consequent loss of height.

Every aeroplane has a stalling speed, and it is the aim of aeroplane design to keep the stalling speed as low as possible for the following reasons:

(1) The speed at which an aeroplane approaches the ground in order to land is limited by the stalling speed, and it is obvious that, for a landing to be made in a confined space, or at short notice, the aeroplane must be capable of being manœuvred at a slow speed.

(2) The perfect landing is one in which the aeroplane is just stalled as it touches the ground, for the shock of landing on the aeroplane structure is a minimum when the landing speed is a minimum.

Equation (11) shows that the factors governing the stalling speed are the ratio $\frac{W}{S}$ and the maximum lift coefficient $k_{L\max}$, a low stalling speed being obtainable with a low value of the former and/or a high value of the latter.

Wing Loading. The ratio $\frac{W}{S}$ is called the wing loading and is measured, of course, in lb. per square foot. On modern aeroplanes the stalling speed varies from about 40 to 60 miles per hour, corresponding to loadings of about 5 to 11 with a value for $k_{L\max}$ of 0.6, which is an average figure for the more common types of aerofoil section used in practice. The choice of loading is a compromise between the demands of a low stalling speed, the necessary performance of the aeroplane with regard to speed and climb, and practical design considerations. In purely racing aeroplanes the wing area is kept so small that it is not unusual to find a wing loading as high as 20.

The Maximum Lift Coefficient. The maximum lift coefficient varies from one aerofoil section to another, the extreme range probably being about 0.4 to 0.8, unless slotted wings are used (see p. 40). High values are desirable, but here again the choice of aerofoil section is a compromise, since a 'high-lift' wing may in a given case possess other features which are undesirable. For instance, its drag coefficient may be too large,

or its minimum drag coefficient may occur at the wrong incidence, for optimum performance.

The Lift-Drag Ratio. The lift-drag ratio is $\frac{L}{D}$ (or $\frac{k_L}{k_D}$) and may be regarded as a measure of the efficiency of a wing. In comparing aerofoils on a lift-drag basis, it is essential to compare the $\frac{L}{D}$ ratios *at the same values of k_L* , and not at the same values of α . The reason for this is that, with different aerofoils,

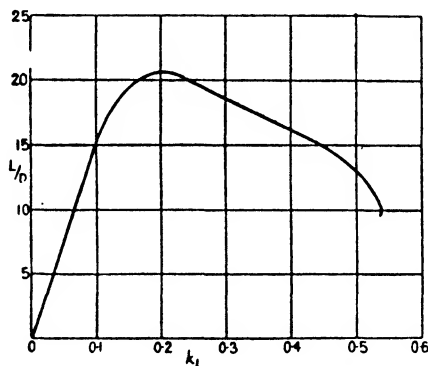


FIG. 12. Lift/ Drag Ratio (R.A.F. 15, Aspect Ratio 6).

a given incidence may correspond to different values of k_L and therefore, for any given aeroplane, to different speeds; and it is at the same speeds that a comparison is required. (The same is true for a k_D comparison. For this reason the curves of Fig. 10 would be misleading if they were used to compare the two aerofoils. If the drag were plotted against a k_L base it would be found that the difference between the two aerofoils is not nearly so pronounced as would appear from Fig. 10).

From the data of Fig. 9 the values of $\frac{k_L}{k_D}$ have been calculated for different values of k_L , and the results are shown plotted in Fig. 12.

On reference to the example on p. 23 it will now be seen that

if, in any particular case, the wing drag only is required (and not the incidence), it is simpler to use the $\frac{L}{D}$ curve than the k_D curve.

For, after k_L is obtained by calculation, $\frac{L}{D}$ can be read direct from this new curve, and D then obtained by means of the equation $D = \frac{W}{\frac{L}{D}}$, since $W = L$.

Indicated Air Speed. Equation (9) may be written in the form

$$\begin{aligned} k_L &= \frac{W}{\rho S V^2} \\ &= \frac{W}{\sigma \rho_0 S V^2} \\ &= \frac{W}{\rho_0 S (\sigma^{\frac{1}{2}} V)^2}, \end{aligned}$$

$$\text{i.e.} \quad k_L = \frac{W}{\rho_0 S V_i^2} \quad . \quad . \quad . \quad . \quad . \quad (12)$$

Hence, if the incidence is fixed and therefore k_L is fixed, V_i is fixed. In other words, *constant indicated air speed means constant incidence*, whatever the height or density may be. Since, however, $V = V_i / \sqrt{\sigma}$, it follows that for a given incidence the true speed rises as the density decreases. As a particular case it may be noted that the indicated stalling speed is constant, but that the true stalling speed increases as the height increases.

The Moment Coefficient and Centre of Pressure. In dealing with questions of the stability and equilibrium of an aeroplane, it is important to know not only the magnitude and direction of the resultant force on a wing, but also the point on the chord through which the line of action of the force passes. This point is called the **Centre of Pressure** or C.P.; it cannot be measured directly, but is found from a wind channel measurement of the moment of the resultant force about a given point.

The Aerofoil

In this country it is usual to measure the moment of the force about the leading edge, and the relation between the moment so obtained and the position of the C.P. is explained below.

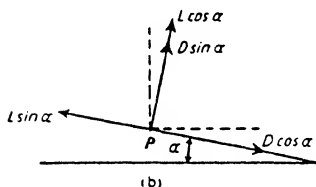
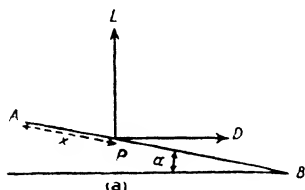


FIG. 13.

Suppose *AB* in Fig. 13 represents an aerofoil section of chord *c* and inclined at an angle α to the air-stream. Let the C.P. be at *P*, and let its distance from the leading edge be *x*.

The resultant force on the aerofoil is equivalent to the forces *L* and *D*, acting at *P* as shown in Fig. 13 (*a*). These may be resolved into their components at right angles to and along the chord. Thus *L* is equivalent to $L \cos \alpha$ at right angles to the chord and $L \sin \alpha$ along it. So *D* is equivalent to $D \sin \alpha$ and $D \cos \alpha$ (Fig. 13 (*b*)).

The forces $L \sin \alpha$ and $D \cos \alpha$ have no moment about the leading edge. Hence the moment *M* is given by

$$\begin{aligned} M &= x(L \cos \alpha + D \sin \alpha) \\ &= x(k_L \cos \alpha + k_D \sin \alpha) \rho S V^2. \end{aligned}$$

Therefore
$$x = \frac{M}{(k_L \cos \alpha + k_D \sin \alpha) \rho S V^2},$$

an equation giving *x* if *M* is known.

The values of *M* and *x*, however, depend upon the conditions of the experiment, e.g. the size of the model and the air speed, and if, as in the case of the lift and drag, characteristics are required which are independent of these quantities, it is necessary to express *M* and *x* in non-dimensional or coefficient form. This can be accomplished by defining the position of the C.P. by the ratio of its distance from the leading edge to the total chord length.

Thus, the above equation may be written (on dividing each side by c)

$$\frac{x}{c} = \frac{1}{c} \frac{M}{(k_L \cos \alpha + k_D \sin \alpha) \rho S V^2},$$

or
$$M = \frac{x}{c} (k_L \cos \alpha + k_D \sin \alpha) c \rho S V^2,$$

and, if k_m is written for the non-dimensional quantity $\frac{x}{c} (k_L \cos \alpha + k_D \sin \alpha)$, this becomes

$$M = k_m c \rho S V^2 \quad \dots \dots \dots (13)$$

Also, if $k_{C.P.}$ (called the centre of pressure coefficient) is written for $\frac{x}{c}$, then

$$\begin{aligned} k_m &= \frac{x}{c} (k_L \cos \alpha + k_D \sin \alpha) \\ &= k_{C.P.} (k_L \cos \alpha + k_D \sin \alpha), \end{aligned}$$

or
$$k_{C.P.} = \frac{k_m}{k_L \cos \alpha + k_D \sin \alpha} \quad \dots \dots \dots (14)$$

Generally $k_D \sin \alpha$ is so small compared with $k_L \cos \alpha$ that it may be neglected. Also, since α is small, $k_L \cos \alpha$ may be replaced by k_L . An approximate formula for the C.P. is therefore

$$k_{C.P.} = \frac{k_m}{k_L} \quad \dots \dots \dots (15)$$

Hence, from the measured value of the moment M , k_m can be found by means of equation (13), and then $k_{C.P.}$ by means of either equation (14) or equation (15).

The variation of k_m and $k_{C.P.}$ with k_L is illustrated in Fig. 14, which gives the characteristics of an aerofoil of R.A.F. 15 section.

It will be noticed that the values of k_m are negative. This is because the moment about the leading edge is an anti-clockwise moment and is considered by convention to be a negative moment. Since k_m is negative, equations (14) and (15) give

negative values for $k_{C.P.}$, but in this case there is no point in retaining the negative sign, and $k_{C.P.}$ is plotted as a positive quantity.

The important features of the diagram are as follows:

(1) The centre of pressure is not fixed, but moves forward as the angle of incidence increases and reaches its most forward position at the critical angle. When the critical angle is passed,

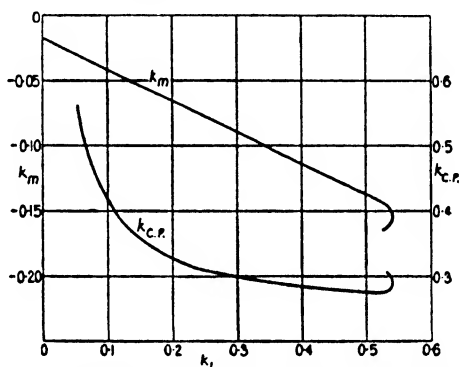


FIG. 14. Moment and Centre of Pressure Coefficients (Aerofoil R.A.F. 15).

the C.P. moves rapidly backwards; this movement explains the automatic nose dive which always follows the stall.

(2) When the lift vanishes and the resultant force, i.e. the drag, is very small, there is still a considerable moment. This is discussed more fully in Chapter III.

(3) Up to the critical angle the slope of the k_m curve is constant ($= -0.24$), and k_m and k_L are connected by the linear law

$$k_m = -0.24k_L - 0.0175$$

It is found that for all aerofoils the k_m curve is practically a straight line, so that, if the value of k_m at $k_L = 0$ is represented by k_{m_0} , then

$$k_m = -bk_L + k_{m_0},$$

where $-b$ is the slope of the line.

Experiment shows that the value of b does not vary much

from one aerofoil to another, and is always in the neighbourhood of 0.25. This is in agreement with the aerofoil theory outlined in the subsequent chapters.

Example 1. For a certain aerofoil at 4° incidence $k_L = 0.27$, $k_D = 0.0134$ and $k_m = -0.0925$. Determine the position of the C.P. using the approximate equation, and show that no appreciable error is introduced by the use of this equation instead of the exact equation.

We have

$$\begin{aligned} k_{C.P.} &= \frac{k_m}{k_L} \\ &= \frac{0.0925}{0.27}, \text{ neglecting the negative sign,} \\ &= 0.343. \end{aligned}$$

Now the exact equation is

$$k_{C.P.} = \frac{k_m}{k_L \cos \alpha + k_D \sin \alpha},$$

$$\begin{aligned} \text{and } k_L \cos \alpha + k_D \sin \alpha &= (0.27 \times 0.9976) + (0.0134 \times 0.0698) \\ &= 0.2693 + 0.0009 \\ &= 0.2702. \end{aligned}$$

The difference between $k_L \cos \alpha + k_D \sin \alpha$ and k_L is negligible, and so the approximate equation is sufficiently accurate.

Example 2. Determine the position of the centre of pressure for an aeroplane flying at 140 miles per hour near the ground, given that the wing loading is 10.5, $k_{m_0} = -0.028$ and the slope of the moment curve is -0.245 .

$$V = 205.3; \text{ hence}$$

$$\begin{aligned} k_L &= \frac{W}{\rho S V^2} \\ &= \frac{10.5}{0.00237 \times (205.3)^2} \\ &= 0.105 \end{aligned}$$

Now

$$k_m = -0.245k_L - 0.028.$$

$$\begin{aligned}\therefore k_{C.P.} &= \frac{k_m}{k_L} \\ &= +0.245 + \frac{0.028}{0.105} \\ &= 0.245 + 0.267 \\ &= 0.512.\end{aligned}$$

EXAMPLES

[All examples refer to standard density $\rho = 0.00237$.]

1. A wind screen is in the form of a flat plate. Find its drag at 100 ft. per second, given that $k = 0.62$ and its area is 0.82 sq. ft.

2. Find the lift coefficient corresponding to a speed of 120 miles per hour for an aeroplane with a wing loading of 9.25.

3. Assuming that, up to an angle of incidence of 7.5° , the lift coefficient of an aeroplane wing may be written in the form

$$k_L = 0.036(\alpha + 2.5),$$

show that, with a wing loading of 9, this equation may be used to find the lift coefficients corresponding to all speeds not less than 70 miles per hour.

4. Calculate the stalling speed of an aeroplane, given that $W = 4,500$, $S = 520$ and $k_{L\max} = 0.56$.

5. Find the increase in the stalling speed of the above aeroplane when it is carrying an overload of 450 lb.

6. An aeroplane with 920 sq. ft. of wing area is estimated to weigh 8,250 lb. with full load. Find the value of the maximum lift coefficient in order that the stalling speed may be 52 miles per hour.

7. The landing or stalling speed of an aeroplane at zero standard height is 55 miles per hour. What would be its landing speed on an aerodrome at a standard height of 5,000 ft.?

8. The lift and drag characteristics of the wings of an aeroplane are given in the following table:

α	-2	0	2	4	6	8	10
k_L	0.003	0.068	0.131	0.197	0.260	0.324	0.387
k_D	0.0069	0.0063	0.0078	0.0111	0.0161	0.0230	0.0306
			12	14			
			0.448	0.500			
			0.0396	0.0518			

Plot k_L and k_D against α , and determine the incidence and wing drag coefficient at speeds of 60 and 80 miles per hour. Find also the actual wing drag in lb.

The aeroplane weighs 1800 lb. and has a wing area of 325 sq. ft.

9. For the aeroplane in the previous example, find the wing drag at a climbing speed of 55 miles per hour, and determine the percentage increase of drag at this speed when the aeroplane is overloaded and weighs 1965 lb.

10. For an aeroplane weighing 7,500 lb. and having a wing surface of 840 sq. ft., the lift and drag characteristics of the wings are given in the following table:

k_L	0.003	0.072	0.140	0.209	0.279	0.348	0.417
k_D	0.0080	0.0078	0.0086	0.0110	0.0151	0.0205	0.0276
		0.482	0.549	0.604	0.640		
		0.0356	0.0453	0.0546	0.0752		

Construct the curve of $\frac{L}{D}$ against k_L , and determine the lift coefficients and speeds corresponding to a $\frac{L}{D}$ ratio of 18.

11. From the $\frac{L}{D}$ curve of the previous example find the wing drag at speeds of 70 and 125 miles per hour.

12. Use the equation $k_{C.P.} = \frac{k_m}{k_L}$ to construct a C.P. curve from the following wind channel data:

α	-2	0	2	4	6	8
k_L	0.034	0.104	0.172	0.243	0.314	0.381
k_m	-0.0293	-0.0429	-0.0627	-0.0788	-0.0960	-0.1119
	10	12	14	16	18	
	0.448	0.508	0.560	0.599	0.602	
	-0.1278	-0.1424	-0.1540	-0.1638	-0.1800	

Hence determine the *C.P.* position at the stall and also its position at a speed of 130 miles per hour for an aeroplane with a wing loading of 8.5.

13. Assuming that the moment coefficient of an aerofoil can be written in the form

$$k_m = -0.25k_L + k_{m_0},$$

find the value of k_{m_0} which gives a *C.P.* position of 0.46 at a speed of 120 miles per hour for an aeroplane weighing 9,250 lb. and having a wing area of 1050 sq. ft.

III ELEMENTS OF AIRFLOW

Introduction. It has already been pointed out that, when an air-stream moves past a body, the momentum of the air is changed owing to the change in the speed and direction of the particles of the air, and that in consequence the body experiences a reaction which is equal to the rate of change of momentum. Early investigators attempted to calculate the reaction by direct application of this principle, but it was found necessary to make many simplifying assumptions with regard to the manner in which the air particles moved.

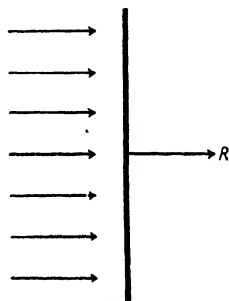


FIG. 15.

A simple illustration of what may be called the Newtonian method is afforded by the case of a flat plate held at right angles to the air-stream, on the assumption that the air is composed of minute inelastic particles which, after impinging on the plate, slide off down its surface. It is further assumed that all the particles immediately in front of the plate come into contact with it, and suffer no change in velocity, either in magnitude or direction, until impact (Fig. 15).

Let V be the air speed, ρ the air density and S the area of the plate.

Then the volume of air striking the plate per second is SV and the mass of this volume is ρSV .

Hence the pressure on the plate = the momentum destroyed per second

$$\begin{aligned} &= \rho SV \times V \\ &= \rho SV^2 \end{aligned}$$

According to experiment, however, the actual pressure or resistance is $k\rho SV^2$, where k depends upon the aspect ratio of the plate but is always less than 1. Thus, although the method

reveals the ρSV^2 law, it fails to give the true magnitude of the resistance.

If the plate is inclined at an angle α to the air-stream and the same assumptions made as before, it may be shown that the plate experiences a force $\rho SV^2 \sin \alpha$ at right angles to itself. This force can be resolved into its lift and drag components at right angles to and along the direction of the air-stream respectively, but again the calculated values do not agree with the measured values.

The failure of the method must be attributed, of course, to the manner in which the air is assumed to move past the plate. Actually the air-stream is disturbed for some distance in front of the plate and closes in again behind it, but the motion is so complex that no simple application of the momentum theory is possible.

The following paragraphs describe the actual manner in which the air particles move past a body, and treat the motion in some detail in order to provide a sound explanation of the nature and origin of air forces.

Airflow. Air is a fluid and 'flows' in a general way like any other fluid. When a fluid flows past a body, or when a body moves through a fluid, the resulting flow may be one of two kinds, *smooth* or *turbulent*. For instance, if a flat plate is dragged broadside on through water, large eddies or whirlpools can be observed in the wake of the plate, and the flow is distinctly turbulent; whereas, if a boat-shaped body is dragged along, the water is seen to flow smoothly past the sides of the body with but little eddying motion in the wake. That air behaves in a similar manner can be proved in a wind channel by admitting smoke into the air-stream; the wisps of smoke reveal the nature of the flow and show if it is smooth or turbulent. It is found that, as in the case of water, the plate creates a turbulent flow while the boat-shaped body allows of a smooth flow.

Streamlines. If the airflow is steady (i.e. does not vary from one moment to another) the type of flow can be illustrated by a simple diagram. For, if the air is supposed to consist of minute

particles, lines can be drawn to represent the paths followed by the particles in their motion past the body. Such lines are called streamlines and give the direction of flow at every point for all time, since each line represents the path of a succession of particles. A typical flow pattern diagram is given in Fig. 16, which illustrates the smooth flow past a symmetrical aerofoil

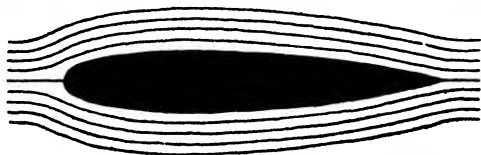


FIG. 16. Smooth Flow over Symmetrical Aerofoil Section.

section at 0° incidence. A flow pattern illustrating turbulent flow is given in Fig. 17.

Viscosity and Skin Friction. Whether the flow is smooth or turbulent, there is always one type of air force experienced by a body, and this is due to viscosity. Viscosity is a property possessed by all fluids and is somewhat analogous to friction in solids. When air is flowing past a body, frictional forces arise between the surface of the body and the air, so that the air is retarded while the body experiences a surface resistance. This resistance is called *skin friction* and always forms a part of the total resistance.

In order to appreciate the effect of viscosity more fully, consider the thin flat plate moving edgewise through the air as in Fig. 7. As the air flows over the plate, the particles of the air adjacent to the surface of the plate are trapped, as it were, by the roughness of the surface and brought to rest. Alternatively the air particles may be regarded as being arrested owing to their intermingling with the surface particles of the plate. Now suppose that the air consists of a succession of layers of particles. Then since the first layer in contact with the plate is stationary, the second layer is in motion over the first, and frictional or viscous forces arise between the two layers, the effect of these forces being to retard slightly the second layer. The third layer

is then moving a little faster than the second, and the relative motion results in viscous forces arising to retard the third layer. This process continues throughout the stream, the retardation clearly diminishing as the distance from the plate increases. Actually the viscosity effects are so small that they are felt only in a very narrow region near the surface of the plate, the thickness of this region probably being of the order of a few thousandth parts of the chord, but in this region the varying velocity causes the streamlines to crumple up and form eddies. (In the case of water an analogy is provided by the breakers on the sea-shore). The surface of the plate is therefore covered by a thin sheet of eddies or vortices, and the energy carried away by these vortices represents the work done in forcing the plate through the air against its 'skin friction.'

Form Drag. In addition to skin friction there is another type of resistance experienced by a body. Unlike skin friction, however, this depends not so much on the extent of the surface as on the shape of the body. It is due essentially to turbulence and the formation of vortex motion in the wake, and can be well illustrated by a flat plate held at right angles to the air-stream, for experiment shows that the flow is very turbulent. The streamlines are as shown in Fig. 17, and it will be seen that the

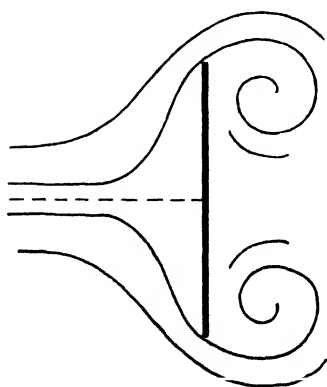


FIG. 17.

Turbulent Flow over Flat Plate

retardation of the air particles near the surface of the plate causes the streamlines close to the edges of the plate to bend inwards and form large vortices. These are continually carrying away energy, and so the plate experiences a resistance. This resistance is called *form drag*, and, since it is not a frictional or rubbing force acting tangentially to the surface, like skin friction, it must appear as a pressure force due to unequal air pressures at the front and rear of the plate.

Streamline Bodies. Since the form drag is due to the vortices shed from the sides of a body and the formation of a region of turbulence, it is clear that low drag can be obtained only by reducing this region to a minimum. Suppose that the plate in Fig. 17 has a tail or *fairing* added as in Fig. 18 (a). The fairing gives the streamlines a chance to resist the tendency to crumple up, and the turbulence is reduced. If, in addition, a nose is added as in Fig. 18 (b), a further improvement is noticeable, for the nose allows a better entry for the streamlines and their deflexion is accomplished more gradually. The net effect of this fairing or 'streamlining' of the plate is to reduce the form drag to such an extent that the total drag is considerably reduced, although the skin friction is increased owing to the increased amount of surface.

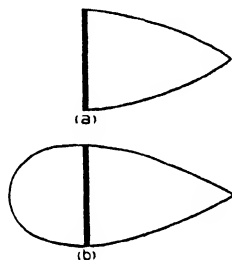


FIG. 18.
Streamlining of Body

A body in which the form drag has been practically eliminated is called a streamline body, and the smooth flow associated with it is generally called streamline flow.

Airflow over an Aerofoil. An aerofoil is a good streamline body at small angles of incidence, but as the incidence increases it loses a little of its streamline properties owing to the development of form drag.

The type of flow occurring over an aerofoil section for different angles of incidence is shown in Fig. 19.

At the lower angles of incidence the flow is fairly smooth, and the eddying motion is confined to a very small region on the upper surface in the neighbourhood of the tail. As the angle increases the eddying motion increases and spreads further along the surface, until at 16° incidence violent eddying extends over the whole upper surface from the nose to the tail. Beyond this angle the eddying is even more violent, and the wake is a region of excessive turbulence. From these diagrams it is clear that at low angles of incidence the form drag must be nearly

negligible, but that it increases as the angle increases. (The reader is warned against concluding that the increase of form drag with incidence accounts for the total increase of the aerofoil drag. It is shown in the next chapter that a lifting surface is subject to another type of drag, and it is the increase of this drag which, up to the critical angle, is responsible for the greater part of the total increase).

More important still is the connexion between the turbulence and the lift. The turbulence is not very great until an angle of incidence of about 12° is reached, and it is in the neighbourhood of this incidence that the lift coefficient is beginning to lose its steady rate of increase, until, at an angle of about 16° , the critical angle is reached and the lift breaks down altogether. From this it would appear that the turbulence not only gives rise to increased form drag but also accounts for the break-down of lift.

The Slotted Wing. In this connexion reference may be made to the slotted wing, which is an invention made to preserve the streamline flow and so delay the approach of the critical angle. In a slotted wing the leading edge is movable with regard to the main aerofoil, and forms a small auxiliary aerofoil whose action is as follows:

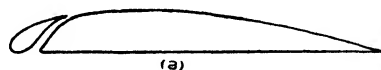
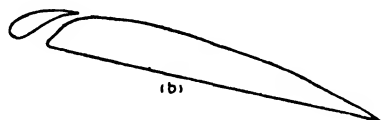


FIG. 20.
The Slotted Wing.



Suppose that the slot is open at an angle at which turbulence would normally have set in over the upper surface. Then Fig. 20 (b) shows that the auxiliary aerofoil is still at a small angle of incidence, and therefore has a smooth flow over it. This smooth flow sweeps down over the upper surface of the main aerofoil and tends to resist the turbulence. In this way a



0° INCIDENCE

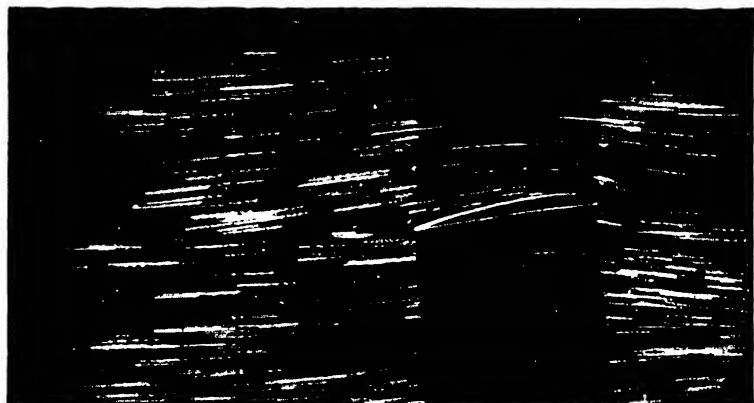
FIG. 19a



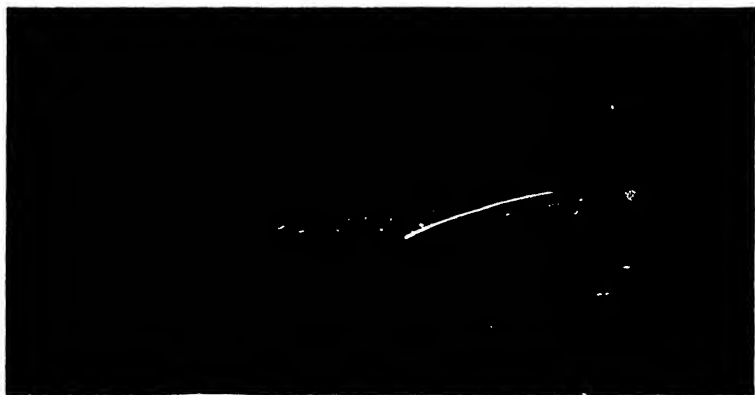
4° INCIDENCE

FIG. 19b

Royal Air Force official.—Crown copyright reserved



8 INCIDENCE



12 INCIDENCE

FIG. 19d

Royal Air Force official. Crown copyright reserved



16° INCIDENCE

FIG. 19e



20° INCIDENCE

FIG. 19f

Royal Air Force official. - Crown copyright reserved

smooth or streamline flow is preserved up to a greater angle of incidence, with a consequent increase in the maximum lift coefficient (see Fig. 21).

In practice the opening of the slot may be either automatic or mechanically controlled by the pilot, and in the automatic type the slot opens progressively as the incidence increases. This is

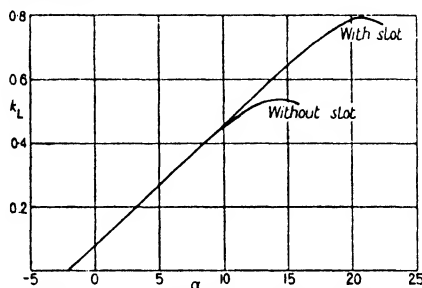


FIG. 21. Lift Curve of Slotted Aerofoil.



FIG. 22. Resultant Force on Auxiliary Aerofoil.

accomplished by so designing the mechanism connecting the main and auxiliary aerofoils that the slot is capable of being moved by the action of the air forces on the auxiliary aerofoil itself, the amount of movement being made to depend upon the position of the centre of pressure of the auxiliary aerofoil. It can easily be seen how the resultant force can be used to open the slot, for Fig. 22 shows that the flow over the auxiliary aerofoil is deflected from its free direction by the presence of the slot, so that the resultant force is inclined as shown and therefore has a forward component.

Pressure Distribution over an Aerofoil. Reference has been made on p. 38 to the difference in pressure at the front and rear of a flat plate held at right angles to the air-stream. Experi-

Elements of Airflow

ments have also been carried out, both on models and on actual aeroplanes in flight, to determine how the air pressure varies over the surface of an aerofoil. It is found that on the under surface of the aerofoil the pressure is everywhere positive, that is to say, the pressure is greater than the atmospheric pressure of the undisturbed stream. On the upper surface, however, the

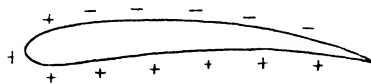


FIG. 23. Pressure Distribution.

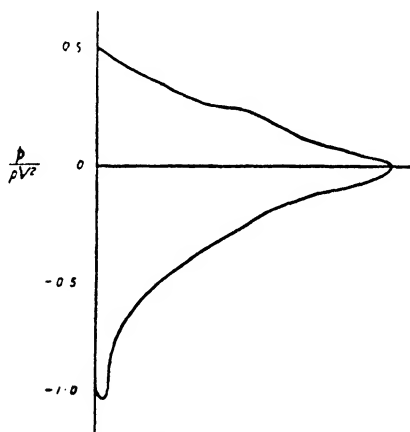


FIG. 24. Pressure Distribution Diagram.

pressure is negative except just on the nose of the aerofoil (Fig. 23). The pressure at any point of the surface acts, of course, at right angles to the surface, the vertical component being the element of lift and the horizontal component the element of drag (excluding skin friction which acts tangentially to the surface and is not a pressure force). Thus it will be seen that the lift is due to a suction force on the upper surface and a direct positive pressure force on the lower surface. Experiment shows further that the suction force contributes more to the lift than the pressure force. A typical pressure distribution diagram is given in Fig. 24; the horizontal scale represents the distance

from the nose measured as a fraction of the chord, and the vertical scale represents the pressure, above or below atmospheric pressure, in lb. per square foot divided by ρV^2 . The positive pressure of the under surface is represented by the area of the curve above the horizontal, and the negative pressure or suction of the upper surface by the area below.

Figs. 23 and 24 show that the maximum positive pressure occurs at the nose and is given by $\frac{p}{\rho V^2} = 0.5$, i.e. $p = \frac{1}{2}\rho V^2$. This is always the magnitude of the pressure at a point which receives the air-stream full on, and can be deduced theoretically from Bernoulli's equation which is given below.

Fig. 24 is roughly representative of the pressure distribution for all angles of incidence up to the stall, except in the neighbourhood of zero lift. As the incidence decreases from its critical value, the suction of the upper surface and the direct pressure of the lower surface both decrease, but the latter decreases more rapidly than the former. Eventually the latter changes into a suction force also, and, when the suction forces of the two surfaces are equal, the aerofoil ceases to lift. Pressure diagrams show, however, that when this happens the resultant forces of the two surfaces do not act at the same point. The aerofoil therefore experiences a couple (Fig. 25), so that the centre of pressure is at infinity. The magnitude of this couple is given, of course, by the value of k_{m_0} (i.e. the moment coefficient at zero lift.)

Bernoulli's Equation. This equation states that, in a stream of fluid in which the velocity is changing, the pressure p and the velocity v at any point are connected by the law

$$p + \frac{1}{2}\rho v^2 = H,$$

where H is a constant.

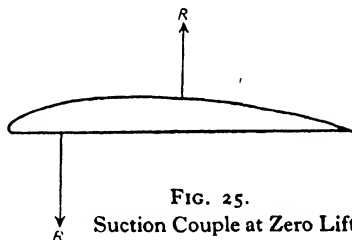


FIG. 25.
Suction Couple at Zero Lift.

The proof of this law is somewhat intricate, and, before it is given, it will first of all be shown how the law leads to the value $\frac{1}{2}\rho V^2$ for the pressure on the nose of an aerofoil and to the value $\frac{1}{2}\rho V^2$ for the pressure difference in the pitot (see p. 8).

Consider an air-stream flowing over an aerofoil. Let p_0 be the pressure of the undisturbed stream and V its velocity, so that the value of H is $p_0 + \frac{1}{2}\rho V^2$ and the equation becomes

$$p + \frac{1}{2}\rho v^2 = p_0 + \frac{1}{2}\rho V^2.$$

Now, at the point on the nose of the aerofoil which receives the stream full on, the velocity of the stream is destroyed. (This point is marked on a flow pattern diagram like Fig. 16 by the abrupt ending of a streamline.) Hence the pressure at this point can be obtained by putting $v = 0$, and the equation giving the pressure becomes

$$p = p_0 + \frac{1}{2}\rho V^2,$$

i.e. the pressure is greater than the ordinary static or atmospheric pressure by $\frac{1}{2}\rho V^2$.

Similarly, at the open end of the fine dynamic tube A (see Fig. 3) of the pitot, the velocity is again arrested, and so the pressure in the tube is $p_0 + \frac{1}{2}\rho V^2$. At the small holes in the static tube B , however, the velocity of the stream is unaltered, and hence the pressure in this tube must be the ordinary stream pressure p_0 . Thus the pressure difference is $\frac{1}{2}\rho V^2$.

This pressure of $\frac{1}{2}\rho V^2$ is called the dynamic pressure of the stream, and the constant H ($= p_0 + \frac{1}{2}\rho V^2$) is called the total pressure head or Pitot pressure.

Proof of Bernoulli's Equation. Consider an air-stream moving to the right with increasing velocity as shown in Fig. 26 (a), and suppose $ABDC$ represents a portion of a stream-tube, i.e. a thin tube of air always enclosing the same stream-lines. Suppose that after a *small* interval of time t the mass of air $ABDC$ takes up the position $A'B'D'C'$ as shown in Fig. 26 (b). Then the mass $ABB'A'$ is equal to the mass $CDD'C'$, i.e. the volume $ABB'A'$ is equal to the volume $CDD'C'$, since the density is constant.

Let p_1, v_1, S_1 be the average pressure, velocity and cross-section of the volume $ABB'A'$, and p_2, v_2, S_2 the corresponding quantities for $CDD'C'$.

Then the volume $ABB'A' = S_1 \times BB' = S_1 \times v_1 t$,
and the volume $CDD'C' = S_2 \times DD' = S_2 \times v_2 t$.

Therefore $S_1 v_1 t = S_2 v_2 t = K(\text{say})$.

[Since $v_2 > v_1$, it follows that $S_2 < S_1$; that is to say, the stream-lines get closer together as the velocity increases.]

Now the difference between the masses $ABDC$ and $A'B'D'C'$ is that the portion $ABB'A'$ at velocity v_1 , has been replaced by an equal portion $CDD'C'$ at velocity v_2 . The mass of each of these portions is ρK ; hence the change in the kinetic energy of the mass $ABDC$ in the small interval of time t is $\frac{1}{2} \rho K (v_2^2 - v_1^2)$. Again, the only forces acting on the mass in the direction of motion are the average pressure $p_1 S_1$ of the air to the left of AB

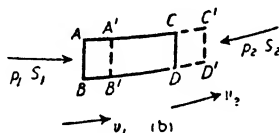
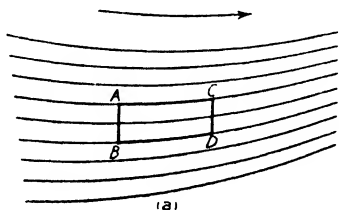


FIG. 26.

and the average pressure $p_2 S_2$ to the right of CD . During the interval of time t the former is moved through a distance $v_1 t$ and the latter through a distance $v_2 t$. Hence the work done by the former is $p_1 S_1 \times v_1 t$, and the work done against the latter is $p_2 S_2 \times v_2 t$, so that the total work done is $(p_1 \times S_1 v_1 t - p_2 \times S_2 v_2 t)$, i.e. $(p_1 - p_2)K$, since $S_1 v_1 t = S_2 v_2 t = K$. Therefore, since the change in the kinetic energy is equal to the work done,

$$\frac{1}{2} \rho K (v_2^2 - v_1^2) = (p_1 - p_2)K,$$

i.e. $\frac{1}{2} \rho v_2^2 - \frac{1}{2} \rho v_1^2 = p_1 - p_2,$

or $p_1 + \frac{1}{2} \rho v_1^2 = p_2 + \frac{1}{2} \rho v_2^2$

In other words $p + \frac{1}{2} \rho v^2$ is constant.

Origin of Lift. Since the lift of an aerofoil is due to reduced pressure on the upper surface and increased pressure on the lower, it follows from Bernoulli's equation that above the aerofoil the velocity of the air is greater than that of the undisturbed stream, and below it is less. The flow over the aerofoil may therefore be considered as a combination of the ordinary translational flow and some form of circulating flow, as shown in Fig. 27; for the circulation has the effect of speeding up the air above the aerofoil and retarding it below. It must be noted that the presence of this circulation does not imply that any particles of

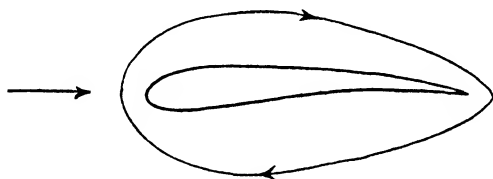


FIG. 27. Circulation Round Aerofoil.

the air actually travel round the aerofoil, but that its existence must be presumed in order to explain the velocity difference above and below the aerofoil.

This conception of a circulation superimposed on the ordinary translational velocity forms the basis of what is known as the Circulation Theory of Lift. The mathematics involved in the development of this theory is far beyond the scope of this book, but a general outline is given in Chapter V, where it is shown that the circulation imposed on the stream as it passes the aerofoil is yet another viscosity effect.

The circulation theory forms, in its turn, the basis of the Vortex Theory of Aerofoils, which deals with the problem of the aeroplane wing in so far as its behaviour is dependent upon such features as aspect ratio and the interference of one wing of a biplane on the other. Again the mathematics must be almost entirely omitted, but in the following chapter an outline of the theory is given, together with the principal formulae established. The whole theory of wing lift rests on the assumption that the

flow is perfectly streamline outside the very thin vortex region surrounding the surface of the aerofoil, and in consequence the formulae are strictly applicable only over the range of incidence in which the turbulence is negligible and the lift preserves its steady rate of increase. In practice, however, the formulae are found to give results in such excellent agreement with experimental data, right up to the critical angle, that they are used universally in aircraft design.

IV

THE AEROPLANE WING

Aspect Ratio. It was shown in Chapter II that the use of non-dimensional coefficients enables the air forces on an aeroplane wing to be calculated from experimental data obtained from a model wing, provided the wings are geometrically similar. This similarity must apply not only to the aerofoil section, but also to the plan form of the wing. In the case of a rectangular wing, plan form is defined by aspect ratio, and the effect of change in aspect ratio on the non-dimensional coefficients is most marked. With all aerofoils, of whatever section, it is found that an increase of aspect ratio results in a higher lift coefficient and a lower drag coefficient at every angle of incidence up to the critical angle. Before an explanation of this phenomenon can be given, reference must be made to one further type of experiment.

Lift Distribution Across the Span. The lift of an aerofoil is not uniformly distributed over the whole span. If pressure

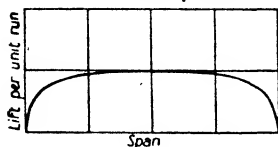


FIG. 28.

Lift Distribution Across Span angular plan form and constant aerofoil section, it is found that the lift distribution curve is of the form shown in Fig. 28. The lift is a maximum at the median or central section, and diminishes towards the wing tips, slowly at first but more rapidly near the tips.

Three-Dimensional Flow. This variation of lift, or pressure, across the span gives rise to a further disturbance of the airflow over an aerofoil. For consider the upper surface of the aerofoil; the pressure is negative over the whole span, but the magnitude of this negative pressure is a maximum at the centre

and decreases towards the wing tips. Hence the air passing over the upper surface tends to flow inwards from the tips towards the centre, i.e. towards the region of lowest pressure. Similarly, on the lower surface which is in a region of positive pressure, the maximum positive pressure occurs at the centre, and so the air passing on the under surface tends to flow outwards from the centre towards the tips. This is illustrated in Fig. 29, the full lines representing the flow above the aerofoil and the dotted lines the flow below. This figure shows that the flow past an aerofoil is three-dimensional, for the streamlines suffer deflexion both in the plane of the aerofoil section and in the plane of the span and chord. Diagrams like Fig. 16 give the flow in the plane of the section only, and are therefore only truly representative of the flow over the median

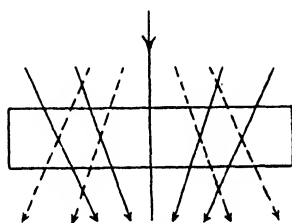


FIG. 29.

section. For such two-dimensional diagrams to be representative of the flow over every section, the span must be considered to extend throughout the whole fluid; in other words, the aerofoil must be regarded as of infinite aspect ratio.

The Trailing Vortices. From Fig. 29 it is clear that transverse vortices (i.e. vortices at right angles to the direction of flow of the free stream) will arise at the trailing edge where streams of different directions unite. For consider the flow to the left of the centre line; the streamlines above the aerofoil have a component of velocity towards the centre of the aerofoil, while those below have a component outwards from the centre. Hence at the trailing edge vortices must arise spinning in a clockwise direction. Similarly, to the right of the centre line, vortices must arise spinning in an anti-clockwise direction. These vortices prove to be unstable, and quickly roll up into two main vortices, one behind each wing tip as shown in Fig. 30 (b). These are called the trailing vortices of the aerofoil, and their presence has been established experimentally, both in

the channel and in actual flight, by attaching streamers to the trailing edge.

The Induced Velocity. The continual shedding of these trailing vortices results in a cylindrical tube of vortex motion being formed behind each wing tip, and such vortex tubes attempt to impart their rotation to all the fluid particles. Hence Fig. 30 (b) shows that an upwash is imparted to all the air outside the

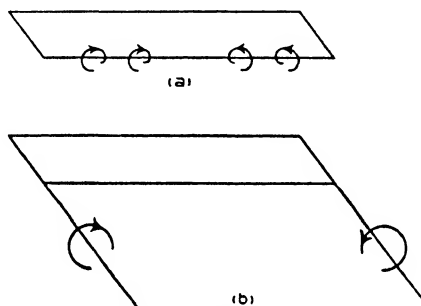


FIG. 30. The Trailing Vortices.

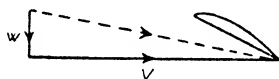


FIG. 31.

wing tips and a downwash to all that inside. The effect of these trailing vortices is damped out, of course, at any great distance in front of the aerofoil or beyond the tips, but clearly the flow past the aerofoil is deflected inwards and downwards. The inward deflexion is unimportant and is neglected in the aerofoil theory, but the downward deflexion is of considerable importance, and the downward velocity imparted is called the induced velocity. If this velocity is denoted by w , the resultant velocity at which the air meets the aerofoil is given by a simple vector diagram like Fig. 31. The effect of w is seen to be a small increase in the actual velocity of the air and a small reduction in the angle of incidence. Since w is very small compared with the velocity V of the undisturbed stream, the difference in magnitude

between V and the true resultant velocity can be neglected, but the slight reduction in the angle of incidence is very important.

Effect of the Induced Velocity. Let α be the angle of incidence, θ the angle through which the air is deflected, and α_0 the *effective* angle of incidence. Then

$$\tan \theta = \frac{w}{V}, \text{ from Fig. 31,}$$

$$\alpha_0 = \alpha - \theta,$$

and the aerofoil experiences the same forces as it would do if it were at an angle of incidence α_0 , and there were no

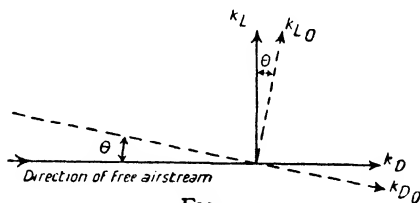


FIG. 32.

trailing vortices. If, however, there were no trailing vortices, the flow over every section would be the same, i.e. the flow would be two-dimensional. Let k_{L_0} and k_{D_0} be the lift and drag coefficients in this ideal two-dimensional flow. Then the true lift and drag characteristics may be obtained by resolving k_{L_0} and k_{D_0} at right angles to and parallel to the direction of the undisturbed stream. Thus

$$k_L = k_{L_0} \cos \theta - k_{D_0} \sin \theta,$$

and

$$k_D = k_{D_0} \cos \theta + k_{L_0} \sin \theta.$$

But θ is very small, and therefore $\cos \theta$ may be taken as unity. Also $k_{D_0} \sin \theta$ may be neglected in comparison with k_{L_0} . Hence the above equations reduce to

$$k_L = k_{L_0},$$

and

$$\begin{aligned} k_D &= k_{D_0} + k_{L_0} \sin \theta \\ &= k_{D_0} + k_L \theta, \end{aligned}$$

since $\sin \theta = \theta$ (in radians) when θ is small.

The Aeroplane Wing

Thus, due to the induced velocity and the consequent tilting back of the flow, a component of the lift becomes drag.

Now the induced velocity w , and therefore the deflexion θ (since $\tan \theta = \frac{w}{V}$), depend upon the strength of the trailing vortices, and these are dependent upon

- (1) the form of the lift distribution curve and the aspect ratio, for these determine the directions of the inflow and outflow of Fig. 29.
- and (2) the magnitude of the lift developed, for this determines the strength of these flows.

If the lift distribution curve is assumed to be a semi-ellipse,

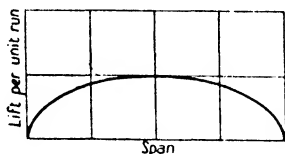


FIG. 33. Elliptic Distribution of Lift.

as shown in Fig. 33, it can be proved that θ is constant over the whole span and has the value $\frac{2}{\pi A} k_L$ radians, where A is the aspect ratio. The lift component which becomes drag is therefore $k_L \theta = \frac{2}{\pi A} k_L^2$. Hence the equations connecting the actual three-dimensional flow with the two-dimensional flow are as follows:

$$\alpha_0 = \alpha - \frac{2}{\pi A} k_L$$

$$k_L = k_{L_0}$$

and

$$k_D = k_{D_0} + \frac{2}{\pi A} k_L^2.$$

These equations show that *the lift coefficient of an aerofoil in actual three-dimensional motion at an angle of incidence α is the*

same as the lift coefficient in two-dimensional motion at a reduced angle of incidence α_0 , where $\alpha_0 = \alpha - \frac{2}{\pi A} k_L$, but the corresponding drag in three-dimensional motion is greater by $\frac{2}{\pi A} k_L^2$.

Thus, for a given lift coefficient k_L ,

$$\alpha = \alpha_0 + \frac{2}{\pi A} k_L \quad . \quad . \quad . \quad . \quad . \quad (1)$$

$$\text{and} \quad k_D = k_{D_0} + \frac{2}{\pi A} k_L^2 \quad . \quad . \quad . \quad . \quad . \quad (2)$$

Although these formulae hold strictly for elliptic distribution only, they can be used with sufficient accuracy for all kinds of lift distribution (see p. 58).

Now, in the ideal two-dimensional flow, each section of an aerofoil provides its own quota of skin friction and form drag, and no other type of drag is encountered. Hence in two-dimensional flow the drag depends solely upon the shape and attitude of the aerofoil, and for this reason the drag is called **profile drag**, k_{D_0} being called the profile drag coefficient. The additional type of drag occurring in actual three-dimensional flow is called the **induced drag**, and its coefficient $\frac{2}{\pi A} k_L^2$ is denoted by k_{D_1} .

This drag is quite independent of the aerofoil section and, for a given lift coefficient, depends only on the aspect ratio of the aerofoil. Equation (2) shows that the induced drag decreases as the aspect ratio increases, eventually disappearing when the aspect ratio becomes infinite and the flow is two-dimensional.

Again, by taking $k_{D_1} = \frac{2}{\pi A} k_L^2$, the induced drag coefficient can be calculated for different values of k_L , and the profile drag coefficient can then be obtained by subtracting the induced drag coefficient from the measured total drag coefficient. This has been done for R.A.F. 15, whose characteristics for $A = 6$ are given in Fig. 9, and the results are shown graphically in

The Aeroplane Wing

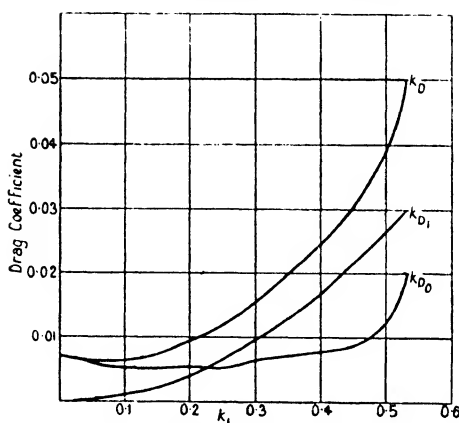


FIG. 34. Profile and Induced Drag.

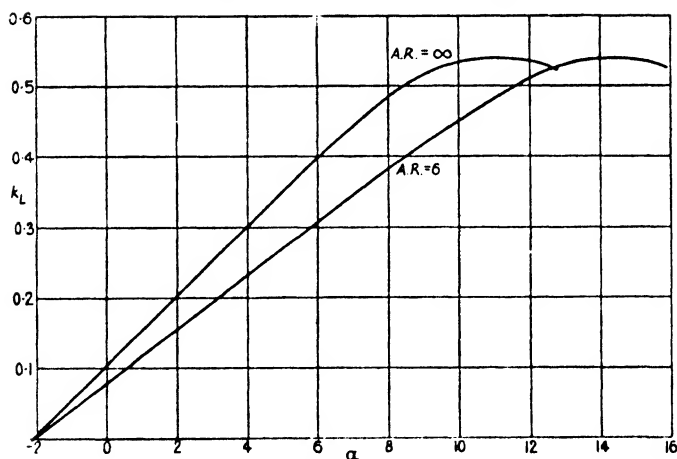


FIG. 35. Lift Curve for Infinite Aspect Ratio.

Fig. 34, where the profile drag coefficient k_{D_0} , the induced drag coefficient k_{D_i} and the total drag coefficient k_D are all shown plotted against k_L .

It will be seen that, except near the critical angle, the increase of aerofoil drag with incidence is due almost entirely to the

induced drag. The profile drag is naturally rather irregular, as it has to bear all the experimental errors.

The k_{D_0} curve of the figure can now be used in conjunction with equation (2) to determine the drag of any aerofoil of R.A.F. 15 section.

Example. An aeroplane having $W = 4200$ and $S = 500$ is climbing at 75 miles per hour in standard density. If the aeroplane is a monoplane of aspect ratio 5 with R.A.F. 15 aerofoil section, calculate the induced drag at this speed, and obtain the ratio of the induced drag to the profile drag.

$$\begin{aligned} V = 110; \text{ therefore } k_L &= \frac{W}{\rho S V^2} \\ &= \frac{4200}{0.00237 \times 500 \times 110^2} \\ &= 0.293. \end{aligned}$$

$$\therefore k_{D_1} = \frac{2}{\pi A} k_L^2 = 0.0109.$$

$$\begin{aligned} \text{Hence the induced drag} &= 0.0109 \times 0.00237 \times 500 \times 110^3 \\ &= 156 \text{ lb.} \end{aligned}$$

[alternatively,

$$\begin{aligned} \text{the induced drag} &= k_{D_1} \rho S V^2 \\ &= \frac{k_{D_1}}{k_L} \times k_L \rho S V^2 \\ &= \frac{0.0109}{0.293} \times 4200 \\ &= 156 \text{ lb.}] \end{aligned}$$

Again, from Fig. 34, the value of k_{D_0} at $k_L = 0.293$ is 0.0062.

Hence,

$$\begin{aligned} \frac{D_1}{D_0} &= \frac{k_{D_1}}{k_{D_0}} \\ &= \frac{0.0109}{0.0062} \\ &= 1.76. \end{aligned}$$

The lift-incidence curve for infinite aspect ratio can be obtained by means of equation (1), and Fig. 35 gives the curve for R.A.F. 15.

This figure shows that, as the aspect ratio increases, the slope of the curve increases, but it reveals no variation in the value of $k_{L\max}$. Actually there is some experimental evidence that $k_{L\max}$ increases as the aspect ratio increases, and the failure of the

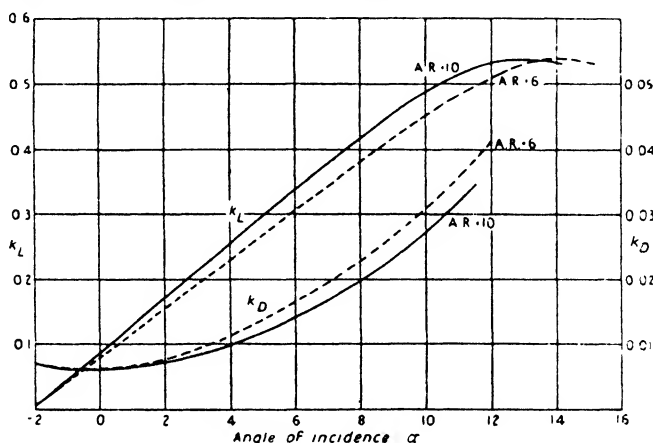


FIG. 36. Effect of Aspect Ratio.

theory in this respect is due to the assumption on which it rests, namely, that the turbulence may be neglected (see p. 47). The variation in the value of $k_{L\max}$ is small, however, and for normal aeroplane wings is of quite secondary importance.

Note that *the angle of no-lift does not change with changing aspect ratio*. This follows from equation (1), since $\alpha = \alpha_0$ when $k_L = 0$.

Corrections for Aspect Ratio. If the characteristics of an aerofoil section are known for one aspect ratio, those for any other aspect ratio can easily be obtained without first constructing the k_{D_0} curve and the corresponding lift-incidence curve for two-dimensional flow.

For suppose it is required to find the characteristics of an

aerofoil of aspect ratio A' , given the characteristics for aspect ratio A . Let the corresponding angles of incidence for a given lift coefficient k_L be α' and α respectively. Then

$$\alpha' = \alpha_0 + \frac{2}{\pi A'} k_L$$

and

$$\alpha = \alpha_0 + \frac{2}{\pi A} k_L,$$

so that

$$\alpha' - \alpha = \frac{2}{\pi} \left(\frac{1}{A'} - \frac{1}{A} \right) k_L \quad . \quad . \quad . \quad (3)$$

Similarly,

$$k_D' - k_D = \frac{2}{\pi} \left(\frac{1}{A'} - \frac{1}{A} \right) k_L^2 \quad . \quad . \quad . \quad (4)$$

It is customary to use the notation of the calculus and denote the incidence difference $\alpha' - \alpha$ by $\Delta\alpha$ and the drag difference $k_D' - k_D$ by Δk_D . Note that $\Delta\alpha$ is expressed in radians.

Example. The lift and drag characteristics for a R.A.F. 15 aerofoil of A.R. 6 are given in the following table:

α	-2	0	2	4	6	8	10
k_L	0.004	0.080	0.155	0.232	0.308	0.383	0.452
k_D	0.0069	0.0063	0.0078	0.0115	0.0165	0.0229	0.0308
			12	14	16		
			0.512	0.539	0.524		
			0.0418	0.0602	—		

Obtain the characteristics for an aerofoil of the same section but of A.R. 10, and compare the lift-incidence and drag-incidence curves of the two aerofoils.

From equations (3) and (4) we have

$$\begin{aligned} \Delta\alpha &= \frac{2}{\pi} \left(\frac{1}{10} - \frac{1}{6} \right) k_L \\ &= -0.0424 k_L \text{ radians} \\ &= -2.43 k_L \text{ degrees,} \end{aligned}$$

and

$$\Delta k_D = -0.0424 k_L^2.$$

The corrections can now be applied at each value of the lift coefficient, and we tabulate as under:

k_L	α	k_D	$\Delta\alpha$	Δk_D	α'	k_D'
0.004	-2	0.0069	-0.01	0	-2.01	0.0069
0.080	0	0.0063	-0.19	-0.0003	-0.19	0.0060
0.155	2	0.0078	-0.38	0.0010	+1.62	0.0068
0.232	4	0.0115	-0.56	-0.0023	3.44	0.0092
0.308	6	0.0165	-0.75	-0.0040	5.25	0.0125
0.383	8	0.0229	-0.93	-0.0062	7.07	0.0167
0.452	10	0.0308	-1.11	-0.0087	8.89	0.0221
0.512	12	0.0418	-1.24	-0.0111	10.76	0.0307
0.539	14	0.0602	-1.31	-0.0123	12.69	0.0479
0.524	16	—	-1.27	—	14.73	—

The curves obtained by plotting the lift and drag coefficients against α for the two aerofoils are given in Fig. 36.

Effect of Lift Distribution. The principal formulae (1) and (2) have been deduced on the assumption that the lift distribution curve is a semi-ellipse, and it has been found that this leads to a constant value for the induced velocity over the whole span. Actually the usual type of lift distribution for a rectangular aerofoil is of a more rectangular form, as shown in Fig. 28, and the induced velocity is not constant. It has been proved, however, that the effect of taking the correct form of distribution is merely to increase the average value of θ by about 5 per cent., so that no great error is introduced by the use of equations (1) and (2).

If desired, this can be allowed for by taking $k_{D1} = N \times \frac{2}{\pi A} k_L^2$, where N has a value of about 1.05.

Aspect Ratio of Non-Rectangular Wings. Aeroplane wings are often not rectangular (Fig. 37), and the determination of the induced velocity is very complex. Nevertheless equations (1) and (2) may again be used with fair accuracy, provided the aspect ratio is defined as the ratio of the mean span to the mean chord. An alternative method of expressing the aspect ratio is given below.

For a rectangular aerofoil, the

$$\begin{aligned} \text{A.R.} &= \frac{\text{span}}{\text{chord}} \\ &= \frac{2s}{c} \\ &= \frac{2s \times 2}{c \times 2s} \end{aligned}$$

$$\text{i.e.} \quad A = \frac{4s^2}{S} \quad . \quad . \quad . \quad . \quad . \quad . \quad (5)$$

In this form for A the chord does not appear, and it is the chord which generally varies most in non-rectangular aerofoils.

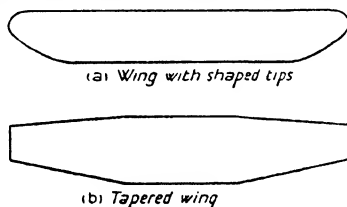


FIG. 37. Non-Rectangular Wings.

Hence the above equation is frequently used to determine the aspect ratio, $2s$ being taken as the overall span.

Biplane Effect. The non-dimensional characteristics of a monoplane cannot be applied to a biplane of the same aerofoil section, even though the two wings of the biplane may be absolutely identical and both of the same aspect ratio as the monoplane, for the trailing vortices of each wing impose an induced velocity on the flow over the other, with the result that the induced velocity of each wing is increased. The interference between the two wings is therefore equivalent to a reduction in aspect ratio, so that, at any angle of incidence, the lift coefficient of the biplane is less and the drag coefficient greater than the corresponding coefficients of the monoplane.

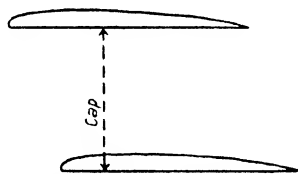


FIG. 38. Gap of Biplane.

The Aeroplane Wing

It is found that, due to the increased induced velocity, the angle θ through which the flow is deflected is increased by an amount equal to $\frac{2k_L}{\pi A} \sigma$, where σ is a quantity which depends on the ratio of the *gap* of the biplane (defined as the shortest distance between the two wings) to the span, and is given by the curves of Fig. 141.

Thus the formulae for a biplane corresponding to equations (1) and (2) for the monoplane are

$$\alpha = \alpha_0 + \frac{2}{\pi A} (1 + \sigma) k_L \quad . \quad . \quad . \quad (6)$$

and
$$k_D = k_{D_0} + \frac{2}{\pi A} (1 + \sigma) k_L^2 \quad . \quad . \quad . \quad (7)$$

The above equations refer to a biplane with wings of the same aspect ratio but not necessarily of the same size.

Example. The lift and drag characteristics of a R.A.F. 15 aerofoil of A.R. 6 are given in the example on p. 57.

Obtain the characteristics of a biplane of the same section and aspect ratio, given that the biplane has equal wings and a gap/span ratio of 1.52.

The corrections to be applied to the monoplane characteristics are

$$\begin{aligned} \Delta\alpha &= \frac{2}{\pi A} \sigma k_L \\ &= \frac{2 \times 0.56}{\pi \times 6} k_L, \text{ for } \sigma = 0.56 \text{ from Fig. 141} \\ &= 0.0594 k_L \text{ radians} \\ &= 3.40 k_L \text{ degrees,} \end{aligned}$$

and $\Delta k_D = 0.0594 k_L^2.$

These corrections are made at each value of k_L as in the example on p. 57. The actual working is not shown, but the curves obtained by plotting the lift and drag coefficients against incidence for the monoplane and biplane are given in Fig. 39.

It will be seen that the theoretical corrections applied indicate

no change in the value of $k_{L\max}$ due to biplane effect. Since, however, biplane effect is of the same nature as an aspect ratio reduction, it is only to be expected that the maximum lift coefficient of the biplane is slightly less than that of the monoplane (see p. 56), and this is confirmed by experiment. The reduction in the value of $k_{L\max}$ is generally of the order of 5 per cent.

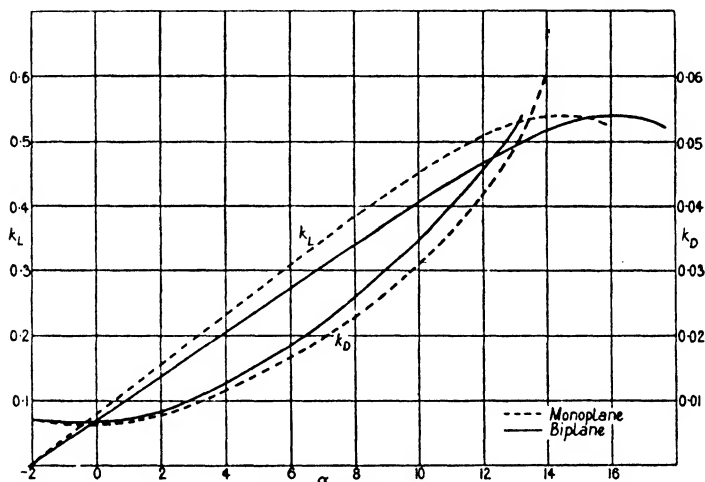


FIG. 39. Biplane Effect.

If the aspect ratio is not the same for both wings of a biplane, the expression $\frac{2}{\pi A}(1+\sigma)$ must be replaced by the general expression $\frac{S}{2\pi s_1^2 - 2\sigma s_1 s_2 + s_2^2}$, where s_1, s_2 are the semi-spans and S is the total area of both wings.

Example. Find the induced drag of the following biplane at a speed of 90 miles per hour:

Weight	2,400 lb.
Top Wing	30 ft. \times 5 ft.
Bottom Wing	26 ft. \times 4 ft.
Gap	4 ft. 3 in.

We have

$$V = 132, S = 254;$$

hence,

$$k_L = \frac{2400}{0.00237 \times 254 \times 132^2}$$

$$= 0.229.$$

Now

$$s_1 = 15, s_2 = 13;$$

$$\therefore \text{gap/mean span} = \frac{4.25}{28} = 0.152,$$

$$\text{and ratio of spans} = \frac{26}{30} = 0.87.$$

Hence from the curves of Fig. 141 we get, by interpolation,

$$\sigma = 0.545.$$

$$\therefore k_{D_1} = \frac{S}{2\pi s_1^2 - 2\sigma s_1 s_2 + s_2^2} \frac{1 - \sigma^2}{k_L^2}$$

$$= \frac{254}{2\pi \cdot 225 - 2 \cdot 12 \cdot 3 + 169} \frac{1 - 0.297}{k_L^2}$$

$$= 0.156 k_L^2.$$

Therefore the induced drag in lb. is given by

$$D_1 = \frac{D_1}{L} \times L$$

$$= \frac{k_{D_1}}{k_L} \times W$$

$$= 0.156 k_L \times W$$

$$= 86 \text{ lb.}$$

Stagger. In order to improve the pilot's view, or from considerations of stability, it is sometimes desirable to have one wing of a biplane forward of the other. The distance of one wing in front of the other is called stagger and is generally measured by the *angle of stagger*. The stagger is said to be positive if the top wing is in front of the bottom one, and nega-

tive if the bottom is in front of the top. This is illustrated in Fig. 40.

Negative stagger is very seldom used, and there is but little aerodynamic advantage to be gained from the use of positive stagger. What little advantage there is lies in a slight increase in the value of $k_{L\max}$ with increasing positive stagger, and a slight increase in the slope of the lift-incidence curve. The theory shows that *the induced drag is independent of the stagger*, for the work done against this drag is equal to the energy carried away by the trailing vortices, and, for a given lift, this is constant

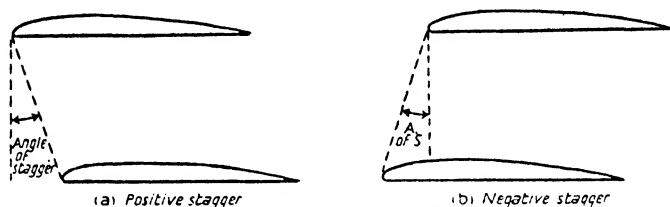


FIG. 40. Biplane Stagger.

whatever the stagger. The effect of stagger on the profile drag is probably negligible.

Curvature of the Streamlines. There is another type of interference between the two wings of a biplane which has not yet been discussed.

When an air-stream flows over an aerofoil, the streamlines are changed from straight lines to curved lines, and therefore any body in the neighbourhood of the aerofoil is subject to a curved type of flow. Hence the two wings of a biplane are each in a curved type of flow due to the presence of the other. The effect of this curvature of the streamlines is found to be equivalent to a further increase in the angle θ , and hence equations (6) and (7) are not strictly accurate. Approximate formulae have been developed to allow for the curvature, and these show that, while the effect on k_{D_1} is negligible, the incidence reduction

amounts to $\frac{1}{8\pi} \left(\frac{c}{h} \right)^2 k_L$ radians, where c is the chord and h is the

gap, provided the stagger is zero. The true incidence formula for zero stagger is therefore

$$\alpha = \alpha_0 + \frac{2}{\pi A}(1+\sigma)k_L + \frac{1}{8\pi}\left(\frac{c}{h}\right)^2 k_L \quad . \quad . \quad . \quad (8)$$

If the stagger is not zero, this new correction is not so large. For an angle of stagger of 10° its value is about 90 per cent. of that for zero stagger, while for an angle of stagger of 20° its value

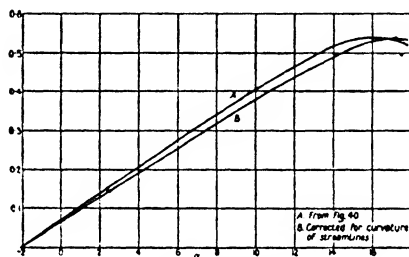


FIG. 41. Lift Curve of Biplane

is about 70 per cent. The magnitude of this correction can be gauged from Fig. 41, which gives the biplane lift curve of Fig. 39 fully corrected for the curvature of the streamlines, assuming zero stagger and a gap/chord ratio of unity.

Frequently, however, this correction is not applied to the incidence, for the most important characteristics of an aeroplane wing are the value of $k_{L\max}$ and the shape of the lift-drag or $\frac{L}{D}$ curves.

Distribution of Lift between Biplane Wings. For structural reasons it is necessary to know how the lift of a biplane arrangement is divided between the two wings. Experiment shows that, even if the two wings are identical, the load intensity on the upper wing is always greater than that on the lower one, provided the stagger is zero or positive.

Aerofoil theory has been developed to take into account the variation in the lift distribution with stagger, and approximate

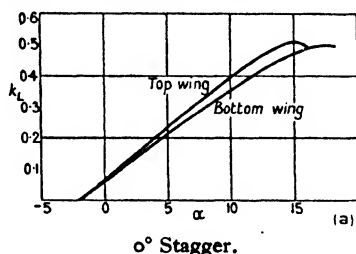
formulae have been deduced, but the theory is lacking in an explanation of the difference in the lift between the two wings at zero stagger.

It is possible, however, to obtain a general explanation of the difference in load intensity between the two wings without a detailed study of the actual flow. For, since the difference is due in some way to the interference of one wing on the flow over the other, it is only reasonable to suppose that the interference effects are greatest on the under surface of the top wing and the upper surface of the bottom wing. But it is known that the upper surface of a wing contributes more to the lift than the under surface; therefore the lower wing must suffer more from interference than the top one.

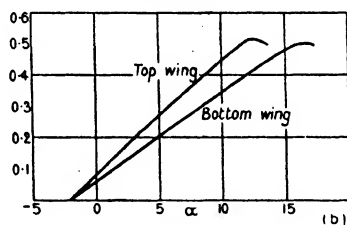
Channel Wall Constraint.

In experimental work on aerofoils it is found that wind channels of different sizes do not give quite the same results. This is due to the fact that the flow in a wind channel

differs from actual free air conditions owing to the constraint of the channel walls on the air-stream, and the effect of this constraint, for a given size of model, must clearly be greater in the case of a small channel than a large one. By means of the vortex theory it has been proved that the effect of the constraint in a closed rectangular channel is in the form of an upwash, and is therefore equivalent to an increase in aspect ratio, so that, for a given lift, both the incidence and drag are under-estimated. The formulae for the correction of wind channel data to free air conditions are :



0° Stagger.



30° Stagger.

FIG.42. Distribution of Lift between Biplane Wings.

The Aeroplane Wing

$$\Delta\alpha = 15.7 \frac{S}{C} k_L (\text{degrees}) \quad . \quad . \quad . \quad (9)$$

and
$$\Delta k_D = 0.274 \frac{S}{C} k_L^2 \quad . \quad . \quad . \quad (10)$$

where S is the area of the model aerofoil and C is the cross-sectional area of the wind channel.

The use of these equations brings the results obtained from different channels into excellent agreement.

There are some circular channels in use, which have an open working portion. For these channels the corrections are

$$\Delta\alpha = -14.3 \frac{S}{C} k_L \quad . \quad . \quad . \quad (11)$$

and
$$\Delta k_D = -0.250 \frac{S}{C} k_L^2 \quad . \quad . \quad . \quad (12)$$

Example. At an angle of incidence of 3° the lift and drag coefficients of a model aerofoil 30 in. by 5 in. were measured in a 4 ft. wind channel and were found to be 0.310 and 0.0158 respectively.

Correct the incidence and drag to free air conditions.

We have
$$S = \frac{30 \times 5}{144} \text{ and } C = 16$$

$$\therefore \frac{S}{C} = 0.065$$

Hence,
$$\begin{aligned} \Delta\alpha &= 15.7 \times 0.065 \times 0.310 \\ &= 0.32, \end{aligned}$$

and
$$\begin{aligned} \Delta k_D &= 0.274 \times 0.065 \times (0.310)^2 \\ &= 0.0017. \end{aligned}$$

The true incidence is therefore 3.32° and the true drag coefficient 0.0175.

EXAMPLES

1. Calculate the induced drag coefficient at $k_L = 0.3$ for a monoplane of aspect ratio 5.5.

2. The following table gives the results of a wind channel test on an aerofoil of aspect ratio 6:

α	-3.8	-2.6	-1.2	-0.1	1.1	2.8	6.6
k_L	0.033	0.081	0.132	0.174	0.217	0.281	0.414
k_D	0.0052	0.0052	0.0060	0.0071	0.0094	0.0140	0.0268
			8.7	10.5			
			0.465	0.500			
			0.0352	0.0466			

Obtain the values of k_{D_0} and plot k_{D_0} against k_L . Draw the mean curve through the points, and show that the minimum value of k_{D_0} is 0.0039 and occurs at a lift coefficient of about 0.18.

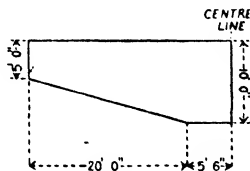
3. A monoplane weighing 7,850 lb. is of 70 ft. span and 12 ft. chord. Calculate the induced drag at speeds of 80 and 120 miles per hour.

4. The profile drag of a certain aerofoil section is given by the following table:

k_L	0.042	0.119	0.190	0.268	0.340	0.413	0.480	0.528
k_{D_0}	0.0063	0.0052	0.0050	0.0052	0.0066	0.0082	0.0107	0.0240

Find k_{D_1} in terms of k_L for a rectangular wing of aspect ratio 7.2. Hence construct the total k_D curve, and from the curve read off the values of k_D at $k_L = 0.15$ and $k_L = 0.35$.

5. The wing of a monoplane is shown in the figure. Find the aspect ratio of the wing, and so obtain an expression for the induced drag coefficient k_{D_1} . Hence, by assuming that the profile drag coefficient is approximately constant at 0.0065 between $k_L = 0.1$ and $k_L = 0.4$, construct the $\frac{L}{D}$ curve



of the wing between these limits of k_L , and determine the maximum value of $\frac{L}{D}$ and the value of k_L at which it occurs.

6. The following table gives the lift and drag characteristics of an aerofoil of aspect ratio 6:

α	-4.4	-2.4	-0.4	1.7	3.7	5.8	7.6	9.5
k_L	0.066	0.141	0.214	0.294	0.366	0.433	0.492	0.526
k_D	0.0066	0.0081	0.0112	0.0160	0.0217	0.0287	0.0363	0.0454

Obtain expressions for the corrections $\Delta\alpha$ and Δk_D which must be applied in order to arrive at the characteristics for an aerofoil of the same section but of $A.R.$ 7.

Determine these characteristics, and draw the lift-incidence and drag-incidence curves. Hence find the incidence and wing drag coefficient at 60 miles per hour of an aeroplane having this aerofoil as a monoplane wing, given that $\frac{W}{S} = 8$.

7. Calculate the induced drag coefficient at $k_L = 0.33$ of a biplane with equal rectangular wings, given that the span is 40 ft., the chord 5.5 ft., and the gap 5 ft.

8. The aerofoil section of example 6 is used in the following biplane:

Top Wing . . .	62 ft. \times 7 ft.
Bottom Wing . . .	56 ft. \times 7 ft.
Gap . . .	7 ft.

Find the $\frac{L}{D}$ ratios at $k_L = 0.294, 0.366$ and 0.433 .

9. Prove that, for a given span and a given area, a biplane is always more efficient than a monoplane of the same aerofoil section.

(Assume the biplane has equal wings, use $A = \frac{4s^2}{S}$ and compare the expressions for k_{D1} .)

10. Prove that, for any given speed, the ratio of the lift to the induced drag is inversely proportional to the 'span loading' [span loading = $\text{weight}/(\text{span})^2$].

(Take $k_{D1} = \frac{2}{\pi A} k_L^2$, as for monoplane.)

V

THE AEROFOIL IN TWO-DIMENSIONAL FLOW

REFERENCE has already been made to the idea of a circulation of flow round an aerofoil, and this forms the basis of all aerofoil theory. In fact all the formulae of the previous chapter have been established on the assumption that such a circulation exists. The present chapter deals with the origin of the circulation, and gives an outline of the Circulation Theory which treats of the lifting properties of an aerofoil in two-dimensional flow.

The Perfect Fluid. The starting-point of aerofoil theory is the conception of a *perfect fluid*. The perfect fluid is the name given to the imaginary fluid free from viscosity. In the motion of the perfect fluid past a body it is possible to calculate the direction and speed of flow at every point. (This branch of mathematical physics is called Hydrodynamics.) If this could be done for a real viscous fluid like air, it would be possible to calculate the reactions experienced by a body, without any simplifying assumptions or approximations. Unfortunately the presence of viscosity renders the problem too difficult for mathematical investigation, and in consequence attention has been directed to studying in what essentials the viscous flow differs from the perfect flow, and to ascertaining to what extent the principles underlying the latter can be applied to the former.

The Boundary Layer. Now the perfect fluid differs from a real fluid only in its freedom from viscosity, and it has been shown how viscosity effects can arise only when there is relative motion between the particles of the fluid. In the case of air flowing past a good streamline body like an aerofoil, the greatest viscosity effects occur near the surface of the body, where the particles of the air next to the surface are arrested while the others move on. The assumption made in the development of the aerofoil theory is that the region in which the viscosity effects

70 The Aerofoil in Two-Dimensional Flow

are important is confined to a very thin layer surrounding the surface of the aerofoil (see p. 38), beyond which layer the effect of viscosity is considered to be so small as to be negligible, and therefore the flow outside the layer is the same as that of the perfect fluid. This layer is therefore referred to as the *boundary layer*, and consists of a thin sheet of vortices surrounding the aerofoil. If then this thin boundary layer is regarded as being part and parcel of the aerofoil and capable of transmitting pressures, the general mass of air may be regarded as flowing past this combined body in the same way that the perfect fluid would flow, and the methods of Hydrodynamics become immediately applicable. It follows at once that the theory can hold good only so long as the flow is streamline and the viscosity effects are small enough to allow the assumption of a thin boundary layer. Obviously, in the region of the critical angle, the flow is so turbulent as to invalidate the theory, which is therefore confined to the range of incidence covering normal flight.

Profile Drag. One of the first rules of Hydrodynamics is that a body exposed to a stream of the perfect fluid in two-dimensional motion experiences no resistance. This can be proved mathematically, but may be regarded as the obvious consequence of the absence of viscosity. Without viscosity there can be no skin friction and no form drag, and these are the only types of drag occurring in two-dimensional flow in a viscous fluid. Hence in the perfect fluid every body is a streamline body, and the streamlines everywhere follow the surface of the body. An aerofoil, however, does experience a certain amount of drag, namely profile drag, but this is small compared with the lift and may be neglected. In any case the profile drag of an aerofoil consists mostly of skin friction due to the presence of the boundary layer, and, since the boundary layer is supposed to be bound to the aerofoil, the existence of the profile drag is not contrary to the assumption that outside this layer the flow is sensibly perfect.

The Origin of Lift. Now an aerofoil section is a complex

The Aerofoil in Two-Dimensional Flow 71

shape mathematically, and, since any shape is streamline in the perfect fluid, the origin of lift is generally illustrated in Hydrodynamics by the simple case of a cylinder of circular cross-section.

If the cylinder is at rest, the streamlines are symmetrical about the centre line, as shown in Fig. 43 (a), and the cylinder experiences no reaction. If, however, the cylinder is rotating about its axis, or is surrounded by a circulating flow, then it can be proved that the combination of the translational flow and the

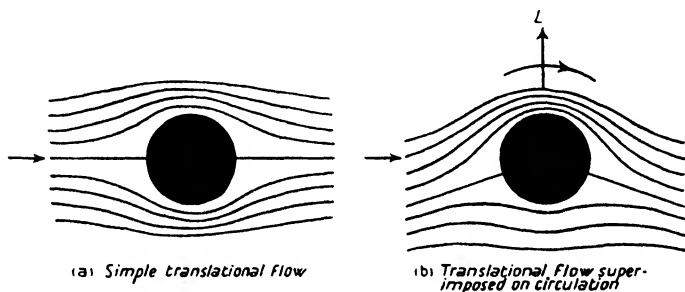


FIG. 43. Origin of Lift.

circulation leads to a flow pattern as in Fig. 43 (b), and the cylinder is found to experience a reaction or lift L as shown. The circulation has the effect of increasing the velocity above the cylinder and decreasing it below, so that, by Bernoulli's equation, there is reduced pressure above and increased pressure below. This pressure difference is revealed by the streamlines, for it can be seen that some of the fluid which passed below the cylinder when the cylinder was at rest is now passing above it, and hence there is a flow from a region of high pressure to one of low pressure.

Although a circular section has been chosen for illustration, it can be proved that, for any section, such pressure conditions can exist only if there is a circulation. In the case of an aerofoil these pressure conditions are known to exist; hence the lift of an aerofoil must be due to some form of circulation.

Circulation. The origin of the circulation round an aerofoil

72 The Aerofoil in Two-Dimensional Flow

is not obvious, and, in order to explain its existence, it is necessary to return to the boundary layer. This layer consists of a thin sheet of vortices, those on the upper surface of the aerofoil clearly spinning in a clockwise direction (if the flow is from left to right), and those on the lower surface in an anti-clockwise direction. Now a vortex attempts to impart its rotation to the general mass of the fluid; hence every elementary vortex in the vortex sheet imparts a rotational velocity to the rest of the stream, the velocity induced at any point depending upon the distance of the point from the centre or core of the vortex, and upon the direction of spin. The resultant velocity at any point is then the vector sum of all the elementary velocities. Owing to the complex and indefinite nature of the boundary layer it is impossible to calculate the actual resultant rotational velocity at any point, but, from what has been said, it is clear that the net effect of the layer must be equivalent to some form of circulation.

Thus it appears that, although viscosity is responsible for skin friction and form drag, without viscosity an aerofoil would not lift.

From Circle to Aerofoil. In the case of the circle of Fig. 43 it is possible to calculate the lift if the 'strength' of the circulation is known. Now, by a mathematical device which cannot be entered into here, it is possible to transform the circle into an aerofoil section and the streamlines for the circle into those for the aerofoil; and the aerofoil lift can be calculated. The shape of the aerofoil section depends upon the actual particulars of the transformation, and, by varying the numerical details of the transformation, an infinite number of shapes can be obtained. Again, the lift obtained for the aerofoil will depend upon the circulation strength assumed, and so far nothing is known as to the correct value to be taken. Clearly, however, the flow pattern is also dependent on the circulation, and if the circulation is assumed to be that which makes the calculated flow pattern agree with the known flow pattern, the true lift will be obtained. The principal feature of the flow pattern in this connexion is

The Aerofoil in Two-Dimensional Flow 73

the manner in which the streamlines meet and leave the aerofoil, and the circulation is determined in the theory by supposing that the flow is absolutely smooth, so that the streamlines divide at the nose and re-unite at the tail.

For all reasonable shapes of aerofoil section obtained in this manner, it is found that the lift coefficient and angle of incidence are connected by the equation

$$k_L = \pi(\alpha + \beta) \quad . \quad . \quad . \quad . \quad . \quad (1)$$

where $-\beta$ is the angle of no-lift, and both α and β are expressed in radians. The theory shows, of course, no critical angle, since it is based entirely on the assumption of streamline flow outside the thin boundary layer; hence this formula can only be regarded as applicable to that range of incidence over which k_L increases uniformly with α . Again, due to the fact that the actual flow does depart slightly from the perfect flow as the angle of incidence increases, it is better to reduce the slope of the lift curve from π to about 3. Then, if α and β are expressed in degrees, the lift-incidence equation becomes

$$k_L = 0.052(\alpha + \beta) \quad . \quad . \quad . \quad . \quad . \quad (2)$$

This equation has been applied to R.A.F. 15, using the measured no-lift angle of -2.1° . The calculated lift curve is shown in Fig. 44, where it is compared with that of Fig. 35, obtained from model data corrected for infinite aspect ratio by

means of the equation $\alpha = \alpha_0 + \frac{2}{\pi A} k_L$. The agreement is seen to be very good indeed, the slight discrepancy being due to the fact that, in the construction of Fig. 35, the above formula for elliptic lift distribution was used instead of that for the true distribution.

From equation (2) and the equation $\alpha = \alpha_0 + \frac{2}{\pi A} k_L$ it follows that *the slope of the straight part of the lift-incidence curve of an aerofoil of finite aspect ratio is independent of the aerofoil section and depends only on the value of the aspect ratio*. For all reasonable shapes of aerofoil section this is very well confirmed by experiment.

74 The Aerofoil in Two-Dimensional Flow

Again, the theory enables the moment of the lift about the leading edge to be calculated, and it is found that, if k_{m_0} is the value of the moment coefficient at zero lift, k_m and k_L are always connected by the equation

$$k_m = -0.25k_L + k_{m_0} \quad (3)$$

This also agrees very well with experiment (see p. 30).

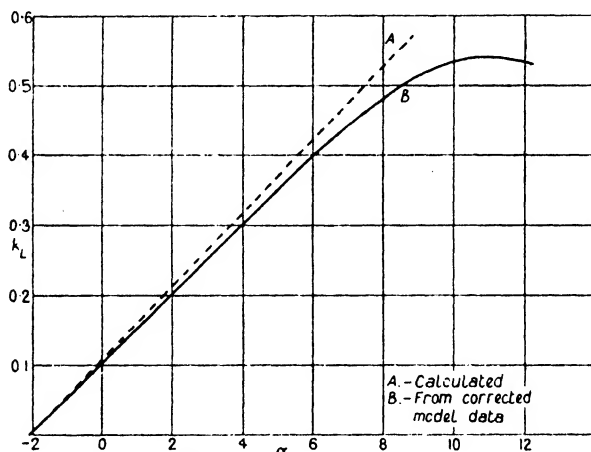


FIG. 44. Lift Curve for Infinite Aspect Ratio.

Calculation of β and k_{m_0} . The values of β and k_{m_0} depend upon the particulars of the transformation, and, given the shape of an aerofoil section, it is a difficult matter to find the exact transformation which will convert a circle into this shape. It has been proved, however, that β and k_{m_0} depend primarily on the shape of the centre line of the aerofoil section, the actual thickness being relatively unimportant. Thus, for the purposes of calculation, the aerofoil section may be replaced by the curved line representing the mean of its upper and lower surfaces, the section itself being regarded merely as a fairing placed round this centre line to render the flow streamline.

(a) *Centre line a straight line.* When the centre line is straight,

The Aerofoil in Two-Dimensional Flow 75

i.e. when the section is a symmetrical one, it is clear from symmetry that the angle of no-lift is zero, and also the value of k_{m_0} .

(b) *Centre line a circular arc.* When the centre line is a circular arc it can be proved that β and k_{m_0} are given by the simple relations

$$\beta = 2\gamma \quad . \quad . \quad . \quad . \quad . \quad . \quad (4)$$

and

$$k_{m_0} = -\frac{\pi}{2}\gamma \quad . \quad . \quad . \quad . \quad . \quad . \quad (5)$$

where β is expressed in radians and γ is the *camber* of the centre

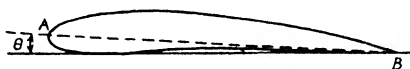


FIG. 45.

line, defined by the ratio of the maximum ordinate of the centre line to the chord. In equation (4) β is taken to be measured from the line joining the leading edge and trailing edge; it must therefore in general be corrected to read from the true chord which is defined as the tangent to the under surface. Thus in Fig. 45 the calculated value of β would be measured from AB and would therefore have to be increased by the angle θ .

Example. Calculate the angle of no-lift and the value of k_{m_0} for an aerofoil with a centre line of camber 0.03, given that the line joining the leading and trailing edges is inclined at 1.66° to the chord.

We have

$$\begin{aligned} \beta &= 2\gamma \\ &= 0.06 \text{ radians} \\ &= 3.44 \text{ degrees} \end{aligned}$$

$$\begin{aligned} \therefore \text{angle of no-lift} &= 3.44 + 1.66 \text{ degrees} \\ &= 5.1^\circ. \end{aligned}$$

Again

$$\begin{aligned} k_{m_0} &= -\frac{\pi}{2}\gamma \\ &= -0.047. \end{aligned}$$

76 The Aerofoil in Two-Dimensional Flow

In order to test the accuracy of the theory, several aerofoil sections have been developed by curving the centre line of symmetrical sections into circular arcs. For instance, the section known as R.A.F. 32 was obtained from the symmetrical section R.A.F. 30 (see Fig. 8) by giving the centre line a camber of 0.05, and another section known as R.A.F. 31 was obtained by using a camber of 0.02. The results of wind channel tests on these two aerofoil sections are given in Table II below and compared with the calculated characteristics. The table also includes particulars of two other sections, R.A.F. 25 and R.A.F. 26, which are of half the thickness of the series R.A.F. 30-2.

TABLE II
COMPARISON OF OBSERVED AND CALCULATED AEROFOIL CHARACTERISTICS

Aerofoil Section	Camber	k_{m_0}		Angle of no-lift	
		(observed)	(calculated)	(observed)	(calculated)
R.A.F. 25	0.01	-0.016	-0.016	-3.2°	-3.2°
„ 26	0.02	-0.028	-0.031	-3.6°	-3.6°
„ 31	0.02	-0.029	-0.031	-6.2°	-6.4°
„ 32	0.05	-0.067	-0.078	-7.3°	-7.7°

It will be seen that, except for the moment coefficient of the aerofoil of greatest camber, the agreement between theory and experiment is quite good.

(c) *Other forms of centre line.* When the centre line is not a circular arc, β and k_{m_0} can be calculated by means of the integral calculus if the equation of the centre line is known, or determined graphically if it is not known. The method is somewhat intricate and is given in the appendix.

Further Camber Effects. Experiment shows that, for a given thickness of section, the maximum lift coefficient increases as the centre line camber increases, so long as the centre line camber does not exceed a value of about 0.08. In practice the camber rarely exceeds a value of 0.06, for reasons which will appear later; hence, if the value of $k_{L_{\max}}$ were the only consideration, it would always be desirable to use a section of high

The Aerofoil in Two-Dimensional Flow 77

camber. In the choice of aerofoil section, however, there are two other points to be considered, namely, the shape of the profile drag curve and the movement of the centre of pressure.

(a) *Profile Drag.* Consider the two aerofoil sections R.A.F. 31 and R.A.F. 32 of the same thickness but of different camber. The profile drags of these sections have been determined from model tests on aerofoils of aspect ratio 6, by using the equation $k_{D_1} = 1.05 \times \frac{2}{\pi A} k_L^2$ (see p. 58), and the drag curves are shown in Fig. 46. It will be seen that, although the value of

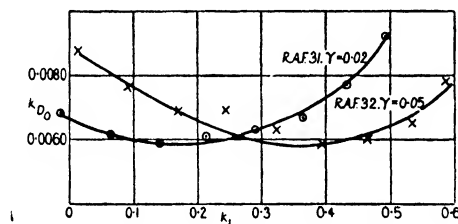


FIG. 46. Profile Drag Curves Illustrating Effect of Camber.

the minimum profile drag coefficient is the same in each case, the value of the lift coefficient at which this minimum occurs is quite different. The figure shows that R.A.F. 31 would be a suitable section for a high speed aeroplane working at a low lift coefficient, whereas R.A.F. 32 would be more suitable for an aeroplane in which the minimum profile drag is required at the slower climbing speeds.

An explanation can be found for this variation in the position of minimum k_{D_0} by considering an aerofoil as a circular arc. For it is only reasonable to suppose that the profile drag will be a minimum when the aerofoil is at an incidence 0° (in two-dimensional flow.) Now $k_L = \pi(\alpha + \beta)$, and therefore the lift coefficient corresponding to $\alpha = 0$ is given by $k_L = \pi\beta = 2\pi\gamma$, since $\beta = 2\gamma$. Hence the minimum value of k_{D_0} might be expected to occur at a lift coefficient of

$$k_L = 2\pi\gamma \quad . \quad . \quad . \quad . \quad . \quad (6)$$

78 The Aerofoil in Two-Dimensional Flow

The application of this equation to R.A.F. 31 and R.A.F. 32 gives the values of k_L for minimum k_{D_0} as 0.13 and 0.31 respectively, and these values agree fairly well with those determined from experiment and revealed by Fig. 46.

The above equation also shows that, if the camber is very great, the profile drag will not reach its minimum value until a very high lift coefficient—probably outside the useful range—is reached, so that for all normal flying speeds the profile drag will be excessive.

(b) *Centre of Pressure Movement.* The use of the equations

$$k_{C.P.} = -\frac{k_n}{k_L} \text{ (taking a negative sign to make } k_{C.P.} \text{ positive)}$$

and

$$k_m = -0.25k_L + k_{m_0}$$

leads to the equation

$$k_{C.P.} = 0.25 - \frac{k_{m_0}}{k_L}.$$

Hence, since k_{m_0} is always negative, a large value for the camber and therefore a large value for $k_{m_0} \left(= \frac{\pi}{2} \gamma \right)$ means a backward position of the centre of pressure. Now structural considerations demand that the travel of the centre of pressure, as given by its most forward position at the stall and its backward position at top speed, should be kept as low as possible, and it can easily be shown from the above equation for $k_{C.P.}$ that a large value of k_{m_0} leads to a large travel. Consider, for instance, a high speed lift coefficient of $k_L = 0.12$ and a stalling speed coefficient of 0.6. Then the C.P. travel when $k_{m_0} = -0.020$ is from 0.417 to 0.283, while when $k_{m_0} = -0.060$ it is from 0.750 to 0.350. A large camber therefore leads to an excessive C.P. travel, besides possibly throwing the position of minimum k_{D_0} outside the normal flying range. For these reasons the camber seldom exceeds a value of 0.06.

It is possible, however, to reduce the value of k_{m_0} by departing from a circular arc centre line, in which the curvature is con-

The Aerofoil in Two-Dimensional Flow 79

stant throughout the length, to a centre line in which the curvature decreases towards the trailing edge; and, if the centre line is given a certain amount of *reflex curvature* (Fig. 47) the value of k_{m_0} may be reduced to zero, so that the C.P. is stationary at 0.25. This is discussed more fully in the appendix.



FIG. 47. Centre Line with Reflex Curvature

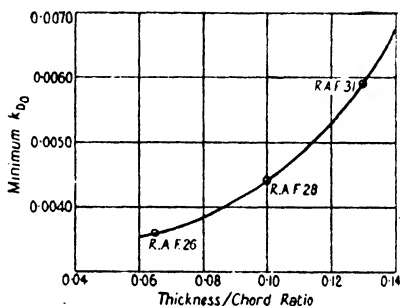


FIG. 48. Variation of Minimum k_{D_0} with Thickness.

Two slight disadvantages attend this method of reducing C.P. travel, viz.:

- (1) the value of $k_{L_{\max}}$ is slightly reduced,
- and (2) the profile drag is slightly increased, although, if the *maximum* camber remains unaltered, the position of minimum k_{D_0} remains practically unchanged.

Effect of Thickness. The theory does not take into account the actual thickness of an aerofoil section, but experiment shows that, for reasonable values of the thickness/chord ratio (called t/c ratio), say not exceeding 0.16, the lift and moment characteristics are almost independent of the thickness and depend upon the centre line camber only, as indicated by the theory. As might be expected, however, the profile drag increases with thickness, and Fig. 48 shows the approximate values of minimum k_{D_0} for varying t/c ratios.

80 The Aerofoil in Two-Dimensional Flow

This curve has been prepared from experimental data on aerofoils obtained by curving the centre lines of symmetrical sections into circular arcs, but it probably gives a good indication of the nature of the increase in min. k_{D_0} which accompanies increase in thickness for all aerofoils of good streamline form.

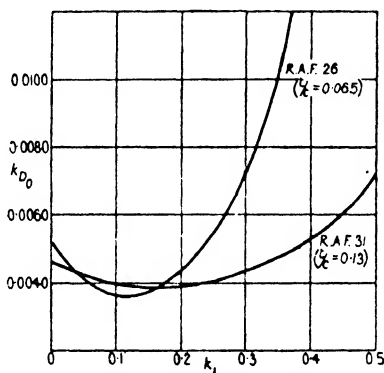


FIG. 49. Profile Drag Curves for different Thickness, Chord Ratios.

Another feature of the profile drag is that, while the profile drag curve of any aerofoil section is roughly parabolic in shape, the curve rises more steeply on either side of the minimum for the thinner sections. This is illustrated in Fig. 49, which gives the mean k_{D_0} curves for R.A.F. 31 and R.A.F. 26. These sections have the same centre line camber of 0.02, but the former is twice as thick as the latter.

VI

PARASITE DRAG

Parasite Drag. In addition to the drag of the wings there is the drag of the remaining parts of the aeroplane, including the fuselage, tail unit, landing gear, struts and wires. Except for the tail plane, which behaves as a small aerofoil, these various parts contribute nothing to the support or propulsion of the aeroplane, and their drag is therefore called parasite drag. Generally a little lift comes from the fuselage, but this is so small as to be negligible in comparison with the main plane lift. (Strictly speaking, the profile drag of the wings should also be labelled parasite drag, for it is only the induced drag which owes its existence to the wing lift.)

Parasite drag consists of skin friction and form drag, and can be kept low only by careful streamlining. Like the profile drag of the wings, it cannot be directly calculated, but must be obtained from wind channel data.

Dynamic Similarity. It has been proved both experimentally and mathematically that every type of air force can be written with a good degree of accuracy in the form

$$R = k\rho l^2 V^2,$$

where l is some typical linear dimension of the body, so that l^2 represents an area. In the case of aeroplane wings l^2 is replaced by the wing area S ; in the case of parasite drag it is convenient to replace it by the frontal or projected area A . The use of the above equation then enables model data to be corrected to full scale.

In estimating the parasite drag of an aeroplane it is usual to express each item in lb. at 100 ft. per second in standard density.

Example 1. The drag of a flat plate 6 in. square and held at right angles to the air-stream is found to be 1.215 lb. at 60 ft. per second. Find the resistance coefficient k and the drag of a plate 1 ft. square at 100 ft. per second.

Parasite Drag

We have

$$A = \frac{1}{2} \times \frac{1}{2} = 0.25; \text{ hence}$$

$$\begin{aligned} k_D &= \frac{R}{\rho A V^2} \\ &= \frac{1.215}{0.00237 \times 0.25 \times 3600} \\ &= 0.57. \end{aligned}$$

Hence the drag when $A = 1$ and $V = 100$ is given by

$$\begin{aligned} R &= 0.57 \times 0.00237 \times 100^2 \\ &= 13.5 \text{ lb.} \end{aligned}$$

Example 2. The drag of a $\frac{1}{12}$ scale fuselage at 40 ft. per second is 0.09 lb. Find the full scale drag at 100 ft. per second.

Let A be the frontal area of the model; then the full scale area is $A \times 12^2$. Hence, if R, R' are the model and full scale drags respectively, we have

$$\begin{aligned} R &= k\rho A \times 40^2 \\ R' &= k\rho A \times 12^2 \times 100^2 \\ \therefore \frac{R'}{R} &= \frac{12^2 \times 100^2}{40^2} \\ \therefore R' &= \frac{12^2 \times 100^2}{40^2} \times 0.09 \\ &= 81 \text{ lb.} \end{aligned}$$

Streamlining. As was stated in Chapter III, the object of streamlining is to reduce the form drag by eliminating as far as possible the turbulent motion in the wake, and it is found that the best streamline forms all possess two common characteristics, namely,

- (1) a fairly blunt nose,
and (2) a shaped profile leading to a 'tail'.

The drag of any bluff-shaped body can be reduced by the addition of a shaped nose and tail, but there is obviously a limit to which useful streamlining can be carried out by these means. For the additional surface of the fairing increases the skin

friction, so that, if the profile is drawn out to a great length, there may be an increase in skin friction without any corresponding reduction in form drag.

The drag or resistance coefficient of a streamline body depends upon

- (1) the actual shape or curvature of the profile,
 - (2) the position of maximum thickness,
- and
- (3) the *fineness ratio*, which is the ratio of the length of the body to its maximum thickness.

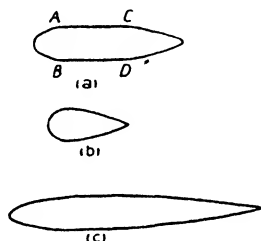


FIG. 50.

Corresponding to these three items, the following points should be noted :

- (1) The profile should possess continuity of curvature. Flats like AC and BD , with discontinuous points like A , B , C and D , should be avoided (Fig. 50 (a)). A smooth flow can only come from a smooth regular contour.
- (2) A very blunt nose, with the maximum thickness close to the nose, is clearly still associated with form drag (Fig. 50 (b)).
- (3) A very long tapering shape as in (c) results in excessive skin friction.

Numerous experiments have been carried out to determine the best form of a streamline body, and it is found that the resistance coefficient has its lowest value when the fineness ratio is about 3 and the maximum thickness occurs at a point about 40 per cent. of the length back from the nose.

The foregoing remarks apply both to solid bodies like fuselages and airship envelopes, and also to the cross-sectional shapes of bodies like struts and wires, which are long in comparison with the length of their cross-sections and over which the flow is therefore approximately two-dimensional.

Struts. The main vertical members connecting the two wings of a biplane are called the *interplane struts*. The *body struts* connect the fuselage to the wings, while struts are also used to connect the undercarriage and the tail plane to the fuselage. A typical type of strut section of fineness ratio 3 is shown in Fig. 51. For values of the



FIG. 51. 3:1 Streamline Strut Section.

fineness ratio between 3 and 4 the resistance coefficient varies but little and has a value of about 0.042. This corresponds to a drag of 1 lb. per square foot of frontal area at 100 ft. per second in standard density.

Example. A 4:1 fineness ratio strut is 6.5 ft. long and 5 in. wide. Find its drag at 120 miles per hour.

Since the fineness ratio is 4, the thickness of the strut

$$= \frac{5}{4} \text{ in.} = \frac{5}{48} \text{ ft.}$$

$$\therefore \text{frontal area} = \frac{6.5 \times 5}{48} \text{ sq. ft.}$$

Also

$$V = 176 \text{ f.p.s.}$$

Hence, taking the resistance to be 1 lb. at 100 f.p.s., we have

$$\begin{aligned} R &= 1 \times \frac{6.5 \times 5}{48} \times \frac{176^2}{100^2} \\ &= 2.1 \text{ lb.} \end{aligned}$$

Where a strut joins the wing, the strut end and socket disturb the flow and so increase the drag. The actual amount of extra drag produced depends upon the type of joint which is used, but an average figure is about 0.2 lb. at 100 ft. per second for each end. In some aeroplanes with thick wing sections the strut ends are buried inside the wings, and the 'end effect' is negligible.

Wires. The interplane and body struts are braced and cross-braced by wires. These wires are called R.A.F. wires and are elliptic in cross-section with a fineness ratio of 4. (Fig. 52) They have a much lower drag coefficient than ordinary circular wires, and the drag could be still further reduced, of course, by using a streamline strut type of cross-section. It is found, however, that the reduction is not worth the increased difficulty of manufacture. The actual drag coefficient is about 0.18, but the drag is usually expressed in lb. per foot run at 100 ft.

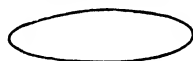


FIG. 52. Streamline Wire

per second. The following table gives the drag for the various sizes of wires, together with the added drag due to end fittings and wiring plates. It will be seen that the end effect is responsible for the greater part of all streamline wire drag. This is due mostly to the interference which arises between the fittings and the wings.

TABLE III
WIRE DRAG

Wire	Drag (lb. per ft. run)	Drag per end fitting (lb.)	Wire	Drag (lb. per ft. run)	Drag per end fitting (lb.)
4 B.A.	0.025	0.21	$\frac{3}{8}$ " B.S.F.	0.052	0.90
2 B.A.	0.027	0.30	$\frac{1}{2}$ " "	0.060	1.06
$\frac{1}{4}$ " B.S.F.	0.034	0.44	$\frac{5}{8}$ " "	0.064	1.15
$\frac{3}{8}$ " "	0.037	0.53	$\frac{3}{4}$ " "	0.067	1.32
$\frac{1}{2}$ " "	0.041	0.68	$\frac{7}{8}$ " "	0.071	1.51
$\frac{3}{4}$ " "	0.049	0.76			

The Fuselage. The fuselage is a long box-like structure consisting essentially of four main longitudinal members (called the *longerons*), braced by struts and wires, and covered with a streamline fairing. Owing to the presence of the engine, cockpits, wind screens, &c., all of which considerably disturb the flow and mar the streamlining, it is often a difficult matter to obtain a good streamline fuselage. In addition, the fuselage of a single-engine machine is situated in the slipstream, i.e. the rotating mass of air thrown backwards by the airscrew,

and this further upsets the streamlining. Thus a good fuselage can only be designed after some difficulty and expense, and in some cases the increased cost of design and manufacture may outweigh the advantages to be gained by careful streamlining. Since, however, the drag of the fuselage may easily be anything up to 75 per cent. of the total parasite drag, high performance can be obtained only by careful fuselage design. It should be noted that, in the case of a twin-engine aeroplane in which the engines are housed either on or between the main planes, the absence of the slipstream and of the disturbing influence of the engine in the nose renders a good streamline body comparatively simple of attainment.

Unfortunately the fuselage varies so much from one aeroplane to another that it is almost impossible to give any generalized data for the estimation of fuselage drag, and the only way of obtaining a low resistance is by systematic wind channel experiments. Obviously, however, the frontal area must be kept as small as possible, but equally important is the necessity for continuity of curvature and absence of flats. Thus the drag of a rectangular type of fuselage with sharp edges can often be reduced by adding a streamline fairing, although by these means the frontal area is increased.

In the case of a single-engine aeroplane with the engine in the nose, the presence of the engine may have a devastating effect. For instance, while it may be possible to obtain a basic shape (i.e. the shape before the engine, cockpits, &c. are added) for about 2 lb. per square foot of frontal area, the final shape with, say, a radial air-cooled engine may give a figure as high as 6 or 7 lb. This is due mostly to the turbulence created by the projecting cylinders, and can often be slightly reduced by careful shaping of the nose in front of the engine and by local fairings behind the cylinders. A new and better scheme, which gives a considerable reduction, consists of the addition of a ring enclosing the cylinders, the section of the ring being of aerofoil shape. This ring is called a *turbulence ring* and acts in a similar manner to the auxiliary aerofoil of the slotted wing. The smooth flow

over the ring sweeps down on to the general mass of air behind the cylinders and tends to break up the turbulence and smooth out the flow (Fig. 53).

An insight into the minimum basic drag obtainable is afforded by some experiments carried out on airship envelopes. Five models were tested, and they were all solids of revolution but of

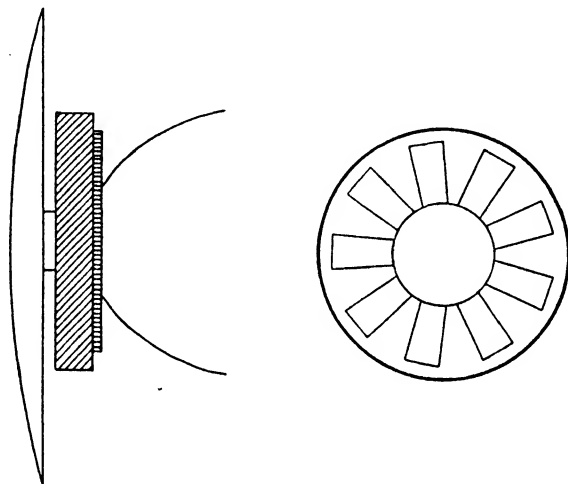


FIG. 53. Turbulence Ring.

varying fineness ratio. The generating curves are shown in Fig. 54, and the resistance characteristics of the bodies are given in Table IV.

TABLE IV.
DRAG OF AIRSHIP ENVELOPES

Model No.	Fineness Ratio	k_D	lb./sq. ft. at 100 f.p.s.
1	6.0	0.0348	0.82
2	4.5	0.0279	0.66
3	4.0	0.0251	0.59
4	3.5	0.0245	0.58
5	3.0	0.0224	0.53

Such low values for the drag cannot, of course, be realized

for aeroplane bodies, even for basic shapes. It is impossible, for instance, to taper a fuselage right down to a point, and the inevitable foreshortening of the ideal streamline body must give rise to form drag. Again it is generally impossible to have a fuselage perfectly symmetrical about its centre line, or of circular cross-section throughout its length. The result of such departures from the ideal form is that a figure of 2 lb. per square foot for the basic shape probably gives the absolute minimum—and that only to be obtained in exceptional cases.

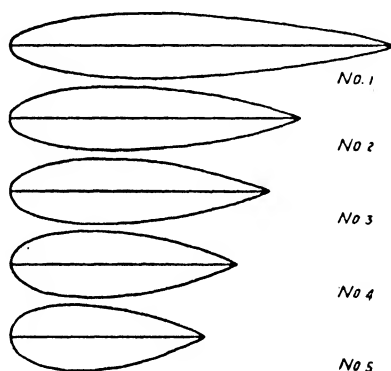


FIG. 54. Airship Envelopes.

The Undercarriage. The undercarriage consists of wheels, axle, struts and cables. The wheel drag depends upon the hub fairing used, but for the normal types of faired wheels a figure of about 4 to 5 lb. per square foot may be taken. Axles are generally streamlined and may be regarded as struts. Cable drag depends upon the ratio of the length of the cable to the diameter, but an average figure is about 10 lb. per square foot.

The Tail Unit. The tail unit comprises fin, rudder and tail plane, all of which are thin symmetrical surfaces of aerofoil shape. The drag of the tail plane depends upon its incidence and the position of its elevators, but, for the purposes of a rapid estimate of parasite drag, the whole tail unit may be considered to be working at a normal aerofoil drag coefficient k_D of about 0.0070.

Interference. When two bodies are in close proximity each affects the flow over the other, and it is not safe to assume that the sum of the drags of the two bodies when tested separately is equal to their drag when tested together. When the drag of the combination is greater than the sum of the individual drags the difference is called *interference drag*.

The interference drag of the two wings of a biplane has already been studied and found to be calculable; that of parasite drag can only be determined by experiment.

It is found that large interference drag may arise at the junction of the struts, axle and wheel of an undercarriage, and the total interference drag of both sides may amount to as much as the drag of the wheels themselves. The true undercarriage drag can therefore be obtained only by testing the undercarriage as a complete unit.

Again, interference may arise between the wings and the fuselage, and in this case the interference may not only increase the drag but also decrease the lift. Experiment appears to show that, in the case of a biplane, the best results are to be obtained by having the fuselage on the lower wing. This results in a loss of lower wing surface, but by careful experimenting it is generally possible to get the same lift from the body-wing combination as from the biplane with full lower wing span, while interference drag is excluded altogether.

Other possible sources of drag are interference effects between fuselage and undercarriage, and between fuselage and tail unit.

Effect of Incidence. Since parasite drag consists of skin friction and form drag, the variation of parasite drag with incidence is of the same order as that of the profile drag of the wings. The drag of struts and wires actually decreases slightly as the incidence increases, owing to the reduction in the projected area at right angles to the air-stream. On the other hand, the drag of the fuselage generally increases with incidence, while the undercarriage drag often decreases at first and then later starts to increase. This is illustrated in Table V, which

Parasite Drag

gives the model fuselage drag and undercarriage drag (tested complete) of an early type of fighting aeroplane.

TABLE V
FUSELAGE AND UNDERCARRIAGE DRAG
Effect of Incidence.

<i>Angle of incidence</i>	<i>Fuselage Drag (model drag in lb.)</i>	<i>Undercarriage Drag (model drag in lb.)</i>
- 2	0·091	0·042
0	0·090	0·041
2	0·090	0·040
4	0·090	0·039
6	0·092	0·039
8	0·095	0·039
10	0·099	0·040
12	0·105	0·042
15	0·113	0·045

With regard to body-wing interference it is quite possible for this to be zero at small angles of incidence but to develop and increase as the incidence increases. Body-wing combinations should therefore be always carefully tested over the complete range of incidence covering normal flight. Especially is this important with twin- or multi-engine aircraft in which the engines are housed in small streamline nacelles and mounted on or between the wings, as it has been found that large interference effects may arise at the higher angles of incidence.

Distribution of Parasite Drag. The relative importance of the various parts of an aeroplane in giving rise to parasite drag varies with the type of aeroplane, but an average distribution of drag for a typical single-engine fighting aeroplane at 0° incidence is given in Table VI.

Drag of Complete Aeroplane. When the total parasite drag of an aeroplane is known for one speed and density (generally 100 f.p.s. and standard density) it can be converted into coefficient form by dividing by ρSV^2 . This is called the parasite drag coefficient, and the addition of this coefficient and the

Parasite Drag

91

wing drag coefficient then gives the total or *overall drag coefficient* of the complete aeroplane.

TABLE VI
PARASITE DRAG OF COMPLETE AEROPLANE

<i>Component</i>	<i>Drag</i> (lb. at 100 f.p.s.)
Fuselage	60
Undercarriage	20
Struts and wires	15
Tail unit and skid	10
Miscellaneous	5
Total Drag	110

Example 1. The parasite drag of an aeroplane at 0° incidence is 122 lb. at 100 ft. per second in standard density. Find the parasite drag coefficient, given that the wing area is 320 sq. ft.

$$\begin{aligned} \text{Parasite } k_D &= \frac{D}{\rho S V^2} \\ &= \frac{122}{0.00237 \times 320 \times 100^2} \\ &= 0.0161 \end{aligned}$$

Example 2. If the parasite drag coefficient of the above example increases by 0.0003 for every 2° decrease or increase of incidence from 0° incidence, find the overall drag coefficient of the aeroplane, given that the wing characteristics are as in the following table:

α	-2	0	2	4	6	8	10	12
k_L	0.003	0.070	0.132	0.199	0.262	0.327	0.390	0.450
k_D	0.0070	0.0066	0.0082	0.0119	0.0175	0.0247	0.0330	0.0428
				14	16			
				0.502	0.530			
				0.0550	0.0740			

Hence construct the L/D curve for the complete aeroplane and determine the maximum value of L/D and the value of k_L at which it occurs.

We tabulate as under:

k_L	0.003	0.070	0.132	0.199	0.262	0.327	0.390
Wing k_D	0.0070	0.0066	0.0082	0.0119	0.0175	0.0247	0.0330
Parasite k_D	0.0164	0.0161	0.0164	0.0167	0.0170	0.0173	0.0176
Overall k_D	0.0234	0.0227	0.0246	0.0286	0.0345	0.0420	0.0506
L/D	0.13	3.08	5.37	6.96	7.60	7.79	7.71
			0.450	0.502	0.530		
			0.0428	0.0550	0.0740		
			0.0179	0.0182	0.0185		
			0.0607	0.0732	0.0925		
			7.41	6.86	5.73		

The curves of k_D and L/D against k_L are shown in Fig. 55,

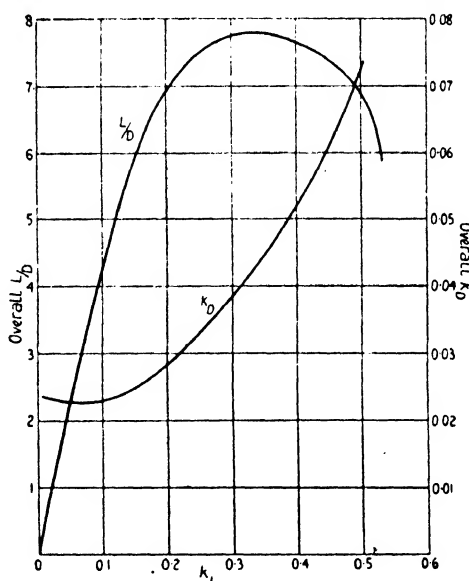


FIG. 55. Overall Lift/Drag Curve.

from which it will be seen that the maximum value of L/D is 7.80 and occurs at about $k_L = 0.33$.

From the overall L/D curve of an aeroplane the total drag at any speed can easily be obtained.

EXAMPLES

1. The drag of a model engine nacelle at 40 ft. per second is found to be 0.156 lb. Find the resistance coefficient, given that the overall diameter is 6 in. Hence find the drag at 100 ft. per second of the full-scale nacelle which is 48 in. in diameter.

2. The resistance coefficient of a certain type of strut section is 0.044. Find the drag at 100 ft. per second of a strut 4 ft. long and 1.25 in. thick.

3. A 3.1 fineness ratio strut is 2.5 ft. long and 3 in. wide. Find its drag at 60 miles per hour. (Take 1 lb. per sq. ft. at 100 f.p.s.)

4. The drag of a $\frac{1}{20}$ scale fuselage of a large passenger-carrying aeroplane at 60 ft. per second is 0.148 lb. Find the full scale drag at 100 ft. per second.

5. The parasite drag of a heavy bombing aeroplane is 315 lb. at 100 ft. per second. Find the parasite drag coefficient, given that the wing area is 920 sq. ft.

6. The following table gives the parasite drag of a single-seater as measured and estimated. Find the parasite drag coefficient, given that the wing area is 310 sq. ft.:

Fuselage	.	.	.	$\frac{1}{8}$ scale at 60 f.p.s.	.	.	0.55 lb.
Undercarriage	.	.	.	$\frac{1}{4}$ scale at 60 f.p.s.	.	.	0.49 lb.
Struts and wires	.	.	.	Estimated full scale at 100			
				f.p.s.	.	.	19 lb.

Tail unit, skid and miscel-

laneous	.	.	.	„	„	„	.	11 lb.
---------	---	---	---	---	---	---	---	--------

7. The profile drag of a certain aerofoil section is given in the following table:

k_L	0.05	0.10	0.15	0.20	0.25	0.30	0.35	0.40
k_{D_0}	0.0066	0.0060	0.0056	0.0055	0.0055	0.0061	0.0068	0.0078

If this section is used on a biplane having equal wings of *A.R.* 7 and a gap/span ratio of 0.13, calculate the total drag coefficient for each value of the lift coefficient, given that the parasite drag coefficient is approximately constant at 0.0142.

Hence construct the $\frac{L}{D}$ curve and determine the maximum value of $\frac{L}{D}$.

VII

AEROPLANE PERFORMANCE

THE previous chapters have described how it is possible to arrive at the lift and drag characteristics of an aeroplane, so that, for any given speed, the drag of the complete aeroplane may be determined. It is proposed in this chapter to deal with the part played by the power unit in overcoming this drag, and with the calculation of the performance of the aeroplane, i.e. its maximum level speed and maximum rate of climb.

The Power Unit. The power unit consists of the engine and airscrew, whose function is to provide a propulsive force which will overcome the drag and so maintain the aeroplane in flight.

The engines used in aeroplanes are mostly internal combustion engines whose essential characteristics are reliability and lightness. In principle they do not differ from the ordinary motor-car engines, and derive their power from the explosion of a mixture of petrol and air in the cylinders. The actual horsepower of an engine is obtained from brake tests, and is called the brake horse-power or B.H.P. and is generally denoted by P .

Airscrews are made of either wood or metal and generally have two or four blades. An airscrew, on being rotated by the engine, discharges a mass of air backwards through the airscrew disc, and therefore develops a forward thrust T which is equal to the rate of change of momentum of the air so discharged. Like any other machine, the airscrew cannot convert into useful work the total work put into it, and the ratio of the useful work to the total work is called the efficiency and denoted by the Greek letter η (eta).

The Slipstream. The rotating mass of air discharged backwards by the airscrew is called the slipstream, and this increases the drag of an aeroplane. For those parts of the aeroplane which are situated in the slipstream are subject to an air speed which is greater than the forward speed of the aeroplane; hence their

drag is greater with the airscrew running than it would be at the same forward speed in free air. The parts of an aeroplane situated in the slipstream are the fuselage (and/or the engine nacelles in the case of multi-engine aeroplanes) and portions of the undercarriage, tail unit, wings and interplane struts and wires, but the increase of drag is due mostly to the fuselage or engine nacelles. In the wind channel it is possible to measure the ratio of the body drag with airscrew running to its drag in free air, and so the body drag can be corrected for slipstream effect. Instead, however, of increasing the body drag, it is sometimes convenient to regard the added drag as equivalent to a loss of thrust and to allow for the slipstream effect by reducing the airscrew efficiency. The corrected efficiency is then called the *net airscrew efficiency*.

Horse-Power Required. Consider an aeroplane flying level at a speed V , and let its drag at this speed be D . Then the work to be done against the drag is DV ft.-lb. per second. Hence the horse-power required ($= H.P.$) to maintain a steady level speed V is given by

$$H.P. = \frac{DV}{550} \quad . \quad . \quad . \quad . \quad . \quad (1)$$

By means of this equation and the overall k_D or L/D curve the horse-power required for any level speed may be calculated.

Example. Given that the aeroplane of the example on p. 91 weighs 2,950 lb. and has 320 sq. ft. of wing area, use the L/D curve of Fig. 55 to find the horse-power required to maintain the aeroplane at a level speed of 120 miles per hour.

We have $k_L = \frac{W}{\rho S V^2}$ and $V = 176$.

$$\begin{aligned} \therefore k_L &= \frac{2950}{0.00237 \times 320 \times 176^2} \\ &= 0.126. \end{aligned}$$

From the $\frac{L}{D}$ curve, $\frac{L}{D} = 5.17$ at $k_L = 0.126$.

Therefore, $D = \frac{W}{L/D}$, since $W = L$

$$= \frac{2950}{5.17}$$

$$= 571 \text{ lb.}$$

Hence, $H.P. = \frac{DV}{550}$

$$= \frac{571 \times 176}{550}$$

$$= 182.7.$$

The horse-power required for the aeroplane in the above

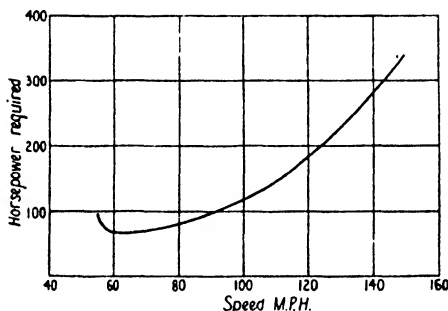


FIG. 56. Horse-Power Required for Level Flight.

example has been calculated over a range of speeds, and is shown graphically in Fig. 56. It will be seen that $H.P.$, decreases continually as the speed decreases until a speed of about 60 to 65 miles per hour is reached, when it begins to increase again owing to the rapid increase of the drag coefficient which outweighs the decreasing speed.

$$\left(\text{Notice that } H.P. = \frac{DV}{550} = \frac{k_D \rho S V^3}{550} \right)$$

Horse-Power Available. The horse-power available ($= H.P_a$)

for driving the aeroplane is the product of the airscrew efficiency and the brake horse-power, that is,

$$H.P_a = \eta P \quad . \quad . \quad . \quad . \quad . \quad (2)$$

The horse-power available is not constant for all speeds of flight, for both the airscrew efficiency and the engine power vary with speed even if the throttle setting remains unaltered. The actual variation depends primarily on the airscrew characteristics, which are discussed in detail in the next chapter; but

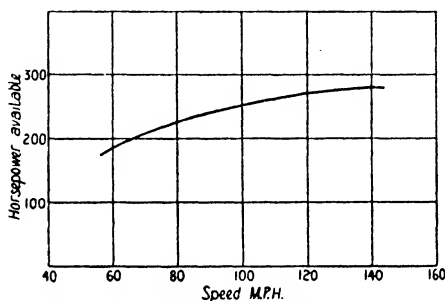


FIG. 57. Horse-power Available at Different Forward Speeds.

if, as is often the case, both the engine power and the airscrew efficiency attain a maximum in the neighbourhood of top level speed, then the general nature of the variation of horse-power available is as shown in Fig. 57.

This curve has been prepared by taking a figure of 400 for the maximum horse-power and a figure of 70 per cent. for the maximum net airscrew efficiency.

Speed and Climb. Fig. 58 below consists of the curves of Figs. 56 and 57 put on the same diagram; such a diagram is called a *performance chart*, for by its use the performance of the aeroplane can be determined.

The intersection of the two curves on the chart clearly gives the maximum level speed, for at the speed given by the point of intersection the horse-power available is just equal to the horse-power required. Thus for the aeroplane chosen the top speed is 139·7 miles per hour.

The excess of $H.P_a$ over $H.P_r$ at any other speed gives the horse-power which is available at that speed for climbing.

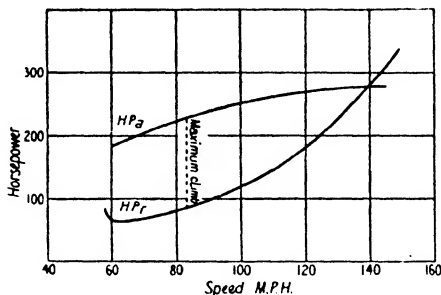


FIG. 58. Performance Chart.

At a given speed let this excess horse-power be denoted by Z , and let V_c denote the rate of climb in feet per second. Then

$$Z = \frac{W \times V_c}{550},$$

for the weight W is lifted a height V_c in 1 second,

i.e.
$$V_c = \frac{Z \times 550}{W}.$$

Generally the rate of climb is measured in feet per minute; hence

$$\text{Rate of climb (ft./min.)} = \frac{Z \times 33000}{W} \quad \dots (3)$$

From the figure the maximum value of Z for this particular aeroplane is read off as 144.4 and occurs at about 83 miles per hour.

$$\begin{aligned} \text{Hence the maximum rate of climb} &= \frac{144.4 \times 33000}{2950} \\ &= 1615 \text{ ft./min.}, \end{aligned}$$

and the best climbing speed is 83 miles per hour.

It is sometimes desirable to find the rate of climb at speeds other than the best climbing speed, and so obtain a curve showing how the climb varies with forward speed. The curve

obtained from Fig. 58 is given in Fig. 59. It will be noticed that the top of the curve is fairly flat, showing that small departures from the best climbing speed do not appreciably effect the rate of climb. This is a property common to all aeroplanes. Another

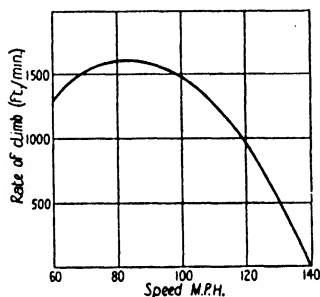


FIG. 59. Variation of Rate of Climb with Forward Speed.

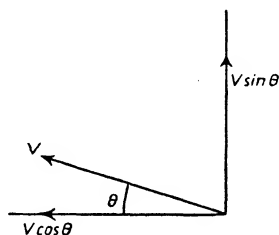


FIG. 60.

interesting feature is that the best climbing speed is not far removed from the speed corresponding to maximum $\frac{L}{D}$. In this case, for instance, maximum $\frac{L}{D}$ occurs at $k_L = 0.33$ (see Fig. 55), corresponding to a speed of 74 miles per hour.

Angle of Climb. Suppose the aeroplane is climbing at an angle θ to the horizontal. Then, since V may be resolved into its components $V \cos \theta$ and $V \sin \theta$ as shown in Fig. 60, the angle of climb is given by

$$V_c = V \sin \theta,$$

$$\text{i.e.} \quad \sin \theta = \frac{V_c}{V}.$$

For the above aeroplane at its best climbing speed of 83 miles per hour, this equation gives

$$\sin \theta = \frac{1615}{121.7}, \text{ since } V = 121.7 \text{ (ft. per second)}$$

$$= 0.2211,$$

$$\text{so that} \quad \theta = 12^\circ 47'.$$

Notice the comparatively small value of the climbing angle. The aeroplane *appears* to be climbing at a much steeper angle, since it is inclined at a considerable angle of incidence to the flight path.

The Equations of Motion. The above method for calculating the performance of an aeroplane is based on certain approxima-

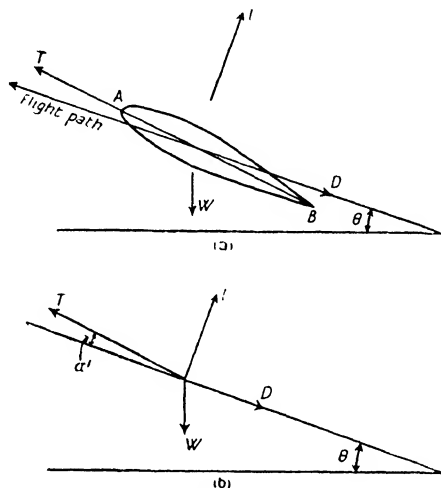


FIG. 61.

tions which will become apparent on considering the equations of motion.

Suppose AB in Fig. 61 (a) represents the centre line or thrust line of an aeroplane flying at a steady forward speed V at an angle θ to the horizontal. The forces acting on it are:

- (1) the weight W vertically downwards,
 - (2) the thrust T along the thrust line,
 - (3) the drag D along the flight path,
- and (4) the lift L at right angles to the flight path.

These forces are shown more clearly in (b). There is also a small force acting on the tail plane, but this is negligible in comparison with L .

Let the angle between the thrust line and the flight path be denoted by α' . This is the incidence of the aeroplane and is not the same thing as the wing incidence, for the wings are generally inclined at an angle of about 2° to 4° to the thrust line (called the *rigging incidence*), so that the wing incidence α is slightly greater than α' . Resolve the forces along and perpendicular to the flight path. Then

$$T \cos \alpha' = D + W \sin \theta$$

and
$$T \sin \alpha' + L = W \cos \theta.$$

Now α' is small; hence $\cos \alpha'$ may be replaced by unity and $T \sin \alpha'$ may be neglected in comparison with L . Hence the equations become

$$T = D + W \sin \theta$$

and
$$L = W \cos \theta;$$

that is,
$$\sin \theta = \frac{T-D}{W} \quad . \quad . \quad . \quad . \quad . \quad . \quad (4)$$

and $L = W$ approximately, since θ is small for normal climbing angles.

But
$$V_c = V \sin \theta.$$

Hence,
$$\text{Rate of climb (ft./min.)} = \frac{T-D}{W} \times V \times 60 \quad . \quad . \quad (5)$$

which is an alternative equation for the determination of the rate of climb.

Now the replacement of $T \cos \alpha'$ by T assumes that the airscrew thrust acts along the flight path, so that the work done by the thrust may be taken to be TV ft.-lb. per second. Hence the airscrew efficiency may be written

$$\begin{aligned} \eta &= \frac{\text{Useful work}}{\text{Total work}} \\ &= \frac{TV}{P \times 550}, \text{ if } P \text{ is the brake horse-power.} \end{aligned}$$

Therefore $TV = \eta P_{550}$ (6)

or $\frac{TV}{550} = \eta P = H.P._a$.

(The expression $\frac{TV}{550}$ is sometimes called the *thrust horse-power*.)

It can now be easily shown that equation (5) is the same as equation (3). For

$$\begin{aligned} \frac{T-D}{W} \times V \times 60 &= (TV-DV) \times \frac{60}{W} \\ &= \frac{TV-DV}{550} \times \frac{33000}{W} \\ &= (H.P._a - H.P._r) \times \frac{33000}{W} \\ &= \frac{Z \times 33000}{W}. \end{aligned}$$

Example 1. The horse-power developed by an engine at a speed of 90 miles per hour is 200 B.H.P. If the airscrew efficiency at this speed is 65 per cent., find the value of the thrust in lb.

We have $V = 132$ and $T = \frac{\eta P_{550}}{V}$.

$$\begin{aligned} \therefore T &= \frac{0.65 \times 200 \times 550}{132} \\ &= 542 \text{ lb.} \end{aligned}$$

Example 2. A twin-engine aeroplane weighs 9,800 lb. and is fitted with two 500 H.P. engines. Calculate the rate of climb and angle of climb at a speed of 65 miles per hour, given that at this speed each engine develops 470 B.H.P., the airscrew efficiency is 60 per cent, and the $\frac{L}{D}$ ratio is 7.5.

Aeroplane Performance

103

First method. We have $P = 470$, $\eta = 0.6$

$$\begin{aligned}\therefore H.P_a &= 2 \times 0.6 \times 470 \\ &= 564.\end{aligned}$$

Again, $\frac{L}{D} = 7.5$

$$\begin{aligned}\therefore D &= \frac{W}{L/D} \\ &= \frac{9800}{7.5} \\ &= 1307 \text{ lb.}\end{aligned}$$

Also, $V = 95.3 \text{ f.p.s.}$

$$\begin{aligned}\therefore H.P_r &= \frac{DV}{550} = \frac{1307 \times 95.3}{550} \\ &= 226.\end{aligned}$$

$$\begin{aligned}\therefore Z &= H.P_a - H.P_r \\ &= 338.\end{aligned}$$

Hence, rate of climb $= \frac{Z \times 33000}{W}$

$$\begin{aligned}&= \frac{338 \times 33000}{9800} \\ &= 1137 \text{ ft./min.}\end{aligned}$$

Second method. From the equation $TV = \eta P_{550}$ we have

$$\begin{aligned}T &= \frac{2 \times 0.6 \times 470 \times 550}{95.3} \\ &= 3255 \text{ lb.}\end{aligned}$$

Also $D = 1307 \text{ lb.}$, as before.

$$\begin{aligned}\therefore \text{rate of climb} &= \frac{T-D}{W} \times V \times 60 \\ &= \frac{1948 \times 95.3 \times 60}{9800} \\ &= 1137 \text{ ft./min.}\end{aligned}$$

Again, since $V_c = V \sin \theta$, we have, by each method,

$$\begin{aligned}\sin \theta &= \frac{V_c}{V} \\ &= \frac{1137}{60} \\ &= 95.3 \\ &= 0.1988,\end{aligned}$$

so that the angle of climb θ is $11^\circ 28'$.

Gliding Angle. It is convenient here to deal with the determination of what is called the *best gliding angle*. Consider an

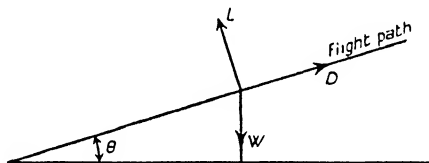


FIG. 62.

aeroplane gliding earthwards with the engine shut off, or throttled down so that the airscrew is just 'ticking over' and developing no thrust. Then the equations of motion become (Fig. 62)

$$L = W \cos \theta$$

$$D = W \sin \theta.$$

$$\therefore \tan \theta = \frac{D}{L},$$

or
$$\tan \theta = \frac{1}{L/D}.$$

Hence $\tan \theta$, and therefore θ , is a minimum when $\frac{L}{D}$ is a maximum. The minimum angle of glide therefore occurs at the incidence and speed corresponding to maximum $\frac{L}{D}$. It is called

the best angle of glide, since it gives the pilot the greatest choice of landing point; it is, in fact, the angle at which all aeroplanes are flown in to land. Any departure from the appropriate incidence and speed results in a steeper path as shown in Fig. 63.



FIG. 63. Gliding Angles and Incidence.

Effect of Change of Weight. It is often required to find the effect on the performance of an aeroplane of carrying an extra load. To do this it is necessary to obtain a new $H.P.$ curve. Obviously the extra weight has no effect on the $H.P_a$ curve, for the horse-power available at any given speed depends only on the engine and airscrew. The new $H.P.$ curve can, of course, be easily obtained by calculating the drag over a range of speeds for the new weight, and so determining the new values of $\frac{DV}{550}$. The

existing $H.P.$ curve can, however, be corrected in a very simple manner without going to so much labour.

For suppose an aeroplane of weight W has its load increased such that the total weight is W' . Let V, V' be corresponding speeds at a given angle of incidence, i.e. at a given lift coefficient k_L . Then

$$k_L \rho S V'^2 = W'$$

and

$$k_L \rho S V^2 = W.$$

$$\therefore \frac{V'^2}{V^2} = \frac{W'}{W},$$

or

$$\frac{V'}{V} = \sqrt{\frac{W'}{W}}. \quad \dots \dots (7)$$

Now, since the aeroplane is flying at the same angle of incidence and at the same lift coefficient, the drag coefficient k_D is the same in each case.

Let D, D' be the corresponding drags. Then

$$\begin{aligned}\frac{D'}{D} &= \frac{k_D \rho S V'^2}{k_D \rho S V^2} \\ &= \frac{V'^2}{V^2} \\ &= \frac{W'}{W}, \text{ from equation (7).}\end{aligned}$$

$$\begin{aligned}\therefore \frac{D' V'}{D V} &= \frac{W'}{W} \times \sqrt{\frac{W'}{W}} \\ &= \left(\frac{W'}{W}\right)^{3/2}.\end{aligned}$$

Hence,
$$\frac{H.P'}{H.P} = \left(\frac{W'}{W}\right)^{3/2} \quad . \quad . \quad . \quad . \quad . \quad (8)$$

It follows then from equations (7) and (8) that the horse-power required for a weight W' at a speed V' is equal to the horse-power required for a weight W at a speed V multiplied by $\left(\frac{W'}{W}\right)^{3/2}$, where V and V' are connected by the equation $\frac{V'}{V} = \sqrt{\frac{W'}{W}}$. This rule may be simply expressed in tabular form as under:

Weight W		Weight W'	
Speed	Horse-power required	Speed	Horse-Power required
V	$H.P.$	$V \sqrt{\frac{W'}{W}}$	$H.P. \times \left(\frac{W'}{W}\right)^{3/2}$

From the original $H.P.$ curve corresponding values of V and $H.P.$ can be read off, and then corresponding values of speed and horse-power required for the new weight can be obtained by means of the above table. The method is further illustrated by the following example.

Example. Determine the performance of the aeroplane of p. 95 when the aeroplane is carrying an extra load of 750 lb.

We have
$$\frac{W'}{W} = \frac{3700}{2950}$$

$$= 1.254.$$

$$\therefore \sqrt{\frac{W'}{W}} = 1.12 \text{ and } \left(\frac{W'}{W}\right)^{3/2} = 1.405.$$

From the $H.P_r$ curve of Fig. 56 or Fig. 58 we read off corre-

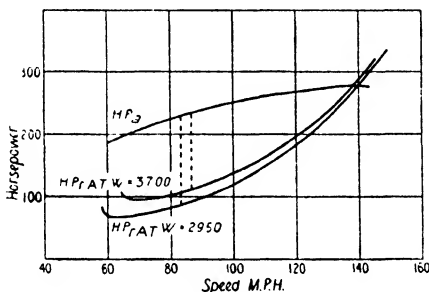


FIG. 64. Effect of Change of Weight.

sponding values of V and $H.P_r$ for $W = 2950$ and correct for the new weight as follows:

V (m.p.h.)	$H.P_r$ (from curve)	V' ($= V \times 1.12$)	$H.P_r'$ ($= H.P_r \times 1.405$)
60	68.7	67.2	96.5
70	70.9	78.4	99.6
80	81.5	89.6	114.5
90	97.8	100.8	137.4
100	118.8	112.0	166.9
110	146.1	123.2	205.2
120	182.6	134.4	256.5

The plotting of the above values of V' , $H.P_r'$ gives the new curve of horse-power required, and this is shown in Fig. 64. The original $H.P_r$ curve is included for comparison, and the $H.P_a$ curve shown is taken from Fig. 58.

The top speed at the new weight is seen to be 138 miles per hour, while the maximum value of Z is 126 and occurs at about 86.5 miles per hour. Hence

$$\begin{aligned}\text{the maximum rate of climb} &= \frac{Z \times 33000}{W} \\ &= \frac{126 \times 33000}{3700} \\ &= 1124 \text{ ft./min.}\end{aligned}$$

A comparative table of the performance of the aeroplane at the two weights is given below:

TABLE VII
EFFECT OF CHANGE OF WEIGHT ON PERFORMANCE

	$W = 2950 \text{ lb.}$	$W = 3700 \text{ lb.}$
Top Speed	139.7 m.p.h.	138 m.p.h.
Max. rate of climb	1615 ft./min.	1124 ft./min.
Best climbing speed	83 m.p.h.	86.5 m.p.h.

The general effects of the extra load may be summarized as follows:

- (1) A *small* reduction of the maximum level speed,
 - (2) A *large* reduction of the rate of climb,
- and (3) A small increase in the best climbing speed.

A further effect is, of course, an increase in the landing or stalling speed.

The most noticeable feature is the vast difference between the effects of the extra load on the top speed and rate of climb respectively, but this can be simply explained. For at high speeds corresponding to low values of k_L , the increase of k_D with increasing k_L is not very great; hence, at a given (high) speed, the higher value of k_L demanded by an extra load does not involve a large drag increase. It is not therefore to be expected that any reasonable extra load will result in a big top speed

reduction. On the other hand, at the slower climbing speeds corresponding to high values of k_L , the drag coefficient k_D increases rapidly with increasing k_L ($k_D \propto k_L^2$, for instance), and so a higher working value of k_L means a relatively large drag increase. This increase of drag, coupled with the extra weight to be lifted, must result in a large reduction of the rate of climb.

Effect of Height. So far the performance of the aeroplane has been calculated for ground level only; it remains now to study the effect of height. As the height increases the density decreases, and in consequence both the drag and the engine power at any given speed are different from those at ground level. Hence both the $H.P_r$ and $H.P_a$ curves vary with height.

With regard to the horse-power required at any given height, fresh calculations may easily be carried out using the appropriate value of the relative density σ , as given in Table I. Alternatively, if the $H.P_r$ curve for ground level has been prepared, it may be corrected for any other height by a method similar to that used for change of weight.

For let V , V' be the speeds at ground level and the given height respectively at a given angle of incidence. Then $V = V'\sqrt{\sigma}$, since constant incidence means constant indicated air speed (see p. 27) and V is both the true and indicated air speed at ground level. But constant indicated air speed means constant drag, for $D = k_D \sigma \rho S V^2 = k_D \rho S V_i^2$ and k_D is constant. Hence, if $H.P_r$ and $H.P'_r$ are the corresponding values of the horse-power required,

$$\begin{aligned} \frac{H.P'_r}{H.P_r} &= \frac{DV'}{DV} \\ &= \frac{V'}{V} \\ &= \frac{1}{\sqrt{\sigma}}, \end{aligned}$$

i.e.

$$H.P'_r = H.P_r \times \frac{1}{\sqrt{\sigma}}.$$

Aeroplane Performance

Thus the following table holds:

Zero Height. Relative density = 1.		Relative density = σ	
Speed	Horse-Power required	Speed	Horse-Power required
V	$H.P.$	$V \frac{1}{\sqrt{\sigma}}$	$H.P. \frac{1}{\sqrt{\sigma}}$

By means of this table the curve of Fig. 56 has been corrected for a height of 10,000 ft., at which $\sigma = 0.738$, and the corrected curve is shown in Fig. 65.

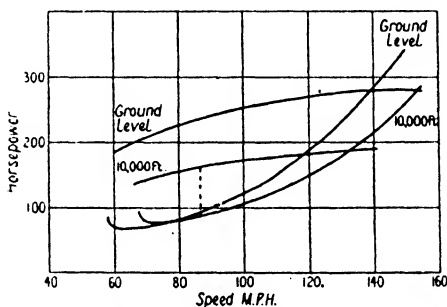


FIG. 65. Effect of Height.

The effect of the reduced density at height on the engine is, of course, a reduction of the engine power. In the early days of flying it was thought that the horse-power varied directly as the density, but it has now been found that the rate of decrease of power is more rapid than the rate of decrease of density and is probably more a function of the pressure than the density. Without going into this involved question more deeply, it may be stated that for most modern engines the engine power appears to be very nearly proportional to the relative pressure, so that at 10,000 ft. the horse-power is about 68.8 per cent. (see Table I) of its ground level power at the same engine revolutions.

It is not sufficiently accurate, however, to assume that the ground level $H.P.$ curve can therefore be corrected for a height of 10,000 ft. simply by multiplying the horse-power scale by

0.688. The next chapter will show that it is inaccurate for two reasons, viz.:

- (1) At a given speed the engine does not develop the same revolutions at different heights; the equivalent ground level horse-power is therefore not the same, for the power is roughly proportional to the revolutions.
- (2) Since the engine revolutions are not the same, the air-screw revolutions are not the same. This results in a different airscrew efficiency.

The full treatment of these points is left till later, but the curve of horse-power available for a height of 10,000 ft. is included in Fig. 65.

From this figure the performance at 10,000 ft. can be estimated. It will be seen that the top speed is 132.5 miles per hour, while the maximum value of Z is 73.4 and occurs at a speed of 86.5 miles per hour. The maximum rate of climb is therefore given by

$$\begin{aligned}\text{Climb} &= \frac{73.4 \times 33000}{2950} \\ &= 820 \text{ ft./min.}\end{aligned}$$

The best climbing speed is slightly greater than that at ground level. It is usual, however, to express climbing speeds as indicated air speeds. Thus the best climbing speed is $86.5 \times \sqrt{0.738} = 73.5$ miles per hour (indicated).

Similar calculations have been carried out for a height of 15,000 ft., and the calculated performance at this height is given in the table below which summarizes the whole performance:

TABLE VIII
CALCULATED SPEED AND CLIMB

<i>Height (feet)</i>	<i>Top Speed (m.p.h.)</i>	<i>Max. Rate of Climb (ft./min.)</i>	<i>Best Climbing Speed (m.p.h. indicated)</i>
0	139.7	1615	83
10,000	132.5	820	73.5
15,000	126.0	475	70.5

Aeroplane Performance

The table shows that speed, climb, and indicated climbing speed all decrease as the height increases.

Ceiling. Since the rate of climb decreases continually as the height increases, there must be a height at which the climb vanishes. This height, which is the greatest height to which an aeroplane can climb, is called the **absolute ceiling**. It can be found by plotting the climb values of Table VIII as in Fig. 66

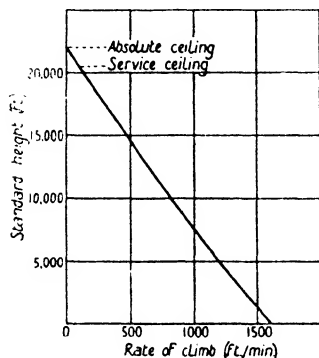


FIG. 66. Variation of Climb with Height.

and by continuing the curve until it cuts the height axis. Experience has shown that in nearly all cases the climb curve may be taken to be a straight line, except at the lower heights, say below 5,000 to 10,000 ft. In this case the absolute ceiling is found to be 22,000 ft. The height at which the rate of climb is 100 ft. per minute is called the **Service Ceiling** and represents roughly the maximum *practical height* at which an aeroplane can operate. Fig. 66 gives a service ceiling of 20,500 ft. The vanishing of the climb at the absolute ceiling shows that the curves of horse-power required and horse-power available at this height touch one another as in Fig. 67, for at no point is there any excess horse-power Z . Hence the absolute ceiling is the height at which there is only one possible speed of flight.

Supercharging. In order to resist the decrease of speed and climb which accompanies increase of height, aero engines are often supercharged. Supercharging means that the air is admitted to the cylinders under pressure, so that compensation is made for the reduction at height of the atmospheric density and pressure. With some supercharged engines the supercharger works in such a manner that, from ground level to a certain pre-determined height, full compensation is made at

every height for the varying atmospheric conditions, and so the full ground level power is maintained. Beyond the given height of course, the supercharger ceases to compensate fully, and the power begins to fall off.

The effect of such supercharging on the performance of an aeroplane is enormous. Up to the given height the $H.P_a$ curve remains approximately the same as the ground level curve, and therefore the speed and climb both increase with height. (Actually the $H.P_a$ curve is not quite constant owing to variations in the engine revolutions and the airscrew efficiency (p. 111), but as an approximation in studying the effect of supercharging the curve may be taken as constant.) For instance, it will be seen from Fig.

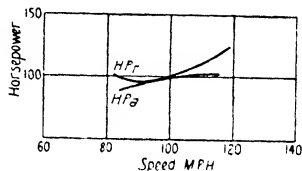


FIG. 67. H.P. Curves at Ceiling.

65 that, if the engine is supercharged to maintain its full ground level power up to a height of 10,000 ft., the top speed at this height will probably rise from 132.5 to 153.5 miles per hour, while the maximum value of Z will rise from 73.4 to 148.5, corresponding to an increase of climb from 820 to 1,660 ft. per minute.

A Useful Approximation in Top Speed Calculations. When an aeroplane is flying level the climb is zero and therefore $T = D$.

But

$$TV = \eta P_{550},$$

$$\therefore \eta P_{550} = DV$$

$$= k_D \rho S V^3.$$

Hence

$$V^3 = \frac{\eta P_{550}}{k_D \rho S} \quad \dots \dots \dots (9)$$

Now, when an aeroplane is flying at its top speed at low heights, it is working at a low value of the lift coefficient, and at low values of the lift coefficient (about $k_L = 0.1$, say) the change of k_D with k_L is not very great (see p. 92). Hence, if it is desired to study the effect on top speed of small changes in the horse-

power available, k_D may be taken to be constant. The above equation then reduces to the approximate form

$$V^3 = k \times \eta P \quad \dots \quad (9a)$$

where k may be taken as constant $\left(= \frac{550}{k_D \rho S} \right)$ for any particular aeroplane.

Example. An aeroplane is capable of a top speed of 120 miles per hour when fitted with an engine of 400 B.H.P. Find the probable top speed when a new engine of 450 B.H.P. is fitted, assuming the weight and efficiency are unaltered and the drag is the same with both engines.

Let $V_{\text{m.p.h.}}$ be the new speed in miles per hour. Then

$$V_{\text{m.p.h.}}^3 = k \times \eta \times 450.$$

Also

$$120^3 = k \times \eta \times 400.$$

[By expressing speeds in m.p.h. instead of f.p.s., k no longer has the value $\frac{550}{k_D \rho S}$, but it is still constant for the two cases if k_D is considered constant.]

Hence, by division,

$$\frac{V_{\text{m.p.h.}}^3}{120^3} = \frac{450}{400},$$

$$\begin{aligned} \therefore V_{\text{m.p.h.}} &= 120 \times \sqrt[3]{\frac{450}{400}} \\ &= 124.8. \end{aligned}$$

Rapid Prediction of Top Speed. In order to make a rapid prediction of the probable top speed of an aeroplane near the ground without going to the trouble of preparing the $H.P.$ and $H.P_a$ curves, it is often customary to make the following assumptions:

- (1) The horse-power and the airscrew efficiency both have their maximum values at top speed,
 - and (2) The lift coefficient is that corresponding to minimum drag, so that the minimum value of overall k_D may be taken.
- By substituting these values in equation (9) a value can be

found for the probable speed. Generally not much error is introduced by this method, but a second approximation can be made, if desired, by calculating the value of k_L appropriate to the speed obtained, and then using the corresponding value of k_D (as read from the k_D curve) in a second application of equation (9).

Suppose, however, that an estimate of the probable speed is required in the course of design before the airscrew efficiency and the drag have been determined. (This is usually required before the airscrew can be designed). Equation (9) can be written

$$V^3 = k_1 \frac{\eta}{k_D} \frac{P}{S},$$

where $k_1 \left(= \frac{550}{\rho} \right)$ is a constant for all aeroplanes.

If now an *average* value is assumed for $\frac{\eta}{k_D}$, the equation becomes

$$V = k_2 \sqrt[3]{\frac{P}{S}} \quad . \quad . \quad . \quad . \quad . \quad (10)$$

where $k_2 = \sqrt[3]{k_1 \frac{\eta}{k_D}}$ and may be taken as constant.

Such an equation is often used by designers to get a rough and preliminary estimate of the probable top speed. The factor $\frac{\eta}{k_D}$ is a measure of the aerodynamic efficiency of the aeroplane and, if the actual top speed comes out at a higher figure than that suggested by equation (10), it means that aerodynamically the aeroplane is above the average.

To get a value for k_2 , consider the aeroplane previously discussed; in this case $P = 400$, $S = 320$ and $V = 140_{\text{m.p.h.}}$. On substituting these values in (10) and expressing V in miles per hour, the value of k_2 is found to be 130. Hence, if this aeroplane may be taken as an *average*, a rough estimate of the probable top speed is given by the equation

$$V_{\text{m.p.h.}} = 130 \sqrt[3]{\frac{P}{S}} \quad . \quad . \quad . \quad . \quad . \quad (11)$$

This equation has been applied to many existing types of aeroplane, and it is found that the value $k_2 = 130$ represents a fair average figure. It is quite possible, of course, that this value will need to be amended as aeroplane design improves.

The Importance of Wing Loading and Power Loading.

The power loading of an aeroplane is defined as $\frac{W}{P}$, while the wing loading $\frac{W}{S}$ has already been mentioned in a previous chapter. The values of these loadings throw considerable light on the probable performance of an aeroplane. Obviously a low power loading, i.e. a low weight per horse-power, will always mean a high performance, but the effect of a high or low wing loading is not so obvious. In point of fact the demands of top speed and climb in this respect are mutually antagonistic.

Consider first of all top speed. The approximate equation (11) may be written

$$V_{m.p.h.} = 130 \sqrt[3]{\frac{W/S}{W/P}}.$$

A high wing loading and a low power loading are therefore obvious indications of high speed, but it must be remembered that, as the wing loading increases, so also does the landing speed. If all aeroplanes had the same landing speed, then, neglecting the variation in the values of $k_{L_{max}}$ for different aerofoil sections, $\frac{W}{S}$ would be constant and the criterion of top speed

for average aerodynamic efficiency would be $\frac{1}{W/P}$ simply.

Consider now the rate of climb; the climb is given by

$$\begin{aligned} \text{Climb (ft./sec.)} &= \frac{H.P_a - H.P_r}{W} \times 550 \\ &= \frac{\eta P 550}{W} - \frac{DV}{W}, \text{ since } H.P_a = \eta P \text{ and } H.P_r = \frac{DV}{550}. \end{aligned}$$

The first term shows the importance of a low power loading, while the second term may be written

$$\begin{aligned}\frac{DV}{W} &= \frac{V}{L/D}, \text{ since } W = L \\ &= \frac{\sqrt{\frac{W}{k_L \rho S}}}{k_L/k_D} \\ &= \frac{1}{\sqrt{\rho}} \cdot \frac{k_D}{k_L^{1/2}} \sqrt{\frac{W}{S}}\end{aligned}$$

Hence, if all aeroplanes had the same lift and drag characteristics and climbed at the same value of k_L (say at the value corresponding to maximum L/D), $\frac{k_D}{k_L^{3/2}}$ would be constant and the term $\frac{DV}{W}$ would be proportional to $\sqrt{\frac{W}{S}}$. A low wing loading is therefore conducive to a high rate of climb.

The expression $\frac{k_L^{3/2}}{k_D}$ may be regarded as a measure of the aerodynamic efficiency at climbing speeds in the same way that $\frac{\eta}{k_D}$ is a measure of the efficiency at top speed.

The above results may be summarized by stating that, apart from considerations of aerodynamic efficiency,

- (1) *A high wing loading helps top speed,*
- (2) *A low wing loading helps climb.*

Also it is obvious that, for a given power loading, a lightly-loaded aeroplane will take off more quickly than a heavily-loaded one.

Rapid Prediction of Ceiling. The importance of a low wing loading with regard to rate of climb and ceiling has been further illustrated by several writers, who have shown that for constant aerodynamic efficiency the ceiling increases as the ratio

$\frac{1}{W/P\sqrt{W/S}}$ increases. This brings out more clearly the relative

importance of the two loadings. For the rapid prediction of ceiling Bairstow, in his *Applied Aerodynamics*, suggests an approximate formula involving this ratio, and the curve of Fig. 68 has been prepared from a slightly modified form of this formula. Such a curve is sometimes useful in preliminary performance estimates, but it is not of the same order of accuracy as equation (11) for the rapid prediction of speed.

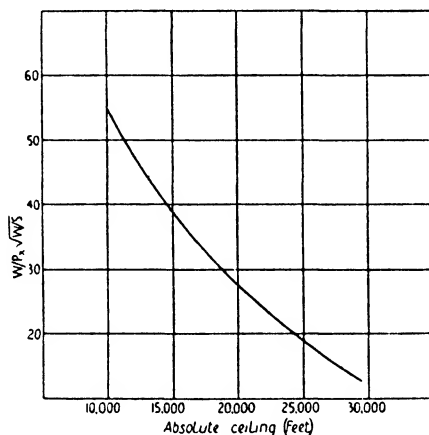


FIG. 68. Ceiling Curve for Rapid Prediction.

Drag Analysis and Application to Design. The foregoing sections have shown how the performance of an aeroplane depends upon its loadings, given average aerodynamic efficiency. The part played by the drag coefficient k_D in determining this efficiency calls for no explanation, but it is important to understand exactly upon what k_D depends and the relative importance of its components.

Now the total drag coefficient k_D consists of the induced drag coefficient k_{D_1} , the profile drag coefficient k_{D_0} and the parasite drag coefficient k_{D_p} , and of these k_{D_1} depends principally on the aspect ratio, k_{D_0} on the aerofoil section and k_{D_p} on the exterior form of the aeroplane. All of them, however, vary with k_L and,

in order to study their relative importance in performance, it is necessary to consider top speed and climb separately. For this purpose an average aeroplane with an aspect ratio of about 6.5 is taken, and it is supposed that its top speed near the ground occurs at $k_L = 0.1$ and its best climbing speed at $k_L = 0.35$.

(a) *Top speed.* Approximate figures for the three types of drag at top speed are given below:

Induced drag coefficient $k_{D_1} = 0.0015$

Profile drag coefficient $k_{D_0} = 0.0055$

Parasite drag coefficient $k_{D_p} = 0.0150$.

The following points should be noted:

(1) $k_{D_1} \propto \frac{k_L^2}{A}$ and its low value is due to the low value of k_L .

Aspect ratio is relatively unimportant as far as top speed is concerned, and little saving in the total drag can be effected by the use of a high aspect ratio. For instance, an increase of aspect ratio from 6.5 to 10 merely reduces k_{D_1} from 0.0015 to $0.0015 \times \frac{6.5}{10}$, i.e. 0.0010.

Furthermore a high aspect ratio probably entails a little extra weight and a little extra parasite resistance (due to the added external bracing drag), while it is definitely unfavourable to rapid manœuvre owing to the increase in span.

(2) k_{D_0} depends upon the thickness and camber of the centre line (see Chapter V). Clearly the thickness should be kept down as much as possible, but its value is generally determined by structural considerations. In addition it is sometimes possible to reduce external bracing drag by the use of a thicker wing.

The profile drag can, however, be kept low by a proper choice of centre line camber. Since the working value of k_L is small, the camber should be small also. Reference to Fig. 46 will show that, in the neighbourhood of $k_L = 0.1$, the section of camber 0.02 shows a saving in k_{D_0} of about 0.0017 over the section of camber 0.05. A low camber section is therefore desirable for

high speed, but it must be remembered that, for a given thickness, $k_{L\max}$ increases with the centre line camber (p. 76).

(3) k_{D_p} forms as much as 70 per cent. of the total k_D ; hence high speed depends primarily on good streamlining and the reduction of frontal area.

(b) *Climb*. With regard to aerodynamic efficiency at climbing speeds the problem of wing design is considerably changed, and the change is revealed by the following points:

(1) at $k_L = 0.35$ the induced drag coefficient is 0.0170. If the comparatively small increase of parasite and profile drag is neglected, it will be seen that the induced drag is now of greater importance than the parasite drag. It represents in fact about 50 per cent. of the total drag. The need for a high aspect ratio is therefore obvious. For instance, an increase of aspect ratio from 6.5 to 10 means a k_{D_i} decrease of 0.0060—a reduction of 16 per cent. of the total drag.

(2) Since the working value of k_L is high, a high centre line camber (about 0.05) is indicated. Fig. 46 shows that at $k_L = 0.35$ the high camber section shows a saving of about $k_{D_0} = 0.0010$ over the low camber section.

The above analysis shows that, with regard to the best choice of aerofoil section and aspect ratio, the requirements of top speed and climb are to some extent irreconcilable, and the choice in any particular case must be governed by the relative importance of speed and climb.

An important point to notice is that what is true for climbing efficiency is also partly true for high speed at great heights. For, as the height increases the top speed and density both decrease, and so the top speed values of k_L increase. Hence the rate of decrease of speed with height may be kept down by the use of a fairly high aspect ratio and a fairly high centre line camber. It is also desirable to use a fairly thick section, since the profile drag for thick sections appears to be more nearly constant than that for thin sections (Fig. 49.)

The Span²/Weight Ratio. For climb, take-off and speed at height, i.e. for performance at the higher values of k_L , it has

now been shown that two desirable characteristics are a low wing loading and a high aspect ratio. Instead, however, of loading and aspect ratio being treated separately, they may be taken together to form a new characteristic called the $\text{span}^2/\text{weight}$ ratio.

For simplicity consider a monoplane. The aspect ratio is defined as $\frac{4s^2}{S}$; hence

$$\frac{\text{Aspect Ratio}}{\text{Wing Loading}} = \frac{4s^2/S}{W/S} = \frac{\text{Span}^2}{\text{Weight}}.$$

A high aspect ratio and a low wing loading are therefore equivalent to a high $\text{span}^2/\text{weight}$ ratio. The reciprocal of this ratio, i.e. $\frac{\text{weight}}{\text{span}^2}$, is sometimes called the *span loading*. This ratio may be obtained in another manner, which brings out more clearly its exact significance. Consider a monoplane, as before. Then the induced drag coefficient is given by

$$\begin{aligned} k_{D_1} &= \frac{2}{\pi A} k_L^2 \\ &= \frac{2S}{\pi \times 4s^2} k_L^2. \end{aligned}$$

Hence the ratio of the lift to the induced drag is given by

$$\begin{aligned} \frac{k_L}{k_{D_1}} &= \frac{k_L \times \pi \times 4s^2}{2S \times k_L^2} \\ &= \frac{\pi \times 4s^2}{2k_L S} \\ &= \frac{\pi}{2} \frac{4s^2}{k_L S V^2} \rho V^2 \\ &= \frac{\pi}{2} \frac{\text{span}^2}{\text{weight}} \rho V^2. \end{aligned}$$

Thus, for a given speed, the $\text{span}^2/\text{weight}$ ratio is a measure of the lift/induced drag ratio.

Aeroplane Performance

The same is true for a biplane, except that the above expression for $\frac{k_L}{k_{D1}}$ is slightly modified by the introduction of the factor $1 + \sigma$ (p. 60).

[NOTE. For a biplane (with equal wings) the aspect ratio is $\frac{4s^2}{S/2}$, i.e. $\frac{8s^2}{S}$, where S is the total area; hence

aspect ratio/wing loading = 2 (span)²/weight.]

From what has been said it follows that, apart from considerations of parasite drag, airscrew efficiency and aerofoil section, the performance of an aeroplane depends upon its power loading and its span²/weight ratio. A very low power loading is always indicative of good performance, both in speed and climb; on the other hand, a high span²/weight ratio helps to offset a high power loading, and especially is this so as regards climb, take-off and general performance at height.

TABLE IX

Type	Aeroplane Characteristics				Remarks
	Power Loading	Wing Loading	Aspect Ratio	Span ² /Weight Ratio	
Racing aeroplane	4	20	5	0.13	Small span to keep down overall size and reduce external bracing. Speed the only consideration.
High-speed fighting aeroplane	6.5	10.5	6	0.20	Small span for above reasons and for manoeuvrability. The low power loading ensures a good climb and ceiling.
Bombing aeroplane	8.5	8.5	9	0.53	A very high span ² /weight ratio since climb, ceiling and performance at height are the main essentials.
Light aeroplane	20	6.5	6.5	0.50	Owing to the very high power loading a high span ² /weight ratio is most important, otherwise the aeroplane would take a large run to get off and would have difficulty in clearing obstacles.
Passenger-carrying aeroplane	10.5	10.5	8.5	0.40	Characteristics are somewhat similar to those of bomber. Power and wing loadings are necessarily high, but take-off and climb are helped by the moderately high span ² /weight ratio.

Aeroplane Characteristics. Table IX given above describes the general characteristics of modern aeroplane types and illustrates the points already discussed, with special reference to the $\text{span}^2/\text{weight}$ ratio. The aeroplanes are all taken to be biplanes, and the $\text{span}^2/\text{weight}$ ratio is calculated from the wing loading and aspect ratio.

EXAMPLES

1. An aeroplane weighs 2,000 lb. and has been designed for a top speed near the ground of 100 miles per hour. If the $\frac{L}{D}$ ratio at this speed is 6.3, find the horse-power required. Hence determine the necessary net airscrew efficiency, assuming the engine develops its maximum horse-power of 120 at this speed.

2. Calculate the probable increase of speed of the above aeroplane when it is fitted with an engine of 150 H.P., the airscrew efficiency remaining unaltered.

[Neglect any change of weight and assume constant k_D .]

3. A certain aeroplane is capable of a speed of 130 miles per hour, the engine developing 350 B.H.P. at this speed and the airscrew being 68 per cent. efficient (net). By gearing the engine so that the airscrew runs at half the engine speed, it is estimated that the airscrew efficiency can be increased to 75 per cent. Find the probable speed with the geared engine, assuming no change in total weight and neglecting any loss of power due to the gearing.

4. An aeroplane is flying on a straight course towards an aerodrome when its engine 'cuts out'. It is then at a height of 2,000 ft. and distant $3\frac{1}{4}$ miles from the aerodrome. What must be the value of its maximum $\frac{L}{D}$ ratio in order that it may just reach the aerodrome?

5. An aeroplane weighing 6,800 lb. is climbing at 72 miles per hour. At this speed the horse-power developed is 590, the net airscrew efficiency 61 per cent. and the $\frac{L}{D}$ ratio 8.1. Calculate the rate of climb and the angle of climb.

6. The measured rates of climb of an aeroplane at various heights (corrected for density, &c.) are as follows:

Standard Height (ft.)	3700	4640	5570	6500	7420	8340	9260	10170
Rate of Climb (ft./min.)	755	660	650	600	525	485	440	370
	11080	11990	12890	13790				
	325	295	240	180				

Assume that the climb curve is a straight line and determine the service and absolute ceilings.

Find also the rate of climb near the ground and the time taken to reach a height of 10,000 ft.

7. The calculated values of the horse-power required and the horse-power available for an aeroplane weighing 1850 lb. are given in the following table:

$V_{m.p.h.}$	55	60	65	70	80	90	100
$H.P_r$	27.2	26.5	28.0	30.9	38.4	50.2	67.0
$H.P_a$	46	48.6	50.8	53.0	56.8	60.1	62.2

Draw the curves of $H.P_r$ and $H.P_a$, and so find the maximum level speed, the maximum rate of climb and the best climbing speed.

8. Determine the top speed and climb of the above aeroplane when it is carrying an overload of 350 lb.

9. An aeroplane weighing 3,300 lb. climbs at 400 ft. per minute at 15,000 ft. at an indicated air speed of 70 miles per hour. At this speed and height the net airscrew efficiency is 65 per cent. and the engine develops 230 B.H.P.

Calculate the rate of climb if the engine is supercharged so that it maintains its full ground level power of 420 B.H.P., assuming that the airscrew efficiency and the drag remain unaltered.

10. From the following data obtain the top speed, the best (indicated) climbing speed and the maximum rate of climb at 10,000 ft. ($W = 4500$ lb.):

$V_{m.p.h.}$	60	65	70	75	80	90	100	110	120
$H.P_r$									
(at ground level)	90	87	89	95	103	123	145	178	217
$H.P_a$									
(at 10,000 ft.)	124	130	135	140	145	155	162	169	175

VIII

THE AIRSCREW

Description. The airscrew is a power-transmitting medium which converts the power of the engine into a forward thrust. Fig. 69 shows a typical two-bladed airscrew and gives the shape of the airscrew in plan and elevation, together with the shape of the cross-section of each blade at various points along the blade.

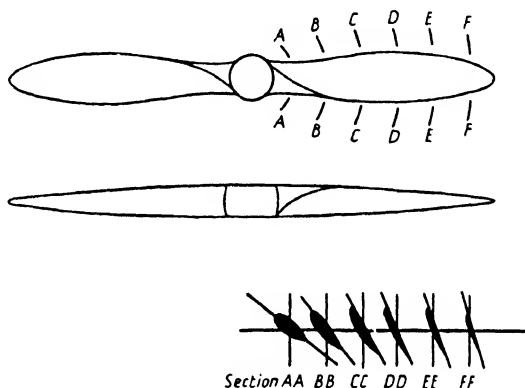


FIG. 69. Typical Two-Bladed Airscrew.

It will be observed that, although the width and thickness of the blade vary, the section at any point (except near the hub or boss) is of aerofoil section with flat undersurface. It will further be noticed that the blade is so twisted that the pitch angle, i.e. the angle between the flat pitch face and the plane of rotation, varies along the blade, the angle decreasing towards the blade tip.

Airscrews are called tractors or pushers according as they are placed in front of or behind the engine.

The ratio of the tip radius (i.e. the distance from the centre of the boss to the blade tip) to the maximum blade width is sometimes called the aspect ratio of the airscrew, and varies in practice from about 4 to 7.

The Airscrew

An airscrew may rotate in either a clockwise or anti-clockwise direction, and is said to be a right-hand airscrew if it rotates in a clockwise direction when viewed from behind.

Engine Power and Engine Torque. Before proceeding to a discussion of the airscrew it is necessary to know something of the general characteristics of the engine—particularly with regard to the power and the torque.

It is shown in books on Applied Mechanics that the B.H.P. of an engine varies directly as the product of the revolutions per

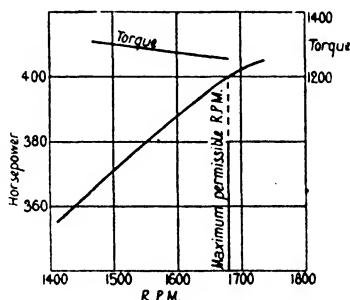


FIG. 70. Engine Power Curve.

minute (R.P.M.) and the brake mean effective pressure in the cylinders.. (The brake mean effective pressure or B.M.E.P. is the actual mean effective pressure multiplied by an efficiency factor to allow for the loss of power due to the internal resistances of the engine itself.) Hence, if the B.M.E.P. were constant for all values of the R.P.M., the B.H.P. would vary directly as the R.P.M., and the curve obtained by plotting B.H.P. against R.P.M. would be a straight line. In practice the B.M.E.P. is not quite constant, and the curve therefore departs slightly from the straight line form. Such a curve which shows the variation of the B.H.P. of an engine with the R.P.M. for full throttle is called the Power Curve, and Fig. 70 shows a typical power curve of a 400 H.P. engine.

The torque of an engine is the mean turning effort exerted on the crank-shaft, and is the turning moment available for rotating

the airscrew. It is connected with the horse-power by a simple relation. For let Q be the torque in pound-feet, P the horse-power and N the R.P.M. Then

$$\text{the work done per revolution} = 2\pi Q \text{ ft.-lb.},$$

so that

$$\text{the work done per minute} = 2\pi NQ \text{ ft.-lb.}$$

Hence,
$$P = \frac{2\pi NQ}{33000}$$

or
$$Q = \frac{33000P}{2\pi N} \dots \dots \dots (1)$$

From this equation it follows that, if the horse-power varied directly as the R.P.M., the torque Q would be constant. The small variation which actually occurs is shown in Fig. 70.

Airscrew Torque. The torque of an airscrew is the moment of resistance which opposes the engine torque.

Consider a rotating airscrew and, for simplicity, suppose the airscrew has no translational velocity. Then each blade experiences a resistance R as shown in Fig. 71, and these resistances form a couple, torque or turning moment about the axis of rotation. Obviously, when the airscrew is rotating at a constant speed, the airscrew torque is just equal to the engine torque.

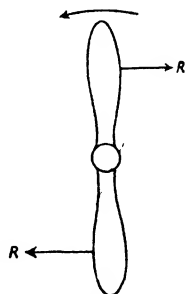


FIG. 71.

For an airscrew working on an aeroplane in flight the value of the airscrew torque depends, of course, on the rotational speed and the forward speed; hence the basis of airscrew design is that at a given forward speed and at a given rate of rotation, the airscrew torque shall equal the engine torque. The general design condition is that the airscrew shall allow the engine to develop its maximum R.P.M. at top speed. If then, the airscrew torque is less than the engine torque at maximum R.P.M.,

The Airscrew

the airscrew will allow the engine to race and it will be necessary to throttle down, while, if the airscrew torque is greater than the engine torque, the airscrew will prevent the engine from developing its full revolutions. In either case there will be a waste of power.

Airscrew Thrust. Since the cross-section of the blade is everywhere of aerofoil section, the blade must experience lift forces as well as drag forces, and it is easy to show that the lift forces provide the thrust of the blade.

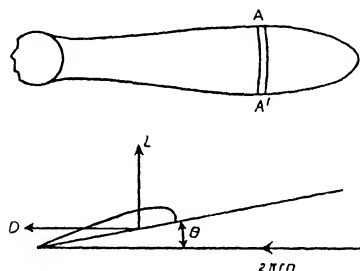


FIG. 72.

Consider, as before, an airscrew rotating with no forward velocity, and consider the behaviour of a small strip or element of the blade AA' as shown in Fig. 72. Then the air passes over this element with a velocity $2\pi nr$, where r is the distance of the element from the axis of rotation and n represents the revolutions per second; for the angular velocity of the blade is $2\pi n$, and so the linear velocity at a distance r from the axis of rotation is $2\pi nr$. Also the angle of incidence of the element is its pitch angle. The element therefore experiences lift and drag forces L and D as shown, and hence the blade behaves as an aerofoil except that the velocity and incidence vary over the blade length. This difference in the conditions under which each element is working complicates the behaviour of the blade as an aerofoil, but each small element may be regarded as supplying its own quota of lift and drag. The summation of all the lift elements gives, of course, the thrust, while

the summation of the drag elements gives the resistance of Fig. 71.

Thrust and Torque Coefficients. Just as it was found convenient to represent the lift and drag characteristics of an aerofoil by the non-dimensional coefficients k_L and k_D , so it is convenient to use non-dimensional coefficients for the thrust and torque characteristics of an airscrew.

Now it was pointed out in Chapter VI that any air force experienced by a body is of the form $R = k\rho l^2 V^2$, where l is some linear dimension of the body. In the case of an aerofoil it was convenient to replace l^2 by the wing area S ; in the case of an airscrew it is more convenient to replace l by the airscrew diameter D . Again, with the airscrew the velocity ($= 2\pi nr$) varies along the blade, but it is always directly proportional at any point to the tip speed πnD , i.e. to nD . The thrust of an airscrew is therefore generally written

$$T = k_T \rho D^2 \times (nD)^2,$$

or

$$T = k_T \rho n^2 D^4 \quad . \quad . \quad . \quad . \quad . \quad . \quad (2)$$

Similarly, since the moment of an air force ($= \text{force} \times \text{distance}$) is of the form $k\rho l^2 V^2 \times l$, the torque Q may be written

$$Q = k_Q \rho n^2 D^5 \quad . \quad . \quad . \quad . \quad . \quad . \quad (3)$$

k_T and k_Q are called the thrust and torque coefficients respectively, and are numerical quantities which are constant for all geometrically similar airscrews rotating at zero speed of advance.

Effect of Forward Speed. Suppose now the airscrew has a forward translational velocity as well as the rotational velocity. Then the velocity and incidence of each element are changed, for the velocity is the resultant of the forward velocity V and the rotational velocity $2\pi nr$ (Fig. 73 (a)). It can be shown, however, that the total thrust and torque may still be expressed as above, but that the values of k_T , k_Q now depend not only on the shape of the airscrew but also on the ratio $\frac{V}{nD}$.

The Airscrew

For consider a small element, as before. It will be seen from Fig. 73 that the resultant velocity is given by

$$V_r \cos \phi = 2\pi nr,$$

or
$$V_r = 2\pi nr \sec \phi \quad . \quad . \quad . \quad . \quad . \quad (4)$$

while the incidence is reduced from the pitch angle θ to $\theta - \phi$, where ϕ is given by

$$\tan \phi = \frac{V}{2\pi nr} \quad . \quad . \quad . \quad . \quad . \quad (5)$$

Also the lift or thrust of the element, measured in the direction

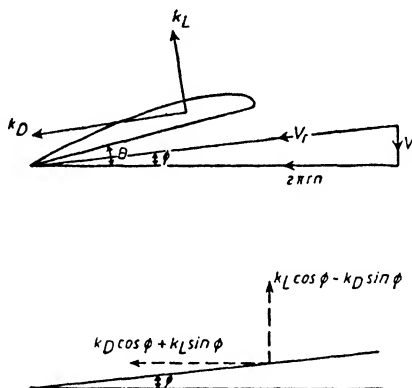


FIG. 73.

of forward motion, is proportional to $k_L \cos \phi - k_D \sin \phi$ and the drag, measured in the plane of rotation, to $k_L \sin \phi + k_D \cos \phi$.

Thus the velocity is again proportional to nD , but in this case it depends on the angle ϕ as well; the lift and drag coefficients of the element also depend on ϕ . But $\tan \phi = \frac{V}{2\pi nr}$, and therefore ϕ is known for every element if $\frac{V}{nD}$ is known, for $2\pi nr$ is proportional to nD . Hence, for a given value of $\frac{V}{nD}$, the thrust and torque of the airscrew may again be written $T = k_T \rho n^2 D^4$ and $Q = k_Q \rho n^2 D^5$, where k_T and k_Q are constants.

In other words k_T , k_Q and $\frac{V}{nD}$ form a system of non-dimensional coefficients for the airscrew analogous to the k_L , k_D and α system for the aerofoil.

Again, just as all aerofoils exhibit the same general charac-

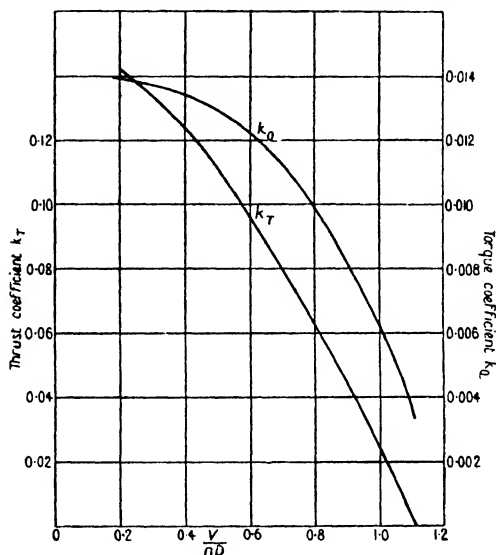


FIG. 74. Variation of k_T and k_Q with $\frac{V}{nD}$.

teristics with regard to the variation of k_L and k_D with α , so do all airscrews with regard to the variation of k_T and k_Q with $\frac{V}{nD}$. The nature of the variation is shown in Fig. 74.

It will be noticed that k_T and k_Q both decrease as $\frac{V}{nD}$ increases, and that k_T vanishes before k_Q . This can be easily explained by returning to the consideration of an element. For equation (5) shows that as $\frac{V}{nD}$ increases the angle ϕ increases also, and therefore the incidence ($= \theta - \phi$) decreases; but k_L and k_D both

decrease as the incidence decreases, and so the thrust of the element must eventually vanish, for the thrust is proportional to $k_L \cos \phi - k_D \sin \phi$. Similarly for the torque of the element, but this cannot vanish until a negative value of k_L is reached, for the torque is proportional to $k_L \sin \phi + k_D \cos \phi$. The same is true for every element, and therefore k_T and k_Q must both decrease as $\frac{V}{nD}$ increases, but k_T must vanish first.

Variation of Engine Speed with Aeroplane Speed. On p. 97 it was stated that the engine speed varies with the forward speed of an aeroplane. It will now be shown how this variation depends upon the k_Q curve of the airscrew and the power curve of the engine. For this purpose an airscrew of 9.25 ft. diameter will be supposed to have the characteristics of Fig. 74 and to be fitted on the engine of Fig. 70.

The calculations start from a selected range of values of N (the R.P.M.), and the following table explains the nature of the calculations and derives the aeroplane speeds corresponding to the chosen engine speeds at full throttle at ground level.

TABLE X
VARIATION OF ENGINE SPEED WITH AEROPLANE SPEED

N	$\frac{n}{(= N/60)}$	$\frac{P}{\text{(from Power Curve)}}$	$\frac{Q}{\left(= \frac{550P}{2\pi n}\right)}$	$\frac{k_Q}{\left(= Q/\rho n^3 D^4\right)}$	$\frac{V/nD}{\text{(from } k_Q \text{ curve)}}$	$\frac{V_{f.p.s.}}{\left(= \frac{V/nD}{\times nD}\right)}$	$V_{m.p.h.}$
1680	28	400	1251	0.00994	0.800	207.2	141.3
1620	27	390.8	1267	0.01083	0.736	183.9	125.3
1560	26	380.7	1281	0.01184	0.647	155.6	106.1
1500	25	370.6	1298	0.01294	0.500	115.6	78.8
1470	24.5	365.6	1306	0.01356	0.365	82.7	56.4

The above table shows that the *engine speed and aeroplane speed decrease together*. Hence, apart from any considerations of airscrew efficiency, the horse-power available decreases as the speed decreases.

Calculation of Thrust. The thrust at any speed may be calculated by the use of the k_T curve. Thus at 141.3 miles per

hour the value of $\frac{V}{nD}$ is 0.8, and the corresponding value of k_T is read from Fig. 74 as 0.0624. Hence the thrust T is given by

$$T = k_T \rho n^2 D^4$$

$$= 848 \text{ lb., on substituting for } \rho, n \text{ and } D.$$

The thrust has been so calculated over the complete range of speeds of Table X, and the variation of thrust with forward

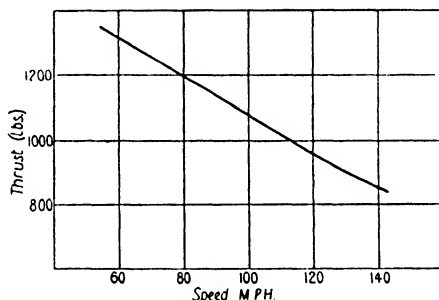


FIG. 75. Variation of Thrust with Forward Speed.

speed is shown graphically in Fig. 75. It will be seen that the thrust decreases as the speed increases, and would eventually vanish at the speed corresponding to the value of $\frac{V}{nD}$ at which $k_T = 0$. In practice this speed would correspond to a very steep dive with the engine full on.

Efficiency. The efficiency of an airscrew is given by

$$\eta = \frac{\text{Work done by airscrew}}{\text{Work done on airscrew}}$$

$$= \frac{TV}{2\pi nQ}$$

$$= \frac{k_T \rho n^2 D^4 V}{2\pi n k_Q \rho n^2 D^5}$$

i.e.

$$\eta = \frac{1}{2\pi} \frac{k_T}{k_Q} \frac{V}{nD} \quad \dots \dots \dots (6)$$

The efficiency has been calculated by means of this formula for the airscrew of Fig. 74 and is shown plotted against $\frac{V}{nD}$ in Fig. 76.

The figure shows that η reaches its maximum value at $\frac{V}{nD} = 0.8$ and decreases to zero at $\frac{V}{nD} = 0$ and $\frac{V}{nD} = 1.11$ (corresponding to $k_T = 0$.) Again, on comparing this figure with Table X, it will

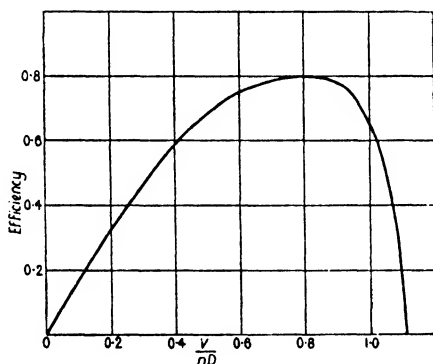


FIG. 76. Airscrew Efficiency.

be seen that the airscrew efficiency attains its maximum value at a forward speed of 141.3 miles per hour, and for all speeds below this the efficiency decreases as the speed decreases. For instance, at a speed of 56.4 miles per hour (corresponding to $\frac{V}{nD} = 0.365$) the efficiency has dropped from its maximum of 80 per cent. to 54.5 per cent. Hence the *decrease of horse-power available with decreasing speed is due to decreasing efficiency and decreasing R.P.M.*

NOTE. The efficiency curve of Fig. 76 is that for the airscrew alone and has not been corrected for slipstream effect on drag.

Pitch. An airscrew resembles an ordinary screw inasmuch as

it rotates about an axis while moving forward along that axis, but differs from an ordinary screw inasmuch as its pitch is not constant. The pitch of a screw is defined as the distance moved forward in one revolution, i.e. the pitch is equal to $\frac{V}{n}$, and, as has been shown above, the airscrew may be working at any value of $\frac{V}{n}$. Two terms, however, are used to define the pitch of an airscrew, viz.:

(a) The Experimental Mean Pitch,

(b) The Geometric Mean Pitch.

The experimental mean pitch is the name given to the ideal pitch, i.e. the maximum value of the pitch at which the airscrew can work without developing a negative thrust. Consider the airscrew already discussed: k_T vanishes when $\frac{V}{nD} = 1.11$, and $D = 9.25$; hence the experimental mean pitch of this airscrew $= \frac{V}{nD} \times D = 1.11 \times 9.25 = 10.27$ ft.

Now it is shown in any book on Applied Mechanics that the pitch of an ordinary screw is $2\pi r \tan \theta$, where θ is the angle which the thread makes with the axis; and the geometric pitch of a section of an airscrew is defined as that of the equivalent screw whose pitch angle is equal to the blade angle of the section. Hence at a distance r from the axis the geometric pitch is $2\pi r \tan \theta$, where θ is the blade or pitch angle at that point. It follows that the geometric pitch is not necessarily constant over the whole blade, but since θ diminishes as r increases the variation is not very great. In practice many airscrews are of constant geometric pitch, but, if the pitch is not constant, the geometric mean pitch is defined as the pitch of a section two-thirds the way along the blade. Hence the geometric pitch

$$= 2\pi \times \frac{2}{3}R \tan \theta$$

$$= \frac{2}{3}\pi D \tan \theta$$

$$= 2.1D \tan \theta,$$

where θ is the blade angle at a radius equal to two-thirds of the tip radius.

The value of the pitch as stamped on all airscrews in this country is defined as above.

There is no consistent connexion between the experimental mean pitch and the geometric mean pitch, but experiment reveals one interesting feature, namely that, if the geometric

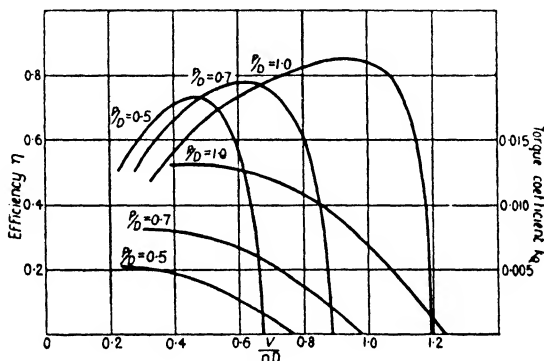


FIG. 77. Effect of Pitch.

mean pitch is denoted by P , then the maximum efficiency always appears to occur at a value of $\frac{V}{nD}$ slightly less than the value of $\frac{P}{D}$ (see Fig. 77).

Effect of Pitch. If experiments are carried out on a series of airscrews, geometrically similar but of varying $\frac{P}{D}$ ratios, the resulting k_Q and η curves will be found to be similar to those of Fig. 77.

This figure shows that high-pitch airscrews are desirable on account of their high efficiencies. Unfortunately the airscrew designer has not a perfectly free choice of pitch. If an airscrew is to be designed for maximum airscrew efficiency at a given forward speed V , and at a given airscrew speed of n revolutions

per second, then the diameter and pitch must be so chosen that the airscrew shall give its maximum efficiency at the correct value of $\frac{V}{nD}$ and also that the airscrew torque shall equal the engine torque. In practice it is found that these considerations of efficiency and torque, together with some considerations of strength, completely determine the choice of pitch and diameter.

As a particular illustration, suppose the characteristics of Fig. 77 all refer to airscrews of the same diameter, and suppose an airscrew of the series is required for an aeroplane in which the engine is to develop a given speed n (revolutions per second) at a given forward speed V . Then the condition of design is that at a given value of $\frac{V}{nD}$ the torque coefficient must be such that the airscrew torque shall equal the engine torque. In other words k_Q must be equal to $\frac{Q}{\rho n^2 D^5}$, i.e. $\frac{550P}{2\pi \rho n^3 D^5}$, where P is the power of the engine at n revolutions per second. The value of k_Q is therefore fixed, and so the $\frac{P}{D}$ ratio is fixed. (For instance, if k_Q must equal 0.0075 at $\frac{V}{nD} = 0.5$, the P/D ratio must be 0.7.)

The obvious way, however, of obtaining high airscrew efficiency is to use an engine with a reduction gear, so that the airscrew runs at a slower rate than the engine. High working values of $\frac{V}{n}$ follow at once, and this is one of the reasons why so many modern engines are now geared.

Fig. 77 also shows the advantage which might be gained by the use of a variable-pitch airscrew. If it were possible to reduce the pitch as the forward speed decreased, then the values of k_Q would be reduced and it would be possible to prevent the R.P.M. from dropping (for $Q = k_Q \rho n^2 D^5$, so that a reduction in the value of k_Q must be accompanied by an increase in the value of n). In addition the efficiencies at the lower values of $\frac{V}{nD}$, i.e. at

the lower speeds, would be increased. Hence a variable-pitch airscrew would give an increase of horse-power available at the slower speeds, and so the rate of climb would be increased.

Effect of Height. At height two factors arise to modify the performance of an airscrew, namely, the loss of engine power and the effect of the reduced density on the air forces experienced by the airscrew. With regard to the engine power, the factor for the loss of power with height, generally denoted by $f(h)$, varies from one type of engine to another, but in the absence of data for any particular engine $f(h)$ may be taken with fair accuracy to be equal to the relative pressure p . (This assumes, of course, that perfect carburation is obtained at all heights by means of some form of altitude control.) Thus the power P and the torque Q at any height can be obtained from the ground level figures at the same value of the R.P.M. by multiplying by p ; the torque coefficient can then be obtained by dividing the torque by $\rho n^2 D^5$. Notice that since $\rho = \sigma \rho_0$, the torque coefficient k_Q may be written

$$\begin{aligned} k_Q &= \frac{Q}{\sigma \rho_0 n^2 D^5} \\ &= \frac{Q_0 \times f(h)}{\sigma \rho_0 n^2 D^5}, \text{ if } Q_0 \text{ is the torque at ground level,} \\ &= \frac{Q_0}{\rho_0 n^2 D^5} \times \frac{f(h)}{\sigma} \\ &= k_{Q_0} \times \frac{f(h)}{\sigma}, \end{aligned}$$

if k_{Q_0} is the torque coefficient at ground level.

Hence the torque coefficient can be obtained from the ground level figure by multiplying by $\frac{f(h)}{\sigma}$.

The performance of the airscrew of Table X is now calculated in this manner for a height of 10,000 ft., at which $f(h) = p = 0.688$ and $\sigma = 0.738$, and is compared with the ground level performance in Table XI.

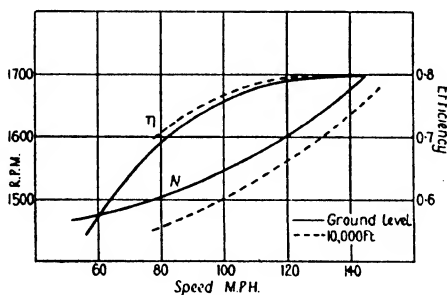
TABLE XI

AIRSCREW PERFORMANCE AT G.L. AND AT 10,000 FT.

G.L.					
N	P	k_q	$\frac{V}{nD}$	$V_{m.p.h.}$	η
1680	400	0.00994	0.800	141.3	0.800
1620	390.8	0.01083	0.736	125.3	0.794
1560	380.7	0.01184	0.647	106.1	0.771
1500	370.6	0.01294	0.500	78.8	0.686
1470	365.6	0.01356	0.365	56.4	0.546

10,000 ft.					
N	P	k_q	$\frac{V}{nD}$	$V_{m.p.h.}$	η
1680	275.2	0.00927	0.840	148.4	0.795
1620	268.9	0.01009	0.790	134.5	0.798
1560	261.9	0.01104	0.720	118.0	0.792
1500	255.0	0.01206	0.622	98.1	0.762
1470	251.5	0.01263	0.556	85.8	0.728

N and η are plotted against V in Fig. 78, and it will be seen

FIG. 78. Effect of Height on N and η .

that the effect of height at any given speed is to reduce the R.P.M., but slightly to increase the efficiency.

Effect of Supercharging. Suppose now the engine in the above is supercharged. Then there is still the same power at,

say, 10,000 ft. as there is at ground level, and therefore the engine drives the airscrew at a much higher rate at this height than it did when unsupercharged. The extra power is so great, however, that it more than compensates for the normal drop in R.P.M. at height, as shown in Fig. 78; the engine will therefore race unless it is throttled down, whence some of the advantage of the supercharging is lost. Conversely, if the airscrew is designed to absorb the full power at 10,000 ft. (as is usually the case), then there will be a large drop in R.P.M. at ground level. Obviously, the greater the height to which the engine is supercharged, the greater the loss of R.P.M. near the ground, and if the loss is very great the aeroplane may experience some difficulty in taking-off. Moreover it is undesirable to run an engine at full throttle at very low R.P.M.

Various means have been devised for overcoming this difficulty, but once again the obvious solution is the variable-pitch airscrew.

Effect of Body Behind an Airscrew. When an airscrew is working in front of a fuselage or engine nacelle, the body modifies to some extent the airflow through the airscrew, and this 'interference' has its effect on the airscrew characteristics. Generally it is found that the presence of the body slightly

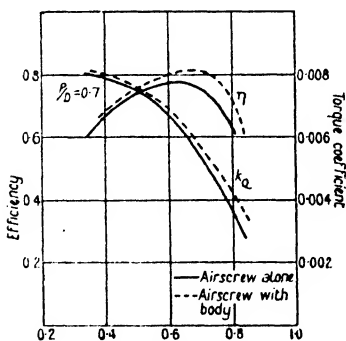


FIG. 79. Effect of Body.

increases the values of k_Q and η , and the type of curves obtained with a body present are shown in Fig. 79. It will be noticed that the maximum efficiency occurs at a slightly greater value of $\frac{V}{nD}$ when the body is present, and so the value of $\frac{V}{nD}$ for η_{\max} is brought still nearer the value of $\frac{P}{D}$.

Effect of Tip Speed. A much more important factor which

affects the behaviour of an airscrew is the actual linear speed of the sections of the blade near the tips. So far it has always been assumed that model wind channel results at low speeds may be applied to the full-scale aeroplane at high speeds by the use of non-dimensional coefficients. When, however, the full-scale speed becomes very high, this assumption ceases to be valid—owing to the fact that, if the speed approaches or exceeds the speed of sound (about 1,120 ft. per second), the type of flow is quite changed. At normal aeroplane speeds the air may be regarded as flowing past the aeroplane without suffering any compression, but when speeds in the neighbourhood of the speed of sound are approached compressibility effects become important. In an airscrew the speeds of the sections near the tips are often very high; for instance, an airscrew of 10 ft. diameter running at 1,800 R.P.M. has a tip speed ($= \pi nD$) of 943 ft. per second.

Now experiments on aerofoils at high speeds show that, beyond a speed of about 0.6 times the speed of sound, the non-dimensional coefficients k_L and k_D begin to change, k_L decreasing and k_D increasing as the speed increases. Hence, since the thrust of an airscrew depends principally on the lift of its elements, and the torque on their drag, it follows that the thrust decreases and the torque increases as the speed of rotation increases; and this has been borne out by special experiments on model airscrews running at very high tip speeds.

Up to a tip speed of about 850 ft. per second these compressibility effects are not very important, but at a speed of about 1,100 ft. per second it is quite possible to get a loss of efficiency of some 20 per cent. or even more. This forms another big argument in favour of gearing.

Effect of Slipstream on Body Drag. Since the fuselage (or engine nacelle) is in the slipstream, its drag is greater with the airscrew running than it is at the same forward speed in free air.

Let the drag at a speed V in free air be R_0 and the drag at the same speed with airscrew running R . Also let the thrust of the

airscrew be T . Then experiment shows that in all cases there is a relationship of the form

$$\frac{R}{R_0} = a + b \frac{T}{\rho V^2 D^2} \quad \dots \quad (7)$$

where a, b are constants for any particular airscrew-body combination.

$\frac{R}{R_0}$ is called the *slipstream factor* and is the factor by which the free air drag must be multiplied to allow for the increased velocity of the slipstream.

It is found that a always has a value very close to unity. This is only to be expected, for, if the thrust is regarded as being equal to the rate of change of momentum of the slipstream, the added slipstream velocity is zero when $T = 0$, and so $R = R_0$. Sometimes the value of a is about 0.85, and this can be explained by supposing that the airscrew 'shields' the body when there is no thrust. The value of b appears to vary from about 2 to 10 for different airscrew-body combinations. If the body is of very good streamline form the value of b is high, since a rotating mass of air like the slipstream is bound to have a greater effect on a good streamline body than on one with a high free air drag. It must not be thought from this that the slipstream always counteracts the effect of streamlining. Although the value of b is high for a good streamline body, the saving in the free air drag more than compensates for the extra slipstream effect. In practice the constant b rarely exceeds a value of 6, and for normal airscrew-body combinations is more likely to lie between 2.5 and 4.

In order to study the effect of the slipstream, take average values $a = 1, b = 3$, so that the slipstream factor may be written

$$\frac{R}{R_0} = 1 + \frac{3T}{\rho V^2 D^2}.$$

Now let k_D' be that part of the parasite drag coefficient due to the body alone. Then the added drag due to the slipstream

$$\begin{aligned}
 &= k_D' \rho S V^2 \times \frac{3T}{\rho V^2 D^2} \\
 &= \frac{3k_D' S T}{D^2}
 \end{aligned}$$

Hence, if the added drag is regarded as equivalent to a loss of thrust (see p. 95), the net thrust T' is given by

$$\begin{aligned}
 T' &= T - \frac{3k_D' S T}{D^2} \\
 &= T \left(1 - \frac{3k_D' S}{D^2} \right).
 \end{aligned}$$

It follows from this that, since k_D' , S and D^2 are constant for any particular aeroplane, the effect of the slipstream is always to reduce the thrust, and therefore the efficiency, by a constant percentage. The expression $\frac{3k_D' S}{D^2}$ can be evaluated in any given case, and so the airscrew efficiency corrected to give the net efficiency. Generally the value of $\frac{3k_D' S}{D^2}$ is of the order of 0.1; hence the net airscrew efficiency is about 90 per cent. of the actual efficiency.

Notice that, if interference effects are present so that k_D' varies with incidence, the effect of the slipstream cannot be allowed for by a simple efficiency reduction factor, for the expression $\frac{3k_D' S}{D^2}$ is no longer constant. In such a case it becomes necessary to apply a correction at every angle of incidence.

EXAMPLES

1. The top speed of an aeroplane near the ground is 120 miles per hour. At this speed the engine runs at 1680 R.P.M. and develops 360 H.P. If the diameter of the airscrew is 9 ft. 6 in., find the values of $\frac{V}{nD}$ and k_D at this speed.

If the corresponding value of k_T is 0.0598, calculate the efficiency.

2. The thrust and torque coefficients of an 8 ft. diameter airscrew are given in the following table:

$\frac{V}{nD}$	0.4	0.5	0.6	0.7	0.8	0.9
k_T	0.1041	0.0956	0.0853	0.0731	0.0591	0.0431
k_Q	0.01231	0.01191	0.01129	0.01043	0.00930	0.00784
			1.0 0.0252 0.00602	1.1 0.0056 0.00379		

Draw the k_T curve and determine the experimental mean pitch.

Calculate the efficiency for each value of $\frac{V}{nD}$ and draw the efficiency curve. Hence obtain the value of the maximum efficiency and the value of $\frac{V}{nD}$ at which it occurs.

3. The airscrew of the above example is fitted on an engine which develops 200 H.P. at 1750 R.P.M. Obtain the aircraft speed corresponding to this engine speed. (Draw the k_Q curve.)

4. An aeroplane is fitted with an engine whose normal H.P. is 500 at 2,000 R.P.M. Find the engine torque.

If the engine is fitted with a reduction gear so that the airscrew speed is half the engine speed, find the R.P.M. of the engine at full throttle when the aeroplane is stationary on the ground, given that the airscrew is 12 ft. in diameter and the estimated value of k_Q at $\frac{V}{nD} = 0$ is 0.0090. The engine torque at full throttle may be assumed constant.

5. Show that for a given airscrew at a given value of $\frac{V}{nD}$ the power absorbed varies as n^3 , where n is the revolutions per second.

An aeroplane is fitted in turn with two engines of the same type. With the first engine the standing R.P.M. at full throttle are 1530; with the second engine they are 1560. If the horse-power of the first engine at 1530 R.P.M. is 380, find the horse-power of the second engine at this speed, assuming that the horse-power is directly proportional to the R.P.M.

6. The following data refer to a light aeroplane:

Engine:	N	1890	1920	1980	2040	2100	2160
	P	76	77.6	80.5	83.3	86.0	88.0
Airscrew:	V						
($D = 6.5$ ft.)	nD	0.4	0.45	0.50	0.55	0.60	0.65
	k_Q	0.00794	0.00777	0.00751	0.00722	0.00681	0.00625
	η	0.653	0.698	0.732	0.759	0.775	0.780
			0.70	0.75			
			0.00559	0.00478			
			0.765	0.734			

Draw the k_Q and η curves, and so find the values of $V_{m.p.h.}$ and ηP corresponding to the given values of N . Hence construct the curve of horse-power available, and read off the horse-power available at the climbing speed of 60 miles per hour and at the top speed of 105 miles per hour.

7. An aeroplane is fitted with a supercharged engine which maintains its full ground level power up to a height of 10,000 ft. The airscrew is 9 ft. 6 in. in diameter and was designed for top speed at this height at the maximum permissible engine speed. From the power curve the maximum permissible R.P.M. are found to be 1800, the ground level power then being 450 B.H.P.

Find the estimated speed on which the airscrew was designed, given that the airscrew torque coefficient is as follows:

$\frac{V}{nD}$	0.3	0.4	0.5	0.6	0.7	0.8
k_Q	0.0143	0.0141	0.0137	0.0130	0.0117	0.0095

Show also that at ground level the engine is unable to develop its normal speed of 1620 R.P.M. below a speed of about 138 miles per hour. (Assume constant torque.)

8. From wind channel experiments on an airscrew-fuselage combination it is found that the slipstream factor $\frac{R}{R_0}$ can be written

$$\frac{R}{R_0} = 1 + 2.8 \frac{T}{\rho V^2 D^2}.$$

If the diameter of the full-scale airscrew is 8 ft. and the estimated drag of the fuselage only in free air is 45 lb. at 100 ft. per second, find the equivalent percentage reduction of airscrew thrust due to the added slipstream drag of the fuselage.

IX

THE EQUILIBRIUM OF THE AEROPLANE

The General Problem. When a number of co-planar forces act on a body, the conditions of equilibrium, or of steady motion, are obtained as follows:

- (1) Resolve the forces in two directions at right angles,
 - (2) Equate to zero the algebraic sum of the resolved parts in each direction,
- and (3) Equate to zero the algebraic sum of the moments of the forces about any convenient point in their plane.

For the aeroplane the equations obtained by resolution have been given in Chapter VII, and these constitute two of the

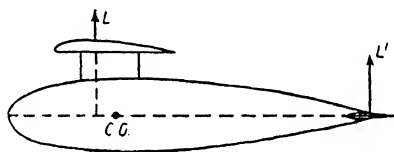


FIG. 80.

equations of motion. The third equation is obtained by taking moments about the centre of gravity, and for the aeroplane to be in balance the algebraic sum of the moments of the forces about the C.G. must be zero.

Consider now an aeroplane flying horizontally, and, for simplicity, suppose that the thrust and drag pass through the C.G., so that they do not enter into the moment equation. Then, unless the centre of pressure is vertically above the C.G., the lift will produce a moment tending to rotate the aeroplane, and this turning moment will be positive or negative (i.e. clockwise or anti-clockwise) according as the C.P. is in front of or behind the C.G. (Fig. 80). It is the function of the tail plane to contribute the necessary righting or balancing moment by giving a small tail plane lift. Obviously, if the C.P. is in front of the

The Equilibrium of the Aeroplane 147

C.G., the lift on the tail plane will be upwards or positive, while if the C.P. is behind the C.G., the tail plane lift will be downwards or negative.

Now the C.P. is not fixed, but has a different position for every angle of incidence; sometimes it may be in front of the C.G. and sometimes behind. Hence the tail plane lift may be sometimes positive and sometimes negative.

In practice the horizontal distance between the C.G. and the C.P. is always small (in normal flight it rarely exceeds a value of about $0.35c$, where c is the chord length), while the distance between the C.G. and the centre of pressure of the tail plane is generally of the order of $2.5c$ or $3.0c$. The tail plane lift is therefore always small in comparison with the main plane lift.

It is the purpose of this chapter to describe in some detail the operation of the tail plane in producing equilibrium.

Determination of the C.G. The position of the C.G. of an aeroplane is determined in two ways, viz.:

- (1) By calculation in the course of design,
- (2) By weighing the actual completed machine.

By calculation. In the first method the weight of each component (i.e. the wings, the fore part of fuselage, the rear frame, the engine, load, &c.) is estimated together with the position of its centre of gravity referred to some convenient axes. Any axes may be chosen—a common practice is to take vertical and horizontal axes through the leading edge of the lower wing. Then, if $w_1, w_2, w_3 \dots$ are the weights of the components and $(x_1, y_1), (x_2, y_2), (x_3, y_3) \dots$ the coordinates of their centres of gravity referred to the chosen axes, the coordinates of the C.G. of the complete aeroplane are given by:

$$\bar{x} = \frac{w_1x_1 + w_2x_2 + w_3x_3 + \dots}{W}$$

and

$$\bar{y} = \frac{w_1y_1 + w_2y_2 + w_3y_3 + \dots}{W},$$

where $W (= w_1 + w_2 + w_3 + \dots)$ is the total weight of the aeroplane.

148 The Equilibrium of the Aeroplane

This is a well-known theorem in ordinary mechanics.

By weighing. The aeroplane is weighed in two positions, generally called 'tail up' and 'tail down', and measurements are recorded in each case at the wheels and tail skid. In the 'tail up' position (Fig. 81 (a)), let W_1, W_2 be the weights at the wheels and tail skid respectively. Then the C.G. must lie on the vertical line XY which divides the line AB in the ratio of $W_2 : W_1$.

Similarly, if W'_1, W'_2 refer to the weights in the 'tail down' position, the C.G. must lie on the vertical line $X'Y'$ which divides $A'B'$ in the ratio of $W'_2 : W'_1$.

Hence, if the two lines $XY, X'Y'$ are inserted on the same diagram as in Fig. 81 (c), their intersection gives the position of the C.G.

The Mean Chord. In problems of equilibrium and stability it is convenient to replace the two wings of a biplane by a single equivalent wing.

Suppose A_1B_1, A_2B_2 represent the chords of the two wings of a biplane and, first of all, consider the case of a biplane with equal wings (Fig. 82 (a)). Then, if AB

is midway between A_1B_1, A_2B_2 and if the difference in load intensity between the two wings is neglected (see p. 64), the two wings may clearly be replaced by a single wing AB of double the area of a single wing. The line AB is called the mean chord.

Suppose now the wings are unequal, both in span and chord. Then the mean chord AB is the line which divides the distance between the two wings A_1B_1, A_2B_2 in the inverse ratio of

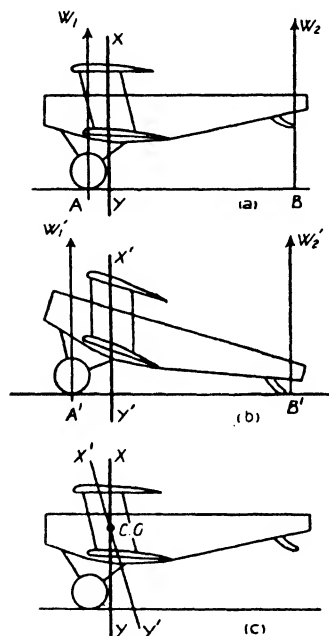


FIG. 81. C. G. Determination.

The Equilibrium of the Aeroplane 149

their areas. Thus, if the upper wing is of twice the area of the lower,

$$\frac{A_1 A}{A A_2} = \frac{1}{2}.$$

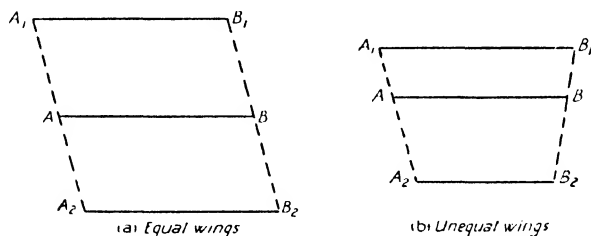


FIG. 82. Mean Chord of Biplane.

Coordinates of the C.G. Let AB (Fig. 83) represent the mean chord of an aeroplane, G the centre of gravity, and let

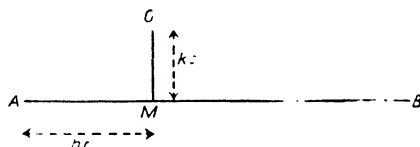


FIG. 83. C. G. Coordinates.

GM be the perpendicular from G on AB . Then the C.G. is always referred to by its coordinates (h, k) defined by

$$h = \frac{AM}{AB}, \quad k = \frac{GM}{AB},$$

or $AM = hc$, $GM = kc$, where c is the length of the mean chord. Note that if the C.G. falls below the mean chord, k is negative.

Wing Moment about the C.G. In order to find the moment of the wing forces about the C.G., the forces may be replaced by $k_L \rho S V^2$, $k_D \rho S V^2$ acting at P , the centre of pressure of the mean chord AB , as in Fig. 84 (a). Hence, if the lift and drag are known, the wing moment may be easily determined.

150 The Equilibrium of the Aeroplane

It is desirable, however, to work in non-dimensional coefficients so that the wing moment for any combination of aerofoil and C.G. position may be expressed non-dimensionally without any reference to the actual weight and wing area of any particular aeroplane.

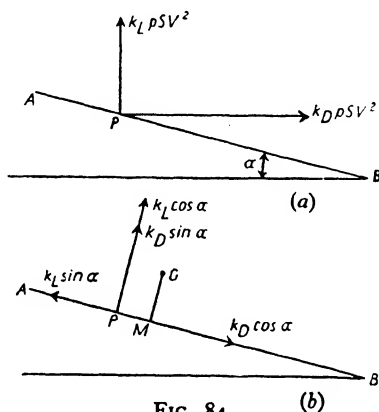


FIG. 84.

The lift and drag forces may be resolved along and perpendicular to the mean chord as in Fig. 84 (b). (Compare Fig. 13, Chapter II.)

The moment about G of the forces at right angles to the mean chord is

$$\begin{aligned}
 & (k_L \cos \alpha + k_D \sin \alpha) \rho S V^2 \times PM \\
 &= (k_L \cos \alpha + k_D \sin \alpha) (AM - AP) \rho S V^2 \\
 &= (k_L \cos \alpha + k_D \sin \alpha) \rho S V^2 \times AM \\
 &\quad - (k_L \cos \alpha + k_D \sin \alpha) \rho S V^2 \times AP.
 \end{aligned}$$

But $-(k_L \cos \alpha + k_D \sin \alpha) \rho S V^2 \times AP$ is the moment about the leading edge and is therefore equal to $k_m c \rho S V^2$ (see p. 29).

Also $k_L \cos \alpha + k_D \sin \alpha$ may be replaced by k_L , since α is small.

Hence the moment becomes $(k_L \rho S V^2 \times hc) + k_m c \rho S V^2$, since $AM = hc$,

i. e.

$$(k_m + h k_L) c \rho S V^2.$$

$$k_m = -0.24k_L - 0.0175.$$

152 The Equilibrium of the Aeroplane

Hence, by assuming the gap/chord ratio of the aeroplane to be 1, the equation for the biplane becomes

$$k_m = -0.21k_L - 0.0175.$$

The C.G. of the aeroplane is taken to be at

$$h = 0.31, k = -0.25,$$

so that

$$k_m + hk_L = -0.21k_L - 0.0175 + 0.31k_L = 0.1k_L - 0.0175.$$

TABLE XII
CALCULATION OF THE WING MOMENT COEFFICIENT \bar{k}_m

α	k	k_D	$k_m + hk_L$ ($= 0.1k_L - 0.0175$)	k_x ($= k_L \sin \alpha - k_D \cos \alpha$)	kk_x	\bar{k}_m ($= k_m + hk_L + kk_x$)
-2	0.003	0.0070	-0.0172	-0.0070	0.0018	-0.0154
0	0.070	0.0066	-0.0105	-0.0066	0.0017	-0.0088
2	0.132	0.0082	-0.0043	-0.0036	0.0009	-0.0034
4	0.199	0.0119	+0.0024	+0.0020	-0.0005	+0.0019
6	0.262	0.0175	0.0087	0.0099	-0.0025	0.0062
8	0.327	0.0247	0.0152	0.0210	-0.0053	0.0099
10	0.390	0.0330	0.0215	0.0352	-0.0088	0.0127
12	0.450	0.0428	0.0275	0.0517	-0.0129	0.0146
14	0.502	0.0550	0.0327	0.0680	-0.0170	0.0157
16	0.530	0.0740	0.0355	0.0750	-0.0188	0.0167

The curve of \bar{k}_m against α is given in Fig. 85.

This figure shows that the wing moment is negative at low incidence and positive at all angles of incidence above 3.3° . Hence for equilibrium the tail plane must give a negative lift at the higher speeds and a positive at the lower, the dividing line being 101.5 miles per hour (corresponding to $\alpha = 3.3^\circ$), at which speed no tail plane lift is required at all.

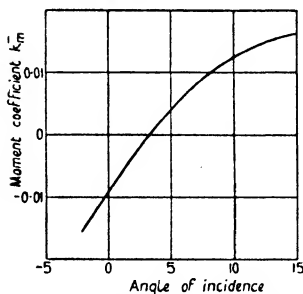


Fig. 85. Wing Moment Curve. **Thrust and Body Moments.** So far the wing moment only has been considered. There may be a further moment due to the

The Equilibrium of the Aeroplane 153

fuselage, landing gear, &c., but this is generally small and may be neglected. Hence, so far as gliding flight is concerned, the total moment may be taken to be equal to that of the wings alone. If, of course, wind channel data are available for the body moment, a correction can easily be applied.

Again, when the airscrew is developing a thrust, a thrust moment may arise if the thrust line does not pass through the C.G., and this must always be taken into account. Especially is this important in the case of a flying boat in which the engines are necessarily well above the C.G. (see Fig. 86).

As an introduction, however, to the behaviour of the tail plane, attention will be confined to gliding flight.

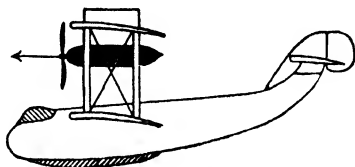


FIG. 86.

Downwash. Fig. 85 shows then the pitching moment which must be counteracted by the tail plane, but, before the operation of the tail plane can be discussed more fully, it is necessary to study the effect of what is called downwash. As the air passes over the wings of an aeroplane it is deflected downwards from its original direction, and the incidence of the tail plane is therefore decreased. The angle through which the air is turned is called the angle of downwash, and its value at the tail is denoted by the Greek letter ϵ (epsilon). Clearly, at a great distance behind the wings the downwash has been dissipated, but in the region of the tail the downwash is considerable and of great importance.

In terms of the aerofoil theory the downwash is the effect of the induced velocity behind the wings of the system of trailing vortices. Now the downward deflexion *at* the wings is proportional to $\frac{k_L}{A}$ (see p. 52); it is therefore only to be expected that at a given distance behind the wings it must still be proportional to $\frac{k_L}{A}$. Clearly it must also vary with the distance, and it is found,

154 The Equilibrium of the Aeroplane

in fact, that a governing factor is the ratio of the distance behind the wings to the span. For normal aeroplanes, however, the ratio of the distance of the tail behind the wings to the span does not vary much, and experiment shows that good average values for the downwash are given by

$$\epsilon = \frac{70k_L}{A} \text{ (for a monoplane) (4)}$$

and
$$\epsilon = \frac{110k_L}{A} \text{ (for a biplane) (5)}$$



FIG. 87. Downwash.

These equations may be modified in certain cases by the interference of the fuselage on the flow near the tail and by the cutting-away of the upper wing at the centre to improve the pilot's view, but no allowances can be made for any such effects without wind channel data.

Tail Setting. If the chord of the tail plane is parallel to the chord of the main planes, the downwash reduces the angle of incidence of the tail plane from the main plane incidence α to

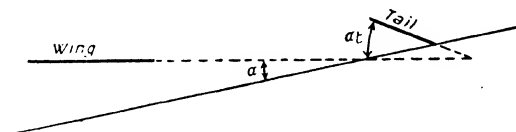


FIG. 88. Tail Setting.

$\alpha - \epsilon$. Generally the tail plane is not parallel to the main planes, and the angle between them is called the tail setting and denoted by α_t ; it is considered positive if the rigging incidence of the tail plane is greater than that of the main planes. Hence the angle of incidence α' of the tail plane is given by

$$\alpha' = \alpha - \epsilon + \alpha_t \text{ (6)}$$

The Equilibrium of the Aeroplane 155

[The angle α_t is sometimes called the *longitudinal dihedral angle*, the name tail setting being reserved for the angle between the tail plane chord and the thrust or centre line of the aeroplane.]

By means of this equation α' may be calculated for any speed of flight if α_t is known. If then the lift and drag characteristics of the tail plane are known, the moment of the forces on the tail plane can be calculated in a similar manner to that used in obtaining the moment of the wing forces, but it is sufficient always to make the following approximations:

- (1) The moment of the longitudinal force $k_L' \sin \alpha' - k_D' \cos \alpha'$ (see p. 151), where k_L' and k_D' are the lift and drag coefficients of the tail plane at an incidence α' , may be neglected altogether.
- (2) The normal force $k_L' \cos \alpha' + k_D' \sin \alpha'$ may be replaced by k_L' .
- (3) The variation in the position of the centre of pressure of the tail plane may be neglected for it is very small compared with the distance of the centre of pressure from the C.G.
- (4) The length of the moment arm may therefore be considered constant and is usually taken to be the distance of the C.G. from the point on the tail plane chord c' situated at $0.3c'$ from the leading edge.

Hence the moment of the tail plane forces is given by

$$M_t = -k_L' \rho S' V^2 \times l$$

i. e.
$$M_t = -k_L' l \rho S' V^2 \quad . \quad . \quad . \quad . \quad . \quad . \quad (7)$$

where l is the length of the moment arm and S' is the area of the tail plane. (The negative sign is included since a positive lift gives a negative moment.)

The Tail Plane as an Aerofoil. It is necessary now to study the behaviour of the tail plane as an aerofoil in order to determine the lift coefficient k_L' at an angle of incidence α' . In the first place mention must be made of the elevators, which are the hinged movable portions at the rear of the tail plane. These elevators are under the control of the pilot who, by fore and aft

156 The Equilibrium of the Aeroplane

movement of the control column, is able to depress or raise the elevators and so vary the shape of the tail plane section. In this way the pilot can vary the tail moment and thus obtain control over the fore and aft or pitching movement of the aeroplane. For the present, however, the elevators will be supposed to be held always in the neutral position so that the tail plane may be regarded as an ordinary rigid aerofoil.

Now the tail plane is generally of a thin symmetrical aerofoil section, and therefore, if the elevators are in the neutral position, the angle of no-lift is zero. Hence the lift coefficient may be written

$$k_L' = a\alpha',$$

where a is a constant depending primarily on the aspect ratio of the tail plane.

The aspect ratio is generally of the order of 3, and the corresponding value of a is 0.03.

This value for the slope a refers to the tail plane when it is acting alone. When it is in position on the aeroplane, the interference of the fuselage and the rest of the aeroplane, together with the presence of the hinges, results in a considerable reduction of the value of a . The ratio of the value of a when the tail plane is in position to its value when the tail plane is operating as a simple aerofoil on its own is called the tail plane efficiency, and in practice the efficiency is generally about 0.6 or 0.7.

For the aeroplane under discussion a will be taken to have the net value of 0.019, so that the lift coefficient of the tail plane is given by

$$k_L' = 0.019\alpha' \quad . \quad . \quad . \quad . \quad . \quad . \quad (8)$$

Calculation of the Moment for Given Tail Setting. Suppose the tail plane has a fixed tail setting of -1° . The tail moments for this setting are now calculated in Table XIII. The data on which the calculations are based are as follows:

$$\text{Tail moment} = -k_L' \rho l S' V^2,$$

$$S' = 40$$

$$l = 2.5c, \text{ where } c \text{ is the length of the mean chord.}$$

∴ tail moment coefficient

$$\begin{aligned}
 &= \frac{\text{Tail Moment}}{\rho c S V^2}, \text{ in order to be comparable with } k_m \\
 &= -\frac{k_L' \rho l S' V^2}{\rho c S V^2} \\
 &= -\frac{k_L' \times 2.5c \times 40}{c \times 320}, \text{ since } S = 320, \\
 &= -0.3125 k_L' \\
 &= -0.3125 \times 0.019 \alpha', \text{ since } k_L' = 0.019 \alpha', \\
 &= -0.00594 \alpha'.
 \end{aligned}$$

Also $\alpha' = \alpha - \epsilon + \alpha_i$, from equation (6)

$$= \alpha - \epsilon - 1, \text{ since } \alpha_i = -1;$$

and $\epsilon = \frac{110 k_L}{A}$, from equation (5)

$$= 18.33 k_L, \text{ since } A = 6.$$

TABLE XIII
CALCULATION OF TAIL MOMENT

α	k_L (from Table XII)	ϵ (= 18.33 k_L)	α' (= $\alpha - \epsilon - 1$)	Tail Moment Coefficient (= -0.00594 α')
-2	0.003	0.1	-3.1	0.0184
0	0.070	1.3	-2.3	0.0137
2	0.132	2.4	-1.4	0.0083
4	0.199	3.6	-0.6	0.0036
6	0.262	4.8	+0.2	-0.0012
8	0.327	6.0	1.0	-0.0059
10	0.390	7.1	1.9	-0.0113
12	0.450	8.2	2.8	-0.0166
14	0.502	9.2	3.8	-0.0226
16	0.530	9.7	5.3	-0.0315

The total moment coefficient of the whole aeroplane is the sum of the last columns of Table XII and Table XIII. If, then,

158 The Equilibrium of the Aeroplane

this total coefficient is plotted against incidence, the point at which the curve cuts the incidence axis gives the incidence at which the aeroplane is in balance or trim with a tail setting of -1° and the elevators neutral. Alternatively, if the tail moment is reversed in sign and plotted against incidence, the intersection of the wing moment and the tail moment curves gives the incidence at which the aeroplane trims. This is illustrated in Fig. 89, and it will be seen that the aeroplane trims at an angle

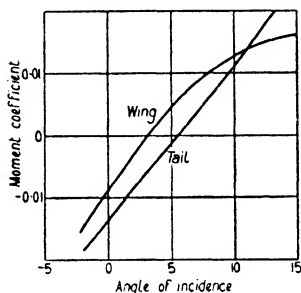


FIG. 89. Wing and Tail Moments.

of incidence of 11° .

When the aeroplane is said to be in trim in this sense it does not necessarily follow that the pilot need not exert any force on the control column, for, if the control column is left free, the elevators will not necessarily trail in the neutral position. Generally, however, the force required to bring the elevators into the neutral position would be small.

Calculation of Tail Setting to Trim. Fig. 89 shows that at any angle of incidence other than 11° the aeroplane would not trim with a tail setting of -1° , and it would therefore be necessary for the pilot to use the elevators.

To avoid this and to allow the pilot to fly 'hands off' it is customary to provide some tail adjusting gear, by means of which the tail plane as a whole may be adjusted to give the correct setting for trim at all speeds.

The 'tail setting to trim' for any angle of incidence may easily be obtained. Since the tail moment must be equal and opposite to the wing moment, the equation for equilibrium is

$$\bar{k}_m c \rho S V^2 = k_L' l \rho S' V^2. \quad \therefore \quad (9)$$

or

$$k_L' = \frac{\bar{k}_m c S}{l S'}.$$

Now for any angle of incidence \bar{k}_m is known (Table XII), and

The Equilibrium of the Aeroplane 159

so k_L' may be determined. Equation (8) then gives α' , and the tail setting follows from equation (6) since ϵ is known.

For the particular aeroplane equation (9) gives

$$k_L' = \frac{\bar{k}_m c \times 320}{2.5c \times 40} = 3.2\bar{k}_m.$$

The calculations are given in Table XIV below; the first two columns are taken from Table XIII and the third from Table XII.

TABLE XIV
CALCULATION OF TAIL SETTING TO TRIM

α	ϵ	\bar{k}_m	k_L' ($= 3.2 \bar{k}_m$)	α' ($= k_L' / 0.019$)	α_t ($= \alpha' - \alpha + \epsilon$)
-2	0.1	-0.0154	-0.0493	-2.6	-0.5
0	1.3	-0.0088	-0.0282	-1.5	-0.2
2	2.4	-0.0034	-0.0109	-0.6	-0.2
4	3.6	+0.0019	+0.0061	+0.3	-0.1
6	4.8	0.0062	0.0198	1.0	-0.2
8	6.0	0.0099	0.0317	1.7	-0.3
10	7.1	0.0127	0.0406	2.1	-0.8
12	8.2	0.0146	0.0467	2.5	-1.3
14	9.2	0.0157	0.0502	2.6	-2.2
16	9.7	0.0167	0.0534	2.8	-3.5

The above table shows that for gliding flight at normal flight speeds the necessary tail setting range is from about 0° to -3.5° .

The Elevators. In practice the tail adjusting gear is naturally rather slow in operation, and it is only used when it is required to fly at a constant speed for some length of time. Otherwise the tail setting is kept constant, and fore and aft trim is maintained by means of the elevators. This is explained more fully in the next chapter on controls.

Effect of Thrust on Tail Setting to Trim. When the air-screw is developing a thrust, the tail setting required at any given speed is different from the tail setting on the glide owing to

- (1) the moment of the thrust about the C.G.,
 - and (2) the effect of the slipstream on the tail plane.
- For instance, suppose the thrust line is $0.12c$ below the C.G. Then the moment coefficient due to the thrust is positive and

160 The Equilibrium of the Aeroplane

equal to $\frac{T \times 0.12c}{\rho c S V^2} = \frac{0.12 T}{\rho S V^2}$, and this must be added to the value of k_m .

In order to allow for the increased velocity over the tail plane, an *effective tail plane area* is obtained as follows:

Let S_1' , S_2' be the areas outside and inside the slipstream respectively. Then the air forces on S_2' must be multiplied by the slipstream factor $\frac{R}{R_0}$ (see p. 142), and so the tail plane lift is given by

$$\begin{aligned} L' &= k_L' \rho S_1' V^2 + k_L' \rho S_2' V^2 \frac{R}{R_0} \\ &= \left(S_1' + S_2' \frac{R}{R_0} \right) k_L' \rho V^2. \end{aligned}$$

Hence the effective area of the tail plane is $S_1' + S_2' \frac{R}{R_0}$, where $\frac{R}{R_0}$ is determined from the equation $\frac{R}{R_0} = a + b \frac{T}{\rho V^2 D^2}$.

In this case suppose $S_1' = 10$, $S_2' = 30$ and the slipstream factor is given by $\frac{R}{R_0} = 1 + \frac{3T}{\rho V^2 D^2}$.

To save labour one value of α only is considered, namely, $\alpha = 2^\circ$. At this incidence $k_L = 0.132$ and the corresponding speed (from $W = 2950$, $S = 320$) is 171.7 ft. per second or 117 miles per hour. From Fig. 57 the value of ηP at this speed is obtained as 267, so that $T = \frac{\eta P 550}{V} = 855$. Hence the thrust

$$\begin{aligned} \text{moment coefficient} &= \frac{0.12 \times 855}{\rho S V^2} \\ &= 0.0046. \end{aligned}$$

Therefore the total moment coefficient

$$\begin{aligned} &= k_m + 0.0046 \\ &= -0.0034 + 0.0046, \text{ for } k_m = -0.0034 \text{ (Table XII)} \\ &= +0.0012. \end{aligned}$$

$$\begin{aligned}
 \text{Again, } \frac{R}{R_0} &= 1 + 3 \frac{855}{\rho V^2 D^2} \\
 &= 1.43, \text{ taking } D = 9.25. \\
 \therefore S' &= 10 + (30 \times 1.43) = 53. \\
 \therefore k_L' &= \frac{k_m c S}{l S'}, \text{ from equation (9),} \\
 &= \frac{0.0012 \times 320}{2.5 \times 53}, \text{ since } l = 2.5c, \\
 &= 0.0029. \\
 \therefore \alpha' &= \frac{k_L'}{0.019} = \frac{0.0029}{0.019} = 0.2.
 \end{aligned}$$

$$\begin{aligned}
 \text{Hence, } \alpha_t &= \alpha' - \alpha + \epsilon \\
 &= 0.2 - 2 + 2.4 \\
 &= 0.6, \text{ as against } -0.2 \text{ on the glide.}
 \end{aligned}$$

But for gliding flight the necessary tail setting range was found to be from 0° to -3.5° ; hence in this case the range would have to be extended to cover power flight.

Tail Plane Drag. Reference may conveniently be made at this point to the effect on the tail plane drag of the slipstream and the downwash. In Chapter VI it was stated that an approximate figure for the drag of the tail plane might be obtained by assuming a constant drag coefficient of 0.0070. Table XIV shows that the assumption of constant k_D' is justified, for the values of k_L' are so small that the induced drag of the tail plane is negligible, and the profile drag cannot vary greatly over the small range of incidence encountered. Owing to the slipstream, however, the area of the tail plane should be taken to be the effective area corrected for the slipstream factor $\frac{R}{R_0}$. In esti-

imating the amount of the tail plane area in the slipstream allowance should be made for the contraction of the slipstream which occurs at some distance behind the airscrew. Generally

162 The Equilibrium of the Aeroplane

the slipstream is assumed to contract to a diameter $0.8D$, where D is the diameter of the airscrew.

The effect of the downwash is also of interest. Since the air is deflected downwards a certain portion of the tail plane lift becomes drag in exactly the same way as a portion of the lift of an aerofoil becomes (induced) drag due to the induced velocity. Thus the true drag along the flight path is $D' \cos \epsilon + L' \sin \epsilon$ or $D' + L' \sin \epsilon$, since $\cos \epsilon$ is always nearly unity (compare p. 51, Chapter IV). Hence the effect of the downwash is to reduce the drag if the tail lift is negative and to increase it if the tail lift is positive. In Table XV below, the true drag coefficient ($= k_D' + k_L' \sin \epsilon$) is obtained, taking $k_D' = 0.0070$; the values of ϵ and k_L' are taken from Table XIV.

TABLE XV
TRUE T.P. DRAG DUE TO DOWNWASH

α	ϵ	k_L'	$\sin \epsilon$	$k_L' \sin \epsilon$	$k_D' + k_L' \sin \epsilon$
0	1.3	-0.0282	0.0227	-0.0006	0.0064
2	2.4	-0.0109	0.0419	-0.0005	0.0065
4	3.6	+0.0061	0.0628	+0.0004	0.0074
6	4.8	0.0198	0.0837	0.0017	0.0087
8	6.0	0.0317	0.1045	0.0033	0.0103
10	7.1	0.0406	0.1236	0.0050	0.0120
12	8.2	0.0467	0.1426	0.0067	0.0137

This table shows that, if the downwash is taken into account, the true drag coefficient is far from constant and increases fairly rapidly with incidence.

Again, since the thrust increases as the speed decreases (see Fig. 75), the value of $\frac{R}{R_0}$ increases and therefore the effective area increases. Hence at high angles of incidence the drag of the tail plane may be considerably underestimated by neglecting the slipstream and downwash. The effect on performance, however, is not very great.

EXAMPLES

1. The top wing of a biplane is 30 ft. by 6 ft., the bottom wing 20 ft. by 3.5 ft., the gap 4 ft. and the angle between the gap and the line joining the leading edges of the two wings is $20^\circ 33'$. Find the length and position of the mean chord.

If the C.G. is 7.2 in. behind the leading edge of the lower wing and 20 in. above it, these distances being measured along and perpendicular to the chord respectively, find the C.G. coordinates h and k .

2. In a light aeroplane the wing chord c is 5 ft. and the wing area 310 sq. ft. Calculate the lift on the tail plane when the aeroplane is travelling at its top speed of 90 miles per hour at ground level, given that the wing moment coefficient \bar{k}_m is -0.014 , $l = 2.7c$ and the moments due to fuselage, thrust, &c. may be neglected.

3. The lift and drag characteristics of the wings of a biplane are given in the following table:

α	— 3	0	3	6	9	12	15
k_L	0.036	0.140	0.244	0.348	0.450	0.549	0.626
k_D	0.0076	0.0086	0.0127	0.0205	0.0313	0.0453	0.0650

Construct the curve of \bar{k}_m against k_L , given that the moment coefficient of the wings about the leading edge is $k_m = -0.215k_L - 0.025$ and the C.G. coordinates are $h = 0.305$, $k = -0.195$.

If the aeroplane has a wing loading of 8.5, at what speed will the aeroplane be in trim with no lift on the tail plane?

4. Use the calculated \bar{k}_m values of the previous example to determine the tail setting to trim at angles of incidence of 0° , 6° and 12° . The slope of the tail lift curve is 0.026, the tail plane efficiency 65 per cent., the aspect ratio of the wings 8.6, the moment arm $l = 2.9c$ and $\frac{S}{S'} = 9$.

5. In order to make a rapid prediction of the performance of an aeroplane it was assumed that the tail plane was always working at a constant drag coefficient, and this assumption led to a figure for the tail plane drag of 12 lb. at 100 ft. per second. Find the drag at 60 miles per hour, and compare this with the more probable figure obtained by taking into account the lift component of drag due to downwash.

The aeroplane is a biplane of aspect ratio 6, and at 60 miles per hour $k_L = 0.42$ and $k_L' = 0.078$.

X

CONTROL AND MANŒUVRE

Axes of Reference. In order to deal with questions relating to control, manœuvre and stability, it is convenient to refer the motion of an aeroplane to a system of mutually perpendicular axes through the C.G. The standard axes used in this country are as shown in Fig. 90. The longitudinal axis is GX forwards,

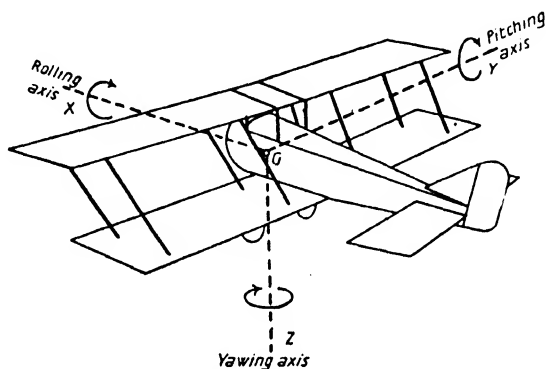


FIG. 90. Axes of Reference.

the lateral axis GY to starboard (i.e. to the right as viewed from behind) and the normal axis is GZ vertically downwards and at right angles to the other two.

A rotation about the longitudinal axis is called *rolling*, about the lateral axis *pitching* and about the normal axis *yawing*. The axes are therefore sometimes referred to as the rolling, pitching and yawing axes respectively. Rotations are considered positive if they are in the directions shown by the arrows.

Control Surfaces. The control surfaces consist of the elevators, ailerons and rudder. The principle of working is the same in each case and is described below.

Consider an aerofoil with the rear portion hinged and capable of motion about the line of hinges (see Fig. 91). When the hinged portion is depressed, the angle of incidence is increased

and the effective centre line camber is increased; the lift is therefore increased. Similarly, when the hinged portion is raised, the lift is reduced.

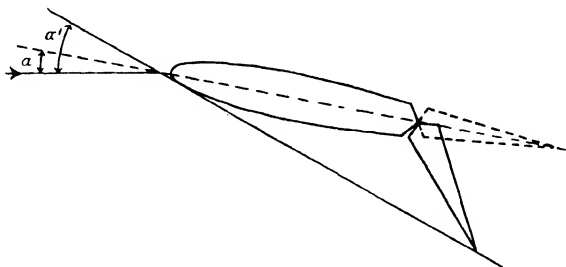


FIG. 91.

The Elevators. The elevators form the rear part of the tail plane, and control the motion of the aeroplane about the lateral

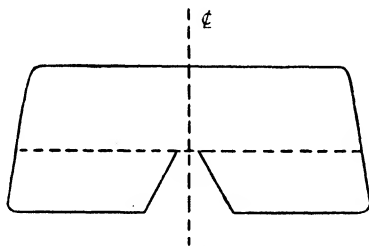


FIG. 92. Elevators.

or pitching axis. They are operated by means of cables attached to the control column in the pilot's cockpit, a forward movement of the column depressing the elevators and a backward movement raising them. If the elevators are depressed when the aeroplane is in trim, the lift on the tail plane is increased and the moment of the tail plane lift about the C.G. is greater than the wing moment. There is thus set up a moment tending to depress the nose of the aeroplane. Hence a forward movement of the control column pushes the nose down; similarly a backward movement pulls the nose up.

Notice (Fig. 92) that the elevators must be cut away to allow rudder movement.

The Ailerons (or wing flaps) are the outer rear portions of the main planes and control the motion about the longitudinal or rolling axis. They are operated in a similar manner to the elevators, except that ailerons on opposite wings work in opposite directions. A movement of the control column to the right

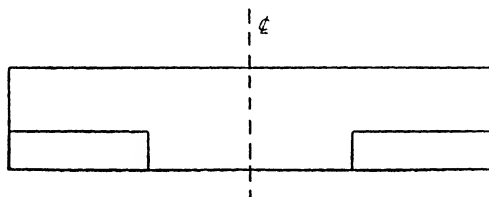


FIG. 93. Ailerons.

depresses the aileron on the port or left-hand wing and raises the aileron on the starboard or right-hand wing. Hence the lift on the port wing is increased, and that on the starboard wing is decreased; a positive rolling moment is therefore set up tending to roll the aeroplane to starboard.

The rudder. The rudder is the vertical hinged surface which

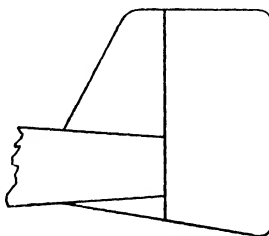


FIG. 94. Fin and Rudder.

controls the motion about the normal or yawing axis, and acts in a similar manner to an ordinary boat rudder. The fixed portion of the vertical surface is called the fin and is a stabilizing surface which will be discussed in the next chapter. Unlike the elevators and the ailerons, the rudder is not operated from the

control column but from a rudder bar at the pilot's feet. If the pilot presses on the rudder bar with his right foot, say, the rudder is moved as shown in Fig. 95, and air forces are set up on

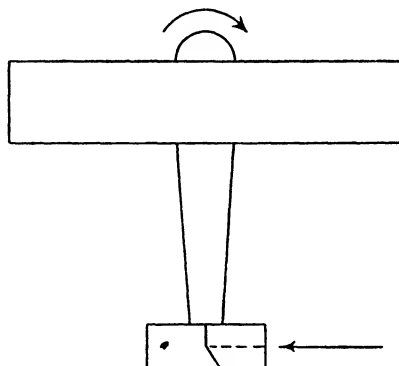


FIG. 95.

the fin and rudder which provide a yawing moment tending to turn the nose of the aeroplane to starboard.

Balanced Controls. Consider a horizontal control surface depressed as in Fig. 96. Then the resultant air force R on the

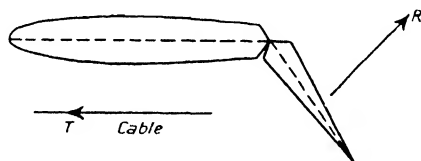


FIG. 96.

control surface tends to rotate it upwards about the hinge; hence the control can be kept in position only by the pilot exerting a load on the control column such that the moment about the hinge of the tension set up in the control cable just balances the moment of R , called the hinge moment. At large angular displacements of a control surface, or even at small ones on a large aeroplane, the hinge moments may be so large that the loads at the pilot's hands and feet become excessive, and it is necessary

to reduce these loads by some form of 'balancing'. In a balanced control a portion of the control surface lies in front of the line of hinges, so that the moment of the air forces on the front part helps to relieve the pilot (Fig. 97). In other words the resultant air force R on the control surface acts nearer to the hinge, and so the hinge moment is reduced.

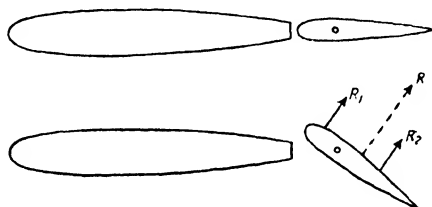


FIG. 97. Balanced Control.

Some typical forms of balance are shown in Fig. 98.

Types (a) and (b) are called *horn balances*, the relieving moments being obtained from the air forces on the horns only. In type (c), called an *inset balance*, the hinge is set back behind the leading edge of the control surface, and the balancing is carried throughout the whole length.

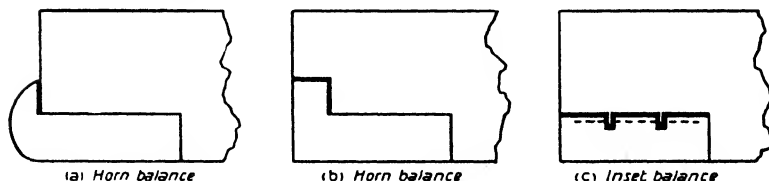


FIG. 98. Types of Balanced Control.

In all cases, of course, partial balancing only is required; no attempt is made to reduce the hinge moment to zero at all angular displacements, for it is always desirable to have some 'feel' to the controls. Furthermore, if the balanced area is too large it is quite possible that (1) large vibrations of the surface may occur, and (2) although the balancing is effective at large displacements, the surface may be overbalanced at the smaller

ones; this means that the resultant force acts in front of the line of hinges, so that the hinge moment is negative and the surface 'takes charge.'

The Elevators. When a tail plane is working at an incidence α' with the elevators neutral, the lift coefficient is given by $k_L' = a\alpha'$, where a is the slope of the lift-incidence curve and depends upon the aspect ratio and efficiency of the tail plane. Suppose now the elevators are moved through an angle η . (This angle is called the *elevator angle* and is considered positive when the elevators are depressed.) Then it is found by experiment that, over a large range of elevator angles, the lift coefficient is increased (or decreased) by an amount $b\eta$, where b is a constant depending upon the ratio of the elevator chord to the total tail plane chord. This is true over the normal range of tail plane incidence encountered, and so the lift coefficient may be written

$$k_L' = a\alpha' + b\eta. \quad (1)$$

Obviously the value of b increases as the ratio of the elevator chord to the tail plane chord increases, but the rate of increase of b is not so great as the rate of increase of the hinge moment. Small elevators are therefore in general more efficient than large ones, but the extent to which the elevators may be cut down is determined by the question of maximum control. For 40 per cent. elevators an average value of b is 0.0130; the lift coefficient of the tail plane of the previous chapter may therefore be written (assuming 40 per cent. elevators)

$$k_L' = 0.019\alpha' + 0.013\eta. \quad (2)$$

The term 0.013η gives the extra lift coefficient (positive or negative) due to elevator movement, and the extra lift is $0.013\eta \times \rho S' V^2$, so that the control moment generated is $0.013\eta \times \rho S' V^2 \times l$, where l is the moment arm of the tail plane.

Equation (2) may also be used to determine the elevator angles to trim at various speeds when the tail plane is fixed at one particular setting. Calculations for the aeroplane of the previous chapter are given in Table XVI below. A fixed tail setting of -1° has been taken, and the first three columns of the table—

which give the downwash angle and the tail plane lift coefficient required for trim at various angles of incidence—are reproduced from Table XIV.

TABLE XVI
ELEVATOR ANGLES TO TRIM WITH FIXED TAIL
SETTING ($\alpha_t = -1^\circ$)

α	ϵ	k_L'	α' ($= \alpha - \epsilon - 1$)	$0.019\alpha'$	0.0137 ($= k_L' - 0.019\alpha'$)	η
-2	0.1	-0.0493	-3.1	-0.0589	0.0096	0.7
0	1.3	-0.0282	-2.3	-0.0437	0.0155	1.2
2	2.4	-0.0109	-1.4	-0.0266	0.0157	1.2
4	3.6	+0.0061	-0.6	-0.0114	0.0175	1.3
6	4.8	0.0198	+0.2	+0.0038	0.0160	1.2
8	6.0	0.0317	1.0	0.0190	0.0127	1.0
10	7.1	0.0406	1.9	0.0361	0.0045	0.3
12	8.2	0.0467	2.8	0.0532	-0.0065	-0.5
14	9.2	0.0502	3.8	0.0722	-0.0220	-1.7
16	9.7	0.0534	5.3	0.1007	-0.0473	-3.6

The Ailerons. With normal ailerons the angular displacement, or aileron angle, for a given movement of the control column is the same on both the port and starboard wings, and it is found that the rolling moment generated is approximately proportional to the aileron angle. As the wing incidence is increased, however, the turbulence which exists over the upper surface of the wings reduces to some extent the effectiveness of the ailerons, and so the rolling moment for a given aileron angle falls off as the wing incidence is increased (Fig. 99).

Another undesirable feature of all normal aeroplanes is that, when the ailerons are moved, a yawing moment is set up due to the difference in drag of the opposite wings. Since the lift on the downward moving aileron is increased, the induced drag on that side must also be increased; similarly the induced drag on the side of the upward-moving aileron is decreased. This drag difference generates a yawing moment which, for a given aileron angle, clearly increases as the incidence (and therefore the lift coefficient) increases. With regard to the profile drag, it is probable that the change of aerofoil shape results in an increase

on both sides, so that little yawing moment is set up by any profile drag difference.

The high values of the yawing moment at the higher angles of incidence may be a serious matter, for the yaw operates against the roll and may render the ailerons ineffective. Suppose, for instance, the pilot wishes to roll to *starboard*. The port side aileron is depressed and the starboard side aileron raised, so that the yawing moment generated starts to turn the aeroplane to *port*. The starboard wing is then moving forward at a greater speed than the port wing. Hence the lift on the starboard wing is increased and that on the port wing decreased, so that the effect of the yawing moment is to generate a roll to *port*. Thus, although the movement of the ailerons starts the required roll to starboard, it is almost immediately opposed by a roll to port due to the induced

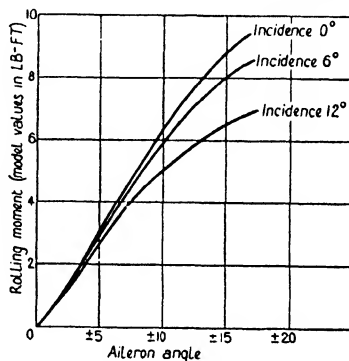


FIG. 99. Effect of Incidence on Aileron Rolling Moment.

yawing moment. If, then, the increase of yawing moment with incidence is large, the aileron control gradually falls away as the incidence is increased, *although the loss of direct aileron rolling moment may be quite small* (Fig. 99). This loss of aileron control is quite noticeable on most machines fitted with normal ailerons, the ailerons appearing to become 'sloppy' at the higher angles of incidence. In point of fact the sloppiness is often regarded as a warning of the near approach of the stall. (Some of the sloppiness is due, of course, to the falling speed.)

The yawing moment may be reduced in some measure by shaping the nose of the aileron as shown in Fig. 100. The shaping is such that the downward-moving aileron is screened by the wing proper, while the upward-moving aileron protrudes well below the wing. In this way the profile drag of the upward-

moving aileron is increased, the increase tending to counteract the increased induced drag of the downward-moving aileron.

A large reduction in the yawing moment can be effected by the use of differential ailerons. In this scheme the angular displacements of the ailerons on opposite wings are unequal, the downward-moving aileron having a small displacement and the upward-moving one a very large displacement. In this way the drag of the upward-moving aileron is considerably increased, the aileron acting more as a wind brake.

A further scheme, called the slot-cum-aileron scheme, is described on a later page (p. 182).

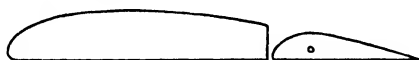


FIG. 100.

The Rudder. The rudder, like the ailerons, is subject to an incidence effect. At the higher angles of incidence the yawing moment provided by the rudder is decreased owing to the partial screening and interference of the rest of the aeroplane. The loss of rudder yawing moment, however, is generally greater than the loss of aileron rolling moment, and this loss is of great importance at slow speeds in the neighbourhood of the critical angle, for the rudder is the only means whereby any adverse aileron yawing moment may be overcome. Unless the rudder is sufficiently powerful to overcome the aileron yaw, it may happen that aileron control is completely lost at the minimum flying speed. Thus the need for adequate control at slow speeds is probably a more important factor in determining the area of the fin and rudder than considerations of normal control and manœuvre.

Taxiing conditions are also important in the fixing of rudder area; for the air speed when taxiing is low, and so the forces on the rudder are small.

Another important point in rudder design arises in the case of a twin-engine aeroplane in which the engines are mounted on or between the wings on either side of the fuselage. The rudder

must be sufficiently powerful to overcome the thrust yawing moment which occurs when one engine fails and the other is kept running; otherwise it would be impossible to keep the aeroplane on a straight course.

The Controls in Manœuvre. A complete study of the action of the controls in manœuvring and of the air forces called into play is quite beyond the scope of this book, but the comparatively simple problems of turning and looping may easily be studied. The general nature of the spin may also be easily explained.

Turning in a Horizontal Circle. In order to make a correct turn it is necessary to apply both rudder and ailerons. When an aeroplane is turning there must be a centripetal force acting on the aeroplane, i.e. a force towards the centre of the turning circle (equal and opposite to the centrifugal force). This force can be obtained only by using the ailerons to bank the aeroplane, if an outward sideslip is to be avoided. Suppose, for instance, the pilot wishes to make a turn to the right. By pressing on the rudder bar with his right foot, he throws the rudder over and an air force is set up on the rudder as shown in Fig. 95. This force tends to move the aeroplane outwards to the left, at the same time rotating the aeroplane about its C.G., but there is no inward centripetal force making the aeroplane turn. Very quickly, however, the action of the force on the rudder results in the aeroplane acquiring a sideways velocity (i.e. an outward sideslip), and a lateral air force arises on the outside of the aeroplane, thus enabling the aeroplane to turn.

To avoid this sideslip in a turn the aeroplane is banked so that the horizontal component of the main plane lift provides the necessary centripetal force, and it will be shown that there is a correct angle of bank for any given speed and radius of turn.

Suppose Fig. 101 represents an aeroplane turning without sideslip in a circle of radius r at a speed V and at an angle of bank ϕ . Then, if the centrifugal force $F \left(= \frac{WV^2}{gr} \right)$ is added, the three forces L , W and F are in equilibrium.

Hence,
$$L \sin \phi = F = \frac{WV^2}{gr} \quad (3)$$

and
$$L \cos \phi = W \quad (4)$$

By division,
$$\tan \phi = \frac{V^2}{gr} \quad (5)$$

an equation giving the required angle of bank.

If the angle of bank is less than that given by this equation, the horizontal component of the lift L will not be large enough to balance the centrifugal force, and the aeroplane will sideslip outwards; similarly, if the angle is greater, the aeroplane will sideslip inwards. In a sideslip the pilot feels the wind blowing on the side of his face; he can therefore tell if he is over- or under-banking.

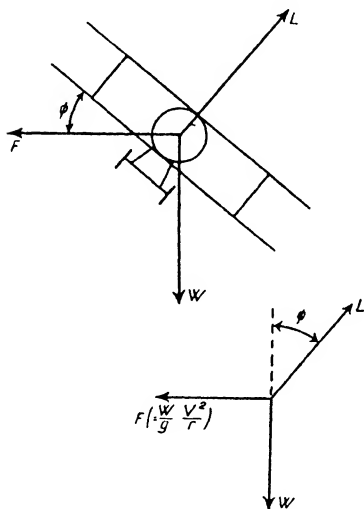


FIG. 101. Forces in a Banked Turn.

Thus there is a tendency for the aeroplane to overbank owing to the rolling moment introduced by the unequal lift on the two wings. Hence, when the turn has been established, it becomes necessary for the pilot to reverse the ailerons; this is known as 'holding off' the bank.

Again, if the bank is at all steep, the elevators and rudder have partially interchanged their functions. Thus in the extreme case of a vertical bank the elevators act as the rudder, and vice versa.

Speed in Turning. Since only a portion of the wing lift, namely $L \cos \phi$, is available for supporting the aeroplane, it

follows that for a given angle of incidence the speed in a turn is greater than that in straight flight.

Let V , V' be corresponding speeds at the same angle of incidence in straight and circling flight respectively, and let ϕ be the angle of bank appropriate to the speed V' . Then

$$W = L \cos \phi$$

$$= k_L \rho S V'^2 \cos \phi, \text{ for circling flight,}$$

$$\text{and} \quad W = k_L \rho S V^2, \text{ for straight flight.}$$

$$\text{Hence,} \quad V'^2 \cos \phi = V^2$$

$$\text{i. e.} \quad V' = \frac{V}{\sqrt{\cos \phi}}.$$

In the particular case when the angle of incidence is the critical angle, the speeds become the stalling speeds; hence the *stalling speed is increased in a steady horizontal turn* and is given by

$$V'_s = \frac{V_s}{\sqrt{\cos \phi}} \quad \dots \dots \dots (6)$$

where V_s is the stalling speed in straight flight.

Loading in a Turn. In normal straight flight the lift on the wings is approximately equal to the weight of the aeroplane, and this condition is referred to as unit wing loading. In a turn equation (4)

shows that $L = \frac{W}{\cos \phi}$, and the loading is therefore increased.

The ratio of the actual loading in any manœuvre to the unit wing loading, i.e. $\frac{L}{W}$, is called the **load factor**, and in a turn the load factor

is $\frac{1}{\cos \phi}$. Thus, at an angle of bank

of 60° where $\cos \phi = \frac{1}{2}$, the load factor is 2. Fig. 102 expresses graphically the relation between the load factor and

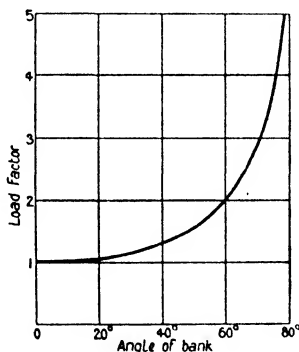


FIG. 102. Loads in a Turn.

angle of bank and shows the large loads which may be thrown on the wings if an attempt is made to keep the aeroplane turning horizontally at a steady speed, without sideslip, at a large angle of bank.

Vertically-Banked Turns. So far only steady continuous turns in which the speed is constant and the aeroplane is turning in a horizontal plane have been considered. In a very sharp and rapid turn an aeroplane may become vertically banked, but, since there is then no wing lift component to support the weight, the bank cannot be maintained continuously without loss of height. On such a turn the speed is varying also, and so the condition of flight is not one of steady motion, and the study of the behaviour of the aeroplane becomes a complicated matter.

It is possible, however, to obtain some idea of the loads imposed upon the wings.

Consider an aeroplane turning with a vertical bank. Then, neglecting sideslip, the lift is equal to the centrifugal force and therefore

$$L = k_L \rho S V^2 = \frac{W V^2}{g r}.$$

Hence for a given speed the load is a maximum when r is a minimum.

Now from the conditions of normal straight flight

$$W = k_{L\max} \rho S V_s^2.$$

The combination of these two equations leads to

$$\frac{k_L V^2}{k_{L\max} V_s^2} = \frac{V^2}{g r},$$

i. e.
$$r = \frac{V_s^2}{g} \times \frac{k_{L\max}}{k_L},$$

which shows that the radius is a minimum when $k_L = k_{L\max}$. Hence the minimum radius is obtained by pulling back the control column so that the angle of incidence of the wings is the

critical angle. The turning radius is then $\frac{V_s^2}{g}$, while the load factor is given by

$$\frac{L}{W} = \frac{k_{L\max}\rho S V^2}{k_{L\max}\rho S V_s^2} = \frac{V^2}{V_s^2}.$$

Suppose, for instance, an aeroplane whose stalling speed is 60 miles per hour turns on a vertical bank of minimum radius at 120 miles per hour. Then the load factor = $\frac{120^2}{60^2} = 4$.

Looping. A loop is a turn in a vertical plane, and the motion therefore has something in common with the ordinary turn. It differs from the steady turn in that the speed and the radius of turn are not constant. The variation in the speed is obvious; on the upward climbing part of the loop the speed is gradually dissipated; it is then regained on the downward diving part.

In looping some aeroplanes they must first be put into a mild dive in order to acquire sufficient energy to carry them over the top of the loop; with the faster types a loop can be made straight off from the level. The entry into a loop should be gradual, otherwise the load thrown on the wings may be excessive. For instance, suppose that at the bottom of a loop the control column is pulled hard back and the aeroplane attains the incidence corresponding to the maximum lift coefficient before the speed has time to fall appreciably. Then, if V is the speed at which the loop is commenced and V_s the stalling speed,

$$L = k_{L\max}\rho S V^2$$

and

$$W = k_{L\max}\rho S V_s^2,$$

so that the load factor is $\frac{V^2}{V_s^2}$, as in the case of a vertically banked turn with the wings at the critical angle. Thus, if an aeroplane whose stalling speed is 50 miles per hour, entered a loop at 150 miles per hour, the control column being pulled hard back, the load imposed on the wings would be 9 times normal. In many aeroplane types this would be sufficient to tear off the wings.

Similarly, in the recovery from the dive on the second part of the loop, the aeroplane should be pulled out gradually. It follows that the path followed by an aeroplane in a loop is never a circle, but more elliptical in shape as shown in Fig. 103. The radius at the entry to the loop and in the recovery from the dive is large. The figure also shows the nature of the variation of the load

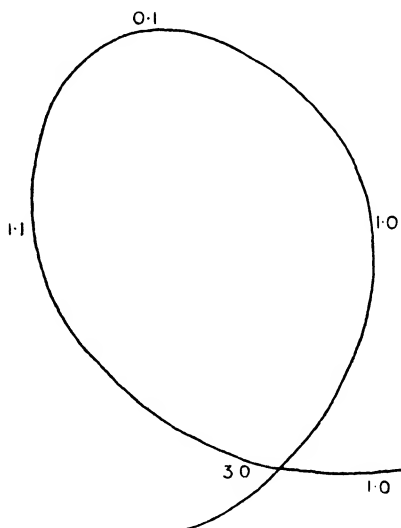


FIG. 103. Path and Load Factor in a Loop.

factor. At the top of the loop the factor is small, showing that at this point the weight of the aeroplane itself is almost sufficient to supply the necessary centripetal force. The vanishing of the load factor at this point would indicate that the pilot is just about to leave his seat.

It is interesting to see what approximate load would come on the wings at the bottom of the loop if the path were truly circular. Suppose the radius of the path is r , and let V_1 , V_2 be the speeds at the bottom and top of the loop respectively. Let L_1 , F_1 be the lift and centrifugal force at the bottom, and L_2 , F_2 the corresponding quantities at the top (Fig. 104). Then

$$L_1 = W + \frac{WV_1^2}{gr} = W \left(1 + \frac{V_1^2}{gr} \right)$$

and
$$L_2 = \frac{WV_2^2}{gr} - W = W \left(\frac{V_2^2}{gr} - 1 \right).$$

Suppose now that the thrust of the airscrew always just

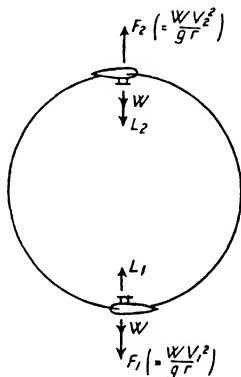


FIG. 104.

balances the drag of the aeroplane. Then the energy lost in the upward climb is $\frac{1}{2} \frac{W}{g} (V_1^2 - V_2^2)$, and the work done is $W \times 2r$.

Hence,
$$\frac{1}{2} \frac{W}{g} (V_1^2 - V_2^2) = W \times 2r$$

i.e.
$$V_1^2 - V_2^2 = 4gr.$$

If it be further assumed that the load is just zero at the top of the loop, then $L_2 = 0$ and so $V_2^2 = gr$. Hence

$$\begin{aligned} V_1^2 &= 4gr + V_2^2 \\ &= 4gr + gr \\ &= 5gr. \end{aligned}$$

Then
$$\begin{aligned} L_1 &= W \left(1 + \frac{V_1^2}{gr} \right) \\ &= 6W. \end{aligned}$$

Hence the load factor at the bottom is 6.

Load Factors in Design. The maximum load factor for which the wings are designed depends upon the type of aeroplane. For a heavy bombing or passenger-carrying aeroplane in which rapid manœuvre is impossible, it is probably sufficient to design for a load factor of about 5, while for a high-speed highly-manœuvrable aeroplane the necessary figure may be as high as 10. Whatever the design factor, however, the wings could probably be torn off by mishandling.

Spinning. Spinning is another common form of manœuvre, but it is also a condition of flight into which an aeroplane may

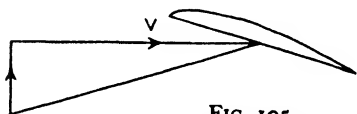


FIG. 105.

Increased Incidence of Falling Wing.

easily fall as a result of an involuntary stall, and is one of the most frequent causes of accident. Before the nature of the spin can be discussed, it is necessary to understand

the conditions of the phenomenon known as autorotation.

Suppose a model is mounted in a wind channel in such a manner that it is free to rotate about the longitudinal or rolling axis. Suppose further that the angle of incidence is less than the critical angle and that the model receives a slight disturbance depressing one wing. Then the rolling motion results in the angle of incidence of this wing being increased (Fig. 105), while that of the other wing is decreased. Hence, since the lift coefficient increases with the angle of incidence (below the stalling angle), the lift on the falling wing is greater than that on the rising wing, and so a rolling moment is set up opposing the original roll. Thus the rolling disturbance is automatically stopped or 'damped'. This state of affairs only occurs, however, so long as the critical angle is not exceeded.

For suppose now that the original angle of incidence is greater than the critical angle and the aeroplane receives a disturbance depressing one wing as before. Again the incidence of the falling wing is increased and that of the rising wing decreased, but in this case the lift of the falling wing is less than that of the rising wing, as shown by the points B, B' of Fig. 106, and so a rolling

moment is set up increasing the original roll. Thus the model is subject to an angular acceleration in roll, but it is found that the rate of roll quickly reaches a constant value. Hence, if the critical angle is exceeded, any disturbance generating a roll results in the model rotating continuously of its own accord. This motion is called **autorotation** and forms the basis of the spin.

Consider now an aeroplane in flight, and suppose that it is suddenly stalled. If it suffers no lateral disturbance it will immediately commence a steep

straight dive, but, if a disturbance occurs to generate a roll, autorotation will set in at the same time as the nose drops, and the aeroplane will therefore start a spinning nose dive or spin. The motion of the spin is actually a combination of

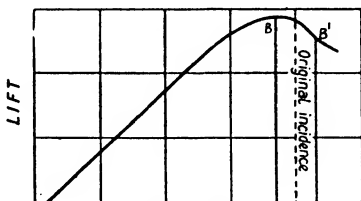


FIG. 106.

rotation about all the axes, and the aeroplane spins earthwards in a steep helical path. The longitudinal axis is inclined at a large angle to the horizontal, usually about 70° or so, but the speed is comparatively low and varies with normal types of aeroplanes from about 50 to 75 miles per hour. The angle of incidence obviously varies over the span of the wings, but the average angle may be as high as 30° , so that the aeroplane is well stalled.

When an aeroplane is spinning with the nose pointing earthwards, it might at first sight be thought that to recover from the spin the nose should first be pulled up. Since, however, the aeroplane is in the stalled state, a backward movement of the control column does not bring up the nose as in normal flight but, if anything, holds the aeroplane more firmly in the spin. Hence the first thing to do for recovery is to get the aeroplane out of the stalled state by easing the control column forward. If at the same time the rudder and ailerons are centralized, the average aeroplane will go into a steep normal dive from which it

may be gradually pulled out. With some aeroplanes it is necessary to use the rudder against the spin, as well as putting the control column forward.

It is clear from the above that considerable height is lost in recovering from a spin, and herein lies the danger if an involuntary spin occurs near the ground.

The involuntary spin. Suppose an aeroplane is suddenly stalled and at the same time the starboard wing is depressed. The pilot instinctively uses the ailerons to correct the lateral disturbance, but the restoring aileron rolling moment is almost immediately neutralized by the aileron yawing moment which is very large at angles of incidence above the critical angle. This yawing moment acts against the ailerons and tends to turn the aeroplane to starboard, so that, unless the rudder is sufficiently powerful to overcome the yaw, the port wing moves faster than the starboard wing, and therefore an additional roll is set up of the same sign as the original disturbing roll, and the aeroplane falls into a spin. It is possible that for a fraction of a second the restoring aileron moment may stop the original roll, but there is then no restoring moment available to stop the roll generated by the yaw.

The likelihood of an involuntary spin may obviously be reduced by the use of (1) a very large and powerful rudder or (2) powerful ailerons which do not give any yaw. Large rudders are undesirable owing to structural and weight considerations and to the fact that a heavily-ruddered aeroplane may be uncomfortable to fly at normal angles of incidence owing to a tendency to swing, although many aeroplanes have been designed with rudders which seem to be sufficiently powerful at the stall and to have no undesirable characteristics in normal flight. The most successful scheme, however, appears to be the **slot-cum-aileron device**. In this scheme the leading edge of the wing in front of the ailerons is slotted, and the aileron and the slotted portion are interconnected so that the amount of slot opening varies with the aileron movement. When an aileron is in the neutral position or raised, the slot remains closed, but

when the aileron is depressed the slot opens. Hence, when an aileron is depressed, the wing on that side behaves as a slotted wing, and the value of the critical angle is raised. It can be shown that in this way the aileron yaw is reduced, the aileron rolling moment increased and the chances of autorotation minimized. In the first place, the large increase of the yaw which occurs when the critical angle is exceeded must be due in great part to the profile drag. Now the slot on the side of the upward-moving aileron slightly increases the profile drag due to a certain amount of spoiling of the aerofoil section, while the action of the slot on the downward-moving aileron is to smooth out the turbulence and so reduce the drag. Hence the aileron yawing moment is reduced. Consider now the above case of an aeroplane in

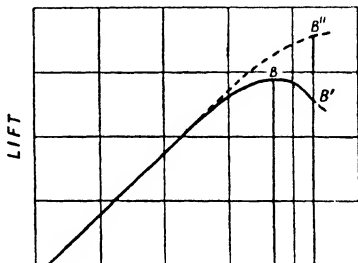


FIG. 107.

which the starboard wing falls on stalling. The use of the ailerons to restore the aeroplane to an even keel results in the aileron of the starboard wing being depressed. If then the aeroplane is fitted with the slot-cum-aileron device, it follows that, apart altogether from any lift difference on the wings due to the aileron movement, the action of the slot has replaced the point B' of Fig. 106 by the point B'' of Fig. 107. Hence the condition for autorotation is not realized; in addition the aileron rolling moment is greatly increased.

The spin as a manœuvre. In order to put an aeroplane into a spin, the control column is pulled back until the aeroplane is stalled, and the rudder is then kicked over. The rudder starts a yaw which, in turn, generates a rolling moment due to the extra speed of the outer wing, and the aeroplane commences to spin. It is not often that the ailerons are used to start a roll in the same direction as the yaw induced by the rudder, owing to the large aileron yawing moment which would operate against the

rudder. In fact with normal conventional ailerons it is customary to apply opposite aileron in order to utilize the aileron yaw to help the rudder yaw.

The efficacy of the slot-cum-aileron device in reducing the possibility of an involuntary spin may be gauged from the fact that some aeroplanes which spin quite easily when fitted with conventional ailerons have become quite difficult to spin with the slot control.

EXAMPLES

1. An aeroplane weighing 1,800 lb. is turning without sideslip in a horizontal circle of 360 ft. radius at 75 miles per hour. Find the angle of bank and the lift on the main planes.

2. An aeroplane whose stalling speed in straight flight is 52 miles per hour is making a horizontal turn of 60° bank. If the aeroplane is on the point of stalling, find the radius of the turn.

3. An aeroplane weighing 3,500 lb. has a wing area of 360 sq. ft. If the maximum lift coefficient is 0.62, find the stalling speed and so determine the load factor when the aeroplane is suddenly pulled up to stalling incidence when flying at 120 miles per hour.

4. An aeroplane weighing 2,400 lb. executes two loops in succession. At the top of the first loop it is travelling horizontally at 45 miles per hour along a path of radius 120 ft. At the bottom of the first loop it is again moving horizontally at 100 miles per hour along a path of radius 300 ft. Find the load factor in each case.

5. Find the minimum speed at which the aeroplane described below can maintain a straight course in the event of one engine 'cutting out'.

Type of aeroplane Twin-engine. Engines on lower plane.

Distance between engine centres 18 ft.

Maximum rudder yawing moment

$N = 1.08V^2$, where N is the yawing moment in lb.-ft.

$H.P._a$ for each engine as follows:

$V_{m.p.h.}$	60	70	80	90
$H.P._a$	203	222	239	254

[Plot thrust moment and rudder moment against speed.]

XI

STABILITY

Definitions. An aeroplane is said to be **stable** if, after receiving some small disturbance from a position of equilibrium in steady flight, it eventually returns to its original flying position and speed without any aid from the pilot; conversely, if it fails to return, it is said to be **unstable**.

Stability is sometimes further sub-divided into static stability and dynamic stability. An aeroplane is said to be *statically stable*

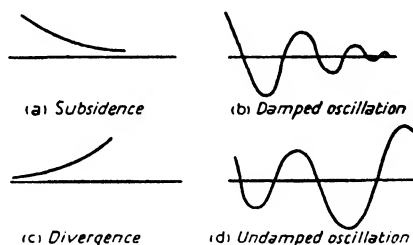


FIG. 108. Disturbed Motion.

if, after receiving a small disturbance, restoring forces and moments are called into play tending to bring the aeroplane back towards its condition of steady flight. These forces and moments may, however, cause the aeroplane to oscillate about the equilibrium position, and the aeroplane is said to be *dynamically stable* only if the oscillations gradually decrease so that the original steady flight is resumed.

Consider an aeroplane flying at a steady speed on a straight course, and suppose it receives a disturbance—due to a gust, say—deflecting it from this course. Then a stable aeroplane will return of its own accord to its original steady flight conditions either by way of a **subsidence** as in Fig. 108 (a) or a **damped oscillation** as in (b); an unstable aeroplane will depart from the steady flight conditions either by way of a **divergence** as in (c) or

an **undamped oscillation** as in (d). It will be realized that (d) illustrates a case of static stability but dynamic instability.

Longitudinal and Lateral Stability. It is convenient to study the longitudinal and lateral stability of an aeroplane separately. The problem of longitudinal stability deals with the disturbed motion in the pitching plane or plane of symmetry, while the lateral stability covers the motion in the rolling and yawing

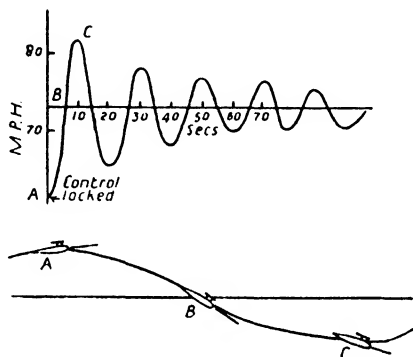


FIG. 109. Uncontrolled Motion of a Stable Aeroplane.

planes. The longitudinal stability is more easily dealt with, for the motion in the pitching plane does not affect the motion in either of the other two planes; for instance, a disturbance which alters the forward velocity or starts the aeroplane pitching cannot cause any sideslipping, rolling or yawing. On the other hand the motions in the rolling and yawing planes are interconnected; for instance, a disturbing yaw generates a roll.

The full mathematical treatment of the problem of stability involves such complicated mathematics that it cannot be included in a book of this type. It is possible, however, to put a great deal of the subject into simple language and show the main characteristics of an aeroplane which make for stability.

SECTION A. LONGITUDINAL STABILITY

Motion of a Stable Aeroplane. Fig. 109 illustrates the uncontrolled motion of a stable aeroplane and shows how the

aeroplane behaves after it has suffered a disturbance. The record was actually obtained by locking the control column at 62 miles per hour in a position which gave equilibrium at 73 miles per hour, and then leaving the aeroplane to take care of itself. It will be seen that the incidence, speed and path are changing all the time in the disturbed motion, but the oscillations are gradually dying down showing that the aeroplane will eventually settle down to its steady equilibrium speed of 73 miles per hour.

An uncontrolled unstable aeroplane would eventually stall and possibly go into a spin, or acquire a very steep dive and possibly turn on its back.

Longitudinal Static Stability. Since static stability is the first essential to complete stability, this will be treated first. Suppose an aeroplane is flying at a steady speed and the tail plane is set to trim so that the tail moment balances the moments of the wings, fuselage, &c. Then any departure from the condition of steady flight means that these moments have changed so that the total moment is not zero. The condition for static stability is that the unbalanced moment at any instant shall always be such as to tend to restore the aeroplane to its original incidence.

Consider the aeroplane of Chapter IX and take the case of $\alpha_t = -1^\circ$. Fig. 89 shows that with this tail setting the aeroplane is in trim at an angle of incidence of 11° . If, however, the wing moment and tail moment for this particular setting are added together as explained on p. 158, a curve can be drawn showing how the total moment varies with incidence. This curve has been drawn in Fig. 110, the wing moment being taken from Table XII and the tail moment from Table XIII.

The figure reveals the magnitude and sign of the total moment when the incidence is changed from the trimming incidence of

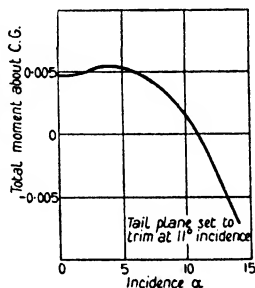


FIG. 110. Total Moment Curve.

11° . (It has been tacitly assumed that the elevators are always at 0° , i.e. the control column is locked to give equilibrium at 11° incidence. If the elevators are allowed to remain free, further complications are introduced, but these are not found to affect the general conclusions drawn.) It will be seen at once that at the speed corresponding to 11° incidence the aeroplane is statically stable, for if the incidence is slightly increased due to any disturbance the total moment is negative and therefore tends to reduce the incidence, while if the incidence is decreased the

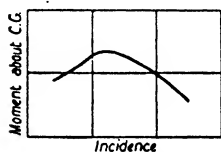


FIG. 111.

moment is positive and tends to increase the incidence. It follows that a *condition for static stability is that the total moment curve shall have a negative slope*. It is also a necessary condition for stability that the curve shall not cut the incidence axis at more than one point. For consider the imaginary moment curve of Fig. 111. This curve cuts the axis in two points and therefore shows that the aeroplane is in trim at two different angles of incidence with the same tail setting. At the lower incidence the slope of the curve is positive and the aeroplane is definitely unstable, while at the higher incidence the aeroplane is stable for small disturbances but may be unstable for large ones. The positive slope is often a feature of the moment curve at very low angles of incidence but seldom at high angles; in other words static instability is more likely to occur at high speeds (generally diving speeds) than at low.

(Static stability is often called weathercock stability, since a statically stable aeroplane will always turn its nose into the wind in the same way as a weathercock. Suppose, for instance, an aeroplane receives a vertically upward gust. Then the incidence is increased and a negative moment arises forcing the nose of the aeroplane into the gust.)

Now the total moment is the sum of the moments due to the wings, tail, fuselage, &c., but only the wing moment and the tail moment are being considered here, for these are quite the most important. For the aeroplane chosen the wing moment curve

itself has a positive slope, while the tail moment curve has a negative slope. (See Fig. 112, which is produced from the data of Tables XII and XIII.) This is in general true for all aeroplanes, and therefore static stability can be achieved either by decreasing the positive slope of the wing moment curve or by increasing the negative slope of the tail moment curve. These two curves will now be more fully discussed.

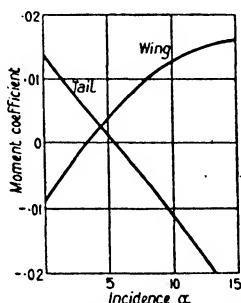


FIG. 112. Wing and Tail Moments.

The Wing Moment Curve. The wing moment coefficient is given by

$$\bar{k}_m = k_m + h k_L + k k_x.$$

If, as an approximation, the small term $k k_x$ is neglected (see Table XII for magnitude of $k k_x$), the equation becomes

$$\begin{aligned}\bar{k}_m &= k_m + h k_L \\ &= (-b k_L + k_{m_0}) + h k_L \\ &= (h - b) k_L + k_{m_0},\end{aligned}$$

where the value of b is about 0.25 for a monoplane and 0.22 for a biplane. This equation shows that for any wing arrangement the slope of the curve of \bar{k}_m against k_L is always $h - b$. But over a considerable range of incidence k_L increases uniformly with α , and so the slope of the curve of \bar{k}_m against α must also be approximately proportional to $h - b$. It follows that the slope of this curve will always be positive provided that h is greater than 0.25 (for a monoplane) or 0.22 (for a biplane), but that its value

decreases as h decreases. Hence a forward position of the Centre of Gravity is desirable for static stability, and in practice the value of h is generally in the neighbourhood of 0.3, the extreme range in modern aeroplanes probably being from about 0.25 to 0.40.

If the term kh_x is taken into account and allowance is made for the departure of the lift-incidence curve from a straight line

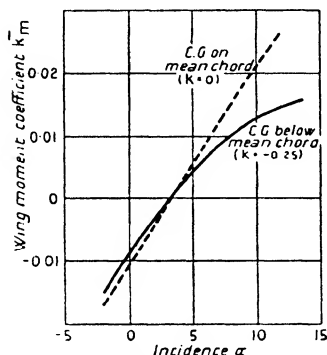


FIG. 113.

at the higher angles of incidence, the value for the slope will change slightly and will not remain constant at $h-b$ for all angles of incidence. This is illustrated in Fig. 113; but the fact remains that the slope of the wing moment curve depends primarily on the value of h . Fig. 113 does show, however, that a low C.G. slightly helps stability, for the true full curve which takes into account the distance of the C.G. below the mean chord is of less slope

than the dotted curve which assumes that the C.G. lies on the mean chord (i.e. $k = 0$).

The Tail Moment Curve. The moment due to the tail plane is given by

$$\begin{aligned} M_t &= -l \times k_L' \rho S' V^2 \\ &= -la\alpha' \rho S' V^2, \end{aligned}$$

since $k_L' = a\alpha'$ where a is the slope of the tail lift-incidence curve multiplied by the tail plane efficiency.

Therefore the tail moment coefficient

$$= \frac{M_t}{\rho S V^2} = -\frac{la\alpha' S'}{cS}.$$

Hence for any given wing area and wing chord the tail moment coefficient is proportional to $la\alpha' S'$, i.e. to $laS'(\alpha - \epsilon - \alpha_i)$. Now ϵ is directly proportional to k_L (p. 154) and therefore approxi-

mately proportional to α . It follows that for a given tail setting the slope of the curve of tail moment coefficient against α is approximately proportional to laS' . Hence the slope can be increased (numerically) and the stability improved by increasing any or all of the values of l , a and S' . Remember that, apart from the tail plane efficiency, the value of a depends upon the aspect ratio of the tail plane.

The above results may be summarized by stating that the features of an aeroplane which are especially favourable to stability are as follows:

- (1) forward position of the C.G., i.e. a low value of h ,
 - (2) large tail leverage l ,
 - (3) large tail plane area S' ,
- and (4) high tail plane aspect ratio.

Longitudinal Dynamic Stability. If an aeroplane is statically unstable, that is to say, if the uncontrolled motion after a disturbance is a divergence, the question of dynamic stability cannot arise. An aeroplane may, however, be statically stable but dynamically unstable, the instability in this case appearing in the form of an increasing oscillation. This is not a serious type of instability.

It is not possible here to deal in simple language with all the factors governing dynamic stability, but mention may be made of what is known as 'damping due to pitch'.

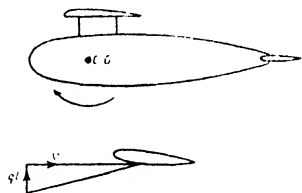


FIG. 114.

Now when an aeroplane is oscillating as shown in Fig. 109, the aeroplane is pitching about its C.G., and one important condition for dynamic stability is that any pitching moment shall be heavily damped. Consider

an aeroplane having a positive angular velocity in pitch q . Then the centre of pressure of the tail plane has a downward velocity ql , and so the incidence of the tail plane is increased (Fig. 114). This increase of incidence results in a positive increment of tail plane lift. But a positive tail lift means a negative moment;

hence there is an added negative moment, and this opposes or tends to damp out the pitching motion. Therefore what is true for the tail plane with regard to static stability is true also with regard to dynamic stability.

The damping due to the wings cannot be very great, for one part of the wing has a downward velocity due to the pitch, while the other part has an upward velocity. Moreover the centre of pressure of the wings is very close to the C.G., and there is no long leverage arm as in the case of the tail plane. There may, however, be a small amount of damping due to the fuselage, &c.

General Remarks. Stability is unfortunately bound up to some extent with controllability, a highly stable aeroplane being probably rather heavy and stiff in responding to the controls. For fighting aeroplanes it is not therefore desirable to aim at too high a degree of stability; on the other hand, for bombing and passenger-carrying aeroplanes which are flown for long distances at a steady speed, a considerable degree of stability is essential in order that the pilot shall not be continually called upon to correct for small disturbances.

Static stability may, however, be carried to excess in any aeroplane. If the stability is very great, it will mean that the restoring moment is always so powerful that the oscillations in any disturbed motion will be of a very rapid period. The motion will not therefore be so comfortable as one in which the period is longer, even if the actual displacement or amplitude of each oscillation is greater. (Compare the oscillations of two springs, one of which is much stiffer than the other; the stiff spring is analogous to the highly stable aeroplane.)

SECTION B. LATERAL STABILITY

Lateral stability may be divided into yawing or directional stability and rolling stability, although these subdivisions cannot be strictly treated separately, since any lateral disturbance must give rise to three-dimensional motion, as already explained. For this reason lateral stability can be treated here only in broad outline.

Directional Stability. Directional or yawing stability is stability in the yawing plane, and is that characteristic of an aeroplane which enables it to return to its straight course after it has suffered some disturbance deflecting it from that course.

Suppose an aeroplane receives a side gust tending to move the aeroplane to the left as shown in Fig. 115 (a). Then the effect of the side wind v , say, is to put the aeroplane in a yawed attitude with regard to the relative wind as shown in (b). The effect of this change of attitude is very marked in the case of the fin and fuselage. If the fin is regarded as a small aerofoil, it will be seen

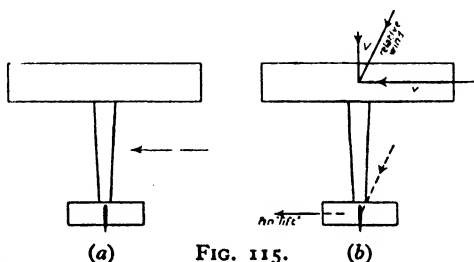


FIG. 115.

that, due to the yaw, the fin is now operating at a definite angle of incidence and therefore experiences a 'lift' in the direction shown. This 'lift' provides a restoring moment tending to turn the nose into the gust; hence the action of the fin in lateral motion is similar to that of the tail plane in longitudinal motion in producing weathercock stability. With regard to the fuselage, the effect of the yaw is clearly to bring the centre of pressure of the fuselage away from the nose. It is found, however, that the centre of pressure is invariably still in front of the C.G., so that there is a body moment of opposite sign to the fin moment. The analogy between directional stability and longitudinal stability is therefore very close. In the one case the body is unstable and the stability is obtained from the fin; in the other case the wings are unstable (for normal values of $h > 0.25$) and the stability is obtained from the tail plane. Hence what holds true for the tail plane is equally true for the fin; that is to say, a large fin of high aspect ratio is favourable to directional stability. Again the

damping in any yawing oscillations is provided by the fin in exactly the same way as the damping in pitch is provided by the tail plane.

Unfortunately an aeroplane which has a very large fin may be unstable in another way as will be shown later.

Rolling Stability. It has already been shown in a previous chapter that the wings of an aeroplane are stable in roll; that is to say, if a small disturbance generates a roll, an opposing moment is immediately called in play owing to the difference in the angles of incidence of the falling and rising wings. This stability, however, is present only so long as the critical angle is not exceeded; otherwise a disturbance in roll will lead to autorotation and spinning. Of course stability, as it is being considered here, is confined to normal flight.

Owing to the difference of the angles of incidence mentioned above, any roll must be accompanied by a yaw due to the drag difference, but mathematical analysis shows that, for small disturbances in roll, the roll is automatically stopped before the yaw becomes important.

Rolling Stability in Sideslip. Suppose, through some disturbance, an aeroplane is flying with one wing down. Then the aeroplane will commence to sideslip towards the lower wing, and it is obviously a condition of stability that a restoring rolling moment shall be called into play to lift the lower wing. This type of stability is achieved by the use of a **dihedral angle**. Most aeroplanes have their wing tips raised as in Fig. 116, the angle Γ being termed the dihedral angle and varying in practice from about 2° to 6° . The action of the dihedral angle in a sideslip is as follows:



FIG. 116. Dihedral Angle.

Suppose an aeroplane has a sideslip velocity to the right as shown in Fig. 117. Then, due to the sideslip, the air meets the aeroplane with a sideways velocity v , say. This velocity can be

resolved into its components along and perpendicular to the inner and outer wings as shown. Thus the inner wing has its incidence increased by an amount $\Delta\alpha$, while the outer wing has its incidence decreased by the same amount. The lift on the inner wing is therefore greater than that on the outer wing, and so a rolling moment is generated lifting the inner wing.

It must be noted that the dihedral angle comes into operation only when the aeroplane has acquired a sideslip velocity; it has

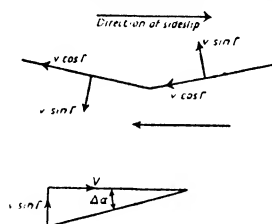


FIG. 117. Action of Dihedral Angle.

no tendency to stop a roll in which there is no sideslip. Thus an aeroplane with a dihedral angle can make a correctly banked turn as easily as one without a dihedral.

Spiral Stability. It has already been mentioned that an aeroplane with a very large fin and rudder, and therefore with a very high degree of directional stability, may be lacking in stability of another form.

Suppose an aeroplane suffers some disturbance which results in the aeroplane having an angular yawing velocity (Fig. 118). Then the outer wing is travelling faster than the inner and consequently has a greater lift, so that a rolling moment is generated tending to roll the aeroplane in the direction of the turn. Thus the aeroplane acquires an angle of bank and sideslips inwards. The dihedral angle immediately comes into operation and tries to lift the inner wing, but the action on the fin of the side wind due to the sideslip is to call into play a moment tending to force the nose into the side wind, i.e. a moment tending to increase the turn. If then the directional stability is so great that the effect of the fin is more powerful than that of the dihedral angle,

the original rate of turn will be increased. This increase of turning velocity will increase the roll; the roll will still further increase the turn, and so on. At the same time the aeroplane will be losing height due to the bank. Hence it will descend in a spiral path of continually decreasing radius. This type of instability is called spiral instability.

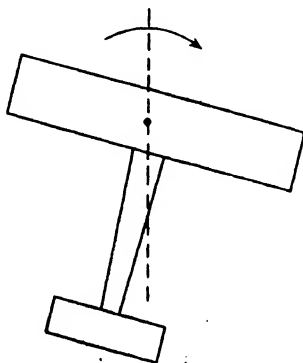


FIG. 118.

XII

SCALE EFFECT

Scale Effect. So far it has always been assumed that any air force experienced by a body can be written in the form $R = k\rho l^2 V^2$, where l is some linear dimension of the body, defining the scale, and k is a constant, depending only on the shape of the body and its attitude to the relative wind. By this means it has been possible to apply model data obtained at low values of l and V to the full-scale aeroplane in which the values of l and V are much higher. Strictly speaking, however, this $\rho l^2 V^2$ law is incomplete, and the true law is given by the Theory of Dimensions. It is not proposed to enter into a discussion of this theory here; it will be sufficient to state that, on theoretical grounds, the correct form for an air force is

$$R = \rho l^2 V^2 \times f\left(\frac{\rho V l}{\mu}\right),$$

where μ is the coefficient of viscosity of air.

Now μ is sensibly independent of pressure and temperature, and therefore, if air of a given density (say standard G.L. density) is considered, $\frac{\rho}{\mu}$ is constant and the expression for R becomes $R = \rho l^2 V^2 \times f(Vl)$. Thus the constant k should be replaced by some function of Vl , and there is nothing in the theory to say whether this function is constant. Hence the simple $\rho l^2 V^2$ law can be used to correct from model to full-scale only if the value of Vl is the same in each case. This is an unfortunate law, for it means that if, say, a model of $\frac{1}{10}$ scale is to be tested in order to obtain the forces on the full-scale aeroplane at 100 miles per hour, the correct wind channel speed should be 1,000 miles per hour, and the forces on the model would then be exactly the same as on the full-scale aeroplane. This is manifestly impossible, and so it becomes necessary to study the manner in which the value of k varies with the value of Vl . Any such variation is called scale effect, and considerable wind channel

and full-scale research have been undertaken to determine its nature.

In dealing with scale effect on aeroplanes it is customary to take the chord length as l ; thus a model of 6 in. chord tested at 60 ft. per second is said to be tested at $VI = 30$. In wind channel practice the working values of VI vary from about 10 to 100, whereas the full-scale value of VI is of the order of 1,000.

A method often employed to determine the scale effect on the resistance coefficient k of any part of an aeroplane is to carry out

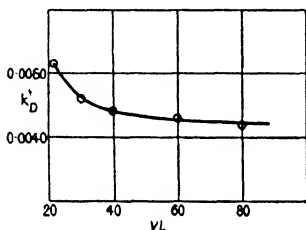


FIG. 119. Typical Scale Effect on k_D .

say, this value still holds at $VI = 1,000$. An illustration of the method is afforded by Fig. 119, which shows the drag coefficient at 0° incidence of a thin symmetrical section R.A.F. 27 obtained experimentally at different VI values. It will be seen that over the whole VI range k_D decreases continually as VI increases but appears to be approaching a constant value.

In some experiments on scale effect the variation of k is found to be irregular, and there is no indication of k acquiring a constant value; in other cases it has been proved that the assumption of an apparent limiting value is definitely erroneous. In any case it is clear that, whatever the variation of k over the model VI range, the value of k even at the highest VI value cannot be confidently applied to the full-scale aeroplane without some further justification, or without possibly some further VI correction. For this reason there have been carried out in this country a large number of full-scale experiments, in which measurements have been made on actual aeroplanes in flight. In America

the problem has been dealt with by the use of a variable-density wind channel, the operation of which is described below. Data obtained by these different methods are now available for the more important resistance coefficients, and a certain amount of generalization seems to be possible.

The Variable-Density Wind Channel. In the expression for R , given by the dimensional theory, it is usual to write ν for $\frac{\mu}{\rho}$ so that the expression becomes $R = \rho l^2 V^2 \times f\left(\frac{Vl}{\nu}\right)$. $\frac{Vl}{\nu}$ is called the Reynolds' number, and so, if viscosity and density are taken into account, the condition for the application of the simple $\rho l^2 V^2$ law is that the Reynolds' number should be constant. It follows that the low model Vl values can be counteracted by using air with a low value of ν (called the kinematic coefficient of viscosity). In America there is a special wind channel in which the air can be compressed; thus, since the density ρ varies as the pressure while μ is practically independent of the pressure, the value of ν can be reduced, and it is possible, even at low channel speeds on small scale models, to work at full-scale values of the Reynolds' number.

It may be noted that for air at standard density the value of ν is about 0.00016, so that a full scale Vl value of 1,000 corresponds to a Reynolds' number of a little over 6×10^6 .

Scale Effect on Aerofoil Lift. This is studied by comparing the lift-incidence curves obtained at different Vl (or $\frac{Vl}{\nu}$) values,

and the first point of importance is that with some aerofoils model results at very low Vl , say $Vl = 10$, are unreliable owing to the falling-away of the curve from its straight line form at small angles of incidence. Fig. 120 shows the lift-incidence curves for an aerofoil of R.A.F. 15 section of aspect ratio 6 at three different Vl values.

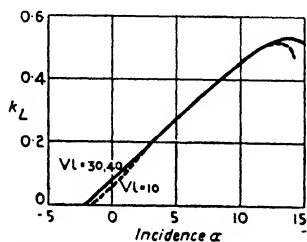


FIG. 120. Scale Effect on k_L at Very Low Vl .

Scale Effect

The curves for $VI = 30$ and $VI = 40$ are practically indistinguishable, but the falling-away of the curve for $VI = 10$ is very noticeable. All model tests carried out at the higher VI values ($VI = 25$ and upwards) have full-scale corroboration in showing that the scale effect on the slope of the curve and on the no-lift angle is negligible; and this is generally true for all aerofoils. Fig. 121 shows the excellent agreement between model and

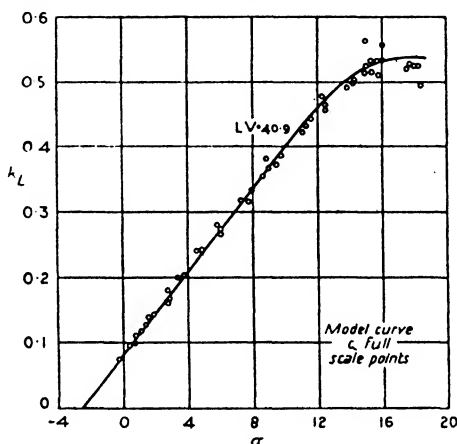


FIG. 121. Model and Full-Scale Lift Curves (R.A.F. 15 Wings).

full-scale for the lift curve of a complete aeroplane fitted with R.A.F. 15 wings. It will be noticed that for this aeroplane there is no appreciable scale effect at all. Generally, however, there is always some scale effect on the maximum lift coefficient, and the nature of the scale effect varies considerably with thickness and centre line camber.

For thin aerofoils of about the thickness of R.A.F. 15 (t/c ratio = 0.063) it appears that the value of $k_{L\max}$ never decreases with increasing VI , but generally increases slightly. The magnitude of the scale effect is illustrated in Fig. 122, which refers to a thin aerofoil R.A.F. 28.

There are no full-scale data available for this aerofoil, but experiments in the variable-density wind channel on other thin

sections would seem to confirm the conclusion which might be drawn from Fig. 122, namely that the scale effect is small but on the right side.

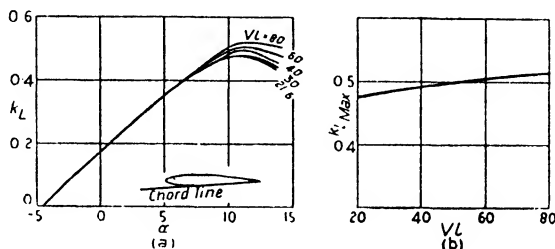


FIG. 122.

(a) R.A.F. 28. Scale Effect on Lift. (b) R.A.F. 28. Scale Effect on $k_{L, Max}$.

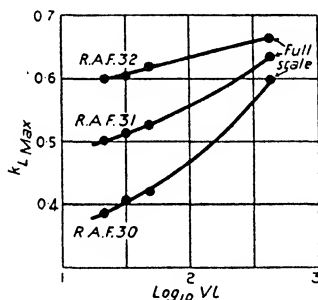


FIG. 123. Scale Effect with Varying Centre Line Camber.

For aerofoils of about twice the thickness of R.A.F. 15 $k_{L, Max}$ again increases with increasing VL , but the rate of increase depends a lot on centre line camber. Model and full-scale experiments have been carried out on an aeroplane fitted in turn with three sets of wings, the wings being all of the same thickness but of different centre line camber. The sections were R.A.F. 30 of zero camber, R.A.F. 31 of camber 0.02 and R.A.F. 32 of camber 0.05 (see Fig. 8). The results of the experiments are shown in Fig. 123, where $k_{L, Max}$ is plotted against $\log_{10} VL$. (VL is plotted on a logarithmic scale to keep the figure to a reasonable

size.) The most noticeable feature is the very large increase of $k_{L\max}$ for the symmetrical section of the series.

Lastly, for very thick aerofoils or for aerofoils of very high camber, $k_{L\max}$ generally decreases with increasing VL , although at times the variation may be irregular. The scale effect on a

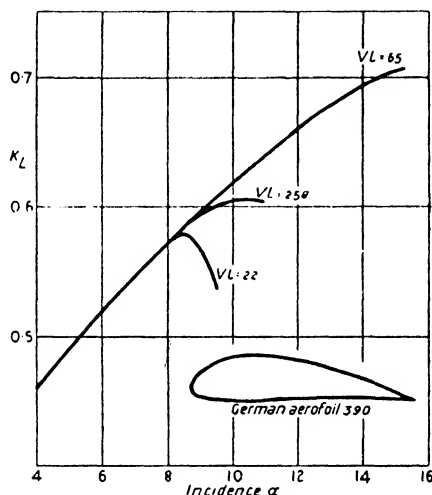


FIG. 124. Scale Effect on Thick Aerofoil.

very thick aerofoil is illustrated in Fig. 124, which is quite typical of sections having a $\frac{t}{c}$ ratio of 0.2 or over. The behaviour of such sections at full-scale $\frac{VL}{v}$ values has been studied in the variable-density wind channel, and the results go to show that it is always unlikely that the high values of $k_{L\max}$ obtained at normal channel speeds will be reproduced full-scale. There is also a little full-scale evidence in support of this.

Another type of 'high-lift' wing section is one of medium thickness but extravagant camber. Such a wing is R.A.F. 19, which gives a very high value for $k_{L\max}$ in the wind channel, but falls a long way short of this value on the full-scale aeroplane.

With this aerofoil there also appears to be a reduction of the slope of the lift curve, but this is unusual. The model lift curve and the full-scale points are given in Fig. 125.

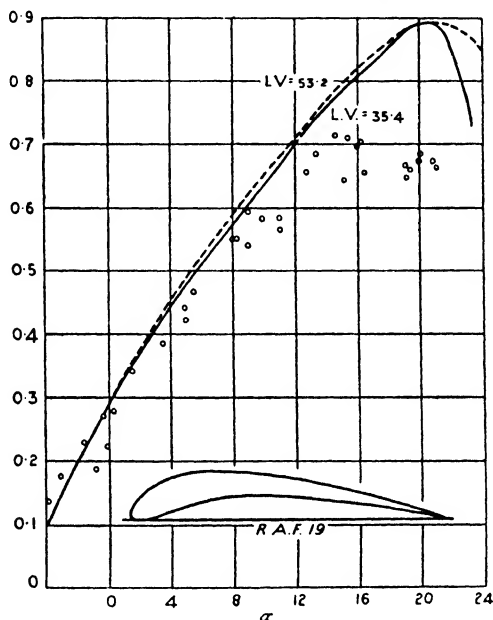


FIG. 125. Model and Full-Scale Lift Curve (R.A.F. 19 Wings).

Scale Effect on Aerofoil Drag. Experiment shows that the drag coefficient k_D of all aerofoils generally decreases as VI increases. The magnitude of the decrease for normal channel VI values is shown in Fig. 126, which gives the drag curves for the thin aerofoil R.A.F. 28 and the medium size aerofoil R.A.F. 31.

The scale effect is better illustrated perhaps in Fig. 127, where minimum k_D is shown plotted against VI . It will be seen that in each case k_D appears to be approaching a limiting value. This is roughly true for all aerofoils, and experiments in the variable-density channel show that this limiting value is probably the full-scale value. For very thick aerofoils the scale effect on k_D is similar in character but much more marked.

Unfortunately there is no full-scale corroboration of this scale effect on k_D , for it is almost impossible to measure the drag of the wings alone. From full-scale observations the drag of the complete aeroplane may be deduced, but any scale effect thus revealed includes the scale effect on the parasite drag.

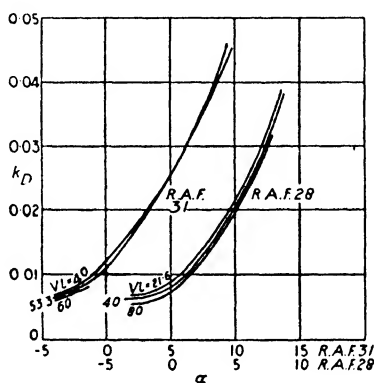


FIG. 126. Scale Effect on Aerofoil Drag.

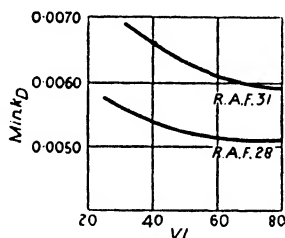


FIG. 127. Scale Effect on $Min k_D$.

Scale Effect on Moment and Centre of Pressure. Scale effect on k_m and $k_{C.P.}$ is not very large and may be neglected. Some full-scale experiments show that the slope of the curve of total k_m against k_L , as obtained in the channel, is substantially correct, but they do reveal some scale effect on the value of k_m at zero lift; and this means, of course, a scale effect on $k_{C.P.}$. Since, however, there is very good agreement between model

and full-scale on k_L , and also on some pressure distribution diagrams, it seems likely that some of the apparent scale effect may be due to scale effect on body moments, &c.

Scale Effect on Parasite Drag. On p. 198 it was stated that the variation of the resistance coefficient k may often be very irregular. Generally speaking, the irregularity increases as the streamline nature of the body decreases. This is due to the fact that, for bodies of high drag which are inevitably associated with turbulent flow, the flow may be unstable, and big changes in the flow pattern may occur as the Reynolds' number changes. On the other hand, for good streamline bodies (e.g. airship envelopes) the scale effect is more of the nature of the scale effect on aerofoils, the drag generally decreasing with increasing VI .

Struts. These are good streamline bodies of thick symmetrical aerofoil section, and the scale effect is similar to that of thick aerofoils. Since the 'chord' of a strut is small compared with the wing chord, it is possible to work at full-scale VI values in the ordinary wind channel, and Fig. 128 shows the scale effect obtained. It will be seen that at full-scale VI the drag is about 1 lb. per square foot at 100 ft. per second, and this is the figure given in Chapter VI.

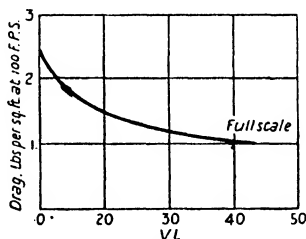


FIG. 128. Scale Effect on Strut Drag.

The wire drag figures given in that chapter are full-scale figures estimated in a similar manner.

Fuselages. If a fuselage is of a very good streamline form, it is probable that the drag decreases as VI increases; on the other hand, if it is a poor shape aerodynamically, the variation in the

drag may be irregular, and the full-scale drag may possibly be greater than the model drag. Fuselages vary so much, however, that generalization is almost impossible. What little evidence there is goes to show that the scale effect is probably small and in most cases, on the right side. Some idea of the possible scale effect may be obtained from the full-scale experiments given below.

Undercarriages. An undercarriage is a collection of struts, wires and wheels, and, like a fuselage, its scale effect is difficult to estimate.

Full-Scale Drag of Complete Aeroplane. Full-scale research has provided some interesting data with regard to the scale effect on the drag of a complete aeroplane. Fig. 129 refers to two

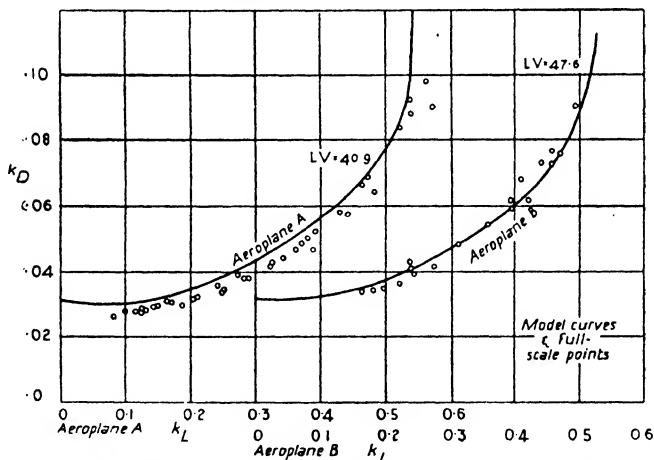


FIG. 129. Model and Full-Scale Drag Curves (R.A.F. 15 Wings).

different aeroplanes, both fitted with wings of R.A.F. 15 section. It will be seen that for aeroplane *A* the full-scale drag is slightly lower than the model drag, while for aeroplane *B* model and full-scale are in good agreement. Since the wing section is the same in each case, it would seem that the discrepancy must be attributed to a difference in scale effect on fuselage, undercarriage, &c., or possibly on interference.

With some aeroplanes having R.A.F. 15 wing section, the scale effect on total drag seems to be slightly adverse, and the full-scale drag is slightly higher than the model drag. On the whole, however, the agreement between model and full-scale must be considered reasonably good.

Fig. 129 may also be compared with Fig. 130, which refers to aeroplane *A* when fitted with wings of R.A.F. 31 section.

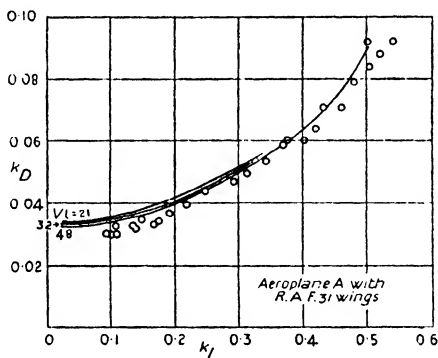


FIG. 130. Model and Full-Scale Drag Curves (R.A.F. 31 Wings).

XIII

AIRSCREW THEORY

(In this chapter the theory of the airscrew is described more fully than in Chapter VIII. Paragraphs marked with an asterisk must be omitted unless the reader has a knowledge of the calculus.)

Introduction. Until the vortex theory of aerofoils was established, the basis of airscrew design consisted of what is known as the Simple Blade Element Theory and the Simple Momentum Theory, and the combination of these two theories led to fairly successful airscrew design. Modern airscrew theory is an extension of the aerofoil theory to the airscrew, and, while it follows more or less the general lines of the older theories, rests on a sounder physical basis.

The Simple Blade Element Theory. This theory has already been mentioned in Chapter VIII. Each portion of the blade is regarded as behaving like an aerofoil so that, if the blade is considered to be split up into small strips or elements, the behaviour of each element can be calculated, and so the behaviour of the whole airscrew determined. Modern airscrew theory also considers the behaviour of the elements of the blade, but not before the actual type of flow occurring at the airscrew has been studied in more detail. The simple theory forms, however, a good introduction to any strip or element theory and throws considerable light on the behaviour of an airscrew.

Consider a small strip of the blade AA' at a radial distance r (see Figs. 72 and 73). Let the chord be c and the width or 'span' of the element Δr . (Δr is the notation of the calculus and simply means a small increment of r ; it is considered so small that the chord, pitch angle and cross-section may be considered constant over the strip.)

Let V be the forward speed and n the revolutions per second. Then, as on p. 130, the following equations hold:

$$\text{Incidence} \quad \alpha = \theta - \phi \quad . \quad . \quad . \quad . \quad . \quad (1)$$

$$V_r = 2\pi nr \sec \phi \quad . \quad . \quad . \quad . \quad . \quad (2)$$

$$\text{and} \quad \tan \phi = \frac{V}{2\pi nr} \quad . \quad . \quad . \quad . \quad . \quad (3)$$

Also, since the area of the element is $c \times \Delta r$, the lift measured in the direction of forward motion is $(k_L \cos \phi - k_D \sin \phi) \rho c V_r^2 \times \Delta r$, and the drag measured in the plane of rotation is $(k_L \sin \phi + k_D \cos \phi) \rho c V_r^2 \times \Delta r$.

Hence the thrust of the element ($= \Delta T$, representing a small fraction of the total thrust T) is given by

$$\Delta T = (k_L \cos \phi - k_D \sin \phi) \rho c V_r^2 \times \Delta r. \quad (4)$$

and the torque (i.e. the moment of the drag about the axis of rotation) by

$$\Delta Q = (k_L \sin \phi + k_D \cos \phi) \rho c r V_r^2 \times \Delta r. \quad (5)$$

Therefore the thrust per unit run at AA' ($= \frac{\Delta T}{\Delta r}$) is $(k_L \cos \phi - k_D \sin \phi) \rho c V_r^2$, and the torque per unit run ($= \frac{\Delta Q}{\Delta r}$) is $(k_L \sin \phi + k_D \cos \phi) \rho c r V_r^2$.

Hence, if $(k_L \cos \phi - k_D \sin \phi) \rho c V_r^2$, i.e. $\frac{\Delta T}{\Delta r}$, is calculated for several points along the blade and is then plotted against the radial distance r , the area bounded by the curve so obtained and the r -axis gives the total thrust of the blade. Similarly for the torque. [If $\frac{\Delta T}{\Delta r}$ were constant at all points of the blade, the total thrust would be $\frac{\Delta T}{\Delta r} \times R$ (where R is the tip radius), i.e. thrust per unit run multiplied by the blade length. The thrust could therefore be represented by the area of a rectangle, of which one side is the thrust per unit run and the other the blade length. Obviously $\frac{\Delta T}{\Delta r}$ is not constant owing to the fact that each section of the blade is of a different aerofoil shape and is working under its own conditions of velocity and incidence, but the area under the curve obtained by plotting $\frac{\Delta T}{\Delta r}$ against r still gives the total thrust. Similarly for the torque.

Airscrew Theory

Compare a velocity-time diagram in which the velocity is varying, or a work diagram in which the force varies.]

Readers having a knowledge of the calculus will prefer to use the more usual notation $\frac{dT}{dr}$, $\frac{dQ}{dr}$ instead of $\frac{\Delta T}{\Delta r}$, $\frac{\Delta Q}{\Delta r}$. For those who have no such knowledge it is sufficient to remember that $\frac{dT}{dr}$, $\frac{dQ}{dr}$ are not ordinary algebraic fractions, but are simply conventional symbols representing the thrust and torque per unit run, and their values vary along the blade.

The equations for the thrust and torque per unit run at any radial distance now become

$$\frac{dT}{dr} = (k_L \cos \phi - k_D \sin \phi) \rho c V_r^2$$

and
$$\frac{dQ}{dr} = (k_L \sin \phi + k_D \cos \phi) \rho c r V_r^2.$$

But $V_r = 2\pi n r \sec \phi$, from equation (2); hence

$$\frac{dT}{dr} = \rho c (k_L \cos \phi - k_D \sin \phi) 4\pi^2 n^2 r^2 \sec^2 \phi \quad . \quad (6)$$

and
$$\frac{dQ}{dr} = \rho c (k_L \sin \phi + k_D \cos \phi) 4\pi^2 n^2 r^3 \sec^2 \phi \quad . \quad (7)$$

Thrust and Torque Grading Curves. By means of the above equations the values of $\frac{dT}{dr}$, $\frac{dQ}{dr}$ at any point along the blade can be calculated for any combination of V and n . For, if V and n are known, the angle ϕ of the section can be obtained from equation (3); the angle of incidence is then given by equation (1), and hence, if the aerofoil characteristics of the section are known, the values of k_L and k_D are known.

The type of curve obtained by plotting the values of $\frac{dT}{dr}$ for various points along the blade against r is shown in Fig. 131 (a); such a curve is called a thrust grading curve and shows how the thrust is distributed along the blade. The area above the dotted

portion represents the drag of the boss and must be subtracted from the big area above the r -axis in order to obtain the net thrust. A typical torque grading curve is shown in (b).

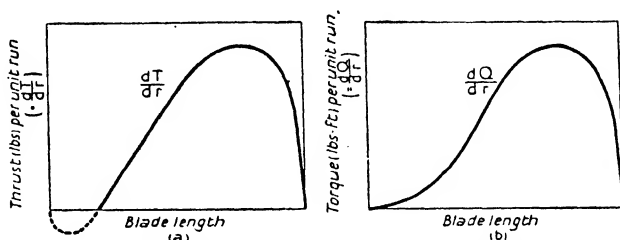


FIG. 131. Thrust and Torque Grading Curves.

It will be seen that the maximum thrust and torque per unit run are both obtained from the section at a radial distance of about three-quarters the tip radius.

Efficiency of an Element. The efficiency of an airscrew is $\frac{TV}{2\pi nQ}$ (see p. 133); hence the efficiency of any element is given by

$$\begin{aligned}\eta &= \frac{\Delta T \times V}{2\pi n \times \Delta Q} \\ &= \frac{(k_L \cos \phi - k_D \sin \phi) \rho c V_r^2 \times \Delta r \times V}{(k_L \sin \phi + k_D \cos \phi) \rho c r V_r^2 \times \Delta r \times 2\pi n},\end{aligned}$$

from equations (4) and (5),

$$= \frac{(k_L \cos \phi - k_D \sin \phi) V}{(k_L \sin \phi + k_D \cos \phi) 2\pi n r}.$$

But $\frac{V}{2\pi n r} = \tan \phi$, from equation (3); hence

$$\begin{aligned}\eta &= \tan \phi \times \frac{k_L \cos \phi - k_D \sin \phi}{k_L \sin \phi + k_D \cos \phi} \\ &= \tan \phi \times \frac{\frac{k_L}{k_D} \cos \phi - \sin \phi}{\frac{k_L}{k_D} \sin \phi + \cos \phi}\end{aligned}$$

$$= \tan \phi \times \frac{\frac{k_L}{k_D} - \tan \phi}{\frac{k_L}{k_D} \tan \phi + 1},$$

on dividing both numerator and denominator by $\cos \phi$,

i.e. $\eta = \frac{\tan \phi (\delta - \tan \phi)}{\delta \tan \phi + 1},$

putting $\frac{k_L}{k_D} = \delta$, for simplicity.

If now a particular value is assigned to δ , the efficiency of the

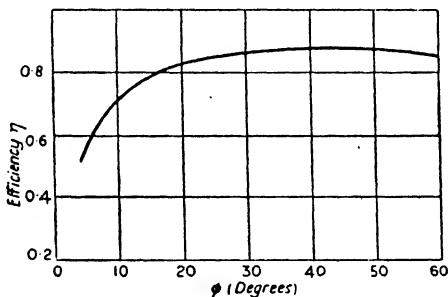


FIG. 132. Effect of Pitch on Efficiency.

element can be calculated for different values of ϕ , and so a curve obtained showing how η varies with ϕ . Such a curve is given in Fig. 132, δ having been given the arbitrary value of 15. It will be seen that the efficiency increases as ϕ increases up to $\phi = 45^\circ$.

Now a given value of δ , i.e. of $\frac{k_L}{k_D}$, means a given value of the incidence α , and therefore increasing values of ϕ correspond to increasing values of θ , for $\phi = \theta - \alpha$. Hence the figure shows that the efficiency of any element increases as θ increases, that is as the pitch increases. (See Chapter VIII, p. 136, and Fig. 77.)

Calculation of $\frac{dT}{dr}$ and $\frac{dQ}{dr}$. If, for simplicity, μ_1 and μ_2 are

written for $(k_L \cos \phi - k_D \sin \phi) \sec^2 \phi$ and $(k_L \sin \phi + k_D \cos \phi) \sec^2 \phi$ respectively, equations (6) and (7) become

$$\frac{dT}{dr} = \mu_1 \rho c 4 \pi^2 n^2 r^2 \quad . \quad . \quad . \quad . \quad . \quad (8)$$

and
$$\frac{dQ}{dr} = \mu_2 \rho c 4 \pi^2 n^2 r^3 \quad . \quad . \quad . \quad . \quad . \quad (9)$$

Also
$$\tan \phi = \frac{V}{2\pi nr}.$$

These equations completely determine the thrust and torque per unit run of any element of an airscrew at any given translational velocity V and rotational velocity $2\pi n$.

Note that the efficiency of the element may be written

$$\eta = \tan \phi \times \frac{\mu_1}{\mu_2} \quad . \quad . \quad . \quad . \quad . \quad (10)$$

Example. A 10 ft. diameter airscrew runs at 1,560 R.P.M. at 120 miles per hour. Show that, under these conditions of working, the incidence of the section at $r = 0.75R$ is about 0.5° , given that the pitch angle of the section is $16^\circ 30'$.

If the lift and drag characteristics at this incidence are $k_L = 0.185$ and $k_D = 0.0120$, find the thrust and torque per unit run and determine also the efficiency. The chord length of the section is 0.722 ft.

We have $V = 176$, $n = 26$, $r = 3.75$.

$$\begin{aligned} \therefore \tan \phi &= \frac{V}{2\pi nr} \\ &= 0.287. \end{aligned}$$

$$\therefore \phi = 16^\circ \text{ approx.}$$

Hence, $\alpha = \theta - \phi = 0.5^\circ.$

Again,
$$\begin{aligned} \mu_1 &= (k_L \cos \phi - k_D \sin \phi) \sec^2 \phi \\ &= (0.178 - 0.003) \times 1.082 \\ &= 0.189, \end{aligned}$$

and

$$\begin{aligned}\mu_2 &= (k_L \sin \phi + k_D \cos \phi) \sec^2 \phi \\ &= (0.0510 + 0.0115) \times 1.082 \\ &= 0.0676.\end{aligned}$$

Hence,

$$\begin{aligned}\frac{dT}{dr} &= \mu_1 \rho c 4 \pi^2 n^2 r^2 \\ &= 0.189 \times 0.00237 \times 0.722 \times (612.5)^2,\end{aligned}$$

for $2\pi nr = 612.5$,

$$= 121 \text{ lb.}$$

and

$$\begin{aligned}\frac{dQ}{dr} &= \mu_2 \rho c 4 \pi^2 n^2 r^3 \\ &= 0.0676 \times 0.00237 \times 0.722 \times (612.5)^2 \times 3.75 \\ &= 163 \text{ lb.-ft.}\end{aligned}$$

Also,

$$\begin{aligned}\eta &= \tan \phi \times \frac{\mu_1}{\mu_2} \\ &= 0.802.\end{aligned}$$

If similar calculations to the above are carried out for other sections of the blade (sections at $\frac{r}{R} = 0.30, 0.45, 0.60, 0.75$ and 0.90 are often taken), the values of $\frac{dT}{dr}$, $\frac{dQ}{dr}$ can be plotted to give the thrust and torque grading curves; and so the total thrust and torque may be obtained. From these values of total thrust T and total torque Q the efficiency of the whole airscrew and the horsepower absorbed by the airscrew can be calculated. T and Q may also be reduced to coefficient form by means of the equations $T = k_T \rho n^2 D^4$ and $Q = k_Q \rho n^2 D^5$. Hence, if a range of arbitrary simultaneous values of V , n are taken, the values of k_T , k_Q may be determined for a range of values of $\frac{V}{nD}$, and so the usual k_T , k_Q curves may be drawn.

***Calculation of k_T and k_Q .** A more convenient method of determining the values of k_T , k_Q for any given value of $\frac{V}{nD}$ is described below.

Consider an element at a radial distance r , and let $\frac{r}{R} = x$.

Then $r = Rx$; and therefore $\tan \phi = \frac{V}{2\pi nr}$

$$= \frac{V}{2\pi Rxn}$$

$$= \frac{V}{nD} \frac{1}{\pi x}, \text{ since } 2R = D,$$

i.e. $\frac{V}{nD} = \pi x \tan \phi. \quad . \quad . \quad . \quad . \quad (11)$

Again,

$$T = k_T \rho n^2 D^4$$

$$\therefore dT = \rho n^2 D^4 \times dk_T.$$

Also, since

$$r = Rx,$$

$$dr = Rdx$$

$$\therefore \frac{dT}{dr} = \frac{\rho n^2 D^4}{R} \times \frac{dk_T}{dx}$$

$$= 2\rho n^2 D^3 \times \frac{dk_T}{dx}.$$

Hence, if B is the number of blades,

$$2\rho n^2 D^3 \times \frac{dk_T}{dx} = B \times \mu_1 \rho c 4\pi^2 n^2 r^2,$$

for $\frac{dT}{dr} = \mu_1 \rho c 4\pi^2 n^2 r^2$ for one blade.

Therefore, $\frac{dk_T}{dx} = \frac{2Bc\mu_1\pi^2 r^2}{D^3}.$

Similarly, $\frac{dk_Q}{dx} = \frac{2Bc\mu_2\pi^2 r^3}{D^4}.$

These equations are generally put into another form as follows :

$$\frac{dk_T}{dx} = \frac{2Bc\mu_1\pi^2 r^2}{8R^3}$$

$$= \frac{Bc}{4\pi r} \mu_1 \pi^3 \left(\frac{r}{R}\right)^3$$

$$= \frac{Bc}{4\pi r} \mu_1 \pi^3 x^3.$$

It is also usual to write σ for the non-dimensional quantity $\frac{Bc}{2\pi r}$. Then the equation for $\frac{dk_T}{dx}$ becomes

$$\frac{dk_T}{dx} = \frac{1}{2}\sigma\mu_1\pi^3x^3. \quad (12)$$

Similarly it may be shown that

$$\frac{dk_Q}{dx} = \frac{1}{4}\sigma\mu_2\pi^3x^4. \quad (13).$$

Equations (11) (12) and (13), together with the expressions for μ_1 , μ_2 and σ , enable $\frac{dk_T}{dx}$, $\frac{dk_Q}{dx}$ to be calculated at once for any given value of $\frac{V}{nD}$. If then the values of $\frac{dk_T}{dx}$, $\frac{dk_Q}{dx}$ for the various sections are plotted against x , the values of k_T , k_Q may be obtained.

Remarks on the Theory. So far nothing has been said about the aerofoil characteristics to be used for the different sections. The aerofoil shape of each section is known, but the shape of the cross-section of an aerofoil does not determine its characteristics unless the aspect ratio is known. The question immediately arises, what aspect ratio characteristics should be used? Each element has a negligible 'span' in the ordinary sense, but at the same time it forms a part of a twisted aerofoil, viz. the blade. In the simple theory no true answer can be found to this question, and the most that can be said is that, if characteristics for an aspect ratio of about 6 are used, the maximum efficiency can be predicted fairly accurately, although the calculated values of k_Q or the horse-power absorbed may be considerably in error.

Again, the theory neglects to take into account the loss of energy due to the axial and rotational velocities imparted to the slipstream, and considers only the loss of efficiency due to the drag of the blades. Now the Simple Momentum Theory, which is discussed in the following paragraph, shows that the axial velocity of the slipstream alone involves a considerable loss of efficiency, and therefore the agreement between the observed

values of the efficiency and those calculated by means of the simple blade element theory must be regarded as fortuitous and due to counteracting errors.

The Simple Momentum Theory. This theory treats the problem from a quite different standpoint by considering the momentum and energy of the system. Since the aircrew develops a forward thrust, there must be an equal and opposite force driving the air backwards. Thus the air which passes

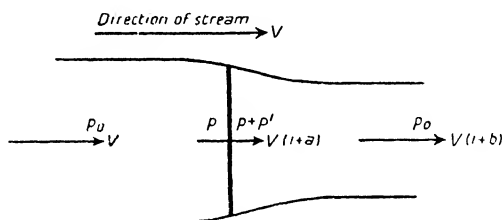


FIG. 133. Actuator Disk.

through the aircrew disk is discharged backwards at a velocity greater than that of the free airstream. This added velocity in the slipstream is sometimes called the *outflow velocity*. The whole of this added velocity does not, however, occur behind the aircrew, for there must be some acceleration of the air in front to take the place of the air driven backwards. Hence the air immediately in front of the aircrew also has an added velocity, and this is called the *inflow velocity*.

Now, in the simple momentum theory, the thrust is supposed to be uniformly distributed over the aircrew blades, and the aircrew is regarded as an 'actuator disk' which imparts a sudden increase of pressure to the air passing through it, so that the thrust is equal to the area of the disk multiplied by the pressure increment. Apart from this discontinuity of pressure, the flow is regarded as streamline in the sense that Bernoulli's equation still holds.

Consider now an actuator disk in an airstream moving with a velocity V and of pressure p_0 . Then the flow diagram is as shown in Fig. 133.

Just in front of the disk the velocity rises to $V(1+a)$, where a is the ratio of the inflow velocity to the free velocity V , and therefore the pressure falls from p_0 to p , say. As the air passes through the disk the velocity remains constant, but immediately behind the disk the pressure is suddenly increased to $p+p'$, where p' is the increment of pressure imparted by the disk. At some distance behind the disk the velocity has risen to $V(1+b)$, where b is the ratio of the outflow velocity to V , and the pressure has resumed its original value p_0 .

(NOTE. The contraction of the stream shown in the figure is due to the fact that, in a given time, a constant volume of air passes through every cross-sectional area, so that increased velocity means reduced cross-sectional area).

Bernoulli's equation is now applied to the flow in front of the disk and to the flow behind.

For the flow in front,

$$p_0 + \frac{1}{2}\rho V^2 = p + \frac{1}{2}\rho V^2(1+a)^2,$$

and for the flow behind,

$$(p+p') + \frac{1}{2}\rho V^2(1+b)^2 = p_0 + \frac{1}{2}\rho V^2(1+b)^2.$$

Hence, by subtraction,

$$\begin{aligned} [(p+p') + \frac{1}{2}\rho V^2(1+b)^2] - [p + \frac{1}{2}\rho V^2(1+a)^2] \\ = [p_0 + \frac{1}{2}\rho V^2(1+b)^2] - [p_0 + \frac{1}{2}\rho V^2]. \end{aligned}$$

$$\begin{aligned} \therefore p' &= \frac{1}{2}\rho V^2(1+b)^2 - \frac{1}{2}\rho V^2 \\ &= \frac{1}{2}\rho V^2[(1+b)^2 - 1] \\ &= \frac{1}{2}\rho V^2(2b+b^2), \end{aligned}$$

$$\text{i.e.} \quad p' = \rho V^2 \left(1 + \frac{b}{2}\right) b. \quad \dots \quad (14)$$

Now the mass of air passing through the disk per second

$$= \rho \times A \times V(1+a),$$

if A is the area of the disk. Also the effect of the disk is to increase the velocity from V to $V(1+b)$. Therefore

the thrust = the rate of change of momentum

$$= \rho AV(1+a) \times bV$$

i.e. $T = \rho AV^2(1+a)b \dots \dots \dots (15)$

But $T = p' \times A = \rho AV^2 \left(1 + \frac{b}{2}\right) b$, from equation (14).

Therefore $\rho AV^2(1+a)b = \rho AV^2 \left(1 + \frac{b}{2}\right) b$

$$\therefore 1+a = 1 + \frac{b}{2}$$

i.e. $a = \frac{b}{2} \dots \dots \dots (16)$

Hence the *inflow is half the outflow*, and equations (15) and (16) give

$$T = 2\rho AV^2(1+a)a \dots \dots \dots (17)$$

An expression can now be found for the efficiency, for

$$\begin{aligned} \text{the efficiency} &= \frac{\text{Useful work done on the air}}{\text{Total work done on the air}} \\ &= \frac{T \times V}{\text{Energy imparted to the stream per second}} \end{aligned}$$

and, if the rotation of the slipstream is ignored, the energy imparted is the difference between the kinetic energy in front and the kinetic energy behind.

Now the mass of air flowing through the disk per second = $\rho AV(1+a)$.

$$\therefore \text{energy in front} = \frac{1}{2} \rho AV(1+a) \times V^2,$$

and $\text{energy behind} = \frac{1}{2} \rho AV(1+a) \times V^2(1+b)^2.$

$$\begin{aligned} \text{Hence, energy imparted} &= \frac{1}{2} \rho AV(1+a) \times V^2[(1+b)^2 - 1] \\ &= \frac{1}{2} \rho AV^3(1+a)(2b+b^2) \\ &= \rho AV^3(1+a) \left(1 + \frac{b}{2}\right) b \\ &= 2\rho AV^3(1+a)^2 a, \text{ since } b = 2a. \end{aligned}$$

Therefore
$$\eta = \frac{TV}{2\rho AV^3(1+a)^2a}$$

$$= \frac{2\rho AV^3(1+a)a}{2\rho AV^3(1+a)^2a}, \text{ from equation (17),}$$

i.e.
$$\eta = \frac{1}{1+a} \quad \dots \dots \dots (18)$$

The efficiency may be obtained in a different way, by considering the disk to be moving forward with velocity V and the stream at rest. Then

$$\begin{aligned} \eta &= \frac{\text{Useful work}}{\text{Useful work} + \text{energy lost in the slipstream}} \\ &= \frac{TV}{TV + \frac{1}{2}\rho AV(1+a) \times b^2 V^2} \\ &= \frac{1}{1+a}, \end{aligned}$$

as before, on substituting for T from equation (17).

This is called the *ideal efficiency* and can never be realized in practice, since it is the efficiency obtained on neglecting the loss of energy due to the drag of the blades and to the rotation of the slipstream. In order to arrive at some idea of the value of this ideal efficiency, it is necessary to put equation (18) into another form.

Now $TV = \eta P_{550}$; hence equation (17) gives

$$2\rho AV^3(1+a)a = \eta P_{550}.$$

But
$$\frac{1}{1+a} = \eta; \text{ therefore } a = \frac{1}{\eta} - 1.$$

Also
$$A = \frac{\pi D^2}{4}.$$

$$\therefore 2\rho \times \frac{\pi D^2}{4} \times V^3 \times \frac{1}{\eta} \left(\frac{1}{\eta} - 1 \right) = \eta P_{550}$$

$$\therefore \frac{1}{2}\pi\rho V^3 D^2 \times \frac{1-\eta}{\eta^2} = \eta P_{550}.$$

Hence
$$\frac{1-\eta}{\eta^3} = \frac{1100}{\pi} \times \frac{P}{\rho V^3 D^2} \quad \dots \quad (19)$$

This relation between η and $\frac{P}{\rho V^3 D^2}$ is illustrated graphically in Fig. 134.

By means of this figure the ideal efficiency may be determined for any speed, provided the horse-power absorbed at this speed is known.

Consider the case of the airscrew of Chapter VII and Chapter VIII; it is of 9.25 ft. diameter and is designed to absorb

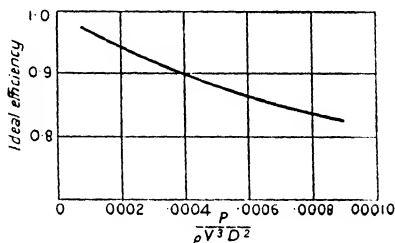


FIG. 134.

400 horse-power at 1,680 R.P.M. at 140 miles per hour. The corresponding value of $\frac{P}{\rho V^3 D^2}$ is 0.000228, and the ideal efficiency is read from the curve as 93.5 per cent. Actually the true efficiency of this airscrew is about 80 per cent., so that the true efficiency would appear to be about 85 per cent. of the ideal efficiency.

The Modified Blade Element Theory. Since the simple blade element theory neglects the energy lost in the slipstream, and the simple momentum theory neglects the drag of the blades, it follows that a better approximation to the true operation of an airscrew can be obtained by incorporating the idea of inflow into the simple blade element theory. In this combined theory the value of the inflow factor a is not, of course, constant over the whole blade, but its value at any section can be determined by using the condition that the inflow is half the outflow. It is

also possible to allow for the rotation of the slipstream by the introduction of a rotational factor a' . The actual equations determining the behaviour of an element are not given here, as they are of the same form as those given in the following paragraph on the vortex theory of airscrews.

This combined theory has been used in airscrew design with a fair measure of success, but it has been found that, if aerofoil characteristics for aspect ratio 6 are used, it is necessary to reduce the theoretical value for the ratio of inflow to outflow from $\frac{1}{2}$ to about $\frac{1}{3}$, in order that calculated values may agree with observed values. This discrepancy is cleared up, however, by the vortex theory.

***The Vortex Theory of Airscrews.** This theory is set forth by H. Glauert in his *Aerofoil and Airscrew Theory*. In it he considers the behaviour of an element as an aerofoil and assumes, as in the aerofoil theory, that the lift of each element is associated with a circulation round it, and that trailing vortices spring from the trailing edge of the blade and pass down-stream in helical paths. The effect of these vortices on the flow near the airscrew is analogous to that of the trailing vortices of an ordinary aerofoil, so that, before the characteristics of any element can be determined, it is necessary to study the manner in which the vortices affect the flow.

It is found that the interference on the two-dimensional flow can be represented by an axial interference velocity and a rotational interference velocity. Further analysis also leads to the result that, if the axial interference velocity is denoted by aV , then the velocity in the wake is $2aV$; and this is in agreement with the momentum theory. Also, if the rotational interference velocity is denoted by $a'\Omega$, where Ω is the angular velocity of the airscrew, then the rotational velocity in the wake is $2a'\Omega$. Now the interference velocities aV , $a'\Omega$ represent the total interference experienced by each element, and therefore, if they are fully taken into account, *the correct aerofoil characteristics to be used for each element are those for two-dimensional motion, i.e. for infinite aspect ratio.* Thus the vortex theory is similar to the

modified blade element theory, except that, by exactly defining the aerofoil characteristics, it calls for no empirical correction to the inflow factor $\frac{1}{2}$.

The true behaviour of an element is now illustrated in Fig. 135. The axial velocity is $V(1+a)$ and the velocity due to the rotation $r\Omega(1-a') = 2\pi nr(1-a')$. Notice that the rotational interference velocity must be subtracted, since it is clearly in the same direc-

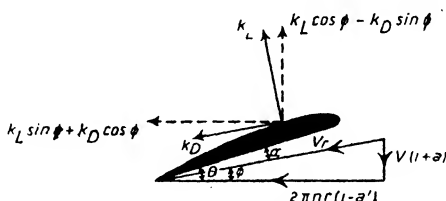


FIG. 135.

tion as the rotation of the airscrew and therefore reduces the relative angular velocity.

$$\text{Hence,} \quad \tan \phi = \frac{V}{2\pi nr} \frac{1+a}{1-a'}, \quad \dots \dots \dots (20)$$

Compare this with equation (3); it will be seen that, for a given value of $\frac{V}{n}$, the angle ϕ is modified by the introduction of the interference factors a, a' .

$$\text{Again,} \quad \frac{dT}{dr} = (k_L \cos \phi - k_D \sin \phi) \rho c V_r^2$$

$$\text{and} \quad \frac{dQ}{dr} = (k_L \sin \phi + k_D \cos \phi) \rho c r V_r^2,$$

exactly as on p. 210, except that k_L and k_D now refer to infinite aspect ratio.

Also V_r is given by

$$V_r = 2\pi nr(1-a') \sec \phi \text{ or } V(1+a) \operatorname{cosec} \phi.$$

It will be found convenient later on to use both these forms for V_r .

Now, in order to obtain equations giving a , a' , it is necessary to return to considerations of momentum. Instead, however, of considering the air flowing through the whole airscrew disk, it is necessary to consider the amount flowing through a small

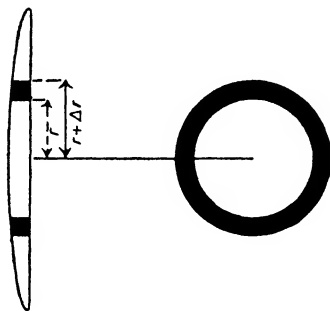


FIG. 136.

annulus, as shown in Fig. 136. The area of the annulus is $2\pi r \times \Delta r$, and so equation (17) becomes

$$\Delta T = 2\rho \times 2\pi r \Delta r \times V^2(1+a)a,$$

on substituting ΔT for T and $2\pi r \Delta r$ for A .

$$\text{Hence,} \quad \frac{\Delta T}{\Delta r} \text{ or } \frac{dT}{dr} = 4\pi r \rho V^2(1+a)a.$$

Therefore, if B is the number of blades,

$$\begin{aligned} 4\pi r \rho V^2(1+a)a &= B(k_L \cos \phi - k_D \sin \phi) \rho c V_r^2 \\ &= B(k_L \cos \phi - k_D \sin \phi) \rho c \times V^2(1+a)^2 \operatorname{cosec}^2 \phi. \end{aligned}$$

$$\begin{aligned} \therefore \frac{a}{1+a} &= \frac{Bc}{4\pi r} \frac{k_L \cos \phi - k_D \sin \phi}{\sin^2 \phi} \\ &= \frac{\sigma}{2} \frac{k_L \cos \phi - k_D \sin \phi}{\cos^2 \phi} \times \frac{\cos^2 \phi}{\sin^2 \phi}, \text{ putting } \frac{Bc}{2\pi r} = \sigma, \end{aligned}$$

$$\text{i.e.} \quad \frac{a}{1+a} = \frac{\sigma \mu_1}{2 \tan^2 \phi}, \quad \dots \dots \dots (21)$$

an equation giving a in terms of ϕ .

[The quantity $\sigma \left(= \frac{Bc}{2\pi r} = \frac{Bc \Delta r}{2\pi r \Delta r} \right)$ is the ratio of the area of

the blade elements at radial distance r to the area of the annulus; it is sometimes called the solidity of the element.]

Again the element of torque ΔQ is equal to the rate of change of angular momentum. Hence, if I is the moment of inertia of the air flowing through the annulus per second, $\Delta Q = I \times 2a'\Omega$, since the angular velocity of the air in front of the airscrew is zero and behind $2a'\Omega$.

Now $I = m r^2$, if m is the mass of air flowing through the annulus per second

$$= \rho \times 2\pi r \Delta r \times V(1+a) \times r^2.$$

$$\text{Therefore, } \Delta Q = \rho \times 2\pi r^3 \Delta r \times V(1+a) \times 2a'\Omega$$

$$\text{i.e. } \frac{\Delta Q}{\Delta r} \text{ or } \frac{dQ}{dr} = 4\pi r^3 \rho V \Omega (1+a)a'.$$

$$\text{But } \Omega = 2\pi n = \frac{V(1+a)}{r(1-a') \tan \phi}, \text{ from equation (20),}$$

$$\begin{aligned} \therefore \frac{dQ}{dr} &= 4\pi r^3 \rho V(1+a)a' \times \frac{V(1+a)}{r(1-a') \tan \phi} \\ &= 4\pi r^2 \rho V^2 (1+a)^2 \frac{a'}{(1-a') \tan \phi}. \end{aligned}$$

Hence,

$$\begin{aligned} 4\pi r^2 \rho V^2 (1+a)^2 \frac{a'}{(1-a') \tan \phi} &= B \times (k_L \sin \phi + k_D \cos \phi) \rho c r V^2, \\ &= B \times (k_L \sin \phi + k_D \cos \phi) \rho c r \times V^2 (1+a)^2 \operatorname{cosec}^2 \phi, \end{aligned}$$

$$\therefore 4\pi r \frac{a'}{(1-a') \tan \phi} = Bc(k_L \sin \phi + k_D \cos \phi) \operatorname{cosec}^2 \phi$$

$$\begin{aligned} \therefore \frac{a'}{1-a'} &= \frac{Bc}{4\pi r} \frac{k_L \sin \phi + k_D \cos \phi}{\sin^2 \phi} \times \frac{\sin \phi}{\cos \phi} \\ &= \frac{\sigma}{2} \frac{k_L \sin \phi + k_D \cos \phi}{\sin \phi \cos \phi} \\ &= \frac{\sigma}{2} \frac{k_L \sin \phi + k_D \cos \phi \cos \phi}{\cos^2 \phi \sin \phi}, \end{aligned}$$

$$\text{i.e. } \frac{a'}{1-a'} = \frac{\sigma \mu_2}{2 \tan \phi} \quad \dots \dots \dots (22)$$

an equation giving a' in terms of ϕ .

Again, on putting $V_r = 2\pi nr(1-a')\sec\phi$, it can easily be seen that the equations for $\frac{dT}{dr}$, $\frac{dQ}{dr}$ are the same as equations (8) and (9), except for the introduction of the factor $(1-a')^2$. Hence,

$$\frac{dT}{dr} = \mu_1 \rho c \ 4\pi^2 n^2 r^2 (1-a')^2 \quad . \quad . \quad . \quad (23)$$

and
$$\frac{dQ}{dr} = \mu_2 \rho c \ 4\pi^2 n^2 r^3 (1-a')^2 \quad . \quad . \quad . \quad (24)$$

Similarly equations (12) and (13) now become

$$\frac{dk_T}{dx} = \frac{1}{2} \sigma \mu_1 \pi^3 x^3 (1-a')^2 \quad . \quad . \quad . \quad (25)$$

and
$$\frac{dk_Q}{dx} = \frac{1}{4} \sigma \mu_2 \pi^3 x^4 (1-a')^2 \quad . \quad . \quad . \quad (26)$$

Also, corresponding to equation (11), the following equation holds

$$\frac{V}{nD} = \pi x \frac{1-a'}{1+a} \tan\phi \quad . \quad . \quad . \quad (27)$$

Summary of Results and Typical Calculation. The full equations for the determination of $\frac{dk_T}{dx}$, $\frac{dk_Q}{dx}$ are summarized below:

$$\begin{aligned} \phi &= \theta - \alpha \\ \frac{V}{nD} &= \pi x \frac{1-a'}{1+a} \tan\phi \\ \frac{a}{1+a} &= \frac{\sigma \mu_1}{2 \tan^2 \phi} \\ \frac{a'}{1-a'} &= \frac{\sigma \mu_2}{2 \tan \phi} \\ \frac{dk_T}{dx} &= \frac{1}{2} \sigma \mu_1 \pi^3 x^3 (1-a')^2 \\ \frac{dk_Q}{dx} &= \frac{1}{4} \sigma \mu_2 \pi^3 x^4 (1-a')^2, \end{aligned}$$

where

$$\sigma = \frac{Bc}{2\pi r}, \quad \mu_1 = \frac{k_L \cos \phi - k_D \sin \phi}{\cos^2 \phi}, \quad \mu_2 = \frac{k_L \sin \phi + k_D \cos \phi}{\cos^2 \phi}$$

and k_L , k_D are the lift and drag characteristics at incidence α for infinite aspect ratio.

Unfortunately the above equations cannot be used to determine the values of $\frac{dk_T}{dx}$, $\frac{dk_Q}{dx}$ at a given value of $\frac{V}{nD}$, except by a method of trial and error. It is necessary to take α as the independent variable and determine the values of $\frac{V}{nD}$, $\frac{dk_T}{dx}$, $\frac{dk_Q}{dx}$ corresponding to different values of α . The method is illustrated in Table XVII, the calculations referring to the section of the example on p. 213. The first three columns give the aerofoil characteristics of this section for infinite aspect ratio, and were obtained from wind channel data on a model aerofoil of aspect ratio 6, corrected to infinite aspect ratio by means of the equations of Chapter IV. The airscrew is supposed to be a two-blader.

TABLE XVII
CALCULATION OF $\frac{dk_T}{dx}$, $\frac{dk_Q}{dx}$

$\theta = 16^\circ 30'$, $\sigma = \frac{Bc}{2\pi r} = 0.0613$, $\pi x = 2.356$									
α	k_L	k_D	ϕ	$\sin \phi$	$\cos \phi$	$\tan \phi$	$k_L \cos \phi$	$k_L \sin \phi$	$k_D \cos \phi$
-4	0.021	0.0192	20° 30'	0.350	0.937	0.374	0.020	0.0074	0.0180
-2	0.137	0.0099	18° 30'	0.317	0.948	0.335	0.130	0.0434	0.0094
0	0.228	0.0069	16° 30'	0.284	0.959	0.296	0.219	0.0648	0.0066
2	0.323	0.0062	14° 30'	0.250	0.968	0.259	0.313	0.0807	0.0060
4	0.430	0.0061	12° 30'	0.216	0.976	0.222	0.420	0.0929	0.0060
6	0.524	0.0070	10° 30'	0.182	0.983	0.185	0.515	0.0953	0.0069
$k_D \sin \phi$	μ_1	μ_2	$\frac{a}{1+a}$	$\frac{a'}{1-a'}$	a	a'	$\frac{V}{nD}$	$\frac{dk_T}{dx}$	$\frac{dk_Q}{dx}$
0.007	0.015	0.0289	0.003	0.0012	0.003	0.0012	0.878	0.006	0.0043
0.003	0.141	0.0587	0.039	0.0129	0.041	0.0127	0.749	0.055	0.0086
0.002	0.236	0.0776	0.083	0.0244	0.090	0.0238	0.624	0.090	0.0111
0.002	0.332	0.0925	0.152	0.0393	0.179	0.0378	0.497	0.123	0.0128
0.001	0.440	0.1038	0.274	0.0607	0.378	0.0572	0.357	0.156	0.0138
0.001	0.532	0.1058	0.470	0.0881	0.908	0.0810	0.208	0.177	0.0132

If the last two columns are plotted against $\frac{V}{nD}$, the values of $\frac{dk_T}{dx}$, $\frac{dk_Q}{dx}$ for any given value of $\frac{V}{nD}$ may easily be read from the resulting curves.

***Efficiency of an Element.** The efficiency of the element is given by

$$\begin{aligned}\eta &= \frac{V \times dT}{2\pi n \times dQ} \\ &= \frac{V}{2\pi n} \frac{\mu_1}{\mu_2 r}, \text{ from equations (23) and (24),} \\ &= \frac{V}{2\pi n r} \frac{\mu_1}{\mu_2} \\ &= \frac{1-a'}{1+a} \tan \phi \frac{\mu_1}{\mu_2}, \text{ from equation (20).}\end{aligned}$$

But $\tan \phi \frac{\mu_1}{\mu_2} = \frac{\tan \phi (\delta - \tan \phi)}{\delta \tan \phi + 1}$, as on p. 212.

This can be written in a simpler form by putting $\tan \gamma = \frac{1}{\delta}$ ($= \frac{1}{k_L/k_D}$), for

$$\begin{aligned}\tan \phi \frac{\mu_1}{\mu_2} &= \frac{\tan \phi \left(\frac{1}{\tan \gamma} - \tan \phi \right)}{\frac{\tan \phi}{\tan \gamma} + 1} \\ &= \frac{\tan \phi (1 - \tan \phi \tan \gamma)}{\tan \phi + \tan \gamma} \\ &= \frac{\tan \phi}{\tan (\phi + \gamma)}.\end{aligned}$$

Hence,
$$\eta = \frac{1-a'}{1+a} \frac{\tan \phi}{\tan (\phi + \gamma)} \quad \dots \quad (28)$$

Thus it can be seen that the efficiency of the element is composed of 3 partial efficiencies, viz.

(1) $\eta_1 = \frac{1}{1+a}$, which is the ideal efficiency and shows the loss due to the axial velocity of the slipstream,

(2) $\eta_2 = \frac{\tan \phi}{\tan(\phi + \gamma)}$ or $\frac{\mu_1}{\mu_2} \tan \phi$, which shows the loss due to the profile drag of the blades,

(3) $\eta_3 = 1 - a'$, which shows the loss due to the rotational velocity of the slipstream.

Table XVIII below is a continuation of Table XVII, and shows the relative importance of the three sources of energy loss.

TABLE XVIII
CALCULATION OF THE EFFICIENCY OF AN ELEMENT

$\frac{V}{nD}$	η_1 $\left(= \frac{1}{1+a} \right)$	η_2 $\left(= \tan \phi \times \frac{\mu_1}{\mu_2} \right)$	η_3 $(= 1 - a')$	η $(= \eta_1 \times \eta_2 \times \eta_3)$
0.878	0.997	0.194	0.999	0.193
0.749	0.961	0.805	0.987	0.763
0.624	0.917	0.900	0.976	0.805
0.497	0.848	0.930	0.961	0.758
0.357	0.726	0.941	0.939	0.642
0.208	0.524	0.930	0.912	0.444

This table shows that at top speed (given in this case by $\frac{V}{nD} = 0.677$, corresponding to $V = 176$, $n = 26$ and $D = 9.25$) the loss due to the profile drag of the blades is the most important, while at the slower climbing speeds the greatest loss is due to the axial velocity imparted to the slipstream, the loss due to the rotation of the slipstream being very small over the whole working range.

Effect of Pitch and Diameter on Efficiency. On referring to Fig. 134, it will be seen that, for a given speed and power, the ideal efficiency of an airscrew increases as the diameter increases; in other words, the inflow factor a decreases as the diameter increases. The same is true, of course, for an element, and therefore the form of the partial efficiency η_1 shows that a large diameter is desirable. Also the form of η_2 shows that a high

pitch is desirable (see p. 112 and Fig. 132). Unfortunately a limit to the maximum diameter and pitch is imposed by structural considerations. An airscrew is designed to absorb a given horse-power at a given speed of rotation, and so an increase of pitch or diameter must be counteracted by a reduction of blade width, in order that the airscrew may allow the engine to develop its full revolutions. But a reduction in blade width involves a reduction of the strength available to withstand the stresses imposed by the air forces and centrifugal forces, and so the blade width is more or less fixed.

APPENDIX

THEORY OF AEROFOILS—CALCULATION OF β AND k_{m_0}

For the general case in which the centre line is not a circular arc the following method is used: Let OA be the chord and OPA the centre line. Take axes as shown and suppose the ordinates and abscissae of

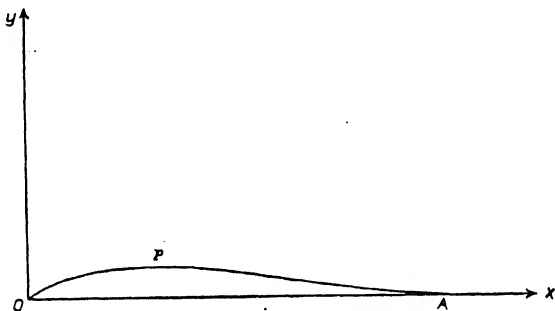


FIG. 137. Axes of Reference for Centre Line.

the centre line are expressed as fractions of the chord. Then the equations giving β and k_{m_0} are found to be

$$\beta = \int_0^1 \frac{y \, dx}{\pi(1-x)\sqrt{x(1-x)}} \quad \dots \quad (1)$$

and

$$k_{m_0} = -\frac{\pi}{4} \beta + \mu_0 \quad \dots \quad (2)$$

where

$$\mu_0 = \int_0^1 \frac{y(1-2x)}{\sqrt{x(1-x)}} \, dx \quad \dots \quad (3)$$

Generally the expressions $\frac{1}{\pi(1-x)\sqrt{x(1-x)}}$ and $\frac{1-2x}{\sqrt{x(1-x)}}$ are written $f_1(x)$ and $f_2(x)$ respectively.

If the equation of the centre line is known, the values of β and k_{m_0} can be obtained at once from equations (1) (2) and (3) by direct integration. A particular and important illustration is afforded by the centre line equation

$$y = hx(1-x)(a-x)$$

where h and a are constants. This equation gives a centre line with a reflex curvature towards the trailing edge when x lies between $\frac{1}{2}$ and 1. The expressions for β and μ_0 can be immediately integrated by the use of the substitution $x = \sin^2 \theta$, with the result that

$$\beta = \frac{1}{8}h(4a-3)$$

and

$$k_{m_0} = \frac{\pi}{64}h(7-8a).$$

Hence k_{m_0} will be zero and the centre of pressure will be stationary if $a = \frac{7}{8}$. This result has been checked by wind channel experiments on an aerofoil known as R.A.F. 33 which was designed by giving the

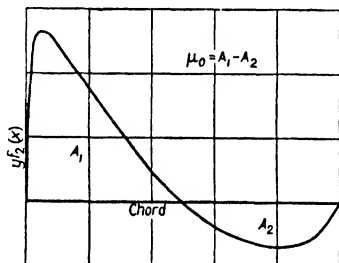


FIG. 138. Calculation of μ_0 .

basic symmetrical section (R.A.F. 30) of R.A.F. 32 a centre line defined by the above equation with the particular values $h = 0.413$, $a = 0.875$. The value for h was so chosen in order that the maximum centre line camber might be 0.05, the same as for R.A.F. 32, the reason for this being that a comparison of the model results for R.A.F. 32 and R.A.F. 33 would then furnish data on the probable effect on lift and drag of reflex curvature. The experiments show that the C.P. is brought to rest at the expense of a small decrease in the maximum lift coefficient (from 0.66 to 0.62) and a small increase in the minimum profile drag coefficient (from 0.0058 to 0.0064).

If the equation of the centre line is unknown the expressions for β and μ_0 must be integrated graphically. To do this it is necessary to take a range of values of x between 0 and 1 and determine the corresponding values of $yf_1(x)$ and $yf_2(x)$. If then these values are plotted against x the areas between the resulting curves and the

x -axis give the values of β and k_{m_0} . The type of curve obtained for the determination of μ_0 is as shown in Fig. 138, the value of μ_0 being the difference between the areas above and below the axis. The type of curve which gives β tends to run to infinity at $x = 1$ since $f_2(x) = \infty$

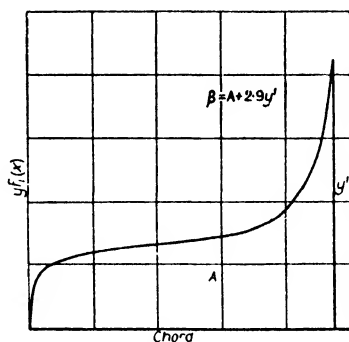


FIG. 139. Calculation of β .

at that point (Fig. 139). It is therefore usual to integrate between $x = 0$ and $x = 0.95$ and to calculate the remaining portion of the area between $x = 0.95$ and $x = 1$ by assuming that this portion of the centre line is a straight line. It can be shown that on this assumption the remaining portion is equal approximately to $2.9y'$, where y' is the ordinate at $x = 0.95$.

This method of calculating β and k_{m_0} has been applied to a few well-known aerofoils and the results obtained have been in very good agreement with experimental results.

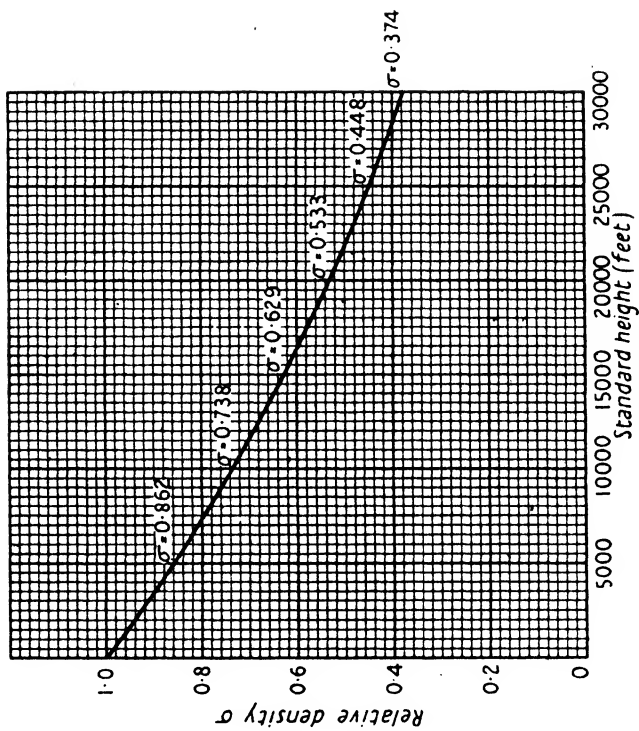


FIG. 140.

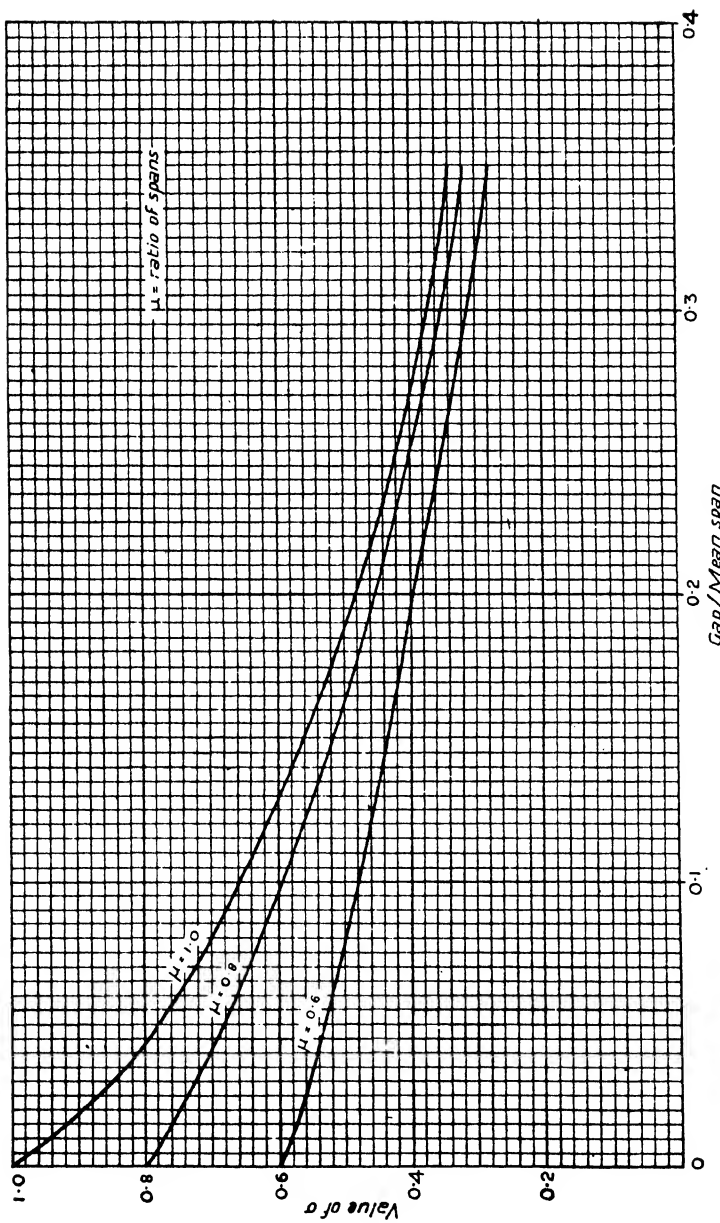


FIG. 141. Values of σ
For determination of Induced Drag of Biplane

INDEX

- Actuator disk, 217.
- Aerofoil, definitions, 18 sq.
 - distribution of pressure over section of, 41.
 - distribution of pressure over span of, 48.
 - flow past section of, 39.
 - forces on; lift and drag, 18.
 - moment and centre of pressure of, 27.
 - slotted, 40, 182.
- Aerofoil characteristics, diagrams of, 20, 26, 30.
 - effect of aspect ratio on, 52 sq.
 - effect of biplane interference, 59 sq.
 - effect of centre line camber, 74 sq.
 - effect of thickness, 79.
 - scale effect on, 197 sq.
- Aeroplane, description of parts, 5.
 - overall drag of, 90.
 - performance of, 94 sq.
- Ailerons, 166.
 - differential, 172.
 - reversal of, on turn, 174.
 - rolling moment of, 170.
 - slot and; action in reducing yawing moment, 182.
 - yawing moment of, 170, 182.
- Airflow, past flat plate, 37 sq.
 - round aerofoil section, 39.
 - across aerofoil span, 48.
- Aircrew, effect of body behind, 140.
 - efficiency, definition, 94.
 - efficiency, expressions for, 102, 133.
 - efficiency, ideal, 220; of element, 211, 228; and forward speed, 134.
 - non-dimensional characteristics of, 129 sq.
 - pitch, definitions, 134; its effect on efficiency and torque, 136; on efficiency of element, 212.
 - theory, blade element, 208; simple momentum, 217; vortex, 222.
 - thrust and torque of, 127 sq.
 - tip speed, 140.
 - variable pitch, 137, 140.
- Air speed, 5.
 - indicated, 10, 27.
 - indicator, 8.
- Altimeter, 11.
- Altitude, and aeroplane performance, 109 sq.
 - and atmospheric conditions, 13.
 - and engine performance, 110, 138.
- Aneroid, 11.
- Angle, of bank, 173.
 - of climb, 99.
 - critical, 21.
 - dihedral, action of, in sideslip, 194; longitudinal, 155.
 - of downwash, 153; its effect on tail plane drag, 161.
 - gliding, 104.
 - of incidence, definition, 17; variation of aerofoil characteristics with, 19.
 - of no-lift, definition, 20; and centre line camber, 74, 75.
 - pitch, of airscrew, 125; *see also* Airscrew.
 - of stagger, 62.
 - stalling, 24.
 - tail setting, 154 sq.
- Aspect ratio:
 - corrections for, 56.
 - and induced drag, 53.
 - and performance, 118 sq.
 - of non-rectangular wings, 58.
- Atmosphere, standard, 13.
- Autorotation, 181.
- Axes of reference, 164.
- Balanced control surfaces, 167.
- Bank, angle of, 173.
- Bernoulli's equation, 8, 43, 71, 218.
- Biplane, lift distribution between wings of, 64.
 - and curvature of streamlines, 63, 151.
 - induced drag of, 59 sq.
 - stagger, 62.
- Blade element theory, 208.
- Body, behind airscrew, effect of, 140.
 - fineness ratio of, 83.
 - pitching moment of, 152.
- Boundary layer, 69, 72.
- Cables, drag of, 88.
- Ceiling, service and absolute, 112.
 - rapid prediction of, 117.

- Centre line camber, 74 sq.
 Centre of gravity, coordinates of, 149.
 — determination of, 147.
 — and stability, 190.
 Centre of pressure, 27.
 — and centre line camber, 78.
 Channel walls, constraint of, 65.
 Channel, wind, description of, 6;
 variable-density, 199.
 Chord, definition, 10.
 — mean, 148.
 Circulation, 46, 71.
 Climb, aerodynamic efficiency on, 117.
 — angle of, 99.
 — calculation of rate of, 98, 101.
 — effect of change of weight on, 105 sq.
 — effect of height, 109 sq.
 — effect of plan form and aerofoil section, 120.
 — effect of supercharging, 112.
 — effect of wing and power loadings, 116.
 Control surfaces, action of, 164.
 — balanced, 167.
 Critical angle, 21.
 Curvature of streamlines, its effect on lift curve, 63; on moment curve, 151.
 Cylinder, non-viscous flow round, 71.
 Damping, in pitch, 191.
 — in roll, 180, 194.
 Density, 8, 9.
 — relative, 10, 13.
 — standard, 9.
 Differential ailerons, 172.
 Dihedral angle, action of, in sideslip, 194.
 — longitudinal, 155.
 Directional stability, 193.
 Distribution, of pressure over aerofoil section, 41.
 — of lift across aerofoil span, 48.
 — of lift between biplane wings, 64.
 — of parasite drag, 90.
 Divergence, 185.
 Downwash, angle of, 153.
 — its effect on tail plane drag, 161.
 Drag, of airship models, 87.
 — of cables, 88.
 Drag, of flat plate, 15 sq.
 — form, 38; of fuselage, 85.
 — induced, of monoplane, 53 sq.; of biplane, 59 sq.
 — interference, 89.
 — overall coefficient, 91.
 — parasite, 81; coefficient, 90.
 — profile, 53 sq., 70; and centre line camber, 77; and thickness of aerofoil, 79.
 — scale effect on, 198 sq.
 — of struts, 84, 205.
 — of undercarriage, 88.
 — of wires, 85.
 Duplex Wind Channel, 7.
 Dynamic Stability, 185, 191.
 Edge, leading and trailing, 19.
 Efficiency, aerodynamic, on climb, 117.
 — at top speed, 115.
 Efficiency, of airscrew, *see* Airscrew.
 — of tail plane, 156.
 Elevators, 5, 159, 165.
 — characteristics of, 169.
 Engines, 94.
 — power and torque of, 126, 138.
 Engine speed, and aeroplane speed, 132.
 Equations of motion, 100.
 Experimental mean pitch, 135.
 Fairing, 39.
 Fin, stabilizing action of, 193.
 — drag of, 88.
 Fineness ratio, 83.
 Flat plate, flow past, 37 sq.
 — forces on, 15 sq.
 Flow, *see* Airflow.
 Fluid, viscosity, 37, 69.
 Flying boat, 153.
 Form drag, 38.
 Friction, skin, 18, 37.
 Full-scale, 197 sq.
 Fuselage, description of, 85.
 — drag of, 85.
 — slipstream effect on, 95, 141.
 Gap of biplane, 59.
 Gap/chord ratio, 63.
 Gap/span ratio, 60.
 Geometric mean pitch, 135.
 Glide, angle of, 104.

- Head, total pressure, 44.
 Height, its effect on aeroplane performance, 109 sq.
 — its effect on airscrew performance, 138 sq.
 — variation of horse-power with, 110, 138.
 Horn balance, 168.
 Horse-power, available, 97.
 — required, 95.
 — variation with height, 110, 138.
 — variation with engine speed, 126.
 Hydrodynamics, 69.
 Incidence, angle of, 17 sq.
 — variation with speed, 23, 24.
 — rigging, 101.
 Indicated air speed, 10, 27.
 Indicator, air speed, 8.
 Induced velocity, 50 sq.
 — drag, 53 sq.
 Inflow, 217, 219.
 Inset balance, 168.
 Instability, spiral, 196.
 Interference drag, 89.
 Landing speed, 25.
 Lateral stability, 192 sq.
 Leading edge, 19.
 Lift, 17.
 — distribution across span, 48.
 — distribution between biplane wings, 64.
 — origin of, 46, 70.
 Lift-drag ratio, 26.
 — of complete aeroplane, 92.
 Load factor, in turn, 175.
 — in loop, 177.
 Loading, power, 116 sq.
 — wing, 25, 116 sq.
 Longerons, 85.
 Longitudinal dihedral, 155.
 Longitudinal stability, 186 sq.
 Looping, 177.
 Mean chord, 148.
 Moment, of body and thrust, 152, 159.
 — of tail plane, 155 sq., 187 sq.
 Moment of wing forces, 27 sq., 74.
 — effect of centre line camber on, 75 sq.
 — effect of curvature of streamlines, 151.
 — and stability, 187 sq.
 Origin of lift, 46, 70.
 Oscillation, 185.
 Overall drag coefficient, 91.
 Parasite drag, 81.
 Perfect fluid, 69.
 Performance, aeroplane, 94 sq.
 Pitch of airscrew, *see* Aircrew.
 Pitching axis, 164.
 Pitching moment, *see* Moment.
 Pitot tube, 7, 44.
 Plate, flat, flow past, 37 sq.
 — forces on, 15 sq.
 Power loading, 116 sq.
 Pressure, atmospheric, 9, 13.
 — and engine power, 110, 138.
 Pressure, centre of, 27, 78.
 Pressure distribution over aerofoil, 41.
 Profile drag, 53 sq., 70.
 — and centre line camber, 77.
 — and thickness of aerofoil, 79.
 Rate of climb, *see* Climb.
 Relative density, 10, 13.
 Reynolds's number, 199.
 Rigging incidence, 101.
 Roll, damping in, 180, 194.
 Rolling axis, 164.
 Rolling moment of ailerons, 170, 183.
 Rudder, 6, 166.
 — yawing moment of, 172.
 Scale effect, 197 sq.
 Sideslip in turning, 173.
 — stability in, 194.
 Skid, tail, 6.
 Skin friction, 18, 37.
 Slipstream, 85, 94.
 — its effect on drag, 141; on tail plane, 160.
 Slipstream factor, 142.
 Slot-cum-aileron control, 182.
 Slotted wing, 40, 182.
 Span, definition, 19.
 — lift distribution across, 48.
 Span²/weight ratio, 120 sq.
 Speed, indicated, 10, 27.
 — maximum level, 97, 108, 111, 113 sq.
 — rapid prediction of, 114.
 — stalling, 24.
 Spin, 80.

- Spiral stability, 195.
- Stability, longitudinal, 186.
- lateral, 192.
- Stagger, 62 sq.
- Stall, 24.
- Stalling speed, 24.
- in turn, 175.
- Standard atmosphere, 13.
- Standard density, 9.
- Static stability, 185 sq.
- Streamlines, 36.
- curvature of, 63, 151
- Streamlining, 82.
- Struts, drag of, 84.
- and scale effect, 205.
- Subsidence, 185.
- Supercharging and aeroplane performance, 112.
- and airscrew performance, 139.
- Tail plane, 5.
- characteristics of, 155, 169.
- drag of, 88, 161.
- efficiency, 156.
- moment, 155 sq., 187 sq.
- Tail setting, 154 sq.
- to trim, 158.
- Tapered wings, 58.
- Thrust, airscrew, 100 sq., 128.
- grading curve, 211.
- moment, 152, 159.
- variation with speed, 133.
- Tip speed, 140.
- Torque, 126 sq.
- grading curve, 211.
- Total pressure head, 44.
- Trailing edge, 19.
- Trailing vortices, 49.
- Turbulence, 36 sq.
- ring, 86.
- Turning, 173 sq.
- Undercarriage, 6.
- drag of, 88.
- Variable-density wind channel, 199.
- Variable pitch airscrew, 137, 140.
- Viscosity, 37, 69 sq.
- kinematic coefficient of, 199.
- Vortices, trailing, 49.
- Weight and performance, 105 sq.
- Weight-lift equation, 22.
- Wheels, drag of, 88.
- Wind channel, variable-density, 199.
- walls, constraint of, 65.
- Wing, slotted, 40, 182.
- tapered, 58.
- Wing loading, 25.
- and performance, 116 sq.
- Wires, drag of, 85.
- Yawing axis, 164.
- Yawing moment, of ailerons, 170, 182.
- of rudder, 172.

ANSWERS TO EXAMPLES

CHAPTER I, p. 14: (1) 0.00149 slugs. (2) 0.629; 15,000 ft. (3) 0.00206 slugs; 4,750 ft. (5) 67.9, 71.1, 74.4, 78.1 m.p.h. (6) 14,500 ft.

CHAPTER II, p. 32: (1) 12 lb. (2) 0.126. (4) 55.1 m.p.h. (5) 2.6 m.p.h. (6) 0.651. (7) 59 m.p.h. (8) $\alpha = 7.3^\circ, 3.2^\circ$; $k_D = 0.0206, 0.0095$; $D = 123$ lb., 101 lb. (9) 135 lb.; 16.2 per cent. (10) $k_L = 0.16, 0.302$; $V_{m.p.h.} = 104.7, 76.2$. (11) 450 lb.; 540 lb. (12) 0.273; 0.420. (13) -0.0252.

CHAPTER IV, p. 67: (1) 0.0104. (2) $k_{D_0} = 0.106k_L$. (3) 245 lb.; 109 lb. (4) $k_{D_1} = 0.0884k_L$; 0.0070; 0.0175. (5) 6.34; $k_{D_1} = 0.1k_L$; About 19.6 at $k_L = 0.255$. (6) $\Delta\alpha = -0.865k_L$ (degrees); $\Delta k_D = -0.0151k_L$; 0.0262; 5.5°. (7) 0.0153. (8) $\Delta k_D = 0.0131k_L$; 17.2, 15.6, 13.9.

CHAPTER VI, p. 93: (1) 61.9 lb. (2) 0.43 lb. (3) 0.16 lb. (4) 164.4 lb. (5) 0.0144. (6) 0.0146. (7) $k_{D_1} = 0.145k_L$; $\text{Max } \frac{L}{D} = 9.05$.

CHAPTER VII, p. 123: (1) 84.7; 70.6 per cent. (2) 7.7 m.p.h. (3) 134.3 m.p.h. (4) 8.58. (5) 964 ft./min.; $8^\circ 45'$. (6) 15,400 ft.; 17,200 ft.; 940 ft./min.; 16 mins. (7) 97.5 m.p.h.; 410 ft./min. at 63 m.p.h. (8) 96 m.p.h.; 260 ft./min. at 68 m.p.h. (9) 1635 ft./min. (10) 118 m.p.h.; 315 ft./min. at 71 m.p.h. (indicated).

CHAPTER VIII, p. 143: (1) 0.662; 0.00783; 0.805. (2) 9 ft.; $\eta_{\max.} = 0.81$ at about $\frac{V}{nD} = 0.815$. (3) 130 m.p.h. (4) 1313 lb.-ft.; 1890. (5) 395.

(6) $\begin{matrix} V_{m.p.h.} & 63.5 & 70.3 & 82.2 & 91.3 & 99.3 & 106.9 \\ \eta P & 53.3 & 56.6 & 61.5 & 64.7 & 67.1 & 68.4 \end{matrix}$; 51.5; 68.2.

(7) 145 m.p.h. (8) 8.3 per cent.

CHAPTER IX, p. 163: (1) 5.3 ft. at 2.88 ft. above lower wing; $h = 0.317$, $k = -0.229$. (2) -66.4 lb. (3) $\bar{k}_m = -0.0199, -0.0108, -0.0030, +0.0032, 0.0078, 0.0108, 0.0120$; 76.5 m.p.h. (4) -0.2° ; -0.9° ; -3° . (5) 9.3 lb.; 23.1 lb.

CHAPTER X, p. 184: (1) $46^\circ 14'$; 2602 lb. (2) 208 ft. (3) 4.68. (4) 0.13; 3.23. (5) 68 m.p.h.

DATE OF ISSUE

This book must be returned
within 3, 7, 14 days of its issue. A
fine of ONE ANNA per day will
be charged if the book is overdue.

C

